Cooperative Control of Multi-Agent Systems

by

Junyi Yang

A thesis submitted in partial fulfillment of the requirements for the degree of

Doctor of Philosophy

in

Control Systems

Department of Electrical and Computer Engineering
University of Alberta

Abstract

Cooperative control of multi-agent systems (MASs) has been a hot topic in control and communication community since it was proposed in last two decades. Cooperative control is applied to a wide range of real world problems, such as search and rescue, resource allocation and multiple robot formation. In order to realize a cooperative goal, a communication network is introduced to facilitate the information flow among MASs, which brings network-induced imperfections at the same time. In addition, the energy of onboard sensors and microprocessors, and the bandwidth of communication networks are limited. It is preferred to reduce the frequency of controller updates and data transmissions. Motivated by the above concerns, this thesis focuses on investigating the robustness of MASs against network-induced imperfections and proposing event-triggered mechanisms (ETMs) to reduce the network load and/or energy consumptions.

Four research topics are considered. Firstly, an affine formation under fixed and switching topologies is studied. An ETM is proposed, such that the controller updates and data transmissions occur only when it is necessary to maintain system stability. To guarantee Zeno-freeness, an absolute term is introduced in the price of introducing steady-state errors. Secondly, a cooperative output regulation (COR) problem is studied. The problem is formulated in a hybrid system framework. By proposing a novel Lyapunov function, robustness against asynchronous samplings and time-varying delays are given in

terms of maximally allowable transmission intervals (MATIs) and maximally allowable delays (MADs). Thirdly, a formation tracking problem of multiple nonholonomic systems without velocity measurements is considered. Two kinds of communication, namely, pull-based communication (PULC), which is enabled by agents' onboard sensors, and push-based communication (PUSC), which is realized by data transmissions through networks, are considered separately. A periodic event-triggered mechanism (PETM) is proposed for PUSC, such that the closed-loop sampled-data system is robust to asynchronous samplings, at the same time, continuous monitoring and Zeno-behavior are avoided. In addition, a hierarchical structure is proposed, according to which, the followers are divided into two levels. Strongly integral input-to-state stability (iISS) is established for the closed-loop system. Finally, a distributed optimization-based formation problem is studied. The control protocol is design based on a modified Lagrangian-based (MLB) algorithm, under which, the agents can reach the global optimal solution and converge to the desirable formation structure simultaneously. A dynamic ETM is proposed to reduce network load. To guarantee Zeno-freeness in the presence of disturbances, an auxiliary variable is introduced to estimate the influence of disturbances. The closed-loop system is proved to be input-to-state exponentially stable (ISES) w.r.t. the disturbances.

The effectiveness of the proposed methods are illustrated by numerical examples. Under the proposed ETMs, unnecessary data transmissions and/or controller updates can be efficiently reduced. Zeno-freeness is guaranteed by event separation properties or computable positive minimum inter-event times. In addition, the proposed methods improve the robustness of closed-loop systems against network-induced imperfections.

Preface

The research work in Chapters 2 and 4 of the thesis was part of an international research collaboration with Dr. Feng Xiao at North China Electric Power University. The algorithms, mathematical derivations, and numerical simulations were my original work, as well as the introduction in Chapter 1.

- Chapter 2 has been published as J. Yang, F. Xiao and T. Chen, Formation tracking of nonholonomic systems on the special Euclidean group under fixed and switching topologies: An affine formation strategy. *SIAM Journal on Control and Optimization*, vol. 59, no. 4, pp. 2850–2874, 2021. A preliminary version has been published as: J. Yang, H. Yu, and T. Chen. Affine formation maneuver control of event-triggered multi-agent systems. *IFAC PapersOnLine*, vol. 53, no. 2, pp. 3391–3396, 2020.

- Chapter 3 has been published as J. Yang, H. Yu, and T. Chen, Cooperative output regulation with asynchronous transmissions and time-varying delays. *IEEE Transactions on Automatic Control*, early access.

- Chapter 4 has been accepted as: J. Yang, H. Yu, and F. Xiao, Hybrid-triggered formation tracking control of mobile robots without velocity measurements. *International Journal of Robust and Nonlinear Control*. A short version has been accepted as J. Yang, H. Yu and F. Xiao, Strong integral-input-to-state stability for cascade-connected systems. *5th International Conference on Control and Fault-Tolerant Systems*, Sept. 29th, 30th and Oct. 1st, 2021, Saint-Raphael, France.

- Chapter 5 has been submitted to *IEEE Transactions on Cybernetics* as: J. Yang, H. Yu, and T. Chen, Distributed optimization-based formation control: a dynamic event-triggered approach.

Acknowledgements

I would like to express my sincere gratitude to many people around me for their help and support. First and foremost, I would like to thank my supervisor, Prof. Tongwen Chen, for his encouragement, guidance, and support. He gave me many valuable opportunities and large freedom to explore interesting research topics and participate in industrial collaborations for getting practical experience. The past years of working under his supervision are unforgettable and irreplaceable in my life.

I would also like to thank my committee members Drs. Zhan Shu and Mahdi Tavakoli Afshari for their precious time and valuable feedback.

Furthermore, I am deeply thankful to those who have contributed to the collaborative research and discussions, with a special mention of Drs. Hao Yu and Feng Xiao (North China Electric Power University).

I also wish to acknowledge the financial support from Natural Sciences and Engineering Research Council of Canada (NSERC).

Moreover, I would like to thank all current and previous members of the research group, especially Hao Yu, Jiarao Huang, Ying Xiong, Jing Zhou, Jun Shang and Mani Hemanth Dhullipalla for their kindness, encouragement, and help.

Last but not the least, greatest thanks are also to my family members and friends for their companion mentally or physically over the past years.

Again, to people mentioned or not, my thankfulness and gratitude are beyond words and can never be written well enough.

Contents

List of Tables

List of Figures

List of Symbols

$\mathcal{G}$	Graph
$\mathcal{N}$	Node Set of a Graph
$\mathcal{E}$	Edge Set of a Graph
I_n	Identity Matrix of Dimension n
$f(r^-)$ $(f(r^+))$	The Limit of Function $f(\cdot)$ from Below (Above) at $r \in \mathbb{R}_{\geq 0}$
Ad	Adjoint Operator
$\mathcal{N}_i$	Neighbor Set of Agent i
$\mathcal{A}(r)$	Affine Image
L	Laplacian Matrix
$\{\mathcal{I}\}$	Inertial Frame
$\{\mathcal{B}_i\}$	Body-Fixed Frame of Agent i
$\mathbb{N}$	Set of Natural Numbers
$\mathbb{R}$	Set of Real Numbers
$\otimes$	Kronecker Product
$\mathcal{K}$	Class K Function
$\mathcal{K}_\infty$	Class K Infinite Function
$\mathcal{KL}$	Class KL Function
$\mathcal{KLL}$	Class KLL Function
$\mathcal{L}_2$	Lebesgue space with 2-norm
$\mathcal{L}_\infty$	Lebesgue space with ∞-norm

List of Acronyms

COR	Cooperative Output Regulation
DOF	Degree of Freedom
DOP	Distributed Optimization Problem
ET	Event-Triggering
ETM	Event-Triggered Mechanism
iISS	Integral Input–to–State Stability
ISES	Input–to–State Exponentially Stability
ISS	Input-to-State Stability
LMI	Linear Matrix inequality
MACP	Maximally Allowable Checking Period
MAD	Maximally Allowable Delay
MAS	Multi-Agent System
MASP	Maximally Allowable Sampling Period
MATI	Maximally Allowable Transmission Interval
MATP	Maximally Allowable Transmission Periods
MLB	Modified Lagrangian-Based
NCS	Network Controlled Systems
PETM	Periodic Event-Triggered Mechanism
PULC	Pull-Based Communication
PUSC	Push-Based Communication
SE(3)	Special Euclidean Group

SO(3)	Special Orthogonal Group
UGAS	Universal Global Asymptotic Stability

Chapter 1

Introduction

In this chapter, the research background for cooperative control of multi-agent systems (MASs) under communication networks is introduced and a literature survey is provided to summarize the recent development in this area. Thereafter, the contributions of the thesis are listed, followed by a thesis outline.

1.1 Research Background

Due to potential applications in search and rescue, monitoring and control, and cooperative localization, MASs have drawn a lot of attention in the areas of control and communication since last two decades [1, 2]. Adapted to different application backgrounds, the fundamental topics in MASs include consensus, flocking, containment, formation, cooperative output regulation (COR) and distributed optimization.

1.1.1 General Topics in Multi-Agent Systems

As one of the basic topics, formation control is suitable for various applications [3]. According to how the desirable formation is defined, most of the existing results on formation control can be classified as distance-based [4, 5, 6, 7], bearing-based [8, 9] and position-based [10, 11] methods. The formation structures defined by the first two kinds are invariant under rotation and scaling, and fixed in the position-based one. It can be seen that, in the

aforementioned results, the formation structures were equipped with at most one degree of freedom (DOF), and as a consequence, the manuverability of the MAS was constrained. This concern was tackled by an affine formation method in [12] and [13] recently, where the formation was invariant under affine transformation. Since the affine transformation can be represented by a combination of rotation, scaling, shearing and translation, more DOF can be provided into the corresponding formation.

Most of the above results are only available when the MASs are composed by subsystems with identical dynamics. To deal with heterogenous systems, COR has been extensively studied since it was proposed [14]. By a well-designed interactive protocol, COR aims at rendering a set of agents to achieve asymptotic tracking or disturbance rejection of an exogenous signal [14, 15]. Significant application potential of COR lies in its generality to include some typical problems in MASs, such as leader-follower formation [3], consensus [1] and flocking [16].

In order to quantitatively evaluate system performance, the distributed optimization problem (DOP) has become a hot topic since it was proposed in [17]. In DOP, we aim to find the optimal point of a global object function by a bunch of network-connected components (agents) who can communicate with each other and be aware of only their local object functions. DOPs were solved in a discrete-time manner in [18] and [19]; while considering that the dynamics of physical systems are generally described by differential equations, they were also solved in a continuous-time manner in [20], [21], [22], and [23].

1.1.2 Network-Induced Imperfections in Multi-Agent Systems

In order to accomplish collaborative operations, a shared network is introduced to facilitate information flow among agents. Communication network allows information to be shared among subsystems, which means that traditional point-to-point wiring in the installation of a control system may be avoided. However, the introduction of networks always comes with inevitable

network-induced imperfections that will degrade the performance properties or even cause instability. The common network-imperfections can be classified into the following five types [24, 25]:

- quantization errors in the signals transmitted over networks due to finite word length of packets;
- packet dropouts caused by unreliability of the networks;
- time-varying sampling/transmission intervals;
- time-varying communication delays;
- communication constraints caused by sharing of networks by multiple nodes and the fact that only one node is allowed to transmit its packet per transmission.

Among all communication imperfections, asynchronous transmissions and time-varying delays are fundamental and critical for MASs. Due to the independence among agents and the inherently digital feature of networked communication, it is hard to synchronize their transmission instants according to a common clock. Therefore, asynchronous transmissions are inevitable. In addition, since signals cannot be transmitted continuously and instantaneous, transmission delays would influence the real-time capability of system operations. Besides the above, another concern in MASs is time-varying topologies. Data transmissions through communication networks can be interrupted by cyber attacks, and the ones that are carried out by detection from onboard sensors are limited by sensing ranges and influenced by the blocks in the concerned areas. As a result, it is more practical to consider the cooperative control problem under switching topologies.

1.1.3 Event-Triggered Mechanism

Cooperative control relies on computations by agents' onborad microprocessors and communications through a shared network. Restricted onboard

energy and communication resources need to be taken into account. Therefore, the scheduling of controller updates and data transmissions has become a critical and practical issue in MASs. The scheduling can be done in a time-triggered or an event-triggered fashion. For the first kind, the sampling periods are predetermined which should guarantee the system performance over a wide range of operating conditions [26]. These off-line designed sampling periods might be conservative, resulting in unnecessary controller updates and data transmissions. High-frequency sampling might cause traffic congestion in the network and increase packet dropouts [27]. Frequent updates and transmissions also cause extra energy consumption [28], which might reduce the lifespan of agents. In light of this concern, event-triggered mechanisms (ETMs) were proposed, which replaced the predetermined sampling periods by an online detected criterion depending on a measurement or time dependent threshold. The controller updates and data transmissions are generated sporadically, only when it is essential for maintaining the system performance. As a result, less communication and energy consumption are required, with some comparable system performance.

The exclusion of Zeno behavior, in the sense that infinite events happen in a finite time interval, is a critical and challenging problem when implementing ETMs. In [29], the authors have pointed out that many existing ETMs would exhibit Zeno behavior when there is disturbance and/or in an output feedback scenario. The Zeno-freeness is usually demonstrated by the event-separation property, where the number of events must be finite within any finite interval, or there exists a computable positive minimum inter-event time.

1.2 Literature Review

Considering unavoidable communication imperfections, researchers focused on investigating the robustness against different types of communication imperfections. To reduce onboard energy and communication resources consumption, a variety of ETMs were proposed. Some of them also provided a

rigorous analysis on Zeno-freeness. This section presents a detailed literature survey on the recent development of such methods.

1.2.1 Research on Robustness Against Network-Induced Imperfections

The introduction of networks always comes with communication imperfections such as asynchronous transmissions, time-varying delays, quantization errors, packet dropouts, and communication constraints [24, 30, 31], which can degrade the system performance or even cause instability. This makes the control problems of MASs under communication networks more challenging compared with their single-plant counterparts. Besides improving the network infrastructure, the focus is also on figuring out the effects of these imperfections and providing a guideline to the system designers. This topic has been widely investigated in the area of networked control systems (NCSs) with one or multiple communication imperfections under consideration [24, 31, 32, 33]. In NCSs, only one node may have access to the network at a transmission instant; thus a proper communication scheduling protocol is necessary to grant the access of the nodes to the network [34]. The scheduling protocol can be static, like Round-Robin (RR) protocols, or dynamic, like Try-Once-Discard (TOD) protocols. The stability under communication constraint was investigated in [34], [35], [24] and [36]. Quantization errors are another network-induced issue, which can be caused by analog-to-digital coders before the data are released to the network. The error between the actual analog value and the converted digital one is usually unavoidable due mainly to the operation of rounding or truncation [37]. Considering different types of quantizers, system performance was investigated for NCSs in [35], [38], and for MASs in [39], [40]. For MASs, the research on data dropouts can be found in [41], [42], which considered stochastic packet dropout; and attack-induced packet dropouts were studied in [43]. Based on the method proposed in [24], the influence of data dropouts can be included in the ones of time-varying delays.

Due to the independence among agents and the inherently digital feature of

network communication, asynchronous transmissions are inevitable. In NCSs, this problem was solved in a hybrid system framework, and an emulation-based approach [44] was used to derive the upper bounds of maximally allowable transmission intervals (MATIs) [24, 45], such that the transmission instants in each node could be decided independently as long as the transmission interval was smaller than MATIs. Following this method, the authors solved a consensus problem under asynchronous transmissions for the MASs with single integrators in [46] and for general linear systems in [47].

Considering time-varying delays, a discrete Lyapunov method was used in [48] and [49] to solve consensus problems for single and double integrators, respectively. Synchronous sampling was assumed in the aforementioned results, in a way that all agents broadcast local information to their neighbors at the same instants. In [24], an emulation-based approach was used to compute the bounds on MATIs and maximally allowable delays (MADs), which can characterize the tolerance of NCSs both on the asynchronous transmissions and time-varying delays. In [50], this method was extended to solve a consensus problem for MASs. Asynchronous transmissions and time-varying delays were tackled simultaneously for MASs with single integrators [51] or marginally stable dynamics [52] in a time-delay approach. However, asynchronous transmissions among agents lift the dimension of system matrices, which brings higher complexities in analysis.

1.2.2 Event-Triggered Mechanism and Zeno-Freeness

The implementation of cooperative control depends on the development of onboard sensors and microprocessors, which only have limited energy resources. Thus, wasted energy consumption would shorten the lifespan of MASs. Under this background, how to efficiently schedule the transmissions among sensors and actuators becomes a critical issue. The classical time-triggered fashion is an open-loop mechanism, where a fixed transmission period is predetermined in spite of the system states. This fixed period

is a bit conservative and results in unnecessary transmissions and updates [26]. On the contrary, the event-triggered fashion can reduce consumption of communication resources by replacing the predetermined transmission period by a closed-loop scheduling mechanism. Specifically, the transmission interval is decided by an online detected criterion with a measurement-dependent [53, 54] or time-dependent [55, 56] threshold. Benefited from that, the frequency of sensor detection and actuator update is reduced, which further results in less utilization of computation and communication resources in some circumstances [27, 28].

A key challenge in adopting ETMs is the exclusion of Zeno behavior, which can be guaranteed by ensuring a positive lower bound of inter-event times or by event-separation properties. The authors in [29] have pointed out that, many existing results in ETM would exhibit Zeno behavior when there is disturbance in systems and/or in an output feedback scenario. A straightforward way to solve this problem is choosing an absolute threshold in the event-triggering (ET) function [22], but with the price of loosing asymptotic stability. In [57] and [58], a time decaying term was introduced to ensure Zeno-freeness for disturbance-free MASs. Considering the situation of unknown disturbances, this problem was tackled by a periodic ETM (PETM) in [51] and [59], and by a time regularization method in [60] and [61], which introduced a pre-specified lower bound to the inter-event times. However, as static ETMs were implemented in the aforementioned results, the transmission behavior were often reduced to approximately periodic communication when the state was close to the origin [32]. Alternatively, dynamic ETMs were considered in [32], [62] and [63] for NCSs. By introducing a dynamic variable to the ET condition, the dynamic ETMs were more robust to unknown disturbances and could provide larger average inter-event times. A similar idea was applied in [50], [47] and [46] to solve the consensus problem of MASs. In addition, the pre-specified minimum inter-event times in time regularization methods are usually calculated in a conservative way [64]; hence, it is better to design ETMs with some

worst-case transmission performance guarantee, which is independent of any pre-specified minimum inter-even times. In [65] and [23], this guarantee was obtained by using an auxiliary variable to estimate the average influence of external disturbances. Single-loop systems were considered in [65] and MASs with undirected underlying graphs were considered in [23].

1.3 Thesis Contributions

Motivated by wide application backgrounds of MASs and the unavoidable communication imperfections, this thesis studies varieties of cooperative control problems and proposes some novel control and communication protocols to guarantee the performance of closed-loop sampled-data systems. The major contributions in this thesis that distinguish them from other work are summarized as follows:

1. Investigate an affine formation tracking problem of general nonholonomic systems on the special Euclidean group (SE(3)) under fixed and switching topologies. A distributed algorithm is proposed to reconstruct a k-rooted graph when some edges are lost. An ETM is proposed such that the affine formation problem can be solved with discontinuous controller updates and data transmissions. However, in order to exclude Zeno behavior, we use an absolute threshold in the ET condition, which sacrifices the asymptotic stability, and the underlying graph is assumed to be acyclic to avoid event accumulation.

2. Investigate a sampled-data COR problem of heterogeneous systems under asynchronous transmissions, time-varying delays and unknown disturbances. The problem is formulated and solved in a hybrid system framework. A novel Lyapunov function candidate is proposed for MASs, based on which, a more intuitive analysis on the trade-off relationship between MATIs and MADs can be given compared with the ones given in [50].

3. Investigate a formation tracking problem for nonholonomic systems without measurements of the leader's velocity. A hierarchical structure is used to divide the followers into two levels, which removes the acyclic assumptions in [66] and [67]. The problem is formulated and solved in a hybrid system framework. An information flow architecture is proposed such that two kinds of communication networks, which enable pull-based communication (PULC) and push-based communication (PUSC), can be considered separately according to their distinct features. The concept of strongly integral input–to–state stability (iISS) in a hybrid system framework and a novel Lyapunov function are proposed to treat the higher order couplings in the closed-loop system. A hybrid-triggered formation control protocol for multi–robot systems is proposed, such that the ET conditions are checked discretely and asynchronously, and the closed-loop system is strongly iISS w.r.t. disturbances.

4. Propose an event-triggered control protocol to solve the optimization-based formation problem. Compared with the existing results in [68], the algorithm considered in this work can guarantee that the MASs converge exactly to the desirable optimal configuration. In addition, the ETM proposed in this work is a dynamic one, where an auxiliary variable is introduced to estimate the average influence of external disturbances. As a result, the closed-loop system can be input–to–state exponentially stable (ISES) w.r.t. unknown disturbances and at the same time, Zeno-freeness is guaranteed by a computable positive minimum inter-event time.

1.4 Thesis Outline

The remainder of the thesis is organized as follows.

In Chapter 2, an affine formation tracking problem is investigated. Section 2.1 gives an overview of the research work of this chapter. Section 2.2 considers the affine formation tracking problem of general nonholonomic systems on

SE(3). Some preliminaries and problem formulation are given in Section 2.2.1. The problem under fixed topologies is solved in Section 2.2.2. In Section 2.2.3, a distributed algorithm is proposed to reconstruct a k-rooted graph when some edges in the graph are lost; thereafter, the problem is solved under switching topologies. Some numerical examples are given in Section 2.2.4 to illustrate the effectiveness of the proposed method. In Section 2.3, an ETM is proposed such that the controller updates and data transmissions are generated discretely only when it is necessary to maintain system stability. A numerical example is given in Section 2.3.3 to verify the validity of the proposed mechanism, followed by conclusion remarks in Section 2.4.

In Chapter 3, a COR problem with time-varying delays, asynchronous transmissions and external disturbances is considered. Section 3.1 gives an overview of the research work in this chapter. Some preliminaries are given in Section 3.2.1. In Section 3.2.2, we formulate the COR problem under communication imperfections and external disturbances and reformulate it in a hybrid system framework in Section 3.2.3. The robustness against asynchronous transmissions and time-varying delays are evaluated in terms of MATIs and MADs in Section 3.3. Numerical examples are provided in Section 3.4 to further illustrate the effectiveness of the method, and conclusions are drawn in Section 3.5.

In Chapter 4, we investigate a formation tracking problem without velocity measurement under a hybrid triggered mechanism. Section 4.1 gives an overview of the research work in this chapter. Preliminaries are given in Section 4.2.1. In Section 4.2.2, we formulate the problem in a continuous-time framework. The information flow architecture is set up in Section 4.2.3. According to the hierarchical structure constructed in Section 4.2, control and estimation strategies are given, respectively, to the agents that belong to different levels in Section 4.3. In Section 4.4, we reformulate the problem in a hybrid system framework. The main results are given in Section 4.5, where finite time convergence, input-to-state stability (ISS) and strongly iISS are

provided for the subsystems that belong to different levels. Numerical examples are given in Section 4.6 to illustrate the effectiveness of the results, followed by concluding remarks in Section 4.7.

In Chapter 5, we investigate a distributed optimization-based formation control problem under ETMs. Section 5.1 gives an overview of the research work in this chapter. Some preliminaries on graph theory and convex functions are given in Section 5.2.1. The event-triggered optimization-based formation problem is formulated in Section 5.2.2. In Section 5.3, we propose an event-triggered optimization algorithm with rigorous proofs on Zeno-freeness and ISS w.r.t. disturbances of the closed-loop system. By a different ETM design, we discuss the trade-off between network load and computation complexity in Section 5.4. Numerical examples are presented in Section 5.5 and conclusions are drawn in Section 5.6.

In Chapter 6, concluding remarks and some potential directions of future work are provided.

Chapter 2

Affine Formation Control under Switching Graphs and Event-Triggered Mechanism*

2.1 Overview

In this chapter, we consider an affine formation tracking problem of MASs. The motivation of investigating an affine formation method is to increase the manuverability of MASs concerning the fact that the formation structure defined by classical methods, such as distance-based, bearing-based and position-based methods, are equipped with at most one DOF. Different from classical methods, generalized Laplacian matrices are used in the affine formation methods. Besides the interaction topology, the elements in the generalized Laplacian matrices are determined by a nominal configuration [13], which describes a typical geometric pattern of the formation. In this way, the generalized Laplacian matrix can be designed with $k+1$ zero eigenvalues in k dimensional (kD) spaces, which results in $k+1$ DOF in the corresponding formation. In [13], the affine formation problem was studied in a consensus sense, that is, the affine formation problem was solved when all agents converged to an unspec-

*A version of this chapter has been published as: J. Yang, F. Xiao, and T. Chen, Formation tracking of nonholonomic systems on the special Euclidean group under fixed and switching topologies: An affine formation strategy. *SIAM Journal on Control and Optimization*, vol. 59, no. 4, pp. 2850–2874, 2021. A preliminary version has been published as: J. Yang, H. Yu, and T. Chen. Affine formation maneuver control of event-triggered multi-agent systems. *IFAC PapersOnLine*, vol. 53, no. 2, pp. 3391–3396, 2020.

ified affine span of the nominal configuration. On the other hand, a different affine formation tracking problem is considered in this work, which was first proposed in [12]. Specifically, the agents could form a time-varying structure, with the centroid of them moving along a specific trajectory. In addition, the formation could be determined with only a small portion of the agents being aware of the desirable formation. Thus, one essential contribution in [12] was to specify an affine span by steering the trajectories of a part of agents.

In Section 2.2, an affine formation tracking problem of general nonholonomic systems is studied. This kind of system model covers most of the mechanical systems such as aerial vehicles, robotics and satellites. However, due to the nonlinearities and nonholonomic constraints, the control and state estimation for this kind of systems are technically challenging. A geometric control method is used in this work. Compared with linear controllers and nonlinear controllers that are based on Euler angles and quaternions, the proposed controller can avoid singularities and it can guarantee almost global convergence of the closed-loop systems [69]. In addition, the controller proposed in this work is designed directly on the Lie algebra of $SE(3)$, which enables a more general representation [70, 71] compared with the ones in [12] and [13].

A critical issue in the existing results on affine formation methods is the requirement of centralized computation when the associated Lapalacian matrices are designed. In [13], the design was formulated as an optimization problem when the graph was universally rigid. For a directed rooted graph, the associated Laplacian matrix could be constructed locally; however, centralized computation was still required to design a stabilizing matrix which guaranteed the semi-positive definiteness of the associated Laplacian [13, 72]. Inspired by [12], a control protocol, which solves the affine formation tracking problem without semi-positive definite Laplacian matrices, is proposed. Hence, for undirected graphs, a globally rigid condition, instead of the universally rigid condition in [13] and [12], is assumed; for directed graphs, the

edge weights can be calculated locally by each agent. By taking advantage of local calculation on weights, the proposed control protocol can be further extended to the case of switching topologies. In addition, to make formation problems realizable in practice, an algorithm, which aims to locally reconstruct a k-rooted graph when some edges in a graph are lost, is proposed. To the best of the authors' knowledge, the affine formation problem under switching topologies has not been investigated in the literature.

In Section 2.3, to reduce network load, an ETM is proposed for affine formation maneuver control problems of single integrators. Benifited from that, the controller updates and information broadcasting are generated only when it is necessary to maintain the system behavior. The practical convergence is guaranteed for the closed-loop system and Zeno behavior is excluded.

2.2 Formation Tracking of General Nonholonomic Systems on the Special Euclidean Group

2.2.1 Preliminaries and Problem Formulation

The special orthogonal group is denoted by $SO(3) = \{R \in \mathbb{R}^{3\times 3} : R^T R = I_3, \det(R) = 1\}$. The special Euclidean group is denoted by $SE(3)$, which can be represented by a matrix as

$$T = \begin{bmatrix} R & p \\ 0 & 1 \end{bmatrix} \in \mathbb{R}^{4\times 4}. \tag{2.1}$$

Here, $R \in SO(3)$, and $p \in \mathbb{R}^3$. The Lie algebra of $SE(3)$ is denoted by $se(3)$, which is defined by

$$se(3)x = \left\{ X \in \mathbb{R}^{4\times 4} | \ \exists\ \omega, v \in \mathbb{R}^3 :\ X = \begin{bmatrix} \omega_\times & v \\ 0 & 0 \end{bmatrix} \right\}. \tag{2.2}$$

Here $\omega_\times$ represents a mapping from $\mathbb{R}^3$ to $\mathbb{R}^{3\times 3}$ associated with ω. Let $\omega = [\omega_x\ \omega_y\ \omega_z]^T$, then $\omega_\times$ is defined by

$$\Omega = \omega_\times = \begin{bmatrix} 0 & -\omega_z & \omega_y \\ \omega_z & 0 & -\omega_x \\ -\omega_y & \omega_x & 0 \end{bmatrix}. \tag{2.3}$$

Furthermore, since the mapping $(\cdot)_\times$ is bijective, denote the inverse mapping by $(\cdot)^\vee$. Then we have $\Omega^\vee = \omega$. The adjoint operator is a mapping $Ad : SE(3) \times se(3) \to se(3)$ defined as $Ad_T X : \ TXT^{-1}$, where $X \in se(3)$, and $T \in SE(3)$, and can be given by

$$Ad_T X = \begin{bmatrix} (R\omega)_\times & -(R\Omega)_\times p + Rv \\ 0 & 0 \end{bmatrix}. \tag{2.4}$$

It acts to change the frame of reference T associated with an element in Lie algebra X.

Let $\mathcal{G} = (\mathcal{V}, \mathcal{E})$ represent the interaction graph of MASs, where $\mathcal{V} = \{1, ..., n\}$ is the node set and $\mathcal{E} \subseteq \mathcal{V} \times \mathcal{V}$ is the edge set. $(j, i) \in \mathcal{E}$ if and only if i can detect the relative information from j. $\mathcal{N}_i = \{j \in \mathcal{V} : (j, i) \in \mathcal{E}\}$ represents the neighbor set of i, and its cardinality is denoted as $|\mathcal{N}_i|$. A configuration in $\mathbb{R}^d$ of the nodes in $\mathcal{V}$ is denoted as $p = [p_1^T, \cdots, p_n^T]^T$, where $p \in \mathbb{R}^{nd}$, $p_i \in \mathbb{R}^d$, $i = 1, \cdots, n$. Based on above, a formation in $\mathbb{R}^d$ is given by a graph $\mathcal{G}$ and the corresponding configuration p, and is denoted as $(\mathcal{G}, p)$. Given a nominal configuration, denoted as $r \in \mathbb{R}^{nd}$, $r = [r_1^T, ..., r_n^T]^T$, with $r_i \in \mathbb{R}^d$, the nominal formation is denoted as $(\mathcal{G}, r)$.

Notations: The Euclidean norm of a vector $x \in \mathbb{R}^n$ is denoted as $\|x\|$. $x \times y$ denotes the cross product of vectors $x \in \mathbb{R}^n$ and $y \in \mathbb{R}^n$. The Euclidean induced matrix norm of $A \in \mathbb{R}^{n \times m}$ is denoted by $\|A\|$. $A \otimes B$ denotes the Kronecker product of matrix A and B. $\mathbb{R}$ denotes the reals and $\mathbb{N}$ denotes the natural numbers. $|\Omega|$ denotes the cardinality of the set Ω. For two sets $\Omega_1, \Omega_2 \subset \mathbb{R}^n$, define $\Omega_1 \backslash \Omega_2 := \{x \in \mathbb{R}^n | x \in \Omega_1, x \notin \Omega_2\}$. $\text{diag}(\cdots)$ denotes a diagonal matrix. For a real number s, $\lceil s \rceil$ denotes the smallest integer larger than or equal to s. Let $\{\mathcal{I}\}$ represent the inertial frame attached to the earth, and $\{\mathcal{B}_i\}$ represent the body-fixed frame attached to agent i. The state expressed in $\{\mathcal{I}\}$ is denoted as p_i; then its expression in $\{\mathcal{B}_i\}$ is denoted as $\bar{p}_i$. The relative state of agent j with respect to agent i is defined as $p_{ij} = p_i - p_j$, if $p_i, \ p_j \in \mathbb{R}^3$; and $\bar{p}_{ij}$ represents the corresponding state given in $\{\mathcal{B}_i\}$. $I_n \in \mathbb{R}^{n \times n}$ is the identity matrix and $\mathbf{1}_n \in \mathbb{R}^n$ is the vector with all entries equal to 1. For a function $f : \mathbb{R}_{\geq 0} \to \mathbb{R}^n$, $f(r^-)$ and $f(r^+)$

denote, respectively, the limit from below and above at the point $r \in \mathbb{R}_{\geq 0}$, i.e., $f(r^-) = \lim_{t \nearrow r} f(t)$ and $f(r^+) = \lim_{t \searrow r} f(t)$. $tr(\cdot)$ represents the trace of a square matrix.

Definition 1 (Affine Image)**.** ([13]) The affine image of the nominal configuration $r \in \mathbb{R}^{nd}$ in $\mathbb{R}^d$ of n nodes is defined by

$$\mathcal{A}(r) = \{p \in \mathbb{R}^{nd} : p = (I_n \otimes A)r + \mathbf{1}_n \otimes b,\ A \in \mathbb{R}^{d \times d}, b \in \mathbb{R}^d\}.$$

Definition 2 (Target Formation)**.** ([12]) The time-varying target formation of the nominal configuration $r \in \mathbb{R}^{nd}$ in $\mathbb{R}^d$ of n nodes is defined by

$$p^*(t) = [I_n \otimes A^*(t)]r + \mathbf{1}_n \otimes b^*(t). \tag{2.5}$$

Here $A^*(t) \in \mathbb{R}^{d \times d}$ and $b^*(t) \in \mathbb{R}^d$ are continuous w.r.t. t.

For a directed graph $\mathcal{G}$, a node i is said to be k-reachable from a non-singleton set $\mathcal{U}$ if there exists a path from a node in $\mathcal{U}$ to i after removing any $k-1$ nodes except for i. In addition, $\mathcal{G}$ is k-rooted if there exists a subset of k nodes called roots, from which every other node is k-reachable.

Definition 3 (Graph Laplacian)**.** For a nominal formation $(\mathcal{G}, r)$ in $\mathbb{R}^d$ containing n nodes, L is its associated graph Laplacian if it satisfies $(L \otimes I_d)r = 0$, and

$$[L]_{ij} = \begin{cases} 0, & i \neq j,\ (j,i) \notin \mathcal{E} \\ -a_{ij}, & i \neq j,\ (j,i) \in \mathcal{E} \\ \sum_{k \in \mathcal{N}_i} a_{ik}, & i = j. \end{cases} \tag{2.6}$$

Here, $[L]_{ij}$ represents the (i,j)-th entry in matrix L and a_{ij} is the edge weight of (i,j). Furthermore, if $\mathcal{G}$ is undirected, the symmetric matrix L is called a stress matrix.

Assumption 1. The undirected graph $\mathcal{G}$ is globally rigid.†

Assumption 2. The directed graph $\mathcal{G}$ is $(d+1)$-rooted.

† The definition of global rigidity follows the one used in [73].

Lemma 1. ([73]) Consider an undirected graph $\mathcal{G}$ containing n nodes with a generic configuration p in $\mathbb{R}^d$, $n \geq d+2$. Under Assumption 1, there always exists a stress matrix L of $(\mathcal{G}, p)$ with its kernel of dimension $d+1$.

Lemma 2. ([13]) Consider a directed graph $\mathcal{G}$ containing n nodes with a generic configuration p in $\mathbb{R}^d$, $n \geq d+2$. Under Assumption 2, there always exists an associated Laplacian matrix L of $(\mathcal{G}, p)$ with its kernel of dimension $d+1$.

Lemma 3. ([74]) Every singular value λ of a matrix $A \in \mathbb{R}^{n\times m}$ satisfies

$$(1 + \|A\|_p)^{-1} \leq |\lambda| \leq \|A\|_p. \tag{2.7}$$

Here $\|A\|_p$ stands for the p norm of A.

Consider an MAS containing n mobile agents maneuvering on $SE(3)$. Each agent is modeled as an underactuated dynamic rigid body as follows

$$\begin{aligned} \dot{p}_i &= u_i, \\ \dot{R}_i &= R_i \bar{\Omega}_i, \ i = 1, \cdots, n. \end{aligned} \tag{2.8}$$

Here, $p_i \in \mathbb{R}^3$ represents the position of the i-th agent, $R_i \in SO(3)$ represents the attitude, $u_i \in \mathbb{R}^3$ represents the linear velocity, and $\bar{\Omega}_i \in \mathbb{R}^{3\times 3}$ satisfies $\bar{\Omega}_i = (\bar{\omega}_i)_\times$, with $\bar{\omega}_i \in \mathbb{R}^3$ representing the angular velocity given in body-fixed frame $\{\mathcal{B}_i\}$ to be designed. In addition, each agent obeys the nonholonomic constraint

$$u_i = R_i E_i v_i. \tag{2.9}$$

Here $E_i \in \mathbb{R}^{3\times q}$ is determined by the mechanical structure of the system. More specifically, if the rigid body can provide one independent direction in translation along the first axis of R_i, then $q = 1$, and $E_i = e_1$; and if it can provide two independent directions in translation along the second and third axes of R_i, then $q = 2$, and $E_i = [e_2\ e_3]$. Here $e_j \in \mathbb{R}^3$ is an unit vector with the j-th element being 1. $v_i \in \mathbb{R}^q$ is the magnitude of the linear velocity along each independent axis to be designed.

Assume that the MAS is connected by a graph $\mathcal{G} = (\mathcal{V}, \mathcal{E})$. Choose n_l agents as leaders and the rest $n_f = n - n_l$ agents are considered as followers. Denote $\mathcal{V}_l = \{1, ..., n_l\}$ as the leader set and $\mathcal{V}_f = \{n_l + 1, ..., n\}$ as the follower set, satisfying $\mathcal{V} = \mathcal{V}_l \cup \mathcal{V}_f$. $p_l = [p_1^T, ..., p_{n_l}^T]^T$ represents the states of the leaders and $p_f = [p_{n_l+1}^T, ..., p_n^T]^T$ represents the states of the followers. Correspondingly, $p_l^* = [p_1^{*T}, ..., p_{n_l}^{*T}]^T$ represents the leaders' target configuration and $p_f^* = [p_{n_l+1}^{*T}, ..., p_n^{*T}]^T$ represents the followers' target configuration. Then, we have $p = [p_l^T, p_f^T]^T$ and $p^* = [p_l^{*T}, p_f^{*T}]^T$. The affine formation tracking problem considered in this work is defined as follows.

Problem 1 (Affine formation tracking)**.** Given a nominal formation $(\mathcal{G}, r)$ in $\mathbb{R}^3$, choose n_l agents as leaders moving along specific trajectories $p_l^*(t)$ determined by the target formation $p^*(t)$. Design the associated Laplacian matrix L and design the control protocols for the rest agents (followers), under which, the trajectories of the followers $p_f(t)$ converge to the target configuration $p_f^*(t)$.

Definition 4 (Affine localizability)**.** ([12]) The nominal formation $(\mathcal{G}, r)$ is affinely localizable by the leaders if for any $p = [p_l^T, p_f^T]^T \in \mathcal{A}(r)$, p_f can be uniquely determined by p_l.

Given a set of points $\{p_i\}_{i=1}^n$ in $\mathbb{R}^d$, the affine span of these points, denoted by $\mathcal{S}$, is

$$\mathcal{S} = \left\{ \sum_{i=1}^{n} a_i p_i : a_i \in \mathbb{R} \ , \ \sum_{i=1}^{n} a_i = 1 \right\}.$$

The affine span $\mathcal{S}$ can always be translated to contain the origin, which forms a linear space. The dimension of the linear space is defined as the dimension of the affine span, and we say points $\{p_i\}_{i=1}^n$ affinely span $\mathbb{R}^d$ if the dimension of its affine span is d.

Assumption 3. For nominal configuration $r = [r_1^T, \cdots, r_n^T]^T$ with $r_i \in \mathbb{R}^d$, $\{r_i\}_{i=1}^n$ affinely span $\mathbb{R}^d$.

Lemma 4. ([12]) Under Assumptions 1 and 3, the nominal formation $(\mathcal{G}, r)$ is affinely localizable by the leaders if and only if (iff) $\{r_i\}_{i \in \mathcal{V}_l}$ affinely span $\mathbb{R}^d$.

Lemma 5. ([75]) Under Assumptions 2 and 3, the nominal formation $(\mathcal{G}, r)$ is affinely localizable by the leaders iff all the roots are chosen from the leaders set $\mathcal{V}_l$.

Referring to Definition 4, **affine localizability** indicates that given a nominal formation $(\mathcal{G}, r)$, the configuration of the MAS can be manipulated by only a part of the agents' (leaders') states p_l. Referring to Definition 2, the target formation $p^*(t)$ is determined by the nominal configuration r as well as the transformation matrix $A^*(t)$ and the translation vector $b^*(t)$. Since r is given, in order to specify $p^*(t)$ by $p_l^*(t)$, the mapping from p_l^* to (A^*, b^*) must be bijective, which can be guaranteed by Assumption 1 and Assumption 3, or Assumption 2 and Assumption 3. More details can be found in [75] and [12].

2.2.2 Affine Formation under Fixed Topologies

In this section, we consider the affine formation tracking problem under fixed topologies. Since the controllers are designed directly on $se(3)$, we introduce auxiliary variables $T_{ij} \in SE(3)$ and $X_{ij} \in se(3)$ as follows

$$T_{ij} = \begin{bmatrix} I_3 & \bar{p}_{ij} \\ 0 & 1 \end{bmatrix}, \; X_{ij} = \begin{bmatrix} \bar{\Omega}_i^T & \dot{\bar{p}}_{ij} - \bar{u}_i \\ 0 & 0 \end{bmatrix}, \tag{2.10}$$

where $\bar{p}_{ij}$ and $\dot{\bar{p}}_{ij}$ represent the relative position and velocity measured in body-fixed frame $\{\mathcal{B}_i\}$, respectively; and $\bar{u}_i = R_i^T u_i$ represents the linear velocity of agent i measured in $\{\mathcal{B}_i\}$. Let $R_i = [a_{xi} \; a_{yi} \; a_{zi}]$, with $a_{xi}, \; a_{yi}, \; a_{zi} \in \mathbb{R}^3$, be the attitude of agent i expressed in inertial frame $\{\mathcal{I}\}$, $R_{di} \in SO(3)$ represent the desirable attitude of agent i expressed in $\{\mathcal{I}\}$, and $R_{di}^i = R_i^T R_{di}$ represent the desirable attitude of agent i expressed in $\{\mathcal{B}_i\}$, where $R_{di}^i = [\bar{b}_{xi} \; \bar{b}_{yi} \; \bar{b}_{zi}]$ with $\bar{b}_{xi}, \; \bar{b}_{yi}, \; \bar{b}_{zi} \in \mathbb{R}^3$ the corresponding vectors to be designed. Considering the underauctuated property, we assume the rigid body can provide one independent direction in translation alone a_{zi}. Then, R_{di}^i is given as follows:

$$\bar{b}_{zi} = \frac{\bar{B}_{zi}}{\|\bar{B}_{zi}\|}, \; \bar{b}_{xi} = \frac{\bar{b}_{zi} \times \bar{B}_{xi}}{\|\bar{b}_{zi} \times \bar{B}_{xi}\|}, \; \bar{b}_{yi} = \bar{b}_{xi} \times \bar{b}_{zi}. \tag{2.11}$$

Here $\bar{B}_{zi}, \bar{B}_{xi} \in \mathbb{R}^3$; $\bar{B}_{zi} = \bar{V}_i$ with

$$\bar{V}_i = \sum_{i \in \mathcal{N}_i} l_{ij}(k_c \bar{p}_{ij} + U_1^T (Ad_{T_{ij}} X_{ij}) U_2) \tag{2.12}$$

aiming to regulate axis a_{zi} to direct at the target configuration; $U_1 = [I_3, \mathbf{0}_3]^T$, $U_2 = [0, 0, 0, 1]^T$, and l_{ij} is (i, j)-th element in the associated Laplacian matrix L; and $\bar{B}_{xi}$ can be designed based on the objective of the operation. Based on above, the control protocol in frame $\{\mathcal{B}_i\}$ is given as

$$\bar{\omega}_i = -k_R e_{R_i} - (\Omega_{di}^i)^\vee, \; v_i = -\frac{1}{\gamma_i} E_i^T \bar{V}_i, \tag{2.13}$$

where $\Omega_{di}^i = R_{di}^i \frac{dR_{di}^i}{dt} - \bar{\Omega}_i$, and $e_{Ri} = (R_{di}^{iT} - R_{di}^i)^\vee$ is defined as the attitude error of agent i. Since all information required in controller (2.13) is included in matrices T_{ij} and X_{ij}, which can be obtained by the detections of agent i via its onboard sensor, no global reference nor communication device is needed. In addition, the relative velocity information required in controller (2.13) is also expressed in local coordinate frames.

Remark 1. It should be noted that the desirable attitude (2.11) is given for the situation when the underactuated rigid body has one independent direction in translation. It is easy to generalize (2.11) to the case when the number of independent directions is two. For example, suppose system (2.8) can move independently along a_{xi} and a_{yi}. Then, R_{di}^i can be given as

$$\bar{b}_{xi} = \frac{\bar{B}_{xi}}{\|\bar{B}_{xi}\|}, \quad \bar{b}_{zi} = \frac{\bar{B}_{zi} \times \bar{b}_{xi}}{\|\bar{B}_{zi} \times \bar{b}_{xi}\|}, \quad \bar{b}_{yi} = \bar{b}_{xi} \times \bar{b}_{z_i}. \tag{2.14}$$

Here, $\bar{B}_{zi} = \bar{V}_i$, and $\bar{B}_{xi} \in \mathbb{R}^3$ can be any vector which is not perpendicular to $\bar{B}_{zi}$.

In the following, we will show that the affine formation tracking problem is solved by controller (2.13), with R_i converging to the desirable attitude R_{di} given in (2.11) and position $p_f(t)$ converging to the target configuration $p_f^*(t)$ for all the followers.

Attitude Convergence:

First, we discuss the attitude convergence of each agent in its body-fixed frame $\{\mathcal{B}_i\}$. Consider Lyapunov function $V_{Ri} = tr[I - R_{di}^{iT}]$. Using Rodrigues' formula, it can be shown that $V_{Ri} = 1 - \cos\|x_i\|$, and

$$\|e_{Ri}\|^2 = \sin^2\|x_i\| = (2 - V_{Ri})V_{Ri}. \tag{2.15}$$

Here, $R_{di}^{iT} = e^{(x_i)\times}$, with $x_i \in \mathbb{R}^3$. Let $\|x_i\| \in (-\pi, \pi]$. Then, $V_{Ri} \geq 0$, $V_{Ri} = 0$ iff $\|x_i\| = 0$, which implies $R_{di}^i = I$, or equivalently, $R_{di} = R_i$. Furthermore, assume $\|x_i\| \neq \pi$. Then, there exists a $\Phi_i < 2$ satisfying $0 < V_{Ri} \leq \Phi_i$ and

$$\frac{1}{2}\|e_{R_i}\|^2 \leq V_{Ri} \leq \frac{1}{2 - \Phi_i}\|e_{Ri}\|^2. \tag{2.16}$$

Refer to [69] for more details.

Taking the derivatives on both sides, and combining with (2.8), one has

$$\begin{aligned} \dot{V}_{R_i} &= tr[-(\dot{R}_{di})^T R_i - R_{di}^T \dot{R}_i] = tr[-(R_{di}\Omega_{di}^d)^T R_i - R_{di}^T R_i \bar{\Omega}_i] \\ &= tr[-R_{di}^i \Omega_{di}^d - R_{di}^{iT}\bar{\Omega}_i]. \end{aligned} \tag{2.17}$$

Here $\Omega_{di}^d = (\omega_{di}^d)_\times$, with $\omega_{di}^d \in \mathbb{R}^3$ representing the angular velocity of R_{di} expressed in R_{di}. Under controller (2.13), we have

$$\begin{aligned} \dot{V}_{R_i} &= tr[-R_{di}^{iT}(-k_R(e_{R_i}) - (\Omega_{di}^i)^\vee)_\times - R_{di}^i \Omega_{di}^d] \\ &= tr[R_{di}^{iT} k_R(e_{Ri})_\times + R_{di}^{iT}(R_{di}^i R_{di}^i \Omega_{di}^d) - R_{di}^i \Omega_{di}^d] \\ &= tr[R_{di}^{iT} k_R(e_{Ri})_\times] = -k_R e_{Ri}^T e_{Ri} = -k_R\|e_{Ri}\|^2. \end{aligned} \tag{2.18}$$

By (2.16) we have

$$\dot{V}_{R_i} \leq -k_\Phi V_{R_i}. \tag{2.19}$$

Here, $k_\Phi = \min_i(2 - \Phi_i)k_R$. Since $\Phi_i < 2$, we have $k_\Phi > 0$. The attitude error of agent i almost globally exponentially converges to zero except for $x_i(0) = \pi$.

Position convergence:

In order to evaluate the convergence of p_f to the target configuration p_f^*, the dynamics of all the agents needs to be evaluated in a common frame, which is chosen as inertial frame $\{\mathcal{I}\}$ in this case. Referring to (2.8) and (2.9), under local controller (2.13), the dynamics in $\{\mathcal{I}\}$ is in the form of

$$\dot{p}_i = R_i E_i v_i = -\frac{1}{\gamma_i} R_i E_i E_i^T \bar{V}_i, \quad i \in \mathcal{V}_f. \tag{2.20}$$

Since

$$\begin{aligned}\dot{\bar{p}}_{ij} &= \frac{d(R_i^T p_{ij})}{dt} = R_i^T \dot{p}_{ij} + \dot{R}_i^T p_{ij} = R_i^T(u_i - u_j) + \bar{\Omega}_i^T R_i^T p_{ij} \\ &= \bar{u}_i - R_i^T u_j + \bar{\Omega}_i^T \bar{p}_{ij},\end{aligned} \tag{2.21}$$

combining with (2.12) leads to

$$\bar{V}_i = \sum_{i\in\mathcal{N}_i} l_{ij}(k_c \bar{p}_{ij} - R_i^T u_j). \tag{2.22}$$

Substituting (2.22) into (2.20), we have

$$\begin{aligned}\dot{p}_i =& -\frac{1}{\gamma_i} R_i E_i E_i^T R_i^T \sum_{j\in\mathcal{N}_i} l_{ij}(k_c p_{ij} - u_j) = -\frac{1}{\gamma_i} R_i E_i E_i^T R_i^T \sum_{j\in\mathcal{N}_i} l_{ij}(k_c p_{ij} - \dot{p}_j) \\ =& -\frac{1}{\gamma_i}\sum_{j\in\mathcal{N}_i} l_{ij}(k_c p_{ij} - \dot{p}_j) + \frac{1}{\gamma_i}\sum_{j\in\mathcal{N}_i} l_{ij}(k_c p_{ij} - \dot{p}_j) - \frac{1}{\gamma_i} R_i E_i E_i^T R_i^T \sum_{j\in\mathcal{N}_i} l_{ij}(k_c p_{ij} - \dot{p}_j).\end{aligned} \tag{2.23}$$

Referring to (2.11), we have

$$\dot{p}_i = -\frac{1}{\gamma_i}\sum_{j\in\mathcal{N}_i} l_{ij}(k_c p_{ij} - \dot{p}_j) + \frac{1}{\gamma_i}(R_{di}E_i - R_i E_i E_i^T R_i^T R_{di} E_i)\|\delta_i\|, \tag{2.24}$$

where $\delta_i = \sum\limits_{j\in\mathcal{N}_i} l_{ij}(k_c p_{ij} - \dot{p}_j)$. Let $\epsilon_i = \sum_{j\in\mathcal{N}_i} l_{ij} p_{ij}$, $i \in \mathcal{V}_f$, represent the formation error of agent i, and multiply γ_i on both sides of (2.24). We have

$$\begin{aligned}\dot{\epsilon}_i &= -k_c\epsilon_i + [R_{di}E_i - R_i E_i E_i^T R_i^T R_{di} E_i]\|\delta_i\| \\ &= -k_c\epsilon_i + R_i[R_i^T R_{di} - R_{di}^T R_i]E_i\|\delta_i\| \\ &= -k_c\epsilon_i + R_i(-e_{Ri})_\times E_i\|\delta_i\|.\end{aligned} \tag{2.25}$$

Consider Lyapunov function $V_p = \frac{1}{2}\epsilon_i^T\epsilon_i$. Taking the derivatives on both sides gives

$$\begin{aligned}\dot{V}_p &= -k_c\epsilon_i^T\epsilon_i + \epsilon_i^T R_i(-e_{Ri})_\times E_i\|\delta_i\| \\ &\le -k_c\|\epsilon_i\|^2 + \|\epsilon_i\|\|e'_{Ri}\|(k_c\|\epsilon_i\| + |\mathcal{N}_i| l_{im} v_{im}) \\ &\le -(1 - \|e'_{Ri}\|)k_c\|\epsilon_i\|^2 + |\mathcal{N}_i| l_{im} v_{im}\|e_{Ri}\|\|\epsilon_i\|.\end{aligned} \tag{2.26}$$

Here $v_{im} = \max(\|v_j\|)$, and $e'_{Ri} = e_{Ri}E_i$. Since $x_i \in (-\pi, \pi)$, $\|e'_{Ri}\| = \|e_{Ri}E_i\| < 1$, there always exist positive constants k_ϵ and k_r satisfying $(1 - \|e'_{Ri}\|)k_c - k_\epsilon > 0$ and

$$\dot{V}_p \le -((1 - \|e'_{Ri}\|)k_c - k_\epsilon)\|\epsilon_i\|^2 + k_r\|e_{Ri}\|^2. \tag{2.27}$$

As a result, ϵ_i is ISS w.r.t. the attitude error. Since e_{Ri} is almost globally exponentially stable, ϵ_i globally converges to zero as $t \to \infty$ except for $x_i(0) = \pi$.

Based on the above discussion, the first main result of this work is summarized as follows.

Theorem 1. Consider the MAS in (2.8), with four agents chosen as leaders moving along the target configuration $p_l^*(t)$ and the rest of agents considered as followers driven by controller (2.13). If (i) the nominal configuration $(\mathcal{G}, r)$ satisfies Assumptions 1 and 3 and (ii) leaders' nominal configuration $\{r_i\}_{i\in\mathcal{V}_l}$ affinely spans $\mathbb{R}^3$, then the followers' state $p_f(t)$ converges to the target configuration $p_f^*(t) = -(L_{ff} \otimes I_3)^{-1}(L_{fl} \otimes I_3)p_l^*(t)$ almost globally. Here, L_{ff} and L_{fl} are obtained by the decomposition of the Laplacian matrix

$$L = \begin{bmatrix} L_{ll} & L_{lf} \\ L_{fl} & L_{ff} \end{bmatrix}, \tag{2.28}$$

where $L_{ll} \in \mathbb{R}^{n_l \times n_l}$ represents the submatrix corresponding to the leaders, and L_{ff}, L_{fl}, and L_{lf} have compatible dimensions.

Proof. Referring to Definition 1, $\mathcal{A}(r) \in \ker(L \otimes I_d)$, and $\dim(\mathcal{A}(r)) = d^2 + d$. By Lemma 1, $\dim(\ker(L \otimes I_d)) = d^2 + d$. Thus, $\mathcal{A}(r) = \ker(L \otimes I_d)$. Since $\{r_i\}_{i\in\mathcal{V}_l}$ affinely span $\mathbb{R}^3$, by Lemma 4, for $p(t) \in \mathcal{A}(r)$, $p_f(t)$ is uniquely determined by $p_l(t)$. In addition, $p(t) \in \mathcal{A}(r)$ implies $p(t) \in \ker(L \otimes I_d)$. Then we have

$$(L_{ff} \otimes I_3)p_f^*(t) + (L_{fl} \otimes I_3)p_l^*(t) = 0. \tag{2.29}$$

Since $p_f^*(t)$ is unique, L_{ff} must be nonsingular, and the follower's target configuration $p_f^*(t)$ can be written as

$$p_f^*(t) = -(L_{ff} \otimes I_3)^{-1}(L_{fl} \otimes I_3)p_l^*(t). \tag{2.30}$$

By (2.27), ϵ_i, $i \in \mathcal{V}_f$, globally converges to zero as $t \to \infty$, except for $x_i(0) = \pi$. Then,

$$\lim_{t\to\infty} \sum_{j\in\mathcal{N}_i} l_{ij}(p_i(t) - p_j(t)) = 0. \tag{2.31}$$

Since L_{ff} is nonsingular, and leaders move along the target configuration $p_l^*(t)$, (2.31) can be written as

$$\lim_{t\to\infty} p_f(t) = -(L_{ff}\otimes I_3)^{-1}(L_{fl}\otimes I_3)p_l^*(t). \tag{2.32}$$

Compared (2.32) with (2.30), the proof is completed. □

Remark 2. Theorem 1 can be established under Assumption 2 and Assumption 3 with all the roots of $\mathcal{G}$ chosen from the leader set $\mathcal{V}_l$ when the underlying graph $\mathcal{G}$ is directed.

Remark 3. Compared with the existing results in [75] and [12], controller (2.13) does not include global information even when leaders' velocities are time-varying; and compared with [76] and [77], which required leaders to move along some prescribed polynomial trajectories, there is no restriction on leaders' trajectories. In addition, taking advantage of the geometric controller design, the singularity problem in [12] is avoided in this thesis.

Remark 4. Assumptions 1 and 2 are milder than the ones in [13], [12] and [75], respectively. Specifically, for an undirected graph, the globally rigid condition in Assumption 1 is milder than the universally rigid condition in [13], [12]. For a k-rooted graph, no centralized computation is needed to guarantee the semi-positive definiteness of the Laplacian matrices. Since the nominal configuration r is predetermined and the graph is directed, the associated Laplacian matrices can be calculated locally by

$$\sum_{j\in\mathcal{N}_i} l_{ij}r_{ij} = 0.$$

2.2.3 Affine Formation under Switching Topologies

One advantage of the proposed method is the exclusion of centralized computation when the edge weights are selected for the associated Laplacian matrix of a rooted graph (Remark 4). Inspired by this property, we study the affine formation under switching topologies in this section.

Consider an MAS containing n agents in $\mathbb{R}^d$. Suppose that there exist an infinite sequence of non-overlapped time intervals $[t_q, t_{q+1})$, $q \in \mathbb{N}$, satisfying $t_0 = 0$, $0 < \tau_0 < t_{q+1} - t_q < \tau_1$. During each time interval, the topology is fixed; and at each time instant t_q the topology switches. τ_0 is called the minimum dwell time. Let $s(t) : [0, \infty) \to \{1, ..., m\}$ denote the switching signal, and let $\hat{\mathcal{G}} := \{\mathcal{G}^1, ..., \mathcal{G}^m\}$ represent the set of all possible topologies of the MAS, where $\mathcal{G}^{s(t)} \in \hat{\mathcal{G}}$ represents the graph at time t.

Assumption 4. Each graph $\mathcal{G}^i \in \hat{\mathcal{G}}$ satisfies Assumption 2.

Since the number of agents is finite, under Assumption 4, the number of possible graphs in $\hat{\mathcal{G}}$ is finite. In practice, it is hard to predetermine the underlying graph for each time interval, especially when the MAS manuevers in an unknown environment. The d-rooted graph constructed at initial time might face edge loss caused by blocking or range limitation. Therefore, before giving the main result, a reconstruction method which can preserve the d-rooted property against unexpected edge loss is proposed in Algorithm 1.

Algorithm 1 Reconstruction of a d-rooted graph

Initial: Construct a d-rooted graph $\mathcal{G} = (\mathcal{V}, \mathcal{E})$. Denote the root set $\mathcal{R} = \{r_1, r_2, ..., r_d\}$. Assume $i \in \mathcal{V} \backslash \mathcal{R}$, $j \in \mathcal{V}$, $(j, i) \in \mathcal{E}$.
while Edge lost: (j, i) is removed from $\mathcal{E}$. **do**
    $\forall q \in \mathcal{V} \backslash R$, $q \neq i$
    if $(i, q) \in \mathcal{E}$ **and** $(j, q) \notin \mathcal{E}$ **then**
        add (j, q) to $\mathcal{E}$.
    end if
    pick one node $p \in \mathcal{V}$ and $(p, i) \notin \mathcal{E}$, add edge (p, i) to $\mathcal{E}$.
end while

An example of reconstructing a 4-rooted graph by Algorithm 1 is shown in Figure 2.1. It can be seen that the 4-rooted property is maintained. Referring to Algorithm 1, when an edge (e.g., (j, i)) is lost, for any node which does not belong to the root set, it needs to know only whether i or j belongs to its neighbor set. Therefore, the d-rooted graph is reconstructed locally.

Proposition 1. Following Algorithm 1, graph $\mathcal{G}$ preserves the d-rooted property.

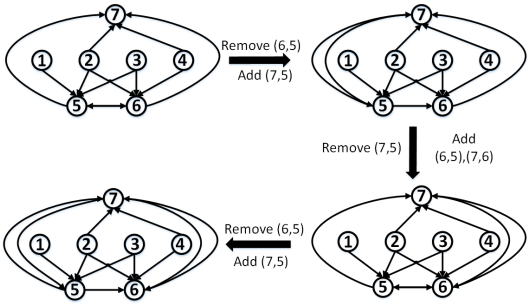

Figure 2.1: Reconstruction of a 4-rooted graph, with $\mathcal{R} = \{1, 2, 3, 4\}$. The graphs are labeled as $\mathcal{G}^i$, $i = 1, 2, 3, 4$, clockwise.

Proof. The essential to prove the d-rooted property remains for graph $\mathcal{G}$ after reconstruction is to provide that there still exist d disjoint paths from the node set $\mathcal{R}$ to every other node belonging to $\mathcal{V}\backslash\mathcal{R}$.

After removing edge (j, i) from $\mathcal{E}$, for a node that does not need (j, i) to complete a path from $\mathcal{R}$, it is still d-reachable from $\mathcal{R}$.

For node q that needs (j, i) to complete a path l_q from $\mathcal{R}$, denote $\mathcal{V}_q$ as the set which includes all the nodes in this path and $l_q^{q'}$ as the segment of l_q which starts from q' and ends at q. Consider the following cases:

1. Remove $d - 1$ nodes from $\mathcal{V}\backslash\mathcal{V}_q$

   When (j, i) is removed, j is still d-reachable from $\mathcal{R}$. Thus, in this case, j is still reachable from $\mathcal{R}$. If node q is directly connected to i, by line 5, an edge (j, q) has been added ($(j, q) \notin \mathcal{E}$ in the original graph) and node q is reachable from $\mathcal{R}$ through j. If node q is not directly connected to i, path l_q leads it to a node q' which is directly connected to i; then, node q is reachable from $\mathcal{R}$ through $(j, q') \rightarrow l_q^{q'}$.

2. Remove $d - 1$ nodes from $\mathcal{V}$, at least one of which belongs to $\mathcal{V}_q$

   At least one node is removed from $\mathcal{V}_q$, and thus at most $d - 2$ nodes are removed from the rest of the graph. For the rest of the graph, there exist $d - 1$ disjoint paths through which node q is reachable from $\mathcal{R}$. Thus, in this case, q is still reachable from $\mathcal{R}$.

For node i, if (j,i) is needed to complete a path from $\mathcal{R}$, we consider the same two cases as follows:

1. Remove $d-1$ nodes from $\mathcal{V}\backslash\mathcal{V}_i$

   Since every node other than i is d-reachable after line 5 in Algorithm 1, line 6 makes node i reachable through p.

2. Remove $d-1$ nodes from $\mathcal{V}$, at least one of which belongs to $\mathcal{V}_i$

   The proof is similar to case 2 for node q above.

The above analysis covers all kinds of nodes in $\mathcal{V}\backslash\mathcal{R}$, and thus, the reconstructed graph is d-reachable. □

After the d-rooted graph is reconstructed, the edge weights of the associated Laplacian matrix need to be recalculated locally by $\sum_{j\in\mathcal{N}_i} r_{ij} = 0$. For agent i, it only needs to know who belongs to its neighbor set $\mathcal{N}_i$ and the nominal configuration r. Since both the d-rooted graph and the associated Laplacian matrix can be reconstructed locally, the study of affine formation under switching topologies is of practical significance.

Denote the reconstructed graph at current time instant as $\tilde{\mathcal{G}}$. Then the value of switching signal $s(t)$ is determined by

$$i := \{j \in \{1,\cdots,m\} | \tilde{\mathcal{G}} = \mathcal{G}^j\}, \tag{2.33}$$

and the associated Lapacian matrix is denoted by $L^{(s(t),t)} \in \mathbb{R}$. L_0 represents the associated Laplacian matrices at t_0.

According to Theorem 1, during $t \in [t_q, t_{q+1})$, the formation error is ISS w.r.t. attitude error. Therefore, in order to guarantee the convergence to the target configuration, the magnitude of attitude error needs to be small, which is provided in the following Lemma.

Lemma 6. Consider the attitude dynamics described in (2.8), with the angular velocity given in (2.13). The length of time intervals, during which the

attitude error $\|e_{R_i}\|$ is larger than a, $0 < a < 1$, is uniformly upper bounded by a positive constant h_a given by

$$h_a = \frac{2\sqrt{1-a^2}}{k_R a^2}. \tag{2.34}$$

Proof. Referring to (2.15), we have

$$V_{R_i} = 1 - \sqrt{1 - \|e_{R_i}\|^2} \ , 0 \le V_{R_i} \le 1; \quad V_{R_i} = 1 + \sqrt{1 - \|e_{R_i}\|^2} \ , 1 < V_{R_i} < 2. \tag{2.35}$$

By (2.18) and (2.35), for $1 < V_{R_i} < 2$, we have

$$\frac{d\sqrt{1 - \|e_{R_i}\|^2}}{dt} \le -k_R \|e_{R_i}\|^2. \tag{2.36}$$

The time $h^1_{a_1}$ for V_{R_i} to travel from an initial $V_{R_i}(t_0) > 1$ to 1 is equal to the one for $\|e_{R_i}\|$ to increase from a constant $a_1 < 1$ to 1. Let $V_i = \sqrt{1 - \|e_{R_i}\|^2}$, $h^1_{a_1}$ is equal to the time for V_i to go from $\sqrt{1 - {a_1}^2}$ to zero. For $V_i \in (0, \sqrt{1 - {a_1}^2}]$, we have

$$\begin{aligned} \frac{dV_i}{dt} = -k_R(1 - V_i^2) &\le -k_R(1 - (1 - {a_1}^2)) \\ V_i(t) - V_i(t_0) &\le -k_R {a_1}^2 (t - t_0). \end{aligned} \tag{2.37}$$

Then, $h^1_{a_1}$ can be estimated by

$$\begin{aligned} 0 - \sqrt{1 - {a_1}^2} &\le -k_R {a_1}^2 (h^1_{a_1} - 0) \\ h^1_{a_1} &\le \frac{\sqrt{1 - {a_1}^2}}{k_R {a_1}^2}. \end{aligned} \tag{2.38}$$

Similarly, for $0 \le V_{R_i} \le 1$, the time $h^2_{a_2}$ for V_{R_i} to go from 1 to $V_{R_i}(t') < 1$ is equal to the time for $\|e_{R_i}\|$ to drop from 1 to a constant a_2, and it is upper bounded by

$$h^2_{a_2} \le \frac{\sqrt{1 - {a_2}^2}}{k_R {a_2}^2}. \tag{2.39}$$

Thus, for $V_{R_i}(t_0) \in (1, 2)$, $\|e_{R_i}\|$ will first increase to 1, and then decrease, and the period of time during which $\|e_{R_i}\| > a$ is $h_a = h^1_a + h^2_a \le \frac{2\sqrt{1-a^2}}{k_R a^2}$. For $V_{R_i}(t_0) \in [0, 1]$, $\|e_{R_i}\|$ will decrease directly, and the time during which $\|e_{R_i}\| > a$ is upper bounded by $h_a = h^2_a \le \frac{\sqrt{1-a^2}}{k_R a^2}$.

To summarize, for any $V_{R_i} \in [0, 2)$, we have $h_a \le \frac{2\sqrt{1-a^2}}{k_R a^2}$. □

Consider piecewise Lyapunov function $V_\epsilon(t) = \frac{1}{2}\epsilon^{qT}\epsilon^q$, $t \in [t_q, t_{q+1})$, which is quadratic of the position error under current topology $\mathcal{G}^{s(t)}$ and the associated Laplacian L^q. Take the derivatives of both sides

$$\begin{aligned}\dot{V}_\epsilon &= -k_c\epsilon^{qT}\epsilon^q + \epsilon^{qT}e_\epsilon \\ &\leq -(1 - \|e'_{R_m}\|)k_c\|\epsilon^q\|^2 + n_f N_m\|e'_{R_m}\|\|\epsilon^q\| \\ &\leq -(1 - \|e'_{R_m}\|)k_c\|\epsilon^q\|^2 + k_r^q\|e'_{R_m}\|^2 + k_\epsilon^q\|\epsilon^q\|^2 \\ &= -((1 - \|e'_{R_m}\|)k_c + k_\epsilon^q)\|\epsilon^q\|^2 + k_r^q\|e'_{R_m}\|^2.\end{aligned} \tag{2.40}$$

Here, $\|e'_{R_m}(t)\| = \max_{i\in\mathcal{V}_f}\|e'_{R_i}(t)\|$, $N_m = \max_{i\in\mathcal{V}_f, t\in[t_q,t_{q+1})} N_i(t)$, $N_i(t) = |\mathcal{N}_i(t)|v_{im}(t)l_{im}(t)$, and $2\sqrt{k_r^q k_\epsilon^q} = n_f N_m$. The above equation implies the ISS property of the formation error ϵ^q w.r.t. the attitude error $\|e_{R_i}\|$ when there exist positive constants k_ϵ^q and k_r^q that guarantee $(1 - \|e'_{R_m}\|)k_c + k_\epsilon^q$ is positive. Such k_r^q and k_ϵ^q always exist since $\|e'_{R_m}\| < 1$. In addition, by (6), during each time interval, $\|e'_{R_m}\|$ is upper bounded by a constant a, $a < 1$ for at least $\tau_0 - h_a$ duration if $\tau_0 > h_a$. Let $k_p^q = (1-a)k_c + k_\epsilon^q$, for a large enough τ_0, then, the formation error ϵ is ensured to converge with a rate higher than k_p^q for a certain period.

In the above, the dynamics during each time interval is discussed. Now, we focus on the system behavior at each switching instant. Assume the leader set $\mathcal{V}_l$ is fixed; then, at each switching instant t_q,

$$V_\epsilon(t_q^+) = \frac{1}{2}\epsilon^{q^+T}\epsilon^{q^+} = \frac{1}{2}\left((L_{ff}^{q^+}\otimes I_3)e_f(t_q^+)\right)^T\left((L_{ff}^{q^+}\otimes I_3)e_f(t_q^+)\right), \tag{2.41}$$

and

$$V_\epsilon(t_q^-) = \frac{1}{2}\epsilon^{q^-T}\epsilon^{q^-} = \frac{1}{2}\left((L_{ff}^{q^-}\otimes I_3)e_f(t_q^-)\right)^T\left((L_{ff}^{q^-}\otimes I_3)e_f(t_q^-)\right), \tag{2.42}$$

where $e_f(t) = p_f(t) - p_f^*(t)$. Since the nominal formation is affinely localizable by leaders, $p_f^*(t_q^+) = p_f^*(t_q^-)$ and $e_f(t_q^+) = e_f(t_q^-) = e_f(t_q)$, which imply

$$\begin{aligned}V_\epsilon(t_q^+) &= \frac{1}{2}\left((L_{ff}^{q^+}\otimes I_3)(L_{ff}^{q^-}\otimes I_3)^{-1}\epsilon^{q^-}\right)^T\left((L_{ff}^{q^+}\otimes I_3)(L_{ff}^{q^-}\otimes I_3)^{-1}\epsilon^{q^-}\right) \\ &\leq f_L^q V_\epsilon(t_q^-).\end{aligned} \tag{2.43}$$

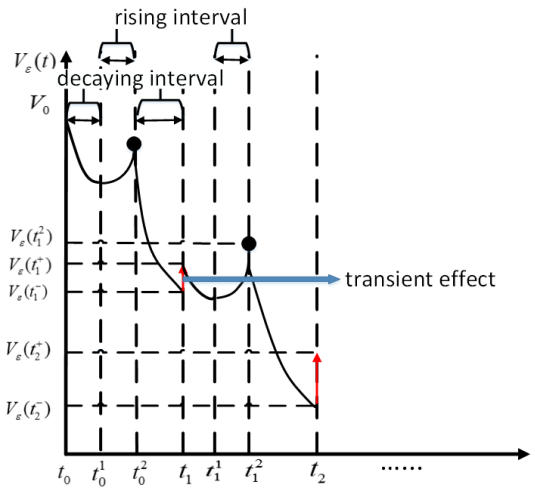

Figure 2.2: Trajectory of $V_\epsilon(t)$ under switching topologies

Here $f_L^q = (\lambda_f^{q-1,q})^2$, and $\lambda_f^{q-1,q}$ is the maximum eigenvalue of $L_{ff}^{q^+}(L_{ff}^{q^-})^{-1}$.

Combining the convergence property during each time interval and the transient effect at each switching instant, the essential to guarantee the convergence of the formation error is to make sure that the dwell time τ_0 is long enough, so that the decrease during each interval can dissipate the transient effect at the switching instant (see Figure 2.2).

Theorem 2. Consider the MAS in (2.8) with four agents chosen as leaders moving along the target configuration $p_l^*(t)$ and the rest of agents considered as followers and driven by controller (2.13). Assume (i) the nominal configuration r satisfies Assumption 3, (ii) the set $\hat{\mathcal{G}}$ satisfies Assumption 4 with the roots for each $\mathcal{G}^i \in \hat{\mathcal{G}}$ chosen from the leader set, and the switching signal $s(t)$ is generated by (2.33), (iii) the dwell time τ_0 satisfies

$$\tau_0 > (1 + \frac{2k_\epsilon}{k_p})h_a + \frac{\ln \lambda_f}{k_p} + \frac{\delta_0}{2k_p}, \tag{2.44}$$

where $\delta_0 > 0$ is a constant, $\lambda_f = \max_{q\geq 1} \lambda_f^{q-1,q}$, $k_p = \min_q k_p^q$, $k_p^q = (1-a)k_c^q + k_\epsilon^q$, $k_c^q - k_\epsilon^q > 0$, $k_\epsilon = \max_q k_\epsilon^q$,

$$h_a = \frac{2\sqrt{1-a^2}}{k_R a^2}, \tag{2.45}$$

$0 < a < 1$ is a constant, and $2\sqrt{k_r^q k_\epsilon^q} = n_f N_m$. Then the followers' state $p_f(t)$ converges into a small ball centered at the target configuration $p_f^*(t) =$

$-(L_{ff_0}\otimes I_3)^{-1}(L_{fl_0}\otimes I_3)p_l^*(t)$ almost globally. Here L_{ff_0} and L_{fl_0} are obtained by the decomposition of the Laplacian matrix at initial time t_0 as follows:

$$L_0 = \begin{bmatrix} L_{ll_0} & L_{lf_0} \\ L_{fl_0} & L_{ff_0} \end{bmatrix}, \tag{2.46}$$

where $L_{ll_0} \in \mathbb{R}^{n_l \times n_l}$ represents the submatrix corresponding to the leaders, and L_{ff_0}, L_{fl_0}, and L_{lf_0} have compatible dimensions.

Proof. Consider the following piecewise Lyapunov function candidate

$$V_\epsilon(t) = \frac{1}{2}\epsilon^{qT}\epsilon^q,\ t \in [t_q, t_{q+1}). \tag{2.47}$$

Separate the time interval $[t_q, t_{q+1})$ into two parts; namely $[t_q^1, t_q^2)$ during which the attitude error $\|e'_{R_m}\| \geq a$, and $[t_q, t_{q+1})\backslash[t_q^1, t_q^2)$ during which the ISS property of the formation error is guaranteed with a lower bounded convergence rate.

If $[t_q, t_q^1) \neq \emptyset$, for $t \in [t_q, t_q^1)$,

$$\begin{aligned} V_\epsilon(t) &\leq e^{-2k_p^q(t-t_q)}V_\epsilon(t_q^+) + k_r^q\int_{t_q}^{t} e^{-2k_p^q(t-\tau)}\|e'_{R_m}\|^2(\tau)d\tau \\ &\leq e^{-2k_p^q(t-t_q)}V_\epsilon(t_q^+) + a^2k_r^q\int_{t_q}^{t} e^{-2k_p^q(t-\tau)}d\tau \\ &= f_{\epsilon_1}^q(t)V_\epsilon(t_q^+) + \Delta_{\epsilon_1}^q(t), \end{aligned} \tag{2.48}$$

where $f_{\epsilon_1}^q(t) = e^{-2k_p^q(t-t_q)}$, $\Delta_{\epsilon_1}^q(t) = \frac{a^2k_r^q}{2k_p^q}(1 - e^{-2k_p^q(t-t_q)})$. In addition, $f_{\epsilon_1}^q(t) = f_{\epsilon_1}^q(t_q^1)$, $\Delta_{\epsilon_1}^q(t) = \Delta_{\epsilon_1}^q(t_q^1)$ for $t \in [t_q^1, \infty)$; $f_{\epsilon_1}^q(t) = 1$, $\Delta_{\epsilon_1}^q(t) = 0$ for $t \in [t_0, t_q)$.

If $[t_q^1, t_q^2) \neq \emptyset$, for $t \in [t_q^1, t_q^2)$, we have

$$\begin{aligned} \dot{V}_\epsilon &\leq k_r^q\|e'_{R_m}\|^2 + k_\epsilon^q\|\epsilon^{s(t)}\|^2 \\ V_\epsilon(t) &\leq e^{2k_\epsilon^q(t-t_q^1)}V_\epsilon(t_q^1) + k_r^q\int_{t_q^1}^{t} e^{2k_\epsilon^q(t-\tau)}\|e'_{R_m}(\tau)\|^2d\tau \\ &\leq f_\Phi^q(t)V_\epsilon(t_q^1) + \Delta_\Phi^q(t) \leq F_\Phi^q(t)V_\epsilon(t_q^+) + \Delta_\Phi^{q\,\prime}(t), \end{aligned} \tag{2.49}$$

where $f_\Phi^q(t) = e^{2k_\epsilon^q(t-t_q^1)}$, $\Delta_\Phi^q(t) = \frac{k_r^q}{2k_\epsilon^q}(e^{2k_\epsilon^q(t-t_q^1)} - 1)$, $F_\Phi^q(t) = f_\Phi^q(t)f_{\epsilon_1}^q(t_q^1)$ and $\Delta_\Phi^{q\,\prime}(t) = f_\Phi^q(t)\Delta_{\epsilon_1}^q(t_q^1) + \Delta_\Phi^q(t)$. In addition, $f_\Phi^q(t) = f_\Phi^q(t_q^2)$ and $\Delta_\Phi^q(t) = \Delta_\Phi^q(t_q^2)$ for $t \in [t_q^2, \infty)$; $f_\Phi^q(t) = 1$ and $\Delta_\Phi^q(t) = 0$ for $t \in [t_0, t_q^1)$.

Similarly, if $[t_q^2, t_{q+1}) \neq \emptyset$, for $t \in [t_q^2, t_{q+1})$,

$$V_\epsilon(t) \leq f_{\epsilon_2}^q(t) V_\epsilon(t_q^2) + \Delta_{\epsilon_2}^q(t) \leq F_{\epsilon_2}^q(t) V_\epsilon(t_q^+) + \Delta_{\epsilon_2}^{q\,\prime}(t), \tag{2.50}$$

where $f_{\epsilon_2}^q(t) = e^{-2k_p^q(t-t_q^2)}$, $\Delta_{\epsilon_2}^q(t) = \frac{a^2 k_r^q}{2k_p^q}(1 - e^{-2k_p^q(t-t_q^2)})$, $F_{\epsilon_2}^q(t) = f_{\epsilon_2}^q(t) F_\Phi^q(t_q^2)$, and $\Delta_{\epsilon_2}^{q\,\prime}(t) = f_{\epsilon_2}^q(t) \Delta_\Phi^{q\,\prime}(t_q^2) + \Delta_{\epsilon_2}^q(t)$. In addition, $f_{\epsilon_2}^q(t) = f_{\epsilon_2}^q(t_{q+1})$, $\Delta_{\epsilon_2}^q(t) = \Delta_{\epsilon_2}^q(t_{q+1})$ for $t \in [t_{q+1}, \infty)$; $f_{\epsilon_2}^q(t) = 1$, $\Delta_{\epsilon_2}^q(t) = 0$ for $t \in [t_0, t_q^2)$.

By Lemma 6, $t_q^2 - t_q^1 \leq h_a$, (2.50) satisfies

$$\begin{aligned} V_\epsilon(t) &\leq f_{\epsilon_2}(t) e^{2k_\epsilon^q h_a} f_{\epsilon_1}^q(t_q^1) V(t_q^+) + \Delta_{\epsilon_2}^{q\,\prime}(t) \\ &\leq e^{-2k_p^q\left((t-t_q^2)+(t_q^1-t_q)\right)+2k_\epsilon^q h_a} V(t_q^+) + \Delta_{\epsilon_2}^{q\,\prime}(t). \end{aligned} \tag{2.51}$$

As a result, if t_{q+1} is large enough, for any $\mu \in (0,1)$, there exists a $\tau(\mu)$, such that for any $t \in [t_q, t_q + \tau(\mu))$,

$$V_\epsilon(t) \leq \mu V(t_q^+) + \Delta_{\epsilon_2}^{q\,\prime}(t), \tag{2.52}$$

and by (2.51), $\tau(\mu)$ can be computed by

$$e^{-2k_p^q(\tau - h_a) + 2k_\epsilon^q h_a} \leq \mu, \quad \tau \geq \frac{\ln \mu}{2k_p^q} + (\frac{k_\epsilon^q}{k_p^q} + 1) h_a. \tag{2.53}$$

In addition, since

$$f_{\epsilon_1}^q(t) \leq F_\Phi^q(t) \leq f_\Phi^q(t) \leq e^{2k_\epsilon^q h_a} \text{ and } \ F_{\epsilon_2}^q(t) \leq F_\Phi^q(t) \leq f_\Phi^q(t) \leq e^{2k_\epsilon^q h_a}, \tag{2.54}$$

for any $t \in [t_q, t_{q+1})$, $q \geq 1$, $V_\epsilon(t)$ is upper bounded by

$$V_\epsilon(t) \leq e^{2k_\epsilon^q h_a} V_\epsilon(t_q^+) + \Delta^{q\prime}(t), \tag{2.55}$$

where $\Delta^{q\prime}(t) = \Delta_{\epsilon_1}^q(t)$ for $t \in [t_q, t_q^1)$; $\Delta^{q\prime}(t) = \Delta_\Phi^{q\,\prime}(t)$ for $t \in [t_q^1, t_q^2)$; and $\Delta^{q\prime}(t) = \Delta_{\epsilon_2}^{q\,\prime}(t)$ for $t \in [t_2, t_{q+1})$.

At each switching instant t_q, by (2.43), we have $V_\epsilon(t_q^+) \leq f_L^q V_\epsilon(t_q^-)$. Combine with (2.52), for the dwell time τ_0 satisfies (2.44)

$$V_\epsilon(t_q^+) \leq e^{-(\delta_0 + 2k_\epsilon h_a)} V(t_{q-1}^+) + \Delta^{q-1}, \tag{2.56}$$

where $\Delta^{q-1} = f_L^q \Delta_{\epsilon 2}^{q-1\prime}(t_q)$. Then, for any $t \in [t_q, t_{q+1})$,

$$\begin{aligned} V_\epsilon(t) &\le e^{2k_\epsilon h_a} V_\epsilon(t_q^+) + \Delta^{q\prime}(t) \\ &\le e^{-\delta_0} V_\epsilon(t_{q-1}^+) + e^{2k_\epsilon h_a}\Delta^{q-1} + \Delta^{q\prime}(t) \\ &\le e^{-(2\delta_0 + 2k_\epsilon h_a)} V(t_{q-2}^+) + e^{-\delta_0}\Delta^{q-2} + e^{2k_\epsilon h_a}\Delta^{q-1} + \Delta^{q\prime}(t) \\ &\le e^{-(q\delta_0 + (q-1)2k_\epsilon h_a)} V(t_0^+) + \Delta(t), \end{aligned} \tag{2.57}$$

where $\Delta(t) = e^{-((q-1)\delta_0 + (q-2)2k_\epsilon h_a)}\Delta^0 + e^{-((q-2)\delta_0 + (q-3)2k_\epsilon h_a)}\Delta^1 + \cdots + e^{2k_\epsilon h_a}\Delta^{q-1} + \Delta^{q\prime}(t)$. In addition, since $V_\epsilon^0(t_0^+) = V_\epsilon^0(t_0^-) = V_\epsilon^0(t_0)$, let $V_0 = V_\epsilon^0(t_0)$ represent the initial value of $V_\epsilon(t)$. We have

$$V_\epsilon(t) \le e^{-(q\delta_0 + (q-1)2k_\epsilon h_a)} V_0 + \Delta(t). \tag{2.58}$$

For $t \in [t_0, t_1)$, referring to (2.48), (2.49) and (2.50), V_ϵ increases during $t \in [t_0^1, t_0^2)$ and decreases during $t \in [t_0, t_0^1) \cup [t_0^2, t_1)$. By Lemma 6, V_ϵ is bounded. Then for any dwell time τ_0 satisfies (2.44), we have

$$V_\epsilon(t_1^+) \le e^{-\delta_0} V_0 + \Delta^0. \tag{2.59}$$

The convergence property is guaranteed for $t \in [t_0, \infty)$. In addition, $\Delta(t)$ is bounded for all $t \in [t_0, \infty)$, and the formation error converges to a small ball entered at the origin almost globally. Based on the above analysis, we reach the conclusion that the followers can gather around the target configuration with the convergence error determined by $\Delta(t)$. The proof is completed. □

Remark 5. Referring to (2.43), centralized computations are required for f_L^q at each switching instant. Since the possible choices of $L_{ff}^{(s(t),t)}$ are infinite, it is difficult to give a precise bound on f_L^q. By constraining the magnitude of l_{ij} as $|l_{ij}| \le \bar{l}$ for all $i, j \in \mathcal{V}_f$, an estimation of f_L^q can be given based on Lemma 3 as

$$\frac{1}{1 + n_f \bar{l}} \le \lambda_{ff}^i \le n_f \bar{l}, \tag{2.60}$$

and

$$f_L^q \le n_f \bar{l}(1 + n_f \bar{l}). \tag{2.61}$$

Remark 6. According to (2.52), the lower bound of dwell time τ_0 is given by

$$\underline{\tau}_0 = (1 + \frac{2k_\epsilon}{k_p})h_a + \frac{\ln \lambda_f}{k_p} + \frac{\delta_0}{2k_p}.$$

Here k_p is the convergence rate of ϵ when the attitude error $\|e'_{R_m}\|$ is smaller than a, and h_a is the maximum duration when the attitude error is larger than a. Both of them are determined by system dynamics, and a higher convergence rate leads to a smaller lower bound of τ_0. A smaller $\underline{\tau}_0$ can also be obtained by a smaller k_ϵ, which is introduced by using the Young's inequality. However, by (2.40), a smaller k_ϵ leads to a larger k_r^q; and by (2.48)–(2.50), it further results in larger convergence error. As a result, there exists a trade-off between the bound on dwell times and convergence errors.

2.2.4 Simulation Results

In this section, we use some simulation examples to further demonstrate the effectiveness of the proposed control protocol. Consider an MAS containing several agents maneuvering on $SE(3)$. Each agent is modeled as an underactuated system as in (2.8), with one independent direction in translation along its third axis. Four of them are chosen as leaders, moving along the pre-determined trajectories and the others are followers, governed by the proposed control protocol in (2.13).

Case I: Affine formation under the fixed graph

In this case, the agents are connected by a 4-rooted graph with nominal configuration $r_1 = [4, 0, 3]^T$, $r_2 = [-2, \frac{-2.5}{\sqrt{3}}, -\frac{4}{6}]^T$, $r_3 = [2, -\frac{2}{\sqrt{3}}, -1]^T$, $r_4 = [0, \frac{4}{\sqrt{3}}, -\frac{2}{5}]^T$, $r_5 = [-\frac{1}{3}, -\frac{2}{3}, \frac{4.5}{\sqrt{3}}]^T$, $r_6 = [\frac{1}{3}, -\frac{1}{3}, \frac{2}{\sqrt{3}}]^T$. The corresponding nominal formations are shown in Figure 2.3. The leaders move along some specific trajectories and the followers need to track the time-varying formation determined by leaders. The initial states for the agents are given by $p_1 = [15, 15, 0]^T$, $p_2 = [-15, -15, 0]^T$, $p_3 = p_5 = [15, -15, 0]^T$, $p_4 = p_6 = [-15, 15, 0]^T$.

The trajectories of the agents are shown in Figure 2.4 (a). The dynamic tracking as well as time-varying formation structures are realized. The formation errors and attitude errors are shown in Figure 2.5. After a transient

process, the attitude errors converge to zero, which means that the axis along which the thrust is provided, has been directed at the target configuration. The formation errors converge to zero as well.

Case II: Affine formation under the switching graph

In this case, the agents are connected by a switching graph with the switching signal $s(t) = \mod(q, 4) + 1,\ t \in [t_q, t_{q+1})$, and the possible graphs $\hat{\mathcal{G}} = \{\mathcal{G}^1, \mathcal{G}^2, \mathcal{G}^3, \mathcal{G}^4\}$ as shown in Figure 2.1. The nominal configuration r is given by $r_1 = [0, 1, -3]^T$, $r_2 = [-1, -3, 1/2]^T$, $r_3 = [1, -3, -1/2]^T$, $r_4 = [0, 2, 1]^T$, $r_5 = [-1/2, -1/2, -2]^T$, $r_6 = [1/2, -1/2, -4]^T$, $r_7 = [1/4, 0, 4]^T$. The parameters in (2.44) are chosen to be $k_c = 4$, $a = 0.4$, $\delta_0 = 0.1$, $k_\epsilon = 0.01$, $k_R = 8$. The initial positions are given by $p_1 = p_3 = p_5 = p_7 = [15, -15, 0]^T$, $p_2 = p_4 = [15, -15, 0]^T$, $p_6 = [-15, -15, 0]^T$. Figure 2.4 (b) shows the trajectories of the agents, which tells that dynamic tracking of a time-varying formation is realized. The formation errors and attitude errors are shown in Figure 2.6. The attitude errors have a jump at each switching instant and converge very quickly after the switching; while the formation errors converge to a small ball centered at zero.

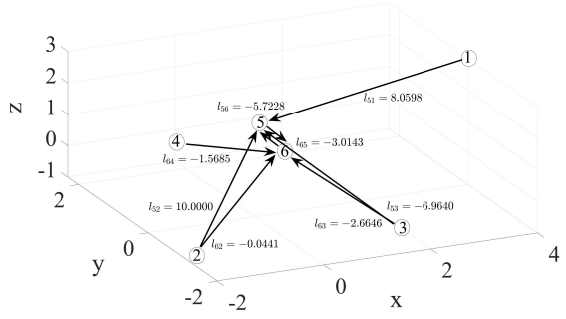

Figure 2.3: Nominal formation for the 4-rooted graph. Here, the arrows represent the directed edges in the graph and the edge weights are labeled aside. The nonzero eigenvalues of the associated Laplacian matrices are -8.9898 and 10.9084.

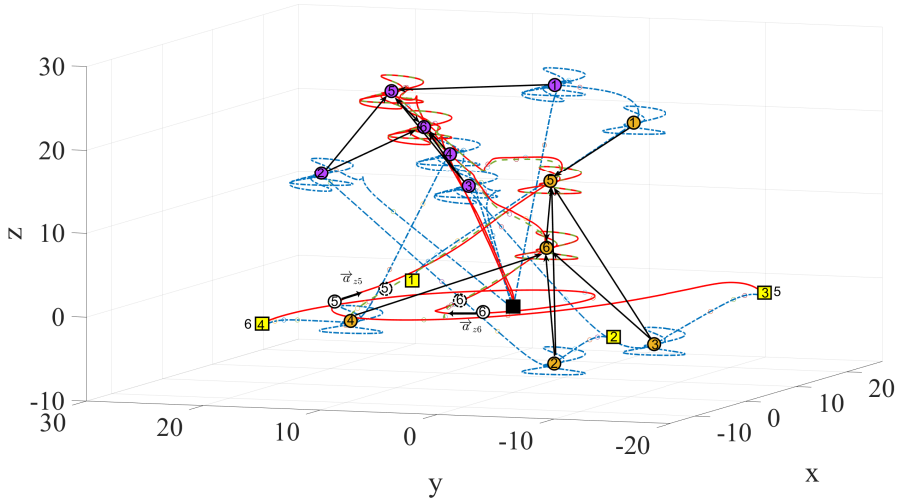

(a) Trajectories of the agents under the 4-rooted graph.

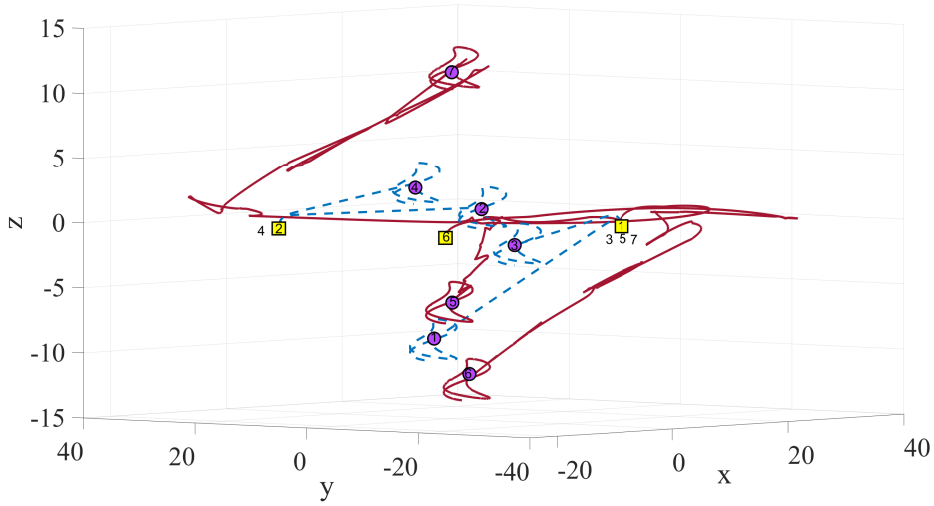

(b) Trajectories of the agents under the switching topology.

Figure 2.4: Trajectories of the agents. Here, the solid lines represent the trajectories of the followers, the dash lines represent the trajectories of the leaders; the squares represent the initial positions of the agents and the circles represent the positions of the agents at a same time instant. The long arrows in (a) represent the edges among agents.

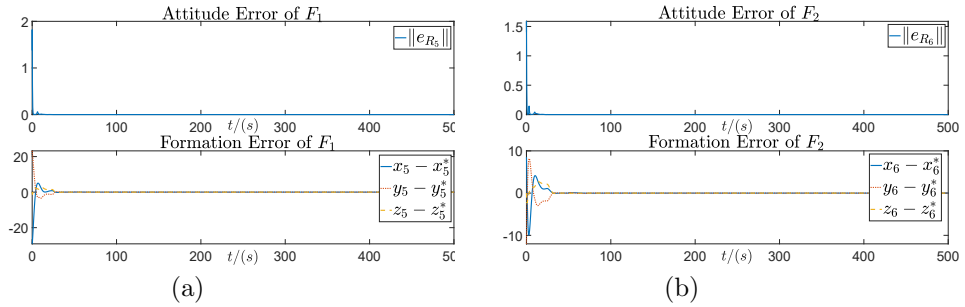

(a) (b)

Figure 2.5: Convergence errors of the followers under the 4-rooted graph.

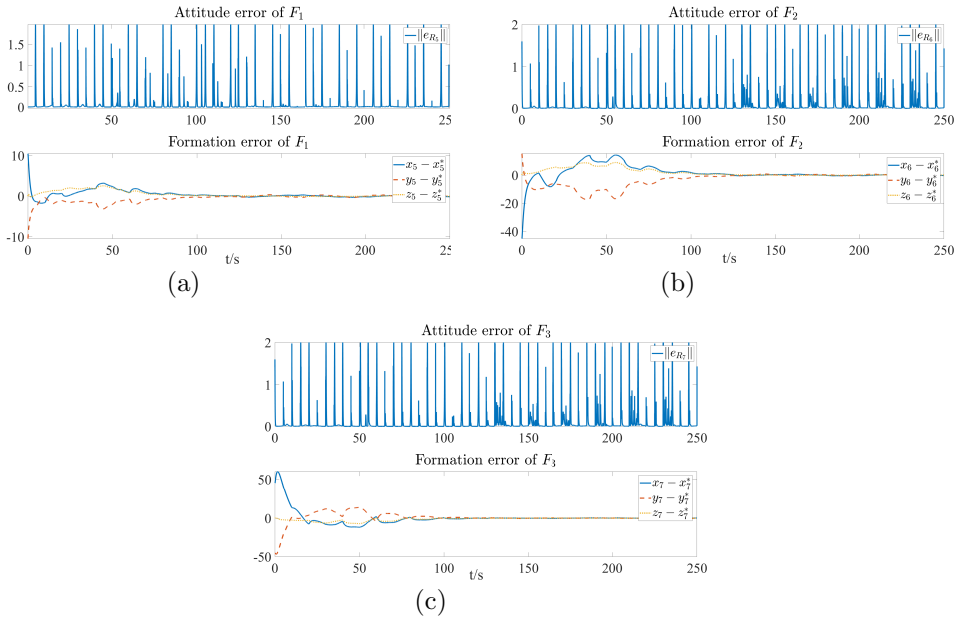

(a) (b)

(c)

Figure 2.6: Convergence errors of the followers under the switching topology.

2.3 Affine Formation under Event-Triggered Mechanism

An ETM for affine formation control of single integrators is presented in the following. The motivation of the following work is derived from a resource-efficient concern.

2.3.1 Problem Formulation

Consider a group of N agents in $\mathbb{R}^d$ with single-integrator dynamics under a signed directed graph $\mathcal{G} = (\mathcal{V}, \mathcal{E})$:

$$\dot{p}_i(t) = u_i(t), \qquad i \in \mathcal{V} = \{1, 2, \ldots, N\}, \tag{2.62}$$

where $p_i \in \mathbb{R}^d$ denotes the position of agent i and u_i is the control input. The initial condition of the configuration is given as $p(0) = p_0 \in \mathbb{R}^{Nd}$. Furthermore, assume that $d \geq 2$ and $N \geq d+2$. The first problem considered in this section is described as follows:

Problem 2. Design event-triggered control protocols $u_i(t), i \in \mathcal{V}_f$, such that the position $p_f(t)$ of followers can track the target configuration $p_f^*(t) = [p_{N_l+1}^{*\mathrm{T}}, \ldots, p_N^{*\mathrm{T}}]^{\mathrm{T}}$ practically, i.e., there is a constant $\varepsilon > 0$ satisfying $\limsup_{t\to\infty} \left\| p_f^*(t) - p_f(t) \right\| < \varepsilon$.

The emulation-based approach is used to design ETM for the system in (2.62). First, a continuous-time control protocol is introduced to ensure asymptotic tracking of the target formation. Then it will be transformed into an event-triggered one.

In the rest of this chapter, we always assume the conditions of Lemma 5 are satisfied and the weights are selected based on (2.6). Then, the associated signed Laplacian can be expressed as

$$L = \left[\begin{array}{c|c} 0_{ll}^{(d+1)\times(d+1)} & 0_{lf}^{(d+1)\times(N-d-1)} \\ \hline L_{fl}^{(N-d-1)\times(d+1)} & L_{ff}^{(N-d-1)\times(N-d-1)} \end{array}\right]. \tag{2.63}$$

By using Lemma 5, one has that $\bar{L}_{ff}$ is nonsingular, and

$$\bar{L}_{fl}p_l^*(t) + \bar{L}_{ff}p_f^*(t) = 0, \tag{2.64}$$

where $\bar{L}_{fl} = L_{fl} \otimes I_d$ and $\bar{L}_{ff} = L_{ff} \otimes I_d$.

Lemma 7 ([75])**.** Under the following continuous control protocols:

$$u_i(t) = -\frac{1}{L_{ii}} \sum_{j \in \mathcal{N}_i} a_{ij}[p_i(t) - p_j(t) - \dot{p}_j(t)], \tag{2.65}$$

where $L_{ii} \neq 0$ is the (i,i)-th element of Laplacian L, the tracking error $\delta_f(t) = p_f(t) - \bar{L}_{ff}^{-1}\bar{L}_{fl}p_l^*(t)$ of followers converges globally and exponentially to zero.

Notice that there are two different parts in (2.65), namely, the (combined) relative position information $y_i(t) = \sum_{j \in \mathcal{N}_i} a_{ij}[p_i(t) - p_j(t)]$ and the in-neighbor's absolute velocity information $\dot{p}_j(t), j \in \mathcal{N}_i$. For these two kinds of information, different ETMs are designed as follows.

Since $y_i(t)$ can be deemed as local information, agent i is able to measure it continuously. At each triggering instant $t_{k_i}^i$, $k_i \in \mathbb{N}$ and $i \in \mathcal{V}_f$, the relative position information will be sent to the local controller to update the control signal u_i. The ET condition is given as

$$\|\epsilon_i(t)\|^2 \leq \sigma_1, i \in \mathcal{V}_f, \tag{2.66}$$

where $\sigma_1 > 0$ is a threshold constant, and the measurement error $\epsilon_i(t) = \hat{y}_i(t) - y_i(t), t \geq 0$, with $\hat{y}_i(t) = y_i(t_{k_i}^i), t \in [t_{k_i}^i, t_{k_i+1}^i)$.

The velocity information $\dot{p}_i(t), i \in \mathcal{V}$, is difficult to be continuously obtained by out-neighbors. Therefore, agent i will first measure its local velocity, then at each triggering instant $\tau_{k_i}^i, k_i \in \mathbb{N}$, broadcast its own velocity information to its out-neighbors for their controller updates. The ET condition is

$$\|e_i(t)\|^2 \leq \sigma_2, i \in \mathcal{V}, \tag{2.67}$$

with a threshold constant $\sigma_2 > 0$, the broadcast error $e_i(t) = \hat{\dot{p}}_i(t) - \dot{p}_i(t), t \geq 0$, and $\hat{\dot{p}}_i(t) = \dot{p}_i(\tau_{k_i}^i), t \in [\tau_{k_i}^i, \tau_{k_i+1}^i)$. Then, the event-triggered control protocols

can be described by

$$\begin{aligned} u_i(t) =& -\frac{1}{L_{ii}}\hat{y}_i(t) + \frac{1}{L_{ii}}\sum_{j\in\mathcal{N}_i} a_{ij}\hat{\dot{p}}_j(t) \\ =& -\frac{1}{L_{ii}}\left[y_i(t) + \epsilon_i(t) - \sum_{j\in\mathcal{N}_i} a_{ij}(\dot{p}_j(t) + e_j(t))\right], \quad i \in \mathcal{V}_f. \end{aligned} \tag{2.68}$$

Due to the discontinuity of $\dot{p}_i(t), i \in \mathcal{V}_f$, under the event-triggered controller in (2.68), it is difficult to ensure a positive minimum inter-event time for the ET condition in (2.67). Hence, we consider the following triggering performance called "separated events".

Problem 3. Show that the ET conditions in (2.66) and (2.67) yield separated events. That is, for any given initial state $p_0 \in \mathbb{R}^{Nd}$, there exist constants $T_y \in (0,\infty)$ and $T_{\dot{p}} \in (0,\infty)$ satisfying, respectively,

$$\limsup_{t\to\infty} \frac{\left|\{t^i_{k_i}\}_{k_i=1}^{\infty} \cap [0,t]\right|}{t} < T_y \in (0,\infty), i \in \mathcal{V}_f,$$

and

$$\limsup_{t\to\infty} \frac{\left|\{\tau^i_{k_i}\}_{k_i=1}^{\infty} \cap [0,t]\right|}{t} < T_{\dot{p}} \in (0,\infty), i \in \mathcal{V}.$$

Remark 7. The event-separation property means that there are a finite number of triggering instants in any finite time interval, thus, it implies Zeno-freeness of the triggering time sequences. Moreover, it further ensures that the average triggering frequency can be upper bounded as the time goes to infinity. Note that if there is a positive lower bound for inter-event times, then the corresponding triggering sequence must be separated.

2.3.2 Main Result

In this section, the main results will be given to solve Problems 2 and 3. First, the following theorem characterizes the tracking performance of the event-triggered controllers.

Theorem 3. The practical tracking property in Problem 2 can be ensured by the event-triggered controller in (2.68) and the ET conditions in (2.66) and (2.67).

Proof. By substituting (2.68) into (2.62), one has for each follower $i \in \mathcal{V}_i$,

$$\dot{y}_i(t) = -y_i(t) - \epsilon_i(t) + \sum_{j \in \mathcal{N}_i} a_{ij} e_j(t). \tag{2.69}$$

Define $\epsilon(t) := [\epsilon_{d+2}^{\mathrm{T}}, \ldots, \epsilon_N^{\mathrm{T}}]^{\mathrm{T}}$, $e(t) := [e_1^{\mathrm{T}}, \ldots, e_N^{\mathrm{T}}]^{\mathrm{T}}$ and $w(t) = \bar{L}_{ff}\delta_f(t)$ with the tracking error δ_f given in Lemma 7. Then, (2.69) can be rewritten in the following compact form:

$$\dot{w}(t) = -w(t) - \epsilon(t) + \mathcal{A}_f e(t), \tag{2.70}$$

where $\mathcal{A}_f$ denotes the last $(n-d-1)$ rows of the adjacency matrix $\mathcal{A}$. According to the ET conditions in (2.66) and (2.67), we have

$$\|\epsilon(t)\|^2 \leq |\mathcal{V}_f|\,\sigma_1, \text{ and } \|\mathcal{A}_f e(t)\|^2 \leq N\,\|\mathcal{A}_f\|^2\,\sigma_2.$$

Let $V(t) = \frac{1}{2}w^{\mathrm{T}}(t)w(t)$, then, its derivative along the solutions of (2.62) and (2.68) satisfies

$$\begin{aligned}\dot{V}(t) \leq & -2V(t) + \|w(t)\|\,\|\epsilon(t)\| + \|w(t)\|\,\|\mathcal{A}_f e(t)\| \\ \leq & -V(t) + |\mathcal{V}_f|\,\sigma_1 + N\,\|\mathcal{A}_f\|^2\,\sigma_2,\end{aligned}$$

which implies that the w-system is Lyapunov stable and

$$\limsup_{t\to\infty} V(t) \leq 2(|\mathcal{V}_f|\,\sigma_1 + N\,\|\mathcal{A}_f\|^2\,\sigma_2) = \frac{1}{2}\sigma_0^2.$$

The fact that $\bar{L}_{ff}$ is nonsingular further leads to

$$\limsup_{t\to\infty} \|\delta_f(t)\| \leq \left\|\bar{L}_{ff}^{-1}\right\|\sigma_0, \tag{2.71}$$

and the proof is completed. □

To study the triggering performance, we introduce the following assumptions.

Assumption 5. For leaders $i \in \mathcal{V}_l$, its velocity $\dot{p}_i(t), t \in [0, \infty)$, is upper bounded by M_0.

Assumption 6. The graph $\mathcal{G}$ is an acyclic graph, i.e., there is no path that begins at a node $i \in \mathcal{V}$ and ends in one of the in-neighbors $j \in \mathcal{N}_i$.

For the events of relative position information, we can provide positive minimum inter-event times in the following theorem.

Theorem 4. For a given initial state p_0, the triggering instants generated by the ET condition in (2.66) satisfy

$$\inf_{k_i \in \mathbb{N}} (t^i_{k_i+1} - t^i_{k_i}) \geq T_0, i \in \mathcal{V}_f,$$

with some positive lower bound $T_0 > 0$.

Proof. By definitions, we have

$$y_f = \begin{bmatrix} y_{d+2} \\ \vdots \\ y_N \end{bmatrix} = \begin{bmatrix} \bar{L}_{fl} & \bar{L}_{ff} \end{bmatrix} \begin{bmatrix} p_l \\ p_f \end{bmatrix} = \bar{L}_{ff}\delta = w.$$

Thus, according to Theorem 3, for any given p_0, there is $M_1(p_0)$ such that $\|w(t)\| \leq M_1, t \in \mathbb{R}_{\geq 0}$. Consequently,

$$\begin{aligned} \|\dot{y}_f(t)\| =& \|w(t) + \epsilon(t) - \mathcal{A}_f e(t)\| \\ \leq& M_1 + \sqrt{|\mathcal{V}_f|\,\sigma_1} + \sqrt{N\,\|\mathcal{A}_f\|^2\,\sigma_2} \\ =& \varphi_0. \end{aligned}$$

Since $\|\dot{y}_i(t)\| \leq \|\dot{y}_f(t)\|$ and $\left\|\epsilon_i(t^i_{k_i})\right\| = 0$ for all $i \in \mathcal{V}_f$ and $k_i \in \mathbb{Z}_{\geq 0}$, one can obtain that the inter-event times of the ET condition in (2.66) are lower bounded by $\frac{\sqrt{\sigma_1}}{\varphi_0}$, and therefore, the proof is completed. □

For the analysis of the ET conditions in (2.67), we introduce the following graph partition algorithm in Algorithm 2.

Recall that both leaders and followers need to broadcast their velocity information. Thus, all nodes in the graph $\mathcal{G}$ are considered in the partition. In an acyclic directed graph, there always exists at least one node that does not have in-neighbors. Hence, the m-th layer $\mathcal{L}_m$ contains all the agents without in-neighbors in the m-th acyclic subgraph $\mathcal{G}_m$. Since there are a finite number of agents in the acyclic graph $\mathcal{G}$, Algorithm 2 must reach an end with finite layers, and denote the last layer as $q \in \mathbb{N}_{\geq 1}$. An example is illustrated in Figure 2.7. Furthermore, we have the following simple facts of the partition.

Algorithm 2 Partition of nodes in $\mathcal{G}$

1: Initial $m = 0$, $\mathcal{V}_0 = \mathcal{V}$, $\mathcal{E}_0 = \mathcal{E}$ and $\mathcal{G}_0 = \mathcal{G}(\mathcal{V}_0, \mathcal{E}_0)$;
2: Select all leaders as the 0-th layer of agents, i.e., $\mathcal{L}_0 = \{i \in \mathcal{V}_l\}$ as the 0-th layer;
3: **while** $\mathcal{V}_m \neq \mathcal{L}_m$
4: $m = m + 1$;
5: Generate a subgraph $\mathcal{G}_m(\mathcal{V}_m, \mathcal{E}_m)$ where

$$\mathcal{V}_m = \{i \in \mathcal{V} | i \notin \cup_{s=0}^{m-1} \mathcal{L}_s\},$$
$$\mathcal{E}_m = \{(i,j) \in \mathcal{E} | i, j \in \mathcal{V}_m\}.$$

6: Define the new m-th layer of agents:

$$\mathcal{L}_m = \{i \in \mathcal{V}_m | \mathcal{N}_i \cap \mathcal{V}_m = \emptyset\}.$$

7: **end while**
8: **end**

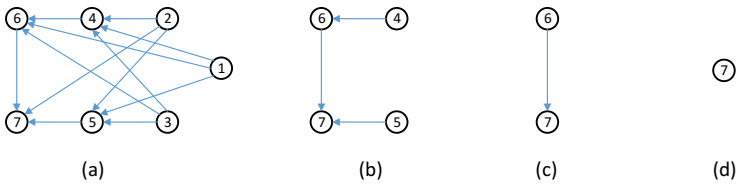

Figure 2.7: An illustration of Algorithm 2. $\mathcal{G}_0(\mathcal{V}_0, \mathcal{E}_0)$ in (a) decides $\mathcal{L}_0 = \{1, 2, 3\}$; $\mathcal{G}_1(\mathcal{V}_1, \mathcal{E}_1)$ in (b) with $\mathcal{V}_1 = \{4, 5, 6, 7\}$ yields $\mathcal{L}_1 = \{4, 5\}$; $\mathcal{G}_2(\mathcal{V}_2, \mathcal{E}_2)$ in (c) with $\mathcal{V}_2 = \{6, 7\}$ yields $\mathcal{L}_2 = \{6\}$; and finally $\mathcal{G}_3(\mathcal{V}_3, \mathcal{E}_3)$ in (d) with $\mathcal{V}_3 = \mathcal{L}_3 = \{7\}$ ends the algorithm.

Proposition 2. For the layers of agents generated by Algorithm 2,

1. $\mathcal{V} = \cup_{m=0}^{q} \mathcal{L}_m$;

2. for any $m \in \{1, 2, \ldots, q\}$, $\cup_{i \in \mathcal{L}_m} \mathcal{N}_i \subset \cup_{j=0}^{m-1} \mathcal{L}_j$.

Based on the analysis above, the event separation property for triggering sequences $\{\tau_{k_i}^i\}_{k_i=0}^{\infty}$, $i \in \mathcal{V}$, is summarized as follows:

Theorem 5. Suppose that Assumptions 5 and 6 hold for the plant in (2.62) associated with the graph $\mathcal{G}$. For a given initial state p_0, the triggering condition in (2.67) generates separated events for all $i \in \mathcal{V}$.

Proof. First, for the leader $i \in \mathcal{L}_0 = \mathcal{V}_l$, the boundedness of $\dot{p}_i(t), t \in [0, \infty)$ guarantees a positive lower bound of inter-event times, which can be given as

$$\inf_{k_i \in \mathbb{N}} (\tau_{k_i+1}^i - \tau_{k_i}^i) \geq \frac{\sqrt{\sigma_2}}{M_0}, i \in \mathcal{L}_0,$$

with M_0 defined in Assumption 5.

Assumption 6 ensures the feasibility of Algorithm 2; hence, we consider the agents in $\mathcal{L}_1 \subset \mathcal{V}_f$. According to the event-triggered controller in (2.68), for any $i \in \mathcal{V}_f$, the events from the ET condition in (2.67) only occur when the relative position information of agent i or the absolute velocity information of its in-neighbors $j \in \mathcal{N}_i$ is updated, i.e., $\tau_{k_i}^i, k_i \in \mathbb{Z}_{\geq 0}$ belongs to $\{t_{k_i}^i\}_{k_i}^{\infty}$ or $\{\tau_{k_j}^j\}_{k_j=0}^{\infty}$ with $j \in \mathcal{N}_i$.

Based on Theorem 4 and item (2) in Proposition 2, one has, for any given interval $[a, b]$ with $a \geq b \geq 0$,

$$\begin{aligned}
\left|[a,b] \cap \{t_{k_i}^i\}_{k_i}^{\infty}\right| &< \left\lceil \frac{(b-a)\varphi_0}{\sqrt{\sigma_1}} \right\rceil + 1, i \in \mathcal{L}_1; \\
\left|[a,b] \cap \{\tau_{k_j}^j\}_{k_i}^{\infty}\right| &< \left\lceil \frac{(b-a)M_0}{\sqrt{\sigma_2}} \right\rceil + 1, j \in \mathcal{N}_i, i \in \mathcal{L}_1.
\end{aligned}$$

Hence, it can be obtained that, for $i \in \mathcal{L}_1$,

$$\begin{aligned}
\left|[a,b] \cap \{\tau_{k_i}^i\}_{k_i}^{\infty}\right| <& \chi_p(b-a) + \sum_{j \in \mathcal{L}_0 \cap \mathcal{N}_i} \chi_v^{0,j}(b-a) \\
=& \chi_v^{1,i}(b-a),
\end{aligned}$$

where $\chi_p(s) = \left\lceil \frac{s\varphi_0}{\sqrt{\sigma_1}} \right\rceil + 1$ and $\chi_v^{0,j}(s) = \left\lceil \frac{sM_0}{\sqrt{\sigma_2}} \right\rceil + 1, j \in \mathcal{L}_0$ for $s \geq 0$. The subscript "p" means position while "v" represents velocity. The superscript (l, i) stands for agent i in layer $\mathcal{L}_l$. Thus, the events for agent $i \in \mathcal{L}_1$ are separated. In detail, we have that for $i \in \mathcal{L}_1$,

$$\limsup_{t\to\infty} \frac{\left|\{\tau_{k_i}^i\}_{k_i=1}^{\infty} \cap [0,t]\right|}{t} < \frac{\varphi_0}{\sqrt{\sigma_1}} + |\mathcal{L}_0 \cap \mathcal{N}_i| \frac{M_0}{\sqrt{\sigma_2}}. \tag{2.72}$$

Suppose that the event-separation property holds for the agents in the layers $\{\mathcal{L}_0, \ldots, \mathcal{L}_m\}$ with $m \leq q-1$ and q being the total number of layers. Specifically, for any given $a \geq b \geq 0$,

$$\left|[a,b] \cap \{\tau_{k_i}^i\}_{k_i}^{\infty}\right| \leq \chi_v^{s,i}(b-a) \tag{2.73}$$

holds for all $i \in \mathcal{L}_s$ and $s \in \{1, \ldots, m\}$.

Now consider the agent $i \in \mathcal{L}_{m+1}$. From Theorem 4,

$$\left|[a,b] \cap \{t_{k_i}^i\}_{k_i}^{\infty}\right| < \chi_p(b-a), i \in \mathcal{L}_{m+1}. \tag{2.74}$$

Since $\mathcal{N}_i \subset \cup_{j=0}^m \mathcal{L}_j, i \in \mathcal{L}_{m+1}$ from Proposition 2, combining (2.73) and (2.74) leads to

$$\begin{aligned} \left|[a,b] \cap \{\tau_{k_i}^i\}_{k_i}^{\infty}\right| <& \chi_p(b-a) + \sum_{t=0}^{m} \sum_{j\in\mathcal{L}_t\cap\mathcal{N}_i} \chi_v^{j,t}(b-a) \\ =& \chi_v^{m+1,i}(b-a). \end{aligned} \tag{2.75}$$

By recursively applying (2.72) to (2.75), one can show that the events caused by the ET condition in (2.67) of agent $i \in \mathcal{L}_{m+1}$ are separated. The analysis above can be extended to all the agents in the graph $\mathcal{G}$ due to item (1) in Proposition 2; and therefore, the proof is completed. □

Remark 8. According to Theorems 3-5, the ET conditions in (2.66) and (2.67) provide a trade-off between the tracking performance and the triggering performance. Smaller thresholds σ_1 and σ_2 could lead to higher tracking accuracy but increases the number of events.

Remark 9. The events of an agent in a higher layer would be triggered more frequently than those in a lower layer. This property demonstrates the relationship between the system size and the communication load.

Remark 10. When there exist cycles in the graph, such as, between agents i and j, each of the agents can be regarded as the lower layer of the other one. In this case, a "positive feedback" effect on their events of absolute velocity information may happen. The events in agent i would promote the events in agent j, which could conversely accelerate the triggering of agent i. As a result, the events would not be separated as they are triggered faster and faster.

2.3.3 Simulation

In this section, the effectiveness of the event-triggered control protocol is illustrated by simulations. The interaction network among agents is shown as in Figure 2.7(a). The nominal formation r and the associated signed Laplacian are chosen the same as the ones used in [75]. The thresholds in (2.66) and (2.67) are chosen as $\sigma_1 = 0.05$ and $\sigma_2 = 0.1$, respectively. The trajectories of the agents are shown in Figure 2.8, with the steady-state errors given in Table 2.1. Here, δ_x and δ_y represent the tracking errors along x axis and y axis, respectively. The number of events are shown in Table 2.2. The agents in the higher layer are triggered more frequently than those in the lower layer, which coincides with the analysis in Remark 9. In addition, the tracking errors of the agents in the higher layer are larger than the ones in the lower layer. This is reasonable, since the control protocol relies on the information collected from the agents in the lower layers. The tracking errors are accumulated layer by layer.

Table 2.1: Steady-state tracking errors

Agent	A_4	A_5	A_6	A_7
Steady-state error δ_x	0.6063	0.5925	1.4063	1.9263
Steady-state error δ_y	0.0131	0.0156	0.0126	-0.0731

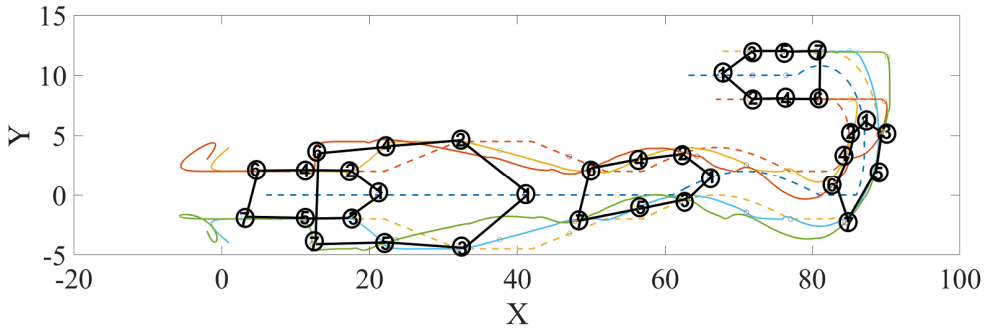

Figure 2.8: Trajectories of the agents, with dash (solid) lines representing leaders' (followers') trajectories.

Table 2.2: Number of events

Agent	A_1	A_2	A_3	A_4	A_5	A_6	A_7
Updates of relative position	-	-	-	373	424	943	1386
Broadcasting of velocity	44	29	49	168	182	333	342

2.4 Summary

An affine formation tracking problem was studied in this chapter. First, we solved the problem for nonholonomic systems on $SE(3)$ under fixed and switching topologies. The geometric control method together with graph theory were used to design the control protocol. The proposed controller was constructed directly on the Lie algebra of $SE(3)$ and only relied on local information. No global reference is required. An algorithm was proposed to reconstruct the k-rooted graph when some edges in the graph were lost. We showed that the system converged to the target configuration under fixed topologies and converged into a small ball centered at the target configuration under switching topologies. Theoretical proof and simulations were given to demonstrate the effectiveness of the proposed controller.

After that, an ETM was proposed for affine formation of MASs modeled by single integrators. Under the proposed control protocol, the followers practically tracked the target configuration. In addition, Zeno behavior was excluded when the MAS was connected by an acyclic graph.

Chapter 3

Cooperative Output Regulation with Communication Imperfections*

3.1 Overview

In this chapter, the COR problem with communication imperfections is investigated. As one of the fundamental problems in MASs, COR has been extensively studied since it was proposed [14]. By a well-designed interactive protocol, COR aims at rendering a set of agents to achieve asymptotic tracking or disturbance rejection of an exogenous signal. In order to accomplish a cooperative goal, agents need to exchange their local information through a shared communication network. The introduction of networks always comes with communication imperfections such as asynchronous transmissions, time-varying delays, quantization errors, packet dropouts and communication constraints. The effects of these imperfections have been widely investigated in the area of NCSs with one or multiple communication imperfections under consideration (see [24, 25]). Following the method proposed in [24], we solve a COR problem with asynchronous samplings and time-varying delays in a hybrid system framework. Compared with the results in [48] and [49], which

*A version of this chapter has been published as: J. Yang, H. Yu, and T. Chen, Cooperative Output Regulation with Asynchronous Transmissions and Time-Varying Delays. *IEEE Transactions on Automatic Control*, early access.

tackled the asynchronous samplings for MASs by a time-delay approach, the method proposed in this work can capture different transmission instants without increasing the dimension of the system.

In NCSs, we assume only one node has access to the network at a transmission instant and a scheduling protocol is implemented to grant the access of the nodes to the network [34]. The performance of the protocol is evaluated by a parameter λ. While in the considered sampled-data MASs, local information of an agent could be packaged and broadcast to its neighbors entirely at a transmission instant, thereby, λ is always set to zero. Since the Lyapunov candidate used in [24] was not consistent when λ approached to zero, simply extending it to sampled-data MASs leads λ to be a redundant variable. Considering the distinction between the sample-data setting in MASs and the protocol used in NCSs, a novel Lyapunov function candidate, with λ being excluded, is proposed in this work. Benefited from that, a more straightforward interpretation on the trade-off design between MATIs and MADs can be given, which can serve as a better guideline for network designers.

The main contributions of this work are summarized as follows:

1. A sampled-data COR problem of heterogeneous systems is solved under asynchronous transmissions, time-varying delays and unknown disturbances. To the best of the authors' knowledge, this is the first time that the above problem is solved in a uniform framework. A hybrid system model is used to incorporate both asynchronous transmissions and time-varying delays. Based on this model, results on universal global asymptotic stability (UGAS) and $\mathcal{L}_2$ ($\mathcal{L}_\infty$) stability are provided.

2. A novel Lyapunov function candidate is proposed for MASs, based on which, a more intuitive analysis on the relationship between MATIs and MADs can be given compared with the ones given in [50].

The effectiveness of the proposed method is verified by numerical examples.

3.2 Preliminaries and Problem Formulation

3.2.1 Definitions and Preliminaries

Preliminaries and notations on graph theory are same as the ones in Section 2.2.1. Let $\mathbf{0}$ denote a vector with all the elements being 0 with appropriate dimensions and 0_n denote an $n \times n$ matrix with all elements being zero. A function $\alpha : \mathbb{R}_{\geq 0} \to \mathbb{R}_{\geq 0}$, is said to be of class $\mathcal{K}$ if it is continuous, strictly increasing and $\alpha(0) = 0$; it is said to be of class $\mathcal{K}_\infty$ if it is of class $\mathcal{K}$ and unbounded. A function $\beta : \mathbb{R}_{\geq 0} \times \mathbb{R}_{\geq 0} \to \mathbb{R}_{\geq 0}$, is said to be of class $\mathcal{KL}$ if it is continuous, and $\beta(\cdot, t)$ is of class $\mathcal{K}$ for each $t \geq 0$, $\lim_{t\to\infty} \beta(s, t) = 0$ for each $s \geq 0$. A function β: $\mathbb{R}_{\geq 0} \times \mathbb{R}_{\geq 0} \times \mathbb{R}_{\geq 0} \to \mathbb{R}_{\geq 0}$, is said to be of class $\mathcal{KLL}$ if it is continuous, and $\beta(\cdot, r, \cdot)$, $\beta(\cdot, \cdot, r)$ are class $\mathcal{KL}$ functions for each $r \geq 0$.

A hybrid system $\mathcal{H}$ is of the form

$$\begin{aligned} \dot{\xi} &= F(\xi, \omega), \ \xi \in C, \\ \xi^+ &\in G(\xi), \quad \xi \in D, \end{aligned} \tag{3.1}$$

where F describes the flow dynamics, G the jump dynamics, C the flow set and D the jump set. The solution of (3.1) is expressed as $\xi(t, j)$ and defined on the hybrid time domain dom ξ, where the elements (t, j) with $t \in \mathbb{R}_{\geq 0}$ and $j \in \mathbb{N}$ record the elapse of time and number of jumps, respectively. For conciseness, we omit the mathematical definitions on some notations in hybrid systems, and refer the readers to [78].

The $\mathcal{L}_2$ norm of a function ξ defined on a hybrid time domain dom $\xi = \cup_{j=0}^{J-1}([t_j, t_{j+1}], j)$ with J possibly ∞ and/or $t_J = \infty$ is given by

$$\|\xi\|_{\mathcal{L}_2} = \sqrt{\sum_{j=0}^{J-1} \int_{t_j}^{t_{j+1}} \|\xi(t, j)\|^2 dt}, \tag{3.2}$$

and its $\mathcal{L}_\infty$ norm is given by

$$\|\xi\|_{\mathcal{L}_\infty} = \text{ess sup}_{(t,j)\in \text{dom } \xi} \|\xi(t, j)\|, \tag{3.3}$$

when the right hand side of (3.2) and (3.3) exist and are finite. Furthermore, we say $\xi \in \mathcal{L}_p$, $p \in \{2, \infty\}$, when $\|\xi\|_{\mathcal{L}_p}$ is finite.

3.2.2 Cooperative Output Regulation

Consider a heterogeneous MAS containing N agents, each of them is modeled as a general linear system as follows

$$\begin{aligned} \dot{x}_i &= A_i x_i + B_i u_i + E_i v + G_i \omega_i \\ e_i &= C_i x_i + D_i u_i + F_i v, \quad i = 1, \cdots, N, \end{aligned} \tag{3.4}$$

where $x_i \in \mathbb{R}^{n_i}$, $u_i \in \mathbb{R}^{m_i}$, $e_i \in \mathbb{R}^{p_i}$ and $\omega_i \in \mathbb{R}^{r_i}$ represent the system state, control input, tracking error and unknown disturbance, respectively, and A_i, B_i, C_i, D_i, E_i, F_i, G_i are constant matrices with compatible dimensions. $v \in \mathbb{R}^q$ represents the exogenous signal to be tracked or rejected, which is labelled as agent 0 and follows the dynamics

$$\dot{v} = Sv + G_0 \omega_0. \tag{3.5}$$

Here $S \in \mathbb{R}^{q \times q}$, $G_0 \in \mathbb{R}^{q \times r_0}$ are constant matrices, and $\omega_0 \in \mathbb{R}^{r_0}$ represents the disturbance. It should be noted that, the disturbances ω_i introduced in (3.4) and (3.5) cannot be merged into the exogenous signal v, as v is deemed as a signal generated by an exosystem with known dynamics while ω_i is unknown disturbances to be attenuated.

The MAS in (3.4) and the exosystem in (3.5) are connected by a communication network. Associate the two systems with a graph $\bar{\mathcal{G}} = (\bar{\mathcal{V}}, \bar{\mathcal{E}})$, where $(i, j) \in \bar{\mathcal{E}}$ iff node j can receive information from node i through the network. $\mathcal{N}_i$ is defined as the neighbor set of agent i, where $j \in \mathcal{N}_i$ iff $(j, i) \in \bar{\mathcal{E}}$. Let $\bar{L} \in \mathbb{R}^{(N+1)\times(N+1)}$ be the Laplacian matrix of graph $\bar{\mathcal{G}}$, where $[\bar{L}]_{ij} = -a_{ij}$, if $i \neq j$; and $[\bar{L}]_{ii} = \sum_{j=0, j\neq i}^{N} a_{ij}$ with $a_{ij} = 1$, if $(j, i) \in \bar{\mathcal{E}}$, and $a_{ij} = 0$, otherwise. Here $[\bar{L}]_{ij}$ represents the (i, j)-th element of the Laplacian $\bar{L}$. For COR problem, the Laplacian $\bar{L}$ can be decomposed as follows

$$\bar{L} = \begin{bmatrix} 0 & \mathbf{0}_N^T \\ a_0 & H \end{bmatrix}.$$

Here $a_0 = [a_{10}, a_{20}, ..., a_{N0}]^T$, and $H \in \mathbb{R}^{N \times N}$ is a submatrix of $\bar{L}$ corresponding to the interconnection among follower agents.

Remark 11. It should be noted that edge $(0,i) \in \bar{\mathcal{E}}$ represents the network connection between agent i and the exosystem. Referring to (2.8), their physical connection is described by matrix E_i. These two kinds of connections are not influenced by each other.

A distributed controller was introduced in [14] to solve the COR problem under continuous communication:

$$\dot{\eta}_i = S\eta_i + \mu(\sum_{j\in\mathcal{N}_i} a_{ij}(\eta_j - \eta_i) + a_{i0}(v - \eta_i)), \tag{3.6}$$

$$u_i = K_{1i}x_i + K_{2i}\eta_i. \tag{3.7}$$

Here, K_{1i}, K_{2i} and μ are the feedback gains to be designed; $\eta_i \in \mathbb{R}^q$ is introduced as a compensator.

Due to the network constraints, η_i and v are transmitted intermittently in a sampled-data manner. Denote the transmission instants of η_j, $j = 1, \cdots, N$, and v by t_0^j, t_1^j, $\cdots$ and t_0^0, t_1^0, $\cdots$, respectively, and assume there exists a $\delta > 0$ such that the transmission intervals satisfy $\delta \leq t_{k_i+1}^i - t_{k_i}^i \leq \tau_{mati}^i$ for all $k_i \in \mathbb{N}$, $i = 0, \cdots, N$. Here, the (sufficiently small) constant δ is used to exclude Zeno behavior; and τ_{mati}^i denote the MATI for agent i to be designed later. Furthermore, transmission delays, $\tau_{k_i}^i \in [0, \tau_{mad}^i]$ are considered for the broadcast of η_i (reference v), where τ_{mad}^i is the MAD for agent i (reference v). Referring to [32], [78] and [24], small delay case is considered in this work, that is, the broadcast data of a node is received by its neighbors before the next transmission. More specifically, the time delays satisfy $\tau_{k_i}^i \leq t_{k_i+1}^i - t_{k_i}^i$ resulting in $\tau_{mad}^i \leq \tau_{mati}^i$.

In order to cope with the communication imperfections, compensator (3.6) will be implemented in a model-based fashion [79] in between the adjacent updates (i.e. $t \in [t_{k_i}^i + \tau_{k_i}^i, t_{k_i+1}^i + \tau_{k_i+1}^i)$). In detail, (3.6) is transformed into the following form:

$$\dot{\eta}_i(t) = S\eta_i(t) + \mu(\sum_{j\in\mathcal{N}_i} a_{ij}(\bar{\eta}_j(t) - \bar{\eta}_i(t)) + a_{i0}(\bar{v}(t) - \bar{\eta}_i(t))), \tag{3.8}$$

where $\bar{\eta}_i$ and $\bar{v}$ satisfy

$$\begin{aligned}
&\dot{\bar{\eta}}_i(t) = S\bar{\eta}_i(t), \quad t \in [t^i_{k_i} + \tau^i_{k_i}, t^i_{k_i+1} + \tau^i_{k_i+1}),\\
&\dot{\bar{v}}(t) = S\bar{v}(t), \qquad t \in [t^0_{k_0} + \tau^0_{k_0}, t^0_{k_0+1} + \tau^0_{k_0+1}),\\
&\bar{\eta}_i((t^i_{k_i} + \tau^i_{k_i})^+) = \eta_i(t^i_{k_i}),\\
&\bar{v}((t^0_{k_0} + \tau^0_{k_0})^+) = v(t^0_{k_0}),
\end{aligned}$$

and we set

$$\bar{\eta}_i(t) = 0,\ t \in [0, t^i_1 + \tau^i_1),\ \text{and}\ \bar{v}(t) = 0,\ t \in [0, t^0_1 + \tau^0_1), \tag{3.9}$$

to generate the control input before receiving the initial broadcast signal from neighbors. Denote ϵ_i, as the measurement errors with $\epsilon_0 = v - \bar{v}$ and $\epsilon_i = \eta_i - \bar{\eta}_i$, $i = 1, \cdots, N$, and $\eta_{e_i} = \eta_i - v$ as the compensator error of agent i. In addition, let $\eta = [\eta_1^T, \cdots, \eta_N^T]^T$, $\hat{v} = \mathbf{1}_N \otimes v$, $\eta_e = [\eta_{e_1}^T, \cdots, \eta_{e_N}^T]^T$, $\epsilon = [\epsilon_1^T, \cdots, \epsilon_N^T]^T$, $\hat{\epsilon}_0 = \mathbf{1}_N \otimes \epsilon_0$, $\hat{\omega}_0 = \mathbf{1}_N \otimes \omega_0$ be the corresponding augmented vectors. Then, the compensator error follows the dynamics:

$$\dot{\eta}_e = \bar{S}_e\eta_e + \bar{H}_e\epsilon - \bar{H}_0\hat{\epsilon}_0 - \bar{G}_0\hat{\omega}_0, \tag{3.10}$$

and the errors ϵ and $\hat{\epsilon}_0$ follow

$$\begin{aligned}
\dot{\epsilon} &= \bar{S}_\eta\epsilon - \bar{H}_e\eta_e - \bar{H}_0\hat{\epsilon}_0,\\
\dot{\hat{\epsilon}}_0 &= \bar{G}_0\hat{\omega}_0,
\end{aligned} \tag{3.11}$$

where $\bar{S}_e = I_N \otimes S - \mu(H \otimes I_q)$, $\bar{H}_e = \mu(H \otimes I_q)$, $\bar{S}_\eta = I_N \otimes S + \mu(H \otimes I_q)$, $\bar{H}_0 = \mu\ \text{diag}([a_{10}, \cdots, a_{N0}]) \otimes I_q$, and $\bar{G}_0 = \mu\ \text{diag}([a_{10}, \cdots, a_{N0}]) \otimes G_0$.

Some commonly used assumptions for COR problems [14] are introduced as follows.

Assumption 7. The pairs (A_i, B_i) are stabilizable, $i = 1, 2, ..., N$.

Assumption 8. There exist solution pairs (X_i, U_i) for the following linear matrix equations

$$\begin{aligned}
X_iS &= A_iX_i + B_iU_i + E_i\\
0 &= C_iX_i + D_iU_i + F_i, \quad i = 1, 2, ..., N.
\end{aligned} \tag{3.12}$$

Assumption 9. The topology of the MAS is directed and contains a spanning tree with the reference signal as a root.

Next, we introduce the following results of COR problem when no network constraints are considered, i.e., all signals can be transmitted continuously.

Lemma 8. ([14]) Consider the MAS in (3.4), with reference signal in (3.5) and distributed controllers in (3.6) and (3.7). Under Assumptions 7–9, let K_{1i}, $i = 1, 2, \cdots, N$, satisfy that $A_i + B_i K_{1i}$ is Hurwitz, and K_{2i} be defined as

$$K_{2i} = U_i - K_{1i} X_i, \quad i = 1, \cdots, N, \tag{3.13}$$

where U_i and X_i are the solutions of (3.12). Then, in the disturbance-free case (i.e., $\omega_j = \mathbf{0}_{r_j}$, $j = 0, \cdots, N$), the COR can be solved asymptotically with a sufficiently large number μ in the sense of $\lim_{t\to\infty} \|e_i\| \to 0$.

According to Lemma 8, controller (3.6) and (3.7) solves the COR problem without communication constraints. To deal with asynchronous transmissions and time-varying delays, the emulation-based approach is applied in this work, that is, for the gains μ, K_{1i} and K_{2i}, $i \in 1, \cdots, N$, selected from Lemma 8, constrain the MATIs and MADs for each agent and the exosystem such that some closed-loop stability is preserved.

Let $e_{xi} = x_i - X_i v$, by (3.4)–(3.8),

$$\dot{e}_{xi} = (A_i + B_i K_{1i}) x_i + (B_i K_{2i} - X_i S) v + B_i K_{2i} \eta_{ei} - X_i \omega_0 + G_i \omega_i.$$

For K_{1i}, K_{2i} selected by Lemma 8, by (3.12) and (3.13), we have

$$\dot{e}_{xi} = (A_i + B_i K_{1i}) e_{xi} + B_i K_{2i} \eta_{ei} - X_i \omega_0 + G_i \omega_i.$$

Then, the tracking error e_i can be written as

$$e_i = (C_i + D_i K_{1i}) e_{xi} + D_i K_{2i} \eta_{ei}.$$

Subsequently, the MAS in (3.4) under controller (3.7) and (3.8), with K_{1i}, K_{2i} selected by Lemma 8 can be represented in terms of e_x, η_e with a tracking

error e as

$$\begin{aligned}\dot{e}_x &= \bar{A}e_x + \bar{B}\eta_e - \bar{X}\hat{\omega}_0 + \bar{G}\omega,\\ \dot{\eta}_e &= \bar{S}_e\eta_e + \bar{H}_e\epsilon - \bar{H}_0\hat{\epsilon}_0 - \bar{G}_0\hat{\omega}_0,\\ e &= \bar{C}e_x + \bar{D}\eta_e,\end{aligned} \tag{3.14}$$

where

$\bar{A} = \text{diag}(A_1 + B_1K_{11}, \cdots, A_N + B_NK_{1N})$, $\bar{B} = \text{diag}(B_1K_{21}, \cdots, B_NK_{2N})$,
$\bar{C} = \text{diag}(C_1 + D_1K_{11}, \cdots, C_N + D_NK_{1N})$, $\bar{D} = \text{diag}(D_1K_{21}, \cdots, D_1K_{2N})$,
$\bar{X} = \text{diag}(X_1, \cdots, X_N)$, $\bar{G} = \text{diag}(G_1, \cdots, G_N)$, $e_x = [e_{x_1}^T, \cdots, e_{x_N}^T]^T$,
$e = [e_1^T, \cdots, e_N^T]^T$, and $\omega = [\omega_1^T, \cdots, \omega_N^T]^T$.

3.2.3 Reformulation in a Hybrid System Framework

In this subsection, a hybrid system model as developed in [32] and [24] is established for the system in (3.14). Introduce auxiliary variables $l_i \in \{0, 1\}$, $s_i \in \mathbb{R}^q$, $k_i \in \mathbb{N}$, $\tau_i \in \mathbb{R}_{\geq 0}$, $i = 0, \cdots, N$, for agent i. The variable l_i is a Boolean that keeps tracking whether the next event of agent i is a transmission ($l_i = 0$) or an update ($l_i = 1$); s_i is introduced as a memory variable that stores the value $-\epsilon_i(t_{k_i}^i)$ at $t_{k_i}^i$ [24]. k_i is a counter that keeps tracking the number of transmissions for agent i, and τ_i is a timer to record the time elapsed since the last transmission. Then, the state vector for hybrid system $\mathcal{H}_{MAS}$ is introduced as $\xi := (e_x, \eta_e, \epsilon, \epsilon_0, s, \tau, k, l) \in \mathbb{X}$ where

$$\begin{aligned}\mathbb{X} = \Big\{&(e_x, \eta_e, \epsilon, \epsilon_0, s, \tau, k, l) \in \mathbb{R}^{(n_1+\cdots+n_N)} \times \mathbb{R}^{qN}\\ &\times \mathbb{R}^{qN} \times \mathbb{R}^q \times \mathbb{R}^{q(N+1)} \times \mathbb{R}_{\geq 0}^{N+1} \times \mathbb{N}^{N+1} \times \{0, 1\}^{N+1}\Big\},\\ s = [s_0^T, \cdots, s_N^T]^T,\ &\tau = [\tau_0, \cdots, \tau_N]^T,\ k = [k_0, \cdots, k_N]^T,\ l = [l_0, \cdots, l_N]^T.\end{aligned}$$

Combining state vector ξ with dynamics (3.14), the flow dynamics has the form of

$$F(\xi,\omega_0,\omega)=\begin{pmatrix}\bar{A}e_x+\bar{B}\eta_e-\bar{X}\hat{\omega}_0+\bar{G}\omega\\ \bar{S}_e\eta_e+\bar{H}_e\epsilon-\bar{H}_0\hat{\epsilon}_0-\bar{G}_0\hat{\omega}_0\\ \bar{S}_\eta\epsilon-\bar{H}_e\eta_e-\bar{H}_0\hat{\epsilon}_0\\ G_0\omega_0\\ \mathbf{0}_{N+1}\\ \mathbf{1}_{N+1}\\ \mathbf{0}_{N+1}\\ \mathbf{0}_{N+1}\end{pmatrix}. \tag{3.15}$$

The corresponding flow set is given by

$$C=\cap_{i=0}^{N}C_i, \tag{3.16}$$

where for $i=0,\cdots,N$, $C_i=\{\xi\in\mathbb{X}|((0\le\tau_i\le\tau^i_{mati})\wedge l_i=0)\vee((0\le\tau_i\le\tau^i_{mad})\wedge l_i=1)\}$.

The jump dynamics is in the form of

$$G(\xi)=\cup_{i=0}^{N}G_i(\xi),\ G_i(\xi)=\begin{cases}\{G_{0,i}(\xi)\}, & \xi\in D_i\wedge l_i=0\\ \{G_{1,i}(\xi)\}, & \xi\in D_i\wedge l_i=1\\ \emptyset, & \xi\notin D_i\end{cases}, \tag{3.17}$$

and

$$G_{0,i}(\xi)=\begin{pmatrix}e_x\\ \eta_e\\ \epsilon\\ \epsilon_0\\ \bar{\Sigma}_i[-\epsilon_0^T,-\epsilon^T]^T+(I_{q(N+1)}-\bar{\Sigma}_i)s\\ (I_{N+1}-\Sigma_i)\tau\\ k+\Sigma_i\mathbf{1}_{N+1}\\ l+\Sigma_i\mathbf{1}_{N+1}\end{pmatrix},$$

$$G_{1,i}(\xi)=\begin{pmatrix}e_x\\ \eta_e\\ \bar{\Sigma}_i s+[\epsilon^T,\epsilon_0^T]^T\\ (I_{q(N+1)}-\bar{\Sigma}_i)s\\ \tau\\ k\\ l-\Sigma_i\mathbf{1}_{N+1}\end{pmatrix}. \tag{3.18}$$

Here, $\bar{\Sigma}_i=\Sigma_i\otimes I_q$, and $\Sigma_i\in\mathbb{R}^{(N+1)\times(N+1)}$ is an diagonal matrix with the $(i+1,i+1)$-th element being 1 and others being 0. The corresponding jump

set is given by

$$D = \cup_{i=0}^{N} D_i, \tag{3.19}$$

where for $i = 0, \cdots, N$, $D_i = \{\xi \in \mathbb{X} | ((\delta \leq \tau_i \leq \tau_{mati}^i) \wedge l_i = 0) \vee ((\delta \leq \tau_i \leq \tau_{mad}^i) \wedge l_i = 1)\}$. Without loss of generality, assume all agents transmit local information at initial instant $t = 0$, then we have $t_1^i = 0$ and $l_i(0,0) = 1$. Combining with (3.9), the initial condition is given by $\xi(0,0) \in \mathbb{X}_0$, with

$$\mathbb{X}_0 = \{\xi \in \mathbb{X} | \epsilon = \eta, \epsilon_0 = v_0, s = [-\epsilon_0^T, -\epsilon^T]^T, l = \mathbf{1}\}.$$

According to the conditions give in [78], one can easily check that the hybrid system in (3.15)-(3.19) is well-posed.

Collecting all the transmission instants $(t_{k_i}^i)$ and update instants $(t_{k_i}^i + \tau_{k_i}^i)$ and rearranging them in an ascending order, a new time sequence is obtained, which is denoted by $\{t_k\}_{k=0}^{\infty}$. The solution domain for the hybrid system $\mathcal{H}_{MAS}$ (eq. (3.15)-(3.19)) is defined as dom $\xi = \cup_{j=0}^{J-1}([t_j, t_{j+1}], j)$ with J possibly ∞ and/or $t_J = \infty$.

Definition 5. ([24]) For the hybrid system $\mathcal{H}_{MAS}$ with $\omega_0 = \mathbf{0}$ and $\omega = \mathbf{0}$, the set given by $\mathcal{E} = \{\xi \in \mathbb{X} | \xi_e = \mathbf{0}\}$ is said to be uniformly globally asymptotically stable (UGAS) if there exists a function $\beta \in \mathcal{KLL}$ such that, for any initial condition $\xi(0,0) \in \mathbb{X}_0$, all corresponding solutions ξ satisfy

$$\|\xi_e(t,j)]\| \leq \beta(\|\xi_e(0,0)\|, t, j),$$

for all $(t,j) \in$ dom ξ, where $\xi_e = [e_x^T, \eta_e^T]^T$.

In the presence of ω_i, we are interested in bounding their influences on the tracking error e in (3.14), which is measured by the $\mathcal{L}_2$ gain when $\omega_i \in \mathcal{L}_2$, or by the $\mathcal{L}_\infty$ gain when $\omega_i \in \mathcal{L}_\infty$. Combining the hybrid model $\mathcal{H}_{MAS}$ with output e, the expanded hybrid system is denoted by $\mathcal{H}_{MAS}^e$.

Definition 6. ([24]) The hybrid system $\mathcal{H}_{MAS}^e$ is said to be $\mathcal{L}_p$-stable, $p \in \{2, \infty\}$, from input ω_i to output e with an $\mathcal{L}_p$-gain less than or equal to θ, if

there exists a $\mathcal{K}_\infty$-function β such that for any exogenous input $\omega_0, \omega \in \mathcal{L}_p$ and any initial condition $\xi(0,0) \in \mathbb{X}_0$, the solution to $\mathcal{H}_{MAS}$ satisfies

$$\|e\|_{\mathcal{L}_p} \leq \beta(\|\xi_e(0,0)\|) + \theta\|[\omega_0^T, \omega^T]^T\|_{\mathcal{L}_p}.$$

Therefore, the main interest of this work is to solve the sampled-data COR problem with asynchronous transmissions and time-varying delays. Specifically, for sufficiently large μ and control gains K_{1i}, K_{2i}, $i = 1, \cdots, N$, selected from Lemma 8, the bounds of τ^i_{mad}, τ^i_{mati} for agent i will be given such that (i) the hybrid system $\mathcal{H}_{MAS}$ in (3.15)-(3.19) is UGAS; (ii) the expanded hybrid system $\mathcal{H}^e_{MAS}$ is $\mathcal{L}_2$ ($\mathcal{L}_\infty$) stable.

3.3 Stability and Performance Analysis

In this subsection, we will first analyze the stability of the closed-loop system without disturbances. Then, the robustness of closed-loop systems (with $\mathcal{L}_2$ or $\mathcal{L}_\infty$ performance) is considered.

Initially, we introduce an auxiliary function $W_i(l_i, \epsilon_i, s_i)$ as

$$W_i(l_i, \epsilon_i, s_i) = \begin{cases} \|\epsilon_i\|, & l_i = 0 \\ \|\epsilon_i + s_i\|, & l_i = 1 \end{cases}, \ i = 0, \cdots, N. \tag{3.20}$$

For convenience, sometimes we will omit (some of) the arguments in $W_i(l_i, \epsilon_i, s_i)$ if there is no confusion from the context.

Lemma 9. The auxiliary function in (3.20) satisfies

$$W_i^+ = 0, \ l_i = 0; \text{ and } W_i^+ = W_i, \ l_i = 1, \tag{3.21}$$

for the jump dynamics in (3.18), and

$$\begin{aligned} \dot{W}_i(l_i, \epsilon_i, s_i) &\leq \|\bar{S}_{\eta_i}\epsilon - \bar{H}_{e_i}\eta_e - \bar{H}_{0_i}\hat{\epsilon}_0\|, \quad i = 1, \cdots, N, \\ \dot{W}_0(l_0, \epsilon_0, s_0) &\leq \|G_0\omega_0\|, \end{aligned} \tag{3.22}$$

for the flow dynamics in (3.15). Here, $\bar{S}_{\eta_i}$, $\bar{H}_{e_i}$ and $\bar{H}_{0_i}$ represent the submatrices composed by the $((i-1)q+1)$-th to (iq)-th rows of $\bar{S}_\eta$, $\bar{H}_e$ and $\bar{H}_0$, respectively.

Proof. According to the jump dynamics in (3.18), we have

$$\begin{aligned} W_j^+ &= W_j(1, \epsilon_j, -\epsilon_j) = \|\epsilon_j - \epsilon_j\| = 0, \quad l_j = 0, \\ W_j^+ &= W_j(0, \epsilon_j + s_j, 0) = \|\epsilon_j + s_j\| = W_i(1, \epsilon_j, s_j) \\ &= W_j, \quad l_j = 1. \end{aligned} \tag{3.23}$$

For the flow dynamics in (3.15), since $\dot{s}_j = 0$, we have

$$\begin{aligned} \dot{W}_j &= \frac{d\|\epsilon_j\|}{dt} \leq \|\dot{\epsilon}_j\|, \quad l_j = 0; \\ \dot{W}_j &= \frac{d\|\epsilon_j + s_j\|}{dt} \leq \|\dot{\epsilon}_j\| + \|\dot{s}_j\| = \|\dot{\epsilon}_j\|, \ l_j = 1, \end{aligned} \tag{3.24}$$

where $j = 0, \cdots, N$. Combining with the third and fourth equations in (3.15), we establish the inequalities in (3.22) and complete the proof. □

In addition, introduce the following differential equations for agent i, $i = 0, \cdots, N$,

$$\dot{\phi}_i(\tau_i) = -\gamma_i(\phi_i^2(\tau_i) + 1), \ \dot{\hat{\phi}}_i(\tau_i) = -\gamma_i(\hat{\phi}_i^2(\tau_i) + 1), \tag{3.25}$$

where $\gamma_i > 0$ are real constants to be designed. It can be noticed that the solutions to (3.25) are strictly decreasing when ϕ_i and $\hat{\phi}_i$ are nonnegative. Next, we will show that under well-designed γ_i and initial conditions of $\phi_i(0)$ or $\hat{\phi}_i(0)$, the time for ϕ_i or $\hat{\phi}_i$ to drop to a relative small value can be used to formulate the constraints on transmission intervals or time delays.

Condition 1. Assumptions 7–9 are satisfied and the control gains μ and K_{1i}, K_{2i}, $i = 1, \cdots, N$, are selected according to Lemma 8.

Condition 2. The transmission intervals and time delays for agent i, $i = 0, \cdots, N$, satisfy

$$\begin{aligned} \hat{\phi}_i(0) \leq \phi_i(\tau_i), \ \delta \leq \tau_i \leq \tau_{mati}^i; \\ \hat{\phi}_i(\tau_i) > 0, \qquad 0 \leq \tau_i \leq \tau_{mad}^i. \end{aligned} \tag{3.26}$$

Condition 3. There exist positive definite matrix $P \in \mathbb{R}^{Nq\times Nq}$, constants $\gamma_i > 0$, $i = 0, \cdots, N$, $\rho_w > 0$, $\rho > 0$, $\rho_\epsilon > 0$ and $\rho_{\epsilon_0} > 0$, such that the following linear matrix inequality (LMI) holds

$$\begin{bmatrix} A_{\eta_e}+\rho I_{qN} & P\bar{H}_e+2\bar{H}_e^T\bar{S}_\eta & -P\bar{H}_0+2\bar{H}_e^T\bar{H}_0 & -P\bar{G}_0 \\ * & A_\epsilon-\Gamma+\rho_\epsilon I_{qN} & -2\bar{S}_\eta\bar{H}_e^T & 0_{Nq\times Nq} \\ * & * & A_{\epsilon_0}-\Gamma_0+\rho_{\epsilon_0}I_q & 0_{q\times Nq} \\ * & * & * & A_w-\rho_w I_{qN} \end{bmatrix} \leq 0, \tag{3.27}$$

where $A_{\eta_e} = P\bar{S}_e + \bar{S}_e^T P + 2\bar{H}_e^T\bar{H}_e$, $A_\epsilon = 2\bar{S}_\eta^T\bar{S}_\eta$, $A_{\epsilon_0} = 2\bar{H}_0^T\bar{H}_0$, $A_\omega = \bar{G}_0^T\bar{G}_0$, $\Gamma = \text{diag}(\gamma_1, \cdots, \gamma_N) \otimes I_q$, $\Gamma_0 = \gamma_0 \otimes I_q$.

Theorem 6. Consider the hybrid system $\mathcal{H}_{MAS}$ in (3.15)-(3.19) with no disturbances (i.e., $\omega_0 = \mathbf{0}$, $\omega = \mathbf{0}$). The set $\mathcal{E}$ is UGAS, if Conditions 1, 2 hold and Condition 3 is satisfied with $\rho_\omega = 0$ and $\bar{G}_0 = 0$.

Proof. Consider a storage function

$$U(\tilde{\xi}) = V + \sum_{i=0}^{N}(\gamma_i\phi_i W_i^2(l_i, \epsilon_i, s_i) + l_i\gamma_i\hat{\phi}_i W_i^2(0, \epsilon_i, s_i)), \tag{3.28}$$

where $V = \eta_e^T P\eta_e$ and $\tilde{\xi} = [\eta_e^T, \epsilon^T, \epsilon_0^T, s^T, \tau^T, k^T, l^T]^T$. With some abuse of notations, we write $W_i(0, \epsilon_i, s_i)$ as $W_{0,i}$, and $W_i(1, \epsilon_i, s_i)$ as $W_{1,i}$.

According to Lemma 9, on the flow domain, we have

$$\begin{aligned} \left\langle \nabla U(\tilde{\xi}), F(\tilde{\xi}, \omega_0) \right\rangle \leq & \dot{V} + \sum_{i=0}^{N} \big(2\gamma_i\phi_i W_{l_i,i}\|\dot{\epsilon}_i\| - \gamma_i^2(\phi_i^2+1)W_{l_i,i}^2 \\ & + l_i(2\gamma_i\hat{\phi}_i W_{0,i}\|\dot{\epsilon}_i\| - \gamma_i^2(\phi_i^2+1)W_{0,i}^2)\big). \end{aligned}$$

Combining with (3.15), we have

$$\begin{aligned} & \left\langle \nabla U(\tilde{\xi}), F(\tilde{\xi}, \omega_0) \right\rangle \leq \\ & -\sum_{i\in L_0}(\gamma_i\phi_i\|\epsilon_i\| - \|\dot{\epsilon}_i\|)^2 - \sum_{i\in L_1}\gamma_i^2 W_i^2 + [\ \eta_e^T,\ \epsilon^T,\ \epsilon_0^T,\ \hat{\omega}_0^T\ ]\Xi[\ \eta_e^T,\ \epsilon^T,\ \epsilon_0^T,\ \hat{\omega}_0^T\ ]^T \\ & -\sum_{i\in L_1}\big((\gamma_i\phi_i W_i - \|\dot{\epsilon}_i\|)^2 + (\gamma_i\hat{\phi}_i\|\epsilon_i\| - \|\dot{\epsilon}_i\|)^2\big), \end{aligned}$$

where $L_j = \{i \in \{0, \cdots, N\} |\ l_i = j\}$, and

$$\Xi = \begin{bmatrix} A_{\eta_e} & P\bar{H}_e+2\bar{H}_e^T\bar{S}_\eta & -P\bar{H}_0+2\bar{H}_e^T\bar{H}_0 & -P\bar{G}_0 \\ * & A_\epsilon-\Gamma & -2\bar{S}_\eta\bar{H}_e^T & 0_{Nq\times Nq} \\ * & * & A_{\epsilon_0}-\Gamma_0 & 0_{q\times Nq} \\ * & * & * & A_w \end{bmatrix}.$$

From Condition 3 we have

$$\begin{aligned}&\left\langle \nabla U(\tilde{\xi}), F(\tilde{\xi},\omega_0)\right\rangle\\ \leq&-\rho\|\eta_e\|^2-\rho_\epsilon^2\|\epsilon\|^2-\rho_{\epsilon_0}\|\epsilon_0\|^2+\rho_\omega\|\hat{\omega}_0\|^2-\sum_{i\in L_1}\gamma_i^2W_{1,i}^2\\ \leq&-\rho\|\eta_e\|^2-\sum_{i=0}^{N}\alpha_i(W_i)+\rho_\omega\|\hat{\omega}_0\|^2\end{aligned}\tag{3.29}$$

where α_i is a class-$\mathcal{K}_\infty$ function.

When there is a reset caused by a transmission event of agent i, referring to Lemma 9 and the first inequality in (3.26), we have

$$\begin{aligned}&U(\tilde{\xi}^+)-U(\tilde{\xi})=\\ &\gamma_i\phi_i(0)W_i^2(1,\epsilon_i,-\epsilon_i)+\gamma_i\hat{\phi}_i(0)W_i^2(0,\epsilon_i,-\epsilon_i)-\gamma_i\phi_i(\tau_i)W_i^2(0,\epsilon_i,s_i)<0.\end{aligned}\tag{3.30}$$

Similarly, when there is a reset caused by an update event of agent i, we have

$$\begin{aligned}&U(\tilde{\xi}^+)-U(\tilde{\xi})\\ =&\gamma_i\phi_i(\tau_i)W_i^2(0,\epsilon_i+s_i,0)-\gamma_i\phi_i(\tau_i)W_i^2(1,\epsilon_i,s_i)-\gamma_i\hat{\phi}_i(\tau_i)W_i^2(0,\epsilon_i,s_i)\\ \leq&-\gamma_i\hat{\phi}_i(\tau_i)W_i^2(0,\epsilon_i,s_i)<0.\end{aligned}\tag{3.31}$$

When $\omega_i=\mathbf{0}$, $i=0,\cdots,N$, (3.29)–(3.31) imply

$$\begin{aligned}\left\langle \nabla U(\tilde{\xi}), F(\tilde{\xi},\omega_0)\right\rangle\leq-\rho\|\eta_e\|^2-\sum_{i=0}^{N}\alpha_i(W_i),\ \ \xi\in C;\\ U(\tilde{\xi}^+)-U(\tilde{\xi})<0,\ \ \xi\in D.\end{aligned}\tag{3.32}$$

According to Lemma 8, $\bar{A}$ is Hurwitz; there always exist positive definite matrices P_e, Q_x and Q_η such that

$$\left[\begin{smallmatrix}P_e\bar{A}+\bar{A}^TP_e+Q_x & P_e\bar{B}\\ \bar{B}^TP_e & -Q_\eta\end{smallmatrix}\right]<0.\tag{3.33}$$

Let the minimum eigenvalues of Q_x and Q_η be λ_x and λ_η, respectively. Consider a Lyapunov candidate

$$U_e(\xi)=V_e+\alpha_eU(\tilde{\xi}),\tag{3.34}$$

where $V_e = e_x^T P_e e_x$, $\alpha_e = \frac{2\lambda_\eta}{\rho}$. According to (3.15) and (3.32), on the flow domain, we have

$$\begin{aligned}
&\langle \nabla U_e, F(\xi, \mathbf{0}, \mathbf{0}) \rangle \\
=&e_x^T (P_e \bar{A} + \bar{A}^T P_e) e_x + 2 e_x^T P_e \bar{B} \eta_e - \alpha_e (\rho \|\eta_e\|^2 + \sum_{i=0}^{N} \alpha_i(W_i)) \\
\leq& -\lambda_x \|e_x\|^2 - \lambda_\eta \|\eta_e\|^2 - \alpha_e \sum_{i=0}^{N} \alpha_i(W_i).
\end{aligned}$$

Referring to (3.18) and (3.32), $U_e^+ \leq U_e$ on the jump domain.

Using the standard Lyapunov arguments in [78], we have

$$U_e(t, j) \leq \beta(\|V_{e0}, V_0, W_0\|, t, j), \tag{3.35}$$

where V_{e0}, V_0 and W_0 represent the initial value of V_e, V and $\sum_{i=0}^{N} W_i$ at $t = 0$, respectively. By (3.20), we have for $\xi(0,0) \in \mathbb{X}_0$, $W_0 = 0$. Then

$$U_e(t, j) \leq \beta(\|V_{e0}, V_0\|, t, j).$$

Furthermore, by the definition of V and V_e, we have $\bar{\alpha}\|\eta_e\|^2 \leq V \leq \underline{\alpha}\|\eta_e\|^2$ and $\bar{\alpha}_e\|e_x\|^2 \leq V_e \leq \underline{\alpha}_e\|e_x\|^2$, where $\bar{\alpha}$, $\underline{\alpha}$ and $\bar{\alpha}_e$, $\underline{\alpha}_e$ represent the maximum and minimum eigenvalues of P and P_e, respectively; and since $V_e + \alpha_e V \leq U_e$, (3.35) can be written as

$$\|\xi_e(t, j)\| \leq \frac{1}{\underline{\alpha}_\xi} \beta(\bar{\alpha}_\xi \|\xi_e(0,0)\|^2, t, j) = \beta_1(\xi_e(0,0), t, j) \tag{3.36}$$

where β_1 is a class–$\mathcal{KLL}$ function, $\bar{\alpha}_\xi = \max\{\bar{\alpha}, \bar{\alpha}_e\}$ and $\underline{\alpha}_\xi = \min\{\underline{\alpha}, \underline{\alpha}_e\}$. By Definition 5, $\mathcal{E}$ is UGAS and the proof is completed. □

Remark 12. Referring to Lyapunov candidate (3.28), the effect of time delay is described by $\gamma_i \hat{\phi}_i W_i^2$ and the effect of transmission intervals is described by $\gamma_i \phi_i W_i^2$. Thereby, the first inequality in Condition 2 characterizes (i) the MATIs due to $\phi_i(\tau_i) > 0$ for all $\tau_i \in [0, \tau_{mati}^i]$, and (ii) how much transmission performance can be sacrificed to cope with delays by requiring $\phi_i(\tau_{mati}^i) \geq \hat{\phi}_i(0)$. The second inequality gives the MADs by ensuring the positive definiteness of U. The LMI in (3.27) in Condition 3 is used to ensure the Lyapunov candidate

decreases during the flow domain, and (3.27) always holds when ρ_ω and γ_i, $i = 0, \cdots, N$, are large enough.

Theorem 7. Consider the hybrid system $\mathcal{H}^e_{MAS}$ with $\mathcal{H}_{MAS}$ given in (3.15)-(3.19) and output e in (3.14). $\mathcal{H}^e_{MAS}$ is finite gain $\mathcal{L}_2$ ($\mathcal{L}_\infty$) stable under $\mathcal{L}_2$ ($\mathcal{L}_\infty$) disturbances (i.e. $\omega_0,\ \omega \in \mathcal{L}_2$ ($\mathcal{L}_\infty$)) if Conditions 1–3 are satisfied.

Proof. Consider the same Lyapunov candidate as in (3.34), referring to (3.29), on the flow domain, we have

$$\begin{aligned}
&\langle \nabla U_e(\xi), F(\xi, \omega, \hat{\omega}_0) \rangle \\
\leq & e_x^T (P_e \bar{A} + \bar{A}^T P_e) e_x + 2 e_x^T P_e \bar{B} \eta_e + 2 e_x^T P_e \bar{X} \hat{\omega}_0 - 2 e_x^T P_e \bar{G} \hat{\omega} \\
& - \alpha_e (\rho \|\eta_e\|^2 + \sum_{i=0}^{N} \alpha_i(W_i) - \rho_\omega \|\hat{\omega}_0\|^2).
\end{aligned}$$

By (3.33), there always exist positive constants λ_{xe}, λ_η, λ_ω and λ_0 such that

$$\begin{aligned}
&\langle \nabla U_e, F(\xi, \omega, \hat{\omega}_0) \rangle \\
\leq & - \lambda_{xe} \|e_x\|^2 - \lambda_\eta \|\eta_e\|^2 - \alpha_e \sum_{i=0}^{N} \alpha_i(W_i) + \lambda_\omega \|\omega\|^2 + \lambda_0 \|\hat{\omega}_0\|^2,
\end{aligned}$$

and by (3.18) and (3.32), $U_e^+ \leq U_e$ on the jump domain.

Using the standard Lyapunov arguments in [78] and following a similar procedure as in Theorem 6, there exist a class–$\mathcal{K}_\infty$ function β_2 and a positive constant θ such that for $\omega,\ \hat{\omega}_0 \in \mathcal{L}_2$, we have

$$\|\xi_e\|_{\mathcal{L}_2} \leq \beta_2(\|(\xi_e(0,0)\|) + \theta \|[\omega^T, \hat{\omega}_0^T]^T\|\|_{\mathcal{L}_2}. \tag{3.37}$$

Furthermore, by (3.14),

$$\|e\| \leq \lambda_C \|e_x\| + \lambda_D \|\eta_e\|,$$

where λ_C and λ_D are the maximum singular values of matrix $\bar{C}$ and $\bar{D}$, respectively. Then,

$$\|e\|_{\mathcal{L}_2} \leq \lambda \|\xi_e\|_{\mathcal{L}_2} \leq \beta_x(\|e(0,0)\|) + \theta_x \|[\omega^T, \hat{\omega}_0^T]^T\|_{\mathcal{L}_2},$$

where $\lambda = \max\{\lambda_C, \lambda_D\}$, θ_x is a positive constant and β_x is a class–$\mathcal{K}_\infty$ function. Then, by Definition 6, we come to the conclusion that $\mathcal{H}^e_{MAS}$ is $\mathcal{L}_2$–stable with ω_0 and ω as inputs.

Following similar arguments, the conclusion for $\mathcal{L}_\infty$–stability can be obtained. The proof is completed. □

Remark 13. The UGAS property with asynchronous transmissions and time-varying delays have been studied in [50] for MASs as well. However, the method used in [50] followed the one proposed in [32] and [24], which was unable to cover the framework proposed in this work. In their method, the auxiliary function $\tilde{W}_i$ satisfied ((17a), (17b) in [24])

$$\tilde{W}_i^+ \leq \lambda \tilde{W}_i, \quad l_i = 0; \text{ and } \tilde{W}_i^+ \leq \tilde{W}_i, \quad l_i = 1,$$

and the constraints on MATIs and MADs are derived according to

$$\hat{\gamma}_i \hat{\phi}_i(0) \leq \lambda^2 \gamma_i \phi_i(\tau_i), \quad 0 \leq \tau_i \leq \tau^i_{mati},$$
$$\hat{\gamma}_i \hat{\phi}_i(\tau_i) \geq \gamma_i \phi_i(\tau_i), \quad 0 \leq \tau_i \leq \tau^i_{mad},$$

with $\hat{\gamma}_i = \frac{M_1 \gamma_i \lambda_W}{\lambda}$ ((48) in [24]) replacing γ_i for the dynamics of $\hat{\phi}$ in (3.25). Therefore, when λ approaches to zero (sampled-data case), $\hat{\gamma}_i$ approaches to infinity, which means $\hat{\phi}_i$ decreases very fast and results in a very small MAD. This is inconsistent with the intuition that a better transmission protocol (smaller λ) usually results in fewer restrictions on the communication infrastructure (e.g., MADs and MATIs). According to the novel Lyapunov candidate proposed in this work, the upper bounds of MADs are derived by the second inequality in Condition 2 and are independent of $\hat{\gamma}_i$. As a result, the inconsistency at $\lambda = 0$ can be avoided. In addition, compared with the $\tilde{W}_i$ used in [24] (Eq. (46)), the auxiliary function W_i in this work (Eq. (3.20)) has a simpler form and a smaller value. Thus, the complexity in analyzing the stability and deriving the results is relived.

Another merit of the method proposed in this work is that after excluding the redundant variable λ, a more intuitive analysis on the trade-off between MATIs and MASs for MASs can be provided.

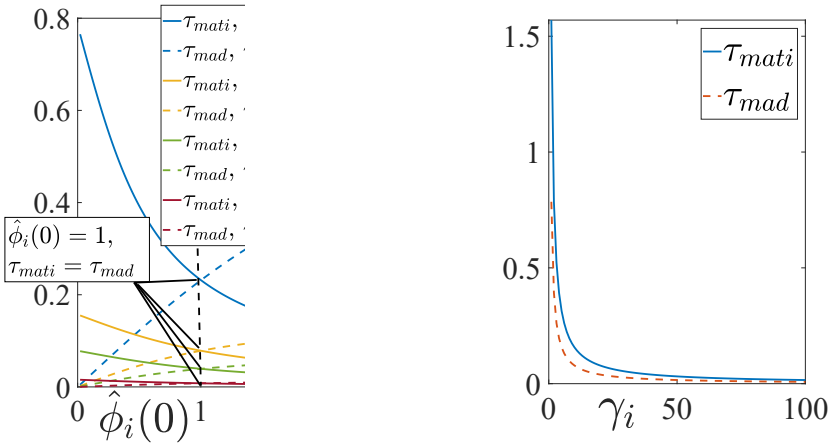

(a) Trade-off curves of MATIs and MADs (b) Maximum values of MATIs and MADs

Figure 3.1: Analysis of MATIs and MADs

Remark 14. Referring to Condition 2 and (3.25), the MATIs and MADs can be expressed explicitly as

$$\begin{aligned} \tau^i_{mad} &= \frac{1}{\gamma_i} \arctan \frac{1 - \sigma_i/\hat{\phi}_i(0)}{1/\hat{\phi}_i(0) + \sigma_i}, \\ \tau^i_{mati} &= \frac{1}{\gamma_i} \arctan \frac{1 - \hat{\phi}_i(0)/\phi_i(0)}{1/\phi_i(0) + \hat{\phi}_i(0)}, \end{aligned} \tag{3.38}$$

where σ_i represents a user-specified lower bound of $\hat{\phi}_i$. It can be seen that, a smaller γ_i is preferred, which results in larger MATIs and MADs. This could be achieved by solving the LMI in (3.27) with minimizing the objective function trace(Γ). In addition, a larger initial value of $\phi_i(0)$ leads to a larger MATI without affecting MADs. Thus, a sufficiently large $\phi_i(0)$ can be chosen at first. For MAD, it can be tuned by the initial value $\hat{\phi}_i(0)$. However, based on the small delay assumption, MADs must be smaller than MATIs.

Consider a bunch of hybrid systems $\mathcal{H}_{MAS}$ with different system matrices (i.e. $\bar{A}$, $\bar{B}$). Assume γ_i for each $\mathcal{H}_{MAS}$ satisfies the corresponding LMI in (3.27) with minimizing trace(Γ). Then, by tuning $\hat{\phi}_i(0)$, trade-off curves between MADs and MATIs are illustrated in Figure 3.1(a). A larger initial value of $\hat{\phi}_i(0)$ increases the MAD but decreases the MATI, and the intersection

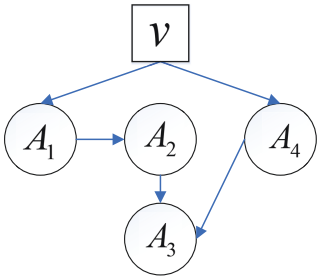

Figure 3.2: Topology of the MAS

always happens at $\hat{\phi}_i(0) = 1$ in spit of γ_i. Therefore, $\hat{\phi}_i(0)$ should be upper bounded by 1 and the corresponding τ^i_{mad} serves as the upper bound of MAD. The maximum value of MATIs happens when MADs approach to zero. The relationship between γ_i and the maximum values of MATI and MAD is shown in Figure 3.1(b).

3.4 Simulation Results

In this section, we use some simulation examples to show the UGAS and the $\mathcal{L}_2$ ($\mathcal{L}_\infty$) performance of the hybrid system $\mathcal{H}_{MAS}$ and $\mathcal{H}^e_{MAS}$, respectively. Consider a heterogeneous MAS containing 4 agents and an exosystem v connected by a communication network as shown in Figure 3.2. The matrices for system (3.4) are given as

$$A_1 = 1, A_2=\begin{bmatrix} 0 & 1 & 0 \\ 0 & 0 & 1 \\ 0 & 0 & -10 \end{bmatrix}, A_3=\begin{bmatrix} 0 & 1 & 0 \\ 0 & 0 & 1 \\ 0 & -10 & -2 \end{bmatrix}, A_4=\begin{bmatrix} 0 & 1 & 0 \\ 0 & 0 & 1 \\ 0 & -1 & -2 \end{bmatrix}, B_1 = 1,\ B_2 = [0\ 0\ 2]^T,$$
$$B_3 = B_4 = [0\ 0\ 1]^T, C_1 = \begin{bmatrix} 1 \\ -1 \end{bmatrix},\ E_1 = [0, -1],\ F_1 = \begin{bmatrix} 1 & 1 \\ -1 & -1 \end{bmatrix},\ G_1 = 1,$$
$$C_i = \begin{bmatrix} 1 & 0 & 0 \\ 0 & 1 & 0 \end{bmatrix}, E_i = \begin{bmatrix} -0.5i & 0 \\ -1 & 0.5i \\ 0 & 0 \end{bmatrix}, F_i = \begin{bmatrix} -1 & 0 \\ -0.5i & -1 \end{bmatrix}, G_i = \mathbf{1}_3,$$
$$S = \begin{bmatrix} 0 & 1 \\ -1 & 0 \end{bmatrix}, G_v = \mathbf{1}_2, i = 2, \cdots, 4.$$

Based on Lemma 8, the feedback matrices are given as $K_{11} = -3$, $K_{1i} = [-1\ \ -1\ \ -1]$, $i = 2, \cdots, 4$, $K_{21} = [-1\ 2]$, $K_{22} = [2\ 1]$, $K_{23} = [17.5\ 11]$, and $K_{24} = [5\ 2]$. The initial values and lower bound are chosen as $\hat{\phi}_i(0) = \pi/5$, $\phi_i(0) = 10000$ and $\sigma_i = 0.0001$.

First, we consider the case without disturbances. The MATIs and MADs computed by (3.38) are shown in Table 3.1. The tracking errors are shown in

Table 3.1: MATIs and MADs for UGAS

Agent/Reference	1	2	3	4	v
MATI	0.0780	0.0525	0.0454	0.0579	0.0553
MAD	0.0308	0.0207	0.0179	0.0228	0.0218

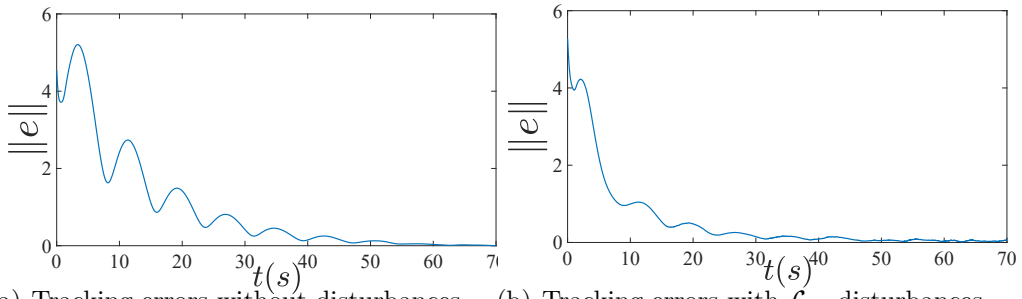

(a) Tracking errors without disturbances (b) Tracking errors with $\mathcal{L}_\infty$ disturbances

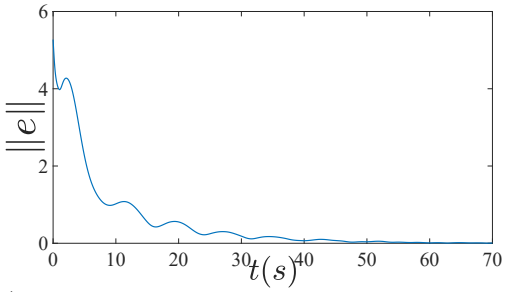

(c) Tracking errors with $\mathcal{L}_2$ disturbances

Figure 3.3: Tracking errors of MASs

Figure 3.3(a), which converge to zero as we expect.

Assume $\mathcal{H}^e_{MAS}$ is subject to $\mathcal{L}_\infty$ disturbances, with $\|\omega_i\|_{\mathcal{L}_\infty} \leq 0.1$, $i = 0, \cdots, N$. The MATIs and MADs computed by (3.38) are shown in Table 3.2. The tracking errors are shown in Figure 3.3(b), which are $\mathcal{L}_\infty$ stable, with

Table 3.2: MATIs and MADs for $\mathcal{L}_\infty/\mathcal{L}_2$ stability

Agent/Reference	1	2	3	4	v
MATI	0.0617	0.0519	0.0430	0.0508	0.0497
MAD	0.0244	0.0205	0.0170	0.0200	0.0196

steady state errors shown in Table 3.3.

For the case when $\mathcal{H}^e_{MAS}$ is subject to $\mathcal{L}_2$ disturbances, we assume $\|\omega_i(t)\| = 0.1e^{-10(t-t_0)}$. The corresponding MATIs and MADs are the same with the $\mathcal{L}_\infty$ case. The tracking errors are shown in Figure 3.3(c), which are $\mathcal{L}_2$ stable.

Table 3.3: Steady-state tracking errors

Agent	1	2	3	4
Steady-State Errors	0.0103	0.0696	0.0339	0.0178

In addition, by assigning a zero initial value to the tracking error e, we use $\theta = (\int_{t_0}^{t_f} \|e\|dt)/(\int_{t_0}^{t_f} \|[\omega^T, \omega_0]^T\|dt)$ to estimate the $\mathcal{L}_2$ gain in a simulation sense. The simulated $\mathcal{L}_2$ gain is given by $\theta = 3.9010$.

3.5 Summary

A sampled-data COR problem with asynchronous transmissions and time-varying delays was investigated in this chapter. We formulated the problem in a hybrid system framework and proposed a new method to establish the constraints on MATIs and MADs. It was proved that if these constraints were satisfied, both UGAS and $\mathcal{L}_2$ ($\mathcal{L}_\infty$) stability could be guaranteed. In addition, we proposed a novel Lyapunov candidate, based on which, MATIs and MADs could be computed in a more straightforward way. Therefore, more intuitive trade-off curves between MATIs and MADs could be given. The effectiveness of the method was also illustrated by a simulation example.

Chapter 4

Formation Tracking Without Velocity Measurements under Hybrid-Triggered Mechanism*

4.1 Overview

This chapter focuses on solving the leader-follower formation tracking problem of multiple mobile robots under a hybrid-triggered mechanism without leader's velocity measurements. In order to accomplish this collaborative goal, the communication among agents is critical, and can be carried out by the detections from agents' on-board sensors or the transmissions via some embedded wireless devices. The first kind is implemented in an active way in a sense that each agent decides when to detect relative information from its neighbors by itself, and defined as PULC; while in the second kind, each agent passively receives the transmitted information from its neighbors, resulting in PUSC. Some situations like cooperative localization require both of them. However, the existing results processed the obtained information from different kinds in a same way [80, 81] which actually ignored the unique features of different communication.

*A version of this chapter has been accepted as: J. Yang, H. Yu, and F. Xiao, Hybrid-triggered formation tracking control of mobile robots without velocity measurements. *International Journal of Robust and Nonlinear Control*. A short version has been accepted as J. Yang, H. Yu and F. Xiao, Strong integral-input-to-state stability for cascade-connected systems. *5th International Conference on Control and Fault-Tolerant Systems, Sept. 29th, 30th and Oct. 1st, 2021, Saint-Raphael, France.*

In practice, the leader's velocity is hard to be measured accurately. Moreover, for mobile robots which will be studied in this work, their velocity estimations are challenging due to the nonholonomic constraints. Because of the unmeasurable leader's velocity, a high gain observer is adopted to estimate leader's velocity with arbitrarily small estimation errors in finite time. Compared with [77], which required the leader's trajectories to follow some predetermined polynomials, we only constrain the upper bounds of leader's velocities and accelerations. According to the detection capacity to leader's information, we formulate the MAS in a hierarchical structure, where an agent belongs to the middle level if it has access to the leader directly, and belongs to the bottom level otherwise. Benefited from this, the cyclic accumulation of estimation errors among followers are cut off at the middle level, resulting in the relaxation of the acyclic assumption in [66].

Two kinds of communication networks are considered separately in this work. The detected information by PULC is used directly. In order to reduce network load, PETC is used for PUSC, in a way that the transmitted data is evaluated by a predetermined ET condition, and updated only when the condition is satisfied. Since PETC is only used for PUSC, the mechanism implemented here is considered as a hybrid-triggered one. However, the separate analysis on PULC and PUSC indicates that the classical Lyapunov function candidates used in [47] and [82], which considered only one kind of communication networks cannot be applied directly in this work. As alternatives, new Lyapunov candidates are proposed to analyze the sampled-data MAS connected by the above networks. Specifically, for agents in the middle level, a novel Lyapunov candidate is proposed to determine the MASPs for detecting relative information from the leader, achieving a small enough estimation error and short enough convergence time. Their explicit expressions reveal the trade-off between better estimation performance and larger MASPs. For the agents in the bottom level, the estimation of leader's velocity and position relies on both PULC and PUSC. MASPs and MACPs are deter-

mined with well-designed PETMs to ensure the stability of the sampled-data system. By investigating the closed-loop dynamics, we reconstruct the system into a cascade-connected structure. Based on that, the problem is tackled by introducing the concept of strongly iISS [83] in a hybrid system framework, in a sense that the sampled-data system is ISS when external disturbances are bounded by a predetermined threshold, while it is iISS otherwise; and a novel Lyapunov method is introduced to solve the problem. Numerical examples are presented to illustrate the effectiveness of the proposed methods.

It should be noted that, although the leader-follower formation tracking of mobile robots is a specific problem, the methods proposed in this work are summarized in general forms, which may enable their utilization in other relevant problems.

4.2 Preliminaries and Problem Formulation

In this section, we first introduce some preliminaries; then, the formation tracking problem of multiple mobile robots in a continuous-time framework is introduced; after that, considering the inherent discrete-time property of data transmissions and detections among agents, we propose a novel information flow architecture for the MAS.

4.2.1 Preliminaries

Some preliminaries on graph theory are the same as those in Section 2.2.1, and the definitions of Laplacian matrix and hybrid systems are the same as those in Section 3.2.1. Given a set $\Xi \subset \mathbb{R}^n$ and $x \in \mathbb{R}^n$, we define the distance from x to Ξ by $|x|_\Xi = \inf_{y\in\Xi} |x - y|$.

Definition 7 (Locally strongly iISS)**.** For the hybrid system in (3.1), the set $\Xi \subset \mathbb{X}$ is said to be locally strongly iISS w.r.t. ς if there exist $R > 0$, $\beta \in \mathcal{KLL}$ and σ_1, σ_2, σ_3, $\sigma_4 \in \mathcal{K}_\infty$ such that for all $\varsigma \in \mathbb{R}^{n_\varsigma}$, $\xi(0, 0) \in \mathbb{X}_1 \subset \mathbb{X}$

and $(t,j) \in \text{dom}\ \xi$, the corresponding solutions ξ satisfy

$$\begin{aligned}|\xi(t,j)|_\Xi \leq & \beta(|\xi(0,0)|_\Xi, t, j) + \sigma_1 \sum_{i=0}^{J-1}\Big(\int_{t_i}^{t_{i+1}} \sigma_2(\|\varsigma(s,i)\|)ds + \sigma_4(\|\varsigma(t_{i+1}, i+1)\|)\Big) \\ & + \sigma_1 \int_{t_J}^{t} \sigma_2(\|\varsigma(s,J)\|)ds, \\ |\xi(t,j)|_\Xi \leq & \beta(|\xi(0,0)|_\Xi, t, j) + \sigma_3(|\varsigma|_{(t,j)}), \quad |\varsigma|_{(t,j)} \leq R,\end{aligned}$$

where $|\varsigma|_{(t,j)}$ represents the supremum norm of ς up to the hybrid time (t,j) (see the reference [84] for a precise definition); J could be ∞ and/or $t_J = \infty$. Furthermore, when $R = \infty$ ($\mathbb{X}_1 = \mathbb{X}$), the set Ξ is said to be ISS (globally strongly iISS).

4.2.2 Continuous-Time Formation Tracking Problem

Consider a MAS consisting of $(n+1)$ mobile robots moving on a plane, with the dynamics of the i-th robot R_i given by

$$\dot{x}_i = v_i \cos(\Phi_i),\ \dot{y}_i = v_i \sin(\Phi_i),\ \dot{\Phi}_i = \omega_i, \quad i = 0, \cdots, n, \tag{4.1}$$

and $i = 0$ stands for the leader's dynamics. Assume the robots are connected by a graph $\mathcal{G}$, where each node i represents a mobile robot and the edge (i,j) represents the information flow among the MAS. Assume that the first n_m followers can detect relative information directly from the leader, and the rest of $n_f = n - n_m$ followers can only detect relative information from their neighbouring followers. Then, the followers are divided into two groups, where $\mathcal{N}_m$ is defined as the middle level set and $\mathcal{N}_f$ is defined as the bottom level set; $i \in \mathcal{N}_m$, if agent i can detect information directly from the leader; and $i \in \mathcal{N}_f$ otherwise. An example of a MAS consisting of six agents with two of them having access to the leader is shown in Figure 4.1.

Assume the available measurements are relative distance d_{ij}, bearing angle β_{ij} and heading angle γ_{ij}, which satisfy

$$d_{ij} = \sqrt{(x_i - x_j)^2 + (y_i - y_j)^2},\ \beta_{ij} = \arctan\frac{y_i - y_j}{x_i - x_j} - \Phi_i,\ \gamma_{ij} = \Phi_i - \Phi_j. \tag{4.2}$$

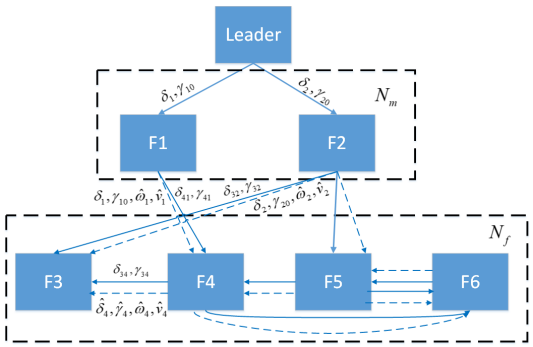

Figure 4.1: Distributed control and estimation based on a sensor network and communication network. Here solid lines and dashed lines represent the topologies of the sensor network and communication network, respectively; and the variables without and with a hat represent the detected relative information and transmitted local estimation, respectively.

Then, the primary objective of this paper is to solve the **formation tracking problem:** Consider a multi-robot system described in (4.1), with R_0 moving at a given velocity $(v_0(t), \omega_0(t))$. For follower R_i, $i = 1, ..., n$, the desirable formation is given by $(\bar{d}_{i0}, \bar{\beta}_{i0})$ w.r.t. the leader. Assume the velocities and accelerations are bounded by $\|v_0\|_{\mathcal{L}_\infty} \leq v_M$, $\|\omega_0\|_{\mathcal{L}_\infty} \leq \omega_M$, $\|\dot{v}_0\|_{\mathcal{L}_\infty} \leq a_v$ and $\|\dot{\omega}_0\|_{\mathcal{L}_\infty} \leq a_\omega$. Design a control input (v_i, ω_i), under which, the relative state $(d_{i0}, \beta_{i0}) \to (\bar{d}_{i0}, \bar{\beta}_{i0})$ as $t \to \infty$.

Notice that the desirable formation is specified w.r.t. the leader. As a result, the stability of the MAS needs to be examined w.r.t. a common coordinate frame, which, in this work, is chosen as the leader's coordinate frame. According to the reference paper [66], the above formation tracking problem is solved when the formation error in leader's coordinate frame $\delta_i = C_3^i(\gamma_{i0}, \beta_{i0})[\ d_{i0} \quad \bar{d}_{i0}\ ]^T$ satisfies $\delta_i(t) \to 0$ as $t \to \infty$. Here

$$C_3^i(\alpha_1, \alpha_2) = \begin{bmatrix} \sin(\alpha_1+\alpha_2) & -\sin(\alpha_1+\bar{\beta}_{i0}) \\ -\cos(\alpha_1+\alpha_2) & \cos(\alpha_1+\bar{\beta}_{i0}) \end{bmatrix}$$

is a function of α_1 and α_2. Combining (4.1) and (4.2), we have

$$\dot{\delta}_i = C_4^i(\gamma_{i0})u_i + [0, -1]^T v_0 + C_2^i(\delta_i)\omega_0, \tag{4.3}$$

where $u_i = [v_i, \omega_i]^T$ is the control input,

$$C_2^i(\mathbf{p}) = \left[\begin{smallmatrix} 0 & 1 \\ -1 & 0 \end{smallmatrix}\right] \mathbf{p}$$

is a function of $\mathbf{p}$, and

$$C_4^i(\alpha) = \begin{bmatrix} -\sin\alpha & -\bar{d}_{i0}\cos(\alpha+\bar{\beta}_{i0}) \\ \cos\alpha & -\bar{d}_{i0}\sin(\alpha+\bar{\beta}_{i0}) \end{bmatrix},$$

is a function of α which has the same interpretation as the one in Eq. (11) of reference [66].

4.2.3 Information Flow Architecture

Assume that the agents are connected by a sensing network and a communication network which have the same topology. For $i \in \mathcal{N}_m$, agent i only takes inflow from the leader and the information flow is one-way out, from itself to agents in $\mathcal{N}_f$; while for agent i, $i \in \mathcal{N}_f$, it takes inflow from agent j, $j \in \mathcal{N}$. Then, the Laplacian matrix can be expressed as follows

$$L = \begin{bmatrix} 0 & \mathbf{0}_{n_m}^T & \mathbf{0}_{n_f}^T \\ \mathbf{1}_{n_m} & L_{mm} & L_{mf} \\ \mathbf{0}_{n_f} & L_{fm} & L_{ff} \end{bmatrix}, \tag{4.4}$$

where $L_{mm} = 0_{n_m \times n_m}$, $L_{mf} = 0_{n_m \times n_f}$ and $L_{ff} \in \mathbb{R}^{n_f \times n_f}$, $L_{fm} \in \mathbb{R}^{n_f \times n_m}$.

Assumption 10. The underlying graph contains a spanning tree with the leader R_0 as a root.

We consider two kinds of information flows which are PUSC and PULC. For PULC, the relative information is detected at sampling instant $s_{s_i}^i$ in an active way; and we assume that the detected information is used immediately after each sampling instant. For PUSC, as the information is received in a passive way, a PETM is designed for agent $i \in \mathcal{N}_f$ such that the ET condition is checked in a discrete-time manner at checking instant $T_{p_{\pi_i}}^{\pi_i}$ and a transmission event is generated at a transmission instant $t_{k_i}^i$ if the ET condition is satisfied. Here π_i is a symbol representing the signal to be checked by the concerned ET condition. For example, if the ET condition is related to δ_i, then the checking instant is given by $T_{p_{\delta_i}}^{\delta_i}$; and the selections of π will be specified in the next section. In addition, we assume whenever an ET condition related to a state π_i is met, all the local information of agent i is packaged

and broadcast together, which means that the transmission sequence $t_1^i, t_2^i, \cdots$ is a subsequence of the union of the checking sequences of all states π_i. The information flow architecture is shown in Figure 4.2. Four kinds of units are

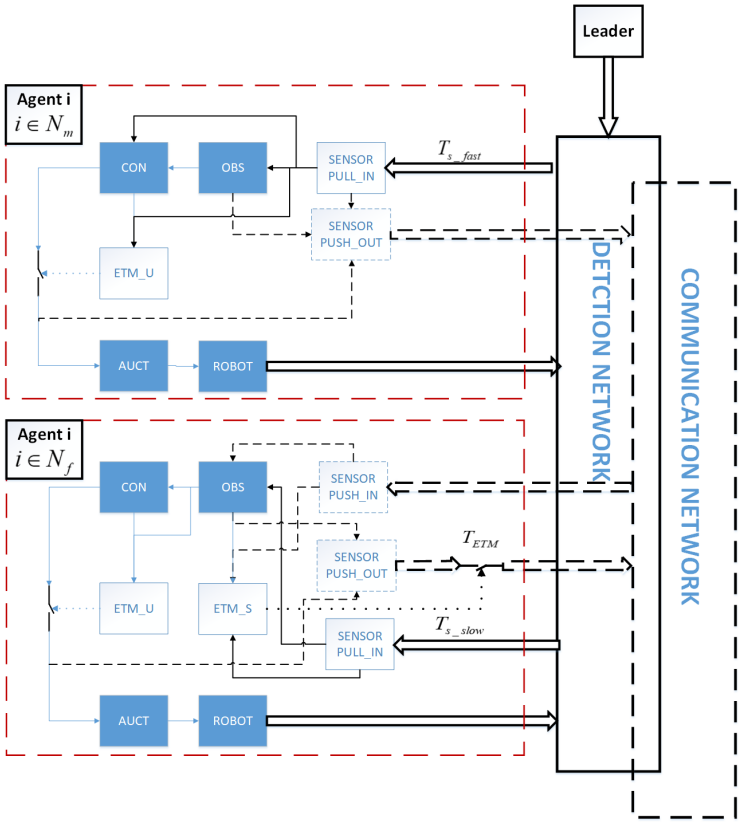

Figure 4.2: Detection and transmission behavior among agents

introduced to facilitate the information flow among MASs. A PULL-IN unit is considered as a detection unit, which collects relative measurements from its neighbors at each sampling instant $s_{s_i}^i$; an ETM_U is a decision unit used to check the ET condition at $T_{p_{u_i}}^{u_i}$ and activate the controller update at $t_{k_{u_i}}^{u_i}$. For agent $i \in \mathcal{N}_f$, an ETM_S is another decision unit used to activate PUSH-OUT unit to broadcast local information at $t_{k_i}^i$ when the ET condition checked at $T_{p_{\pi_i}}^{\pi_i}$ is satisfied; in addition, a PUSH-IN unit is used to receive and store transmitted information from the neighbors of agent i. While for agent $i \in \mathcal{N}_m$, a PUSH-OUT unit is used to collect and transmit local information periodically at $t_{k_i}^i$. The properties of the units are summarized in Table 4.1. It should be

Table 4.1: Description of units

Unit	Information	Network	Device	Function	Agents
PULL-IN	relative	Detection	onboard sensor	detection	$i \in \mathcal{N}$
PUSH-OUT	local	Communication	wireless devices	collecting and transmission	$i \in \mathcal{N}$
PUSH-IN	local	Communication	wireless devices	receiving and storage	$i \in \mathcal{N}_f$
ETM_S	local & relative	- †	micro-processor	activate PUSH-OUT unit	$i \in \mathcal{N}_f$
ETM_U	local & relative	-	micro-processor	drive controller update	$i \in \mathcal{N}$

noted that the sampling intervals are **non-uniform** and the checking instants are **asynchronous**. As a result, instead of giving a fixed sampling period, MASPs and MACPs are determined to maintain some stability properties after introducing the above information flow architecture. The definitions of different time sequences are summarized in Table 4.2. Here τ^i_{masp}, $\tau^{\pi_i}_{macp}$ and

Table 4.2: Notation of sampling instants

Notation	Agents	Action	Information	Constraint
$s^i_{s_i}$	$i \in \mathcal{N}$	‡	relative	$\tau_0 \leq s^i_{s_i+1} - s^i_{s_i} \leq \tau^i_{masp}$
$t^i_{k_i}$	$i \in \mathcal{N}_f$	§	local	ET condition
$t^i_{k_i}$	$i \in \mathcal{N}_m$	¶	local	$\tau_0 \leq t^i_{k_i+1} - t^i_{k_i} \leq \tau^i_{matp}$
$t^{u_i}_{k_{u_i}}$	$i \in \mathcal{N}$	‖	local	ET condition
$T^{\pi_i}_{p_{\pi_i}}$	$i \in \mathcal{N}_f$	**	local	$\tau_0 \leq T^{\pi_i}_{p_{\pi_i}+1} - T^{\pi_i}_{p_{\pi i}} \leq \tau^{\pi_i}_{macp}$
$T^{u_i}_{p_{u_i}}$	$i \in \mathcal{N}$	††	local	$\tau_0 \leq T^{u_i}_{p_{u_i}+1} - T^{u_i}_{p_{u i}} \leq \tau^{u_i}_{macp}$

$\tau^{u_i}_{macp}$ represent, respectively, the MASPs and MACPs related to state π_i and u_i; τ^i_{matp} represents the maximally allowable transmission periods (MATPs) for agent $i \in \mathcal{N}_m$; and $\tau_0 > 0$ is a small constant introduced to avoid Zeno behavior.

4.3 Estimation and Control Strategy

According to the system dynamics and information flow setup, the estimation and control strategies are different for the agents in different groups.

† - represents a null element
‡ detection instant of PULL-IN unit
§ transmission instant of PUSH-OUT unit
¶ transmission instant of PUSH-OUT unit
‖ update instant of actuator
** checking instant of ET condition related to state π_i
†† checking instant of ET condition related to input u_i

For agents in $\mathcal{N}_m$, high-gain observers are used to estimate the leader's velocity according to the relative information δ_{i0} and γ_{i0} detected from the leader; PETM is proposed for controller update; and the local information is transmitted periodically within some MATPs. For agents in $\mathcal{N}_f$, in order to realize the formation tracking in the leader's coordinate frame, the agents need to estimate leader's velocity as well as their relative poses w.r.t. the leader. Local estimation is updated according to the relative measurements as well as the information received from the neighbors, and PETMs are implemented to govern the transmissions and controller updates. The ET conditions for different estimations are checked at different time instants (e.g., $T^{a_i}_{p_{a_i}} \neq T^{b_i}_{p_{b_i}}$, where a_i and b_i represent different signals of agent i).

4.3.1 Estimation and Control Strategies For the Middle Level

High Gain Observer for Velocity Estimation

Only PULC is required for the high gain observers proposed in this subsection. The estimation of angular velocity is given as

$$\begin{cases} \dot{\hat{\gamma}}_i = l_{\eta_1}(\bar{\gamma}_{i0} - \hat{\gamma}_i) + \hat{\omega}_i - \omega_i, \\ \dot{\hat{\omega}}_i = l_{\eta_2}(\bar{\gamma}_{i0} - \hat{\gamma}_i). \end{cases} \tag{4.5}$$

Here $\hat{\gamma}_i$ and $\hat{\omega}_i$ represent the local estimation of γ_{i0} and ω_0, respectively; $\bar{\gamma}_{i0}$ is the relative heading angle detected at sampling instant t_{s_i}; ω_i represents the angular velocity of agent i; and l_{η_1}, $l_{\eta_2} > 0$ are feedback gains to be designed. Implementing PULC and the model-based strategy borrowed from [85] we have

$$\bar{\gamma}_{i0}(t) = \gamma_{i0}(t),\ t = s^i_{s_i};\quad \dot{\bar{\gamma}}_{i0} = l_{\eta_1}(\bar{\gamma}_{i0} - \hat{\gamma}_i) + \hat{\omega}_i - \omega_i,\ t \in [s^i_{s_i}, s^i_{s_i+1}).$$

Let $\eta_i = [\frac{\Delta\gamma_i}{\epsilon_\eta}, \Delta\omega_i]^T$, where $\Delta\gamma_i = \gamma_{i0} - \hat{\gamma}_i$, $\Delta\omega_i = \omega_0 - \hat{\omega}_i$ represent the estimation errors, and $\epsilon_\eta > 0$ is a small constant introduced to constrain the estimation errors and convergence time. Let $S_{\gamma_i} = \gamma_{i0} - \bar{\gamma}_{i0}$ represent the sampling error. Then

$$\begin{bmatrix} \dot{\eta}_i \\ \dot{S}_{\gamma_i} \end{bmatrix} = \frac{1}{\epsilon_\eta} \begin{bmatrix} A_\eta & B_\eta \\ C_\eta & 0 \end{bmatrix} \begin{bmatrix} \eta_i \\ S_{\gamma_i} \end{bmatrix} + \begin{bmatrix} [0, \dot{\omega}_0]^T \\ 0 \end{bmatrix}, \tag{4.6}$$

where $A_\eta = \begin{bmatrix} -\alpha_{\eta_1} & 1 \\ -\alpha_{\eta_2} & 0 \end{bmatrix}$, $B_\eta = \begin{bmatrix} -\alpha_{\eta_1}/\epsilon_\eta \\ -\alpha_{\eta_2}/\epsilon_\eta \end{bmatrix}$, $C_\eta = [0, \epsilon_\eta]$, $\alpha_{\eta_1} = \epsilon_\eta l_{\eta_1}$ and $\alpha_{\eta_2} = \epsilon_\eta^2 l_{\eta_2}$.

Let δ_i^x and δ_i^y represent, respectively, the projection of δ_i along x and y axes in the leader's coordinate frame, and then the high gain observer for leader's linear velocity estimation is proposed as follows

$$\begin{cases} \dot{\hat{\delta}}_i^y = l_{\chi_1}(\bar{\delta}_i^y - \hat{\delta}_i^y) + \hat{v}_i + C_4^i(\bar{\gamma}_i)_{(2,:)}(u_i) + \bar{\delta}_i^x \hat{\omega}_i, \\ \dot{\hat{v}}_i = l_{\chi_2}(\bar{\delta}_i^y - \hat{\delta}_i^y), \\ \bar{\delta}_i(t) = \delta_i(t),\ t = s_{s_i}^i, \\ \dot{\bar{\delta}}_i(t) = C_4^i(\bar{\gamma}_{i0}(t))u_i(t) + [\bar{\delta}_i^y(t), -\bar{\delta}_i^x(t)]^T \hat{\omega}_i(t) + [0,1]^T \hat{v}_i(t),\ t \in [s_{s_i}^i, s_{s_i+1}^i), \end{cases} \tag{4.7}$$

where $\hat{\delta}_i^y$ and $\hat{v}_i$ are the estimations of δ_i^y and v_0; and $\bar{\delta}_i^x$, $\bar{\delta}_i^y$ represent the projections of $\bar{\delta}_i$ along x and y axes, respectively. Let $\chi_i = [\frac{\Delta\delta_i^y}{\epsilon_\chi}, \Delta v_i]^T$, where $\Delta\delta_i^y = \delta_i^y - \hat{\delta}_i^y$, and $\Delta v_i = v_0 - \hat{v}_i$ represent the estimation errors, and $\epsilon_\chi > 0$ be a small constant introduced to constrain the estimation errors and convergence time. $S_{\delta_i} = \delta_i - \bar{\delta}_i$ represents the sampling error. Then

$$\begin{bmatrix} \dot{\chi}_i \\ \dot{S}_{\delta_i} \end{bmatrix} = \frac{1}{\epsilon_\chi} \begin{bmatrix} A_\chi & B_\chi \\ C_\chi & D_\chi \end{bmatrix} \begin{bmatrix} \chi_i \\ S_{\delta_i} \end{bmatrix} + \begin{bmatrix} \varsigma_{\chi_1}^i + \frac{1}{\epsilon_\chi}\varsigma_{\chi 2}^i \\ \varsigma_S^i \end{bmatrix}, \tag{4.8}$$

where

$$A_\chi = \begin{bmatrix} -\alpha_{\chi_1} & 1 \\ -\alpha_{\chi_2} & 0 \end{bmatrix},\ B_\chi = \begin{bmatrix} 0 & -\frac{\alpha_{\chi_1}}{\epsilon_\chi} \\ 0 & -\frac{\alpha_{\chi_2}}{\epsilon_\chi} \end{bmatrix},\ C_\chi = \begin{bmatrix} 0 & 0 \\ 0 & -\epsilon_\chi \end{bmatrix},\ D_\chi = \epsilon_\chi \hat{\omega}_i \begin{bmatrix} 0 & 0 \\ -1 & 0 \end{bmatrix},$$

$$\varsigma_{\chi_1}^i = \begin{bmatrix} 0 \\ \dot{v}_0 \end{bmatrix},\ \varsigma_{\chi 2}^i = \begin{bmatrix} (\Delta\omega_i \delta_i^x + \Delta C_4^i(\bar{\gamma}_{i0}, \gamma_{i0})_{(2,:)} u_i) \\ 0 \end{bmatrix},\ \varsigma_S^i = \Delta C_4^i(\bar{\gamma}_{i0}, \gamma_{i0})u_i + \begin{bmatrix} \delta_i^y \\ -\delta_i^x \end{bmatrix} \Delta\omega_i,$$

$$\Delta C_4^i(\bar{\gamma}_{i0}, \gamma_{i0}) = C_4^i(\gamma_{i0}) - C_4^i(\bar{\gamma}_{i0}) \text{ and } \alpha_{\chi_1} = \frac{l_{\chi_1}}{\epsilon_\chi},\ \alpha_{\chi_2} = \frac{l_{\chi_2}}{\epsilon_\chi}.$$

Event-Triggered Controller

Since high gain observers are used to estimate leader's velocity, to prevent the peaking phenomenon from affecting the robot dynamics, input saturation is implemented [86]. Consider a compact set

$$\mathbb{V}_i = \{\delta_i : \|\delta_i\| < c_\delta\}, \tag{4.9}$$

where $c_\delta > 0$ is a user-specified constant that affects the convergence range of the system. The controller is designed as

$$u_{it} = {C_4^i}^{-1}(\gamma_{i0})(-c\delta_i + [0,1]^T \hat{v}_i), \tag{4.10}$$

where $c > 0$ is a feedback gain to be designed. Let $U_i = \sup_{\delta_i \in \mathbb{V}_i} \|u_{it}(v_0, \omega_0, \gamma_{i0}, \delta_i)\| + \Delta_u$, where Δ_u is introduced to cover the uncertainty caused by the estimation error Δv_i and $\Delta\omega_i$, which will be specified later. The saturated control input is given as $u_{is} = \text{sat}_{U_i}(u_{it}(\delta_i, \gamma_{i0}, \hat{v}_i, \hat{\omega}_i))$, where the saturation function is defined by

$$\text{sat}_{U_i}(u_{it}) = \begin{cases} \text{sign}(u_{it})U_i, & \|u_{it}\| \geq U_i, \\ u_{it}, & \|u_{it}\| < U_i. \end{cases} \tag{4.11}$$

Implementing PETM on controller updates, we have

$$u_i(t) = u_{is}(t^{u_i}_{k_{u_i}}), \quad t \in [t^{u_i}_{k_{u_i}}, t^{u_i}_{k_{u_i}+1}), \tag{4.12}$$

where $t^{u_i}_{k_{u_i}}$ is generated by $t^{u_i}_0 = 0, t^{u_i}_{k_{u_i}+1} = \inf\{t \in \{T^{u_i}_k\}_{k=0}^{\infty},\ t > t^{u_i}_{k_{u_i}} |$ $h_{u_i}(e_{u_i}, \delta_i, t) \geq 0\}$, and $e_{u_i} = C^i_4(\gamma_{i0})(u_{is} - u_i)$ is defined as the measurement error of control inputs. Then, the dynamics of the system can be represented by

$$\begin{cases} \dot{\delta}_i = -c\delta_i + [0,1]\Delta v_i + e_{u_i} + [-\delta^y_i, \delta^x_i]^T\omega_0, \\ \dot{e}_{u_i} = \frac{\partial C^i_4(\gamma_{i0})}{\partial \gamma_{i0}}(\omega_0 - \omega_i)(u_i - u_{is}) + C^i_4(\gamma_{i0})\dot{u}_{is}, \end{cases} \tag{4.13}$$

where $\dot{u}_{is}$ is determined by the system states γ_{i0}, δ_i, Δv_i. $\Delta\omega_i$ and leader's velocities ω_0, v_0.

Periodic Broadcasting of Local Information

Since the agents in the bottom level cannot access information directly from the leader, their estimates of leader's position and velocity rely on the transmitted information $\bar{\delta}_{i0}$, $\bar{\gamma}_{i0}$, $\hat{v}_i$ and $\hat{\omega}_i$ from agents $i \in \mathcal{N}_m$. A discrete broadcasting strategy is implemented with the MATP as follows,

$$t^i_{k_i} = 0,\ t^i_{k_i+1} \in [t^i_{k_i} + \tau_0, t^i_{k_i} + \tau^i_{matp}). \tag{4.14}$$

As the control and estimation of agent $i \in \mathcal{N}_m$ only rely on active detections from the leader and its local information, τ^i_{matp} is determined based on agent's initial conditions and its own dynamics in (4.5), (4.7) and (4.13). On the other hand, since the dynamics of agents $i \in \mathcal{N}_m$ are affected by leader's dynamics, the design of τ^i_{matp} depends on a user-specified constant $r_m > 0$. Furthermore,

in order to take advantage of the finite time convergence provided by high gain observers in (4.5) and (4.7), the design of MATPs will be divided into two phases: before and after convergence (see Subsection 4.5.3 for detailed analysis).

4.3.2 Event-Triggered Distributed Observer-Based Control Strategy For the Bottom Level

For the agents that cannot access the leader, distributed observers are proposed to estimate leader's velocity and position. In order to reduce the occupation of communication networks, the data transmissions and controller updates are generated by PETMs.

Estimation of Leader's Velocities Under PUSC

A consensus-based algorithm is implemented to estimate leader's angular velocity under PUSC as follows

$$\dot{\hat{\omega}}_i = -c_\omega \sum_{j\in\mathcal{N}_i} a_{ij}(\hat{\omega}_i(t^i_{k_i}) - \hat{\omega}_j(t^j_{k_j})), \tag{4.15}$$

where $\hat{\omega}_i$ represents the local estimation of ω_0 given by agent i and c_ω is a feedback gain to be designed. The transmission is generated at $t^i_0 = 0, t^i_{k_i+1} = \inf\{t \in \{T^{\omega_i}_k\}^\infty_{k=0},\ t > t^i_{k_i} | h_{\omega_i}(e_{\omega_i}, q_{\omega_i}, t) \geq 0\}$, where $e_{\omega_i}(t) = \hat{\omega}_i(t^i_{k_i}) - \hat{\omega}_i(t)$ and $q_{\omega_i}(t) = \sum\limits_{j\in\mathcal{N}_i} a_{ij}(\hat{\omega}_i(t) - \hat{\omega}_j(t^j_{k_j}))$. The dynamics of the system can be represented as

$$\begin{cases} \Delta\dot{\omega}_i = -c_\omega \sum\limits_{j\in\mathcal{N}_i} a_{ij}(\Delta\omega_i(t) - \Delta\omega_j(t) + e_{\omega_i}(t) - e_{\omega_j}(t)) - \dot{\omega}_0(t), \\ \dot{e}_{\omega_i} = -\dot{\hat{\omega}}_i = c_\omega \sum\limits_{j\in\mathcal{N}_i} a_{ij}(\Delta\omega_i - \Delta\omega_j + e_{\omega_i} - e_{\omega_j}). \end{cases} \tag{4.16}$$

The observer for linear velocity v_0 follows the same structure as in (4.15) under a feedback gain c_v, with the state given by $\hat{v}_i$ and ET function denoted by $h_{v_i}(e_{v_i}, q_{v_i}, t) \geq 0$; then the errors e_{v_i}, Δv_i have the same dynamics as in (4.16).

Estimation of Leader's Coordinate Frame under PUSC and PULC

In order to realize the formation under the leader's coordinate frame, a consensus algorithm under both PUSC and PULC is proposed to estimate the

relative heading angle w.r.t. the leader as follows

$$\begin{cases} \dot{\hat{\gamma}}_i(t) = -c_\gamma \sum\limits_{j\in\mathcal{N}_i} a_{ij}(\hat{\gamma}_i(t) - \tilde{\gamma}_j(t) - \bar{\gamma}_{ij}(t)) + \hat{\omega}_i(t) - \omega_i(t), & t \in [0,\infty), \\ \tilde{\gamma}_j(t) = \hat{\gamma}_j(t), & t = t^j_{k_j}, \\ \dot{\tilde{\gamma}}_j(t) = \hat{\omega}_j(t^j_{k_j}) - \omega_j(t^{u_j}_{k_{u_j}}), & t \in [t^i_{k_i}, t^i_{k_i+1}), \\ \bar{\gamma}_{ij}(t) = \gamma_{ij}(t), & t = s^i_{s_i}, \\ \dot{\bar{\gamma}}_{ij}(t) = \omega_j(t^{u_j}_{k_{u_j}}) - \omega_i(t^{u_i}_{k_{u_i}}), & t \in [s^i_{s_i}, s^i_{s_i+1}), \end{cases} \tag{4.17}$$

where $\hat{\gamma}_i$ represents the local estimate of γ_{i0}; and $\tilde{\gamma}_j$, $\bar{\gamma}_{ij}$ are the estimates given by model-based mechanisms between adjacent transmission instant $t^i_{k_i}$ and detection instant $s^i_{s_i}$, respectively. The transmission instants generated by PETM satisfies $t^i_0 = 0, t^i_{k_i+1} = \inf\{t \in \{T^{\gamma_i}_k\}^\infty_{k=0},\ t > t^i_{k_i} | h_{\gamma_i}(e_{\gamma_i}, q_{\gamma_i}, t) \geq 0\}$, where $e_{\gamma_i}(t) = \tilde{\gamma}_i - \hat{\gamma}_i$ and $q_{\gamma_i}(t) = \sum\limits_{j\in\mathcal{N}_f} a_{ij}(\hat{\gamma}_i - \tilde{\gamma}_j - \bar{\gamma}_{ij})$. Furthermore, the sampling error is denoted by $S_{\gamma_i} = -\sum\limits_{j\in\mathcal{N}_i} a_{ij}(\bar{\gamma}_{ij} - \gamma_{ij})$ and the estimation error is denoted by $\Delta\gamma_i = \hat{\gamma}_i - \gamma_{i0}$. Then

$$\begin{cases} \Delta\dot{\gamma}_i = -c_\gamma \sum\limits_{j\in\mathcal{N}_i} a_{ij}(\Delta\gamma_i - \Delta\gamma_j + e_{\gamma_i} - e_{\gamma_j}) + c_\gamma S_{\gamma_i} + \Delta\omega_i + e_{\gamma_i}, \\ \dot{e}_{\gamma_i} = c_\gamma \sum\limits_{j\in\mathcal{N}_i} a_{ij}(\Delta\gamma_i - \Delta\gamma_j + e_{\gamma_i} - e_{\gamma_j}) - c_\gamma S_{\gamma_i}, \\ \dot{S}_{\gamma_i} = 0. \end{cases} \tag{4.18}$$

Event-Triggered Observer-Based Controller for the Bottom Level

According to the above estimations, an event-triggered observer-based control protocol is proposed as follows

$$\begin{cases} \dot{\hat{\delta}}_i(t) = -\sum\limits_{j\in\mathcal{N}_i} a_{ij}(\hat{\delta}_i(t^i_{k_i}) - \hat{\delta}_j(t^j_{k_j}) - \bar{\delta}_{ij}(t)) + p_{\delta_i}(t), \\ u_{it} = C_4^{i-1}(\hat{\gamma}_i)(-c\hat{\delta}_i + [0,1]\hat{v}_i), \\ u_i(t) = u_{it}(t), \quad t = t^{u_i}_{k_{u_i}}. \end{cases} \tag{4.19}$$

Here $\hat{\delta}_i$ represents the estimation of δ_i; $t^i_{k_i}$ represents transmission instant of agent i generated by the PETM $t^i_0 = 0, t^i_{k_i+1} = \inf\{t \in \{T^{\delta_i}_k\}^\infty_{k=0},\ t > t^i_{k_i}\ | h_{\delta_i}(e_{\delta_i}, q_{\delta_i}, t) \geq 0\}$, where $e_{\delta_i}(t) = \hat{\delta}_i(t^i_{k_i}) - \hat{\delta}_i(t)$ and $q_{\delta_i}(t) = \hat{\delta}_i(t)$; and the controller is updated at $t^{u_i}_0 = 0, t^{u_i}_{k_{u_i}+1} = \inf\{t \in \{T^{u_i}_k\}^\infty_{k=0},\ t > t^i_{k_i}$ $|h_{u_i}(e_{u_i}, q_{u_i}, t) \geq 0\}$, where $e_{u_i}(t) = C^i_4(\hat{\gamma}_i(t))(u_i - u_{it})$ and $q_{u_i}(t) = \hat{\delta}_i(t)$. p_{δ_i}

is introduced to compensate the dynamics of δ_i, which is designed by

$$\begin{aligned} p_{\delta_i}(t) =& C_4^i(\hat{\gamma}_i(t))u_i(t_{k_{u_i}}^{u_i}) - [0,1]^T\hat{v}_i(t) + [\hat{\delta}_i^y(t), -\hat{\delta}_i^x(t)]^T\hat{\omega}_i(t) \\ =& -c\hat{\delta}_i + e_{u_i} + [\hat{\delta}_i^y, -\hat{\delta}_i^x]^T\hat{\omega}_i; \end{aligned}$$

and $\bar{\delta}_{ij}$ represents the estimated displacement in the leader's coordinate frame, and implements in a model-based fashion in between adjacent measurements

$$\begin{cases} \bar{\delta}_{ij}(t) = & \bar{\delta}_{ijt}(t),\ t = s_{s_i}^i, \\ \dot{\bar{\delta}}_{ij}(t) = & C_4^i(\hat{\gamma}_i(t))u_i(t_{k_{u_i}}^{u_i}) - C_4^j(\hat{\gamma}_j(t_{k_j}^j))u_j(t_{k_{u_i}}^{u_i}) \\ & + \begin{bmatrix} \hat{\delta}_i^y(t_{k_i}^i) - \hat{\delta}_j^y(t_{k_j}^j) \\ -\hat{\delta}_i^x(t_{k_i}^i) + \hat{\delta}_j^x(t_{k_j}^j) \end{bmatrix} \hat{\omega}_i,\ t \in [s_{s_i}^i, s_{s_i+1}^i), \end{cases} \tag{4.20}$$

where $\bar{\delta}_{ijt} = C_4^i(\hat{\gamma}_i)\bar{\delta}_{ij}^i$; $\bar{\delta}_{ij}^i$ represents the displacement measured in the body-fixed frame of agent i; and $\bar{\delta}_{ijt}$ is the estimated displacement in the leader's frame according to the estimated relative heading angle $\hat{\gamma}_i$. Combining with (4.20), we can tell that the difference between the real value δ_{ij} and the estimated one $\bar{\delta}_{ij}$ is introduced by the estimation error of $\hat{\gamma}_i$ and the intermittent detection of $\bar{\delta}_{ij}$, which are denoted by $D_{ij} = \bar{\delta}_{ijt} - \delta_{ij}$ and $S_{ij}^\delta = \bar{\delta}_{ij} - \bar{\delta}_{ijt}$, respectively. Let $D_c(\gamma_i) = \frac{\partial C_4^i(\gamma_i)}{\partial \gamma_i} C_4^i(\gamma_i)^{-1}$ and $D_{\gamma_i}^{\Delta_i} = C_4^i(\hat{\gamma}_i)C_4^i(\gamma_i)^{-1} - 1$. It can be computed that the Frobenius norm of D_c is bounded by 1. Therefore, $D_{\gamma_i}^{\Delta_i} = \int_0^{\Delta\gamma_i} D_c(s)ds \leq |\Delta\gamma_i|$, and $D_{ij} = \bar{\delta}_{ijt} - \delta_{ij} = D_{\gamma_i}^{\Delta_i}\delta_{ij} \leq |\Delta\gamma_i|\|\delta_{ij}\|$. Then,

$$\begin{aligned} \dot{S}_{ij}^\delta =& (-C_4^j(\hat{\gamma}_j(t_{k_j}^j)) + C_4^i(\hat{\gamma}_i)C_4^{i-1}(\gamma_{i0})C_4^j(\gamma_{j0}))u_j(t_{k_j^u}^u) - (\hat{C}_4^i(\hat{\gamma}_i)C_4^{i-1}(\gamma_{i0}) - 1) \\ & \times \begin{bmatrix} \delta_i^y - \delta_j^y \\ -\delta_i^x + \delta_j^x \end{bmatrix} \omega_0 + \begin{bmatrix} \Delta\delta_i^y + e_i^{\delta y} - \Delta\delta_j^y - e_j^{\delta y} \\ -\Delta\delta_i^x - e_i^{\delta x} + \Delta\delta_j^x + e_j^{\delta x} \end{bmatrix} \hat{\omega}_i + \begin{bmatrix} \delta_i^y - \delta_j^y \\ -\delta_i^x + \delta_j^x \end{bmatrix} \Delta\omega_i, \\ |\dot{S}_{ij}^\delta| \leq& (|\Delta\gamma_i| + |\Delta\gamma_i\Delta\gamma_j| + |\Delta\gamma_j|)(\| - c\hat{\delta}_j + [0,1]^T\hat{v}_j + e_j^u\|) + |e_{\gamma_j}|\|e_{u_j}\| \\ & + |\Delta\gamma_i| \left\| \begin{bmatrix} \delta_i^y - \delta_j^y \\ -\delta_i^x + \delta_j^x \end{bmatrix} \omega_0 \right\| + \left\| \begin{bmatrix} \Delta\delta_i^y + e_i^{\delta y} - \Delta\delta_j^y - e_j^{\delta y} \\ -\Delta\delta_i^x - e_i^{\delta x} + \Delta\delta_j^x + e_j^{\delta x} \end{bmatrix} \hat{\omega}_i \right\| + \left\| \begin{bmatrix} \delta_i^y - \delta_j^y \\ -\delta_i^x + \delta_j^x \end{bmatrix} \Delta\omega_i \right\|, \end{aligned} \tag{4.21}$$

where $\Delta\delta_i = \hat{\delta}_i - \delta_i$ represents the estimation error of δ_i. According to (4.19)–(4.21), the dynamics of the formation error can be written as

$$\begin{aligned} \dot{\delta}_i =& C_4^i(\gamma_{i0})u_i(t_{k_i^u}^u) - [0,1]^T v_0 + [\delta_i^y, -\delta_i^x]^T\omega_0 - c\hat{\delta}_i + [0,1]^T\Delta v_0 + e_i^u \\ & + [\delta_i^y, -\delta_i^x]^T\omega_0, \end{aligned} \tag{4.22}$$

and the estimation error satisfies

$$\begin{aligned}\dot{\hat{\delta}}_i &= -c_\delta \sum_{j\in\mathcal{N}_i} a_{ij}(\hat{\delta}_i - \hat{\delta}_j - \delta_{ij} + e_i^\delta - e_j^\delta - D_{ij}) + c_\delta S_{\delta_i} + k_{\delta_i} \\ &= -c\hat{\delta}_i + [0,1]^T \Delta v_0 + e_i^u + [\delta_i^y, -\delta_i^x]^T \omega_0,\end{aligned} \tag{4.23}$$

where $S_{\delta_i} = \sum_{j\in\mathcal{N}_i} S_{\delta_{ij}}$ represents the sampling error of agent i. The dynamics of estimation error follows

$$\Delta\dot{\delta}_i = -c_\delta \sum_{j\in\mathcal{N}_i} a_{ij}(\Delta\delta_i - \Delta\delta_j + e_i^\delta - e_j^\delta - D_{ij}) + c_\delta S_{\delta_i} + \Delta k_{\delta_i}, \tag{4.24}$$

where $\Delta k_{\delta_i} = k_{\delta_i} - \dot{\delta}_i = (C_4^i(\hat{\gamma}_i) - C_4^i(\gamma_{i0}))u_i(t_{k_i^u}^{u_i}) + [0,1]^T \Delta v_i + [\hat{\delta}_i^y, -\hat{\delta}_i^x]^T \hat{\omega}_i - [\delta_i^y, -\delta_i^x]^T \omega_0$. By (4.19)–(4.24), the transmission error e_{δ_i} and control input error e_{u_i} satisfy

$$\begin{cases} \dot{e}_{\delta_i} = -\dot{\hat{\delta}}_i, \\ \dot{e}_{u_i} = \frac{\partial C_4^i(\hat{\gamma}_i)}{\partial \hat{\gamma}_i} \dot{\hat{\gamma}}_i (u_i - u_{it}) - C_4^i(\hat{\gamma}_i)\dot{u}_{it}. \end{cases} \tag{4.25}$$

According to the above estimation and control strategies, the possible choices of the symbol π considered in this work are $\pi \in \{\gamma,\ \delta,\ \omega,\ v,\ \chi,\ \eta,\ m\}$.

The estimation and control strategies proposed in this section are implemented based on the transmitted data by PUSC and the relative information detected by PULC. Thus, the information flows among agents are typical discrete-time dynamics. While for the agents in the MAS, their motions follow the Newton's law, which are typical continuous-time dynamics. This kind of systems fit into the class of hybrid dynamical systems. Therefore, the performance of closed-loop MAS under the control and estimation strategies proposed in this section will be studied in a hybrid system framework in the next section.

4.4 Problem Formulation in a Hybrid System Framework

In this section, we reformulate the formation tracking problem introduced in Section 4.2 in a hybrid system framework. Some auxiliary states and no-

tations are introduced as follows. For agent $i \in \mathcal{N}$, introduce auxiliary variables $\tau_{u_i},\ \tau_{s_i} \in \mathbb{R}_{\geq 0}$ to record the time elapsed since the last checking instant $T^{u_i}_{p_{u_i}}$, and the last detection instant $s^i_{s_i}$, respectively; $k_{u_i},\ k_{t_i} \in \mathbb{N}$, as counters that keep tracking the numbers of controller updates and information transmissions; let $\tau_u,\ \tau_s,\ k_u,\ k_t$ represent the corresponding augmented vectors built upon all followers; in addition, $e_i = [e_{\omega_i}, e_{v_i}, e_{\gamma_i}, e^T_{\delta_i}]^T \in \mathbb{R}^5$, $S_i = [S_{\gamma_i}, S^T_{\delta_i}]^T \in \mathbb{R}^3$, and $e_t,\ S$ represent the corresponding augmented vectors and e_u represent the augmented vector of $e_{u_i} \in \mathbb{R}^2$.

For agent $i \in \mathcal{N}_f$, let $\tau_{\pi_i} \in \mathbb{R}_{\geq 0}$ represent the time elapsed since the last checking instant $T^{\pi_i}_{p_{\pi_i}}$, $\tau_{t_i} = [\tau_{\omega_i}, \tau_{v_i}, \tau_{\gamma_i}, \tau_{\delta_i}]^T \in \mathbb{R}^4$, $x_{f_i} = [\Delta\omega_i, \Delta v_i, \Delta\gamma_i, \delta^T_i, \Delta\delta^T_i]^T \in \mathbb{R}^7$, and $\tau_{t_f},\ x_f$ be the corresponding augmented vectors; while for agent $i \in \mathcal{N}_m$, introduce $\tau_{t_i} \in \mathbb{R}_{\geq 0}$ to record the time elapsed since the last transmission instant $t^i_{k_i}$, $x_{h_i} = [\eta^T_i, \chi^T_i]^T \in \mathbb{R}^4$, $x_{m_i} = [\delta^T_i, \Delta\delta^T_i]^T \in \mathbb{R}^4$, and $\tau_{t_m},\ x_h,\ x_m$ represent the corresponding augmented vectors. In addition, let $x = [x^T_h, x^T_m, x^T_f]^T$, $e = [e^T_t, e^T_u]^T$, $\tau_t = [\tau^T_{t_m}, \tau^T_{t_f}]^T$, $\tau_e = [\tau^T_t, \tau^T_u]^T$, $k = [k^T_t, k^T_u]^T$. Then the state vector can be written as $\xi = (x, e, S, k, \tau_e, \tau_s) \in \mathbb{X},\ \mathbb{X} \in \{\mathbb{R}^{8n_m+7n_f} \times \mathbb{R}^{5n} \times \mathbb{R}^{3n} \times \mathbb{R}^{2n} \times \mathbb{R}^{4n_f+n_m+n} \times \mathbb{R}^n\}$.

Considering the hybrid system in (3.1), a jump dynamics is caused by a detection or a checking event, which we denote by G_s and $(G_t,\ G_u)$, respectively (See Figure 4.3 (a)). Then, on jump domain, the set-valued mapping [78] is given by

$$G(\xi) = G_s(\xi) \cup G_t(\xi) \cup G_u(\xi), \quad \xi \in D,\ D = D_t \cup D_s \cup D_u. \tag{4.26}$$

Since at each detection instant $s^i_{s_i}$, the agent detects all the relative information (i.e., $\gamma_{ij},\ \delta_{ij},\ \forall j \in \mathcal{N}_i$), we have

$$\begin{aligned} &G_s(\xi) = \cup_{i\in\mathcal{N}} G_{s_i}(\xi), \quad \xi \in D_s;\ D_s = \cup_{i\in\mathcal{N}} D_{s_i}, \\ &G_{s_i}(\xi) = \begin{pmatrix} x \\ e \\ (I-\Lambda^s_i)S \\ k \\ \tau_e \\ (I-\Lambda^s_i)\tau_s \end{pmatrix},\ \xi \in D_{s_i};\ D_{s_i} = \{\xi \in \mathbb{X} | \tau_0 \leq \tau_{s_i} \leq \tau^i_{masp}\}, \end{aligned} \tag{4.27}$$

where τ^i_{masp} represents the MASP for detecting relative information. Whenever an ET function h_{π_i} is checked or a transmission event is generated, we

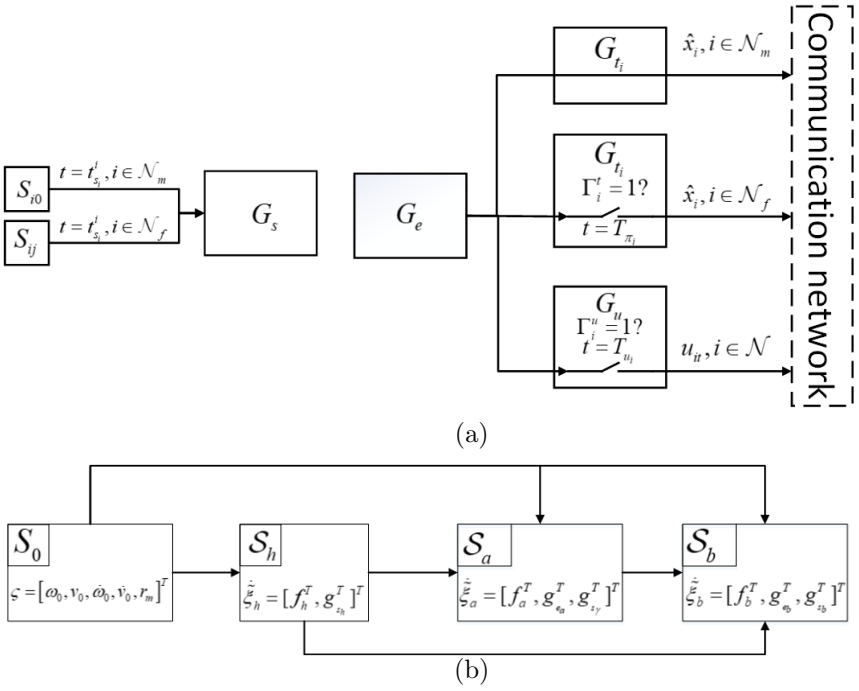

Figure 4.3: (a) Set-valued mapping G for MAS in a hybrid system framework. (b) Cascade Structure of MAS on flow domain

have

$$
\begin{aligned}
&G_t(\xi) = \cup_{i\in\mathcal{N}} G_{t_i}(\xi),\ \xi \in D_t;\ D_t = \cup_{i\in\mathcal{N}} D_{t_i},\\
&G_{t_i}(\xi) = \begin{pmatrix} x \\ (I-\Gamma_i^t(e_{t_i},q_{t_i},k_i)\bar{\Lambda}_i^t)e_t \\ e_u \\ S \\ k_t+\Gamma_i^t(e_{t_i},q_{t_i},k_i)\Lambda_i \\ k_u \\ \tau_m \\ (1-\Gamma_i^t)(I-\bar{\Lambda}_i^t\bar{\Lambda}_\pi^t)\tau_t \\ \tau_u \\ \tau_s \end{pmatrix},\ \xi \in D_{t_i};\\
&D_{t_i} = \cup_{\pi=\omega,v,\gamma,\delta} D_{\pi_i},\ D_{\pi_i} = \{\xi \in \mathbb{X} | \tau_0 \le \tau_{\pi_i} \le \tau_{macp}^{\pi_i}\}, i \in \mathcal{N}_f;\\
&D_{t_i} = \{\xi \in \mathbb{X} | \tau_0 \le \tau_{t_i} \le \tau_{matp}^{i}\}, i \in \mathcal{N}_m,
\end{aligned}
\tag{4.28}
$$

where τ_{matp}^i represents the MATP for agent $i \in \mathcal{N}_m$, $\tau_{macp}^{\pi_i}$ is the MACP for checking the ET condition h_{π_i} of agent $i \in \mathcal{N}_f$, and $q_{t_i}(x_i)$ is a locally Lipschitz

function of state x_i. G_u represents a checking event of h_{u_i}, which satisfies

$$G_u(\xi) = \cup_{i\in\mathcal{N}} G_{u_i}(\xi),\ \ \xi \in D_u,\ D_u = \sum_{i\in\mathcal{N}} D_{u_i};\ G_{u_i}(\xi) = \begin{pmatrix} x \\ e_t \\ (I-\Gamma_i^u(e_{u_i},q_{u_i},k_{u_i})\bar{\Lambda}_i^u)e_u \\ S \\ k_t \\ k_u+\Gamma_i^u(e_{u_i},q_{u_i},k_{u_i})\Lambda_i \\ \tau_t \\ (I-\Lambda_i)\tau_u \\ \tau_s \end{pmatrix},$$

$$\xi \in D_{u_i},\ D_{u_i} = \{\xi \in \mathbb{X} | \tau_0 \le \tau_{u_i} \le \tau_{macp}^{u_i}\}, \tag{4.29}$$

where $\tau_{macp}^{u_i}$ represents the MACP for checking the ET condition h_{u_i}, and $q_{u_i}(x_i)$ is a locally Lipschitz function of state x_i. In (4.27)–(4.29), $\bar{\Lambda}_i = \Lambda_i \otimes I_3$, $\bar{\Lambda}_i^u = \Lambda_i \otimes I_2$, $\bar{\Lambda}_\pi^t = \begin{bmatrix} I_{n_m} & 0 \\ 0 & I_{n_f}\otimes\Lambda_j^\pi \end{bmatrix}$; and $\bar{\Lambda}_i^t = \begin{bmatrix} \Lambda_i^m & 0 \\ 0 & 0 \end{bmatrix}$, $i \in \mathcal{N}_m$, $\bar{\Lambda}_i^t = \begin{bmatrix} 0 & 0 \\ 0 & \Lambda_i^f \otimes I_4 \end{bmatrix}$, $i \in \mathcal{N}_f$; where $\Lambda_i \in \mathbb{R}^{n\times n}$, $\Lambda_i^\pi \in \mathbb{R}^{4\times 4}$, $\Lambda_i^m \in \mathbb{R}^{n_m\times n_m}$, $\Lambda_i^f \in \mathbb{R}^{n_f\times n_f}$, are diagonal matrices with the i-th ($(i-n_m)$-th for Λ_i^f) element being 1 and others being 0; $\Gamma_i^t = \{1\}$, $i \in \mathcal{N}_m$; and $\Gamma_i^t : \mathbb{R}^{e_t} \times \mathbb{R}^{e_t} \times \mathbb{R} \rightrightarrows \{0,1\}$[‡‡], $i \in \mathcal{N}_f$, indicates whether a transmission for an agent in the bottom level occurs and $\Gamma_i^u : \mathbb{R}^{e_u} \times \mathbb{R}^{e_u} \times \mathbb{R} \rightrightarrows \{0,1\}$ indicates whether a controller update occurs, which depends on the ET condition as follows

$$\begin{aligned} \Gamma_i^t(e_{t_i}, q_{t_i}, t) &= \begin{cases} \{0\}, & \cap_{\pi=w,v,\gamma,\delta} h_{\pi_i}(e_{\pi_i}, q_{\pi_i}, t) < 0 \\ \{1\}, & \cup_{\pi=w,v,\gamma,\delta} h_{\pi_i}(e_{\pi_i}, q_{\pi_i}, t) > 0,\ i \in \mathcal{N}_f, \\ \{0,1\}, & \text{otherwise} \end{cases} \\ \Gamma_i^u(e_{u_i}, q_{u_i}, t) &= \begin{cases} \{0\}, & h_{u_i}(e_{u_i}, q_{u_i}, t) < 0 \\ \{1\}, & h_{u_i}(e_{u_i}, q_{u_i}, t) > 0\ ,\ i \in \mathcal{N}. \\ \{0,1\}, & h_{u_i}(e_{u_i}, q_{u_i}, t) = 0 \end{cases} \end{aligned} \tag{4.30}$$

By (4.30), a transmission event is generated when one of the ET conditions is violated (i.e. $h_{\pi_i} \le 0$), and at the same time all the local information of agent i is packaged and broacast entirely.

In order to capture the flow dynamics of the system, we participate the closed-loop MAS in (4.1) into subsystems $\mathcal{S}_\eta$, $\mathcal{S}_\chi$, $\mathcal{S}_\omega$, $\mathcal{S}_v$, $\mathcal{S}_\gamma$, and $\mathcal{S}_\delta$. Then, on flow domain, the dynamics can be described as follows

$$\begin{aligned} F(\xi,\varsigma) =& (f_h(\tilde{\xi}_h,\varsigma), f_a(\tilde{\xi}_a,\xi_h,\varsigma), f_b(\tilde{\xi}_b,\xi_h,\tilde{\xi}_a,\varsigma), g_{e_a}(\tilde{\xi}_a,\xi_h,\varsigma), g_{e_b}(\tilde{\xi}_b,\xi_h,\tilde{\xi}_a,\varsigma), \\ & g_{s_m}(\tilde{\xi}_h,\varsigma), g_{s_\gamma}, g_{s_b}(\tilde{\xi}_b,\tilde{\xi}_h,\tilde{\xi}_a,\varsigma), \mathbf{0}, 1, 1),\ \ \xi \in C, \end{aligned} \tag{4.31}$$

‡‡ $\rightrightarrows$ represents a set-valued mapping [78].

where $\varsigma = [\omega_0, v_0, \dot{\omega}_0, \dot{v}_0, r_m]^T$ represents the external disturbances. It should be noted that, except from the disturbances introduced by leader's dynamics, r_m is introduced by the periodic transmission strategy of agent $i \in \mathcal{N}_m$, which is independent of leader's dynamics and is tunable according to the MATPs. The state vectors are summarized as in Table 4.3. Here, the stabilization

Table 4.3: Structure of the cascade–connected systems

Group	Subsystem	Internal State	Stabilization State	Agent
$\mathcal{S}_h$	$\mathcal{S}_\eta$	$\xi_\eta = (\tilde{\xi}_\eta, e_{\omega_m}, e_{\gamma_m}, \tau_{s_m})$	$\tilde{\xi}_\eta = [\eta_m^T, S_{\gamma_m}^T]^T$	$i \in \mathcal{N}_m$
	$\mathcal{S}_\chi$	$\xi_\chi = (\tilde{\xi}_\chi, e_{v_m}, e_{\delta_m}, \tau_{s_m})$	$\tilde{\xi}_\chi = [\chi_m^T, S_{\delta_m}^T]^T$	*§§
$\mathcal{S}_a$	$\mathcal{S}_m$	$\xi_m = (\tilde{\xi}_m, k_{u_m}, \tau_{u_m})$	$\tilde{\xi}_m = [\delta_m^T, e_{u_m}^T]^T$	*
	$\mathcal{S}_\omega$	$\xi_\omega = (\tilde{\xi}_\omega, k_f, \tau_\omega)$	$\tilde{\xi}_\omega = [\Delta\omega_f^T, e_{\omega_f}^T]^T$	$i \in \mathcal{N}_f$
	$\mathcal{S}_v$	$\xi_v = (\tilde{\xi}_v, k_f, \tau_v)$	$\tilde{\xi}_v = [\Delta v_f^T, e_{v_f}^T]^T$	*
	$\mathcal{S}_\gamma$	$\xi_\gamma = (\tilde{\xi}_\gamma, k_f, \tau_\gamma, \tau_\omega, \tau_{s_f})$	$\tilde{\xi}_\gamma = [\Delta\gamma_f^T, \Delta\omega_f^T, e_{\gamma_f}^T, e_{\omega_f}^T, S_{\gamma_f}]^T$	*
$\mathcal{S}_b$	$\mathcal{S}_\delta$	$\xi_\delta = (\tilde{\xi}_\delta, \tau_\delta, k_f, k_{u_f}, \tau_{u_f}, \tau_{s_f})$	$\tilde{\xi}_\delta = [\delta_f^T, \Delta\delta_f^T, e_{\delta_f}^T, e_{u_f}^T, S_f]^T$	*

states $\tilde{\xi}_\pi$ include the components of ξ_π whose stabilities are relevant to the stabilization set Ξ in Definition 7; ξ_{π_i}, $\tilde{\xi}_{\pi_i}$ are the corresponding states of agent i; π_m and π_f represent the corresponding augmented vectors of π_i for $i \in \mathcal{N}_m$ and $i \in \mathcal{N}_f$, respectively, with π determined by the relevant state (e.g., η, δ). Furthermore, according to the inherent cascade property, we divide the subsystems into three groups, namely, $\mathcal{S}_h$, $\mathcal{S}_a$ and $\mathcal{S}_b$, with the corresponding state vectors $\xi_h = [\xi_\eta^T, \xi_\chi^T]^T$, $\xi_a = [\xi_m^T, \xi_\omega^T, \xi_v^T, \xi_\gamma^T]^T$ and $\xi_b = \xi_\delta$. More specifically, the dynamics of $\mathcal{S}_h$ only depends on its own states and the external disturbances. Besides the states of its own and the external disturbances, the dynamics of $\mathcal{S}_a$ is also influenced by the states of $\mathcal{S}_h$; and the dynamics of $\mathcal{S}_b$ depends on the states of $\mathcal{S}_a$ and $\mathcal{S}_h$ (See Figure 4.3 (b)). In addition, f_{Π_1}, $g_{e_{\Pi_2}}$ and $g_{s_{\Pi_3}}$ with $\Pi_1 \in \{h, a, b\}$, $\Pi_2 \in \{a, b\}$, $\Pi_3 \in \{m, \gamma_f, b\}$ in (4.31) are given by the differential equations in (4.6), (4.8), (4.13), (4.15), (4.18), (4.23), (4.24), (4.25) and (4.21), accordingly. The corresponding flow

§§ * in a table represents the same element with the above cells.

domain is given by

$$\begin{aligned}
&C = C_t \cap C_s \cap C_u,\ C_t = \cap_{i\in\mathcal{N}} C_{t_i},\ C_u = \cap_{i\in\mathcal{N}} C_{u_i};\\
&C_{s_i} = \{\xi \in \mathbb{X} | 0 \le \tau_{s_i} \le \tau^i_{masp}\},\ C_{u_i} = \{\xi \in \mathbb{X} | 0 \le \tau_{u_i} \le \tau^{u_i}_{macp}\};\\
&C_{t_i} = \cap_{\pi=\omega,v,\gamma,\delta} C_{\pi_i},\ C_{\pi_i} = \{\xi \in \mathbb{X} | 0 \le \tau_{\pi_i} \le \tau^{\pi_i}_{macp}\},\ i \in \mathcal{N}_f;\\
&C_{t_i} = \{\xi \in \mathbb{X} | 0 \le \tau_{t_i} \le \tau^i_{matp}\},\ i \in \mathcal{N}_m.
\end{aligned} \tag{4.32}$$

Define $\tilde{\xi} = [\tilde{\xi}_h^T, \tilde{\xi}_a^T, \tilde{\xi}_b^T]^T$, then based on the hybrid system model in (4.26)–(4.32), the problem considered in this work is to prove that the set $\Xi = \{\xi \in \mathbb{X} | \|\tilde{\xi}^T\| = 0\}$ is strongly iISS w.r.t. disturbances ς. According to the cascade-connected structure, we solve the problem step by step as follows:

- For subsystem $\mathcal{S}_h$, determine the bound on τ^i_{masp}, such that the estimation errors Δv_i, $\Delta\omega_i$ converge to small balls centered at the origin with pre-specified small radius in pre-specified short time.

- For subsystem $\mathcal{S}_a$, determine the upper bounds on τ^i_{masp}, $\tau^{\pi_i}_{macp}$, $i \in \mathcal{N}_f$ and $\tau^{u_i}_{macp}$, $i \in \mathcal{N}$, as well as the corresponding ET functions h_{π_i}, h_{u_i}, such that the set $\Xi_a = \{\xi \in \mathbb{X} | \|\tilde{\xi}_a\| = 0\}$ is ISS w.r.t. ς and $\tilde{\xi}_h$.

- For subsystem $\mathcal{S}_b$, determine the upper bounds on τ^i_{masp}, $\tau^{u_i}_{macp}$, $\tau^{\delta_i}_{macp}$, $i \in \mathcal{N}_f$; the functions in ET conditions h_{u_i} and h_{δ_i}, such that the set $\Xi_b = \{\xi \in \mathbb{X} | \|\tilde{\xi}_b^T\| = 0\}$ is ISS w.r.t. ς, $\tilde{\xi}_h$ and $\tilde{\xi}_a$.

4.5 Main Results

In this section, the event-triggered formation tracking problem is solved in a hybrid system framework. The upper bounds on MASPs, MATPs, and MACPs are determined along with well-designed PETMs for detections, transmissions and controller updates. For generalizing the analysis, in each subsection, we will first provide a technical lemma for some general systems, and then, apply it to the concerned one ($\mathcal{S}_h$, $\mathcal{S}_a$, or $\mathcal{S}_b$).

4.5.1 Finite Time Convergence of Subsystem $\mathcal{S}_h$

Consider a hybrid system with state vector $\xi = (\tilde{\xi}, \tau) \in \mathbb{X}$, where $\tilde{\xi} = [x^T, S^T]^T$, $\mathbb{X} = \{(x, S, \tau) \in \mathbb{R}^{n_x} \times \mathbb{R}^{n_s} \times \mathbb{R}_{\geq 0}\}$. On flow domain $C = \{\xi \in \mathbb{X} | 0 \leq \tau \leq \tau_{masp}\}$, its dynamics is described by differential equation $F(\xi, \varsigma)$,

$$\begin{aligned} \dot{\xi} &= F(\tilde{\xi}, \tau, \varsigma) = (f(\tilde{\xi}, \varsigma), 1),\ \xi \in C; \\ f(\tilde{\xi}, \varsigma) &= \frac{1}{\epsilon} f_0(\tilde{\xi}) + [E_1^T, 0]^T f_1(\varsigma_1) + \frac{1}{\epsilon}[E_2^T, 0]^T f_2(\varsigma_2) + [0, E_s^T]^T f_s(\varsigma_s), \end{aligned} \tag{4.33}$$

where $\tau_{masp} > 0$ is the MASP to be determined, $f_0 : \mathbb{R}^{n_x+n_s} \to \mathbb{R}^{n_x+n_s}$, $f_i : \mathbb{R}^{n_{\varsigma_i}} \to \mathbb{R}^{n_i}$ are locally Lipschitz functions; $\varsigma = [\varsigma_1^T, \varsigma_2^T, \varsigma_s^T]^T$ represents the disturbances, with $\varsigma_i \in \mathbb{R}^{n_{\varsigma_i}}$ bounded by $\|\varsigma_i\|_\infty \leq r_i$; $E_i \in \mathbb{R}^{n_x \times n_i}$, $i = 1, 2, s$; and $\epsilon > 0$ is a small constant. On jump set $D = \{\xi \in \mathbb{X} | \tau_0 \leq \tau \leq \tau_{masp}\}$, we have

$$[x^{+T}, S^{+T}, \tau^{+T}]^T = [x^T, \mathbf{0}^T, \mathbf{0}^T]^T,\ \ \xi \in D. \tag{4.34}$$

Introduce an auxiliary variable ϕ with dynamics satisfying

$$\dot{\phi} = -l(\phi^2 + \frac{\alpha_s}{\epsilon}) - 2L\phi,\ \phi(0) = \bar{\rho},\ \phi(\tau) \in [\underline{\rho}, \bar{\rho}],\ \ \forall \tau \in [0, \tau_{masp}), \tag{4.35}$$

where l, α_s, L, $\bar{\rho} > \underline{\rho} > 0$ are positive constants to be designed.

Lemma 10. The maximum value of τ_{masp} satisfies (4.35) can be computed explicitly as

$$\tau_{masp} = \begin{cases} \frac{1}{l\sqrt{\frac{\alpha}{\epsilon} - \frac{L^2}{l^2}}} \arctan\left(\theta \sqrt{\frac{\alpha}{\epsilon} - \frac{L^2}{l^2}}\right), & \frac{L}{l} < \sqrt{\frac{\alpha}{\epsilon}} \\ \frac{1}{l}\theta, & \frac{L}{l} = \sqrt{\frac{\alpha}{\epsilon}} \\ \frac{1}{l\sqrt{\frac{L^2}{l^2} - \frac{\alpha}{\epsilon}}} \arctan\left(\theta \sqrt{\frac{L^2}{l^2} - \frac{\alpha}{\epsilon}}\right), & \frac{L}{l} > \sqrt{\frac{\alpha}{\epsilon}} \end{cases}, \tag{4.36}$$

where $\theta = \frac{\bar{\rho} - \underline{\rho}}{\frac{\alpha}{\epsilon} + \bar{\rho}\underline{\rho} + \frac{L}{l}(\bar{\rho} + \underline{\rho})}$. Especially, when $L = 0$, $\tau_{masp} = \frac{\sqrt{\epsilon\alpha}}{l} \arctan \frac{\sqrt{\epsilon/\alpha}(\bar{\rho} - \underline{\rho})}{1 + \epsilon/\alpha \bar{\rho}\underline{\rho}}$.

Proof. The results can be obtained by solving the differential equation in (4.35). □

The following condition is introduced to provide the finite time convergence of subsystem $\mathcal{S}_h$.

Condition 4. Consider the hybrid system in (4.33)–(4.34). There exist locally Lipschitz functions $W(S) : \mathbb{R}^{n_s} \to \mathbb{R}_{\geq 0}$, $V(x) : \mathbb{R}^{n_x} \to \mathbb{R}_{\geq 0}$, a differential equation $\phi(t) : [0, \tau_s) \to \mathbb{R}_{\geq 0}$ satisfying (4.35), and positive constants $\bar{\alpha} > \underline{\alpha} > 0$, $\alpha > 0$ such that

- $\underline{\alpha}\|\tilde{\xi}\|^2 \leq U(\xi) \leq \bar{\alpha}\|\tilde{\xi}\|^2$,
- $\langle \nabla U(\xi), F(\xi, \varsigma)\rangle \leq -\frac{1}{\epsilon}\alpha U(\xi) + (\beta_1(\|\varsigma_1\|) + \frac{1}{\epsilon}\beta_2(\|\varsigma_2\|))\sqrt{U(\xi)} + \beta_s(\|\varsigma_s\|)$, $\xi \in C$,
- $U^+(\xi) - U(\xi) \leq 0,\ \xi \in D$,

where $U(\xi) = V(x) + l\phi W^2(S)$, β_1, β_2 and β_s are $\mathcal{K}_\infty$ functions.

Lemma 11. Consider the hybrid system described by (4.33)–(4.34). If Condition 4 is satisfied and τ_{masp} satisfies (4.36), then for any $\xi(0,0) \in \mathbb{X}$, the hybrid system converges to set $\Xi = \{\xi(t,j)|\ \|\tilde{\xi}\| \leq \frac{1}{\underline{\alpha}} r_U\}$, within the finite time $T_x = \frac{1}{\alpha_U} \ln \frac{U_0}{r_U^2}$, where $r_U = \frac{2}{\alpha}(\epsilon\beta_1(\|\varsigma_1\|_\infty) + \beta_2(\|\varsigma_2\|_\infty))$, $\alpha_U = \frac{\alpha}{2\epsilon} - \frac{\beta_s(\|\varsigma_s\|)}{r_U^2}$ and U_0 represents the initial value of $U(\xi(0,0))$.

Proof. Let $\mathbb{X}_U = \{\xi(t,j)|U(\xi) \leq r_U^2\}$. By the second item in Condition 4, for all $\xi \in \mathbb{X}\backslash\mathbb{X}_U$ we have

$$\langle \nabla U(\xi(t,j), F(\xi(t,j), \varsigma(t,j))\rangle \leq -\frac{\alpha}{2\epsilon}U(\xi) + \beta_s(\|\xi_s\|) \leq -\alpha_U U(\xi),\quad \xi(t,j) \in C,$$
$$U(\xi(t,j+1)) - U(\xi(t,j)) \leq 0,\quad \xi(t,j) \in D.$$

For $(t,j) \in [t_k, t_{k+1}] \times \{k\}$, $k \in \mathbb{N}$, we have

$$t - t_k \leq \frac{1}{\alpha_U} \ln \frac{U(t_k, k)}{U(t,k)}, \tag{4.37}$$

and when $(t,j) = (t_{k+1}, k+1)$, $U(\xi(t_{k+1}, k+1)) - U(\xi(t_{k+1}, k)) \leq 0$. As a result, for any initial condition $\xi(0,0) \in \mathbb{X}$, after a limited number j of time intervals, $U(t, j-1) \leq r_U^2$. Furthermore, according to (4.37), t can be calculated by $t \leq \frac{1}{\alpha_U} \ln \frac{U(\xi(0,0))}{r_U^2}$, and by the first two items in Condition 4, we have $\Xi \in \mathbb{X}_U$. The proof is completed. □

Theorem 8. Consider subsystem $\mathcal{S}_h$, and assume the following conditions hold:

(i) the initial state $\delta_i(0) \in \mathbb{V}_i$ with $\mathbb{V}_i$ given as in (4.9), and the input saturation satisfies (4.11);

(ii) for subsystem $\mathcal{S}_\pi$, there exist positive definite matrices P_π and Q_π, where $\bar{\alpha}_\pi \geq \lambda(P_\pi) \geq \underline{\alpha}_\pi > 0$, $\lambda(Q_\pi) \geq \alpha_\pi^s > 0$; positive constants α_π, $l_\pi > 0$ and $\bar{\rho}_i^\pi > \underline{\rho}_i^\pi > 0$, such that

$$\begin{aligned} &A_\pi^T P_\pi + P_\pi A_\pi \leq -Q_\pi, \quad \begin{bmatrix} -Q_\pi + \left[\begin{smallmatrix} 0 & 0 \\ 0 & \epsilon_\pi \end{smallmatrix}\right] & P_\pi B_\pi \\ * & -l_\pi^2 \alpha_\pi^s \end{bmatrix} \leq -\alpha_\pi I, \\ &\underline{\alpha}_\pi < l_\pi \underline{\rho}_i^\pi < l_\pi \bar{\rho}_i^\pi < \bar{\alpha}_\pi. \end{aligned} \tag{4.38}$$

Here, π is replaced with η and χ for subsystems $\mathcal{S}_\eta$ and $\mathcal{S}_\chi$, respectively;

(iii) the MASP is upper bounded by $\tau_{masp}^i \leq \min\{\tau_{masp}^{\eta_i}, \tau_{masp}^{\chi_i}\}$, where $\tau_{masp}^{\pi_i}$ is calculated by (4.36), with $\epsilon = \epsilon_\pi$, $l = l_\pi$, $\alpha_s = \alpha_\pi^s$, $L = L_\pi$, $L_\eta = 0$ and $L_\chi = |\omega_M + r_\omega|$.

Then, there exist small enough $\epsilon_\eta, \epsilon_\chi > 0$ such that $\tilde{\xi}_{\eta_i}$ and $\tilde{\xi}_{\chi_i}$ converge into a small ball centered at the origin with radius r_ω, r_v within time T_ω, T_v, where $r_\omega = \frac{4\epsilon_\eta \bar{\alpha}_\eta^2}{\alpha_\eta^s \underline{\alpha}_\eta^{1.5}} a_\omega$, $T_\omega = \frac{2\epsilon_\eta}{\alpha_\eta} \ln \frac{U_\eta(\xi_\eta(0,0))}{r_\omega^2}$, $r_v = \frac{4\epsilon_\chi \bar{\alpha}_\chi^2}{\alpha_\chi \underline{\alpha}_\chi^2}(\max\{c_{\chi 1}^i, c_S^i\} + \frac{c_{\chi 2}^i}{\epsilon_\chi})$ and $T_v = \frac{2\epsilon_\chi}{\alpha_\chi} \ln \frac{U_\chi(\xi_\chi(0,0))}{r_v^2}$ with $c_{\chi 1}^i = a_v$, $c_{\chi 2}^i = r_\omega(c + \frac{U_i}{\sqrt{1+\bar{d}_{i0}^2}} \max(1, \bar{d}_{i0}))$, $c_S^i = \frac{U_i}{\sqrt{1+\bar{d}_{i0}^2}} \max(1, \bar{d}_{i0}) + c r_\omega$.

Proof. The proof is provided in Appendix A.1. □

Remark 15. According to (4.6) and (4.8), subsystem $\mathcal{S}_h$ satisfies (4.33)–(4.34). The small constant $\epsilon > 0$ is introduced to guarantee a small convergence error and a fast convergence rate as shown in Lemma 11. However, referring to (4.36), a smaller ϵ also results in a smaller upper bound on MASP, which means a sufficiently large sampling frequency. Benefited from the hierarchical structure proposed in Subsection 4.2.3, only a few agents $i \in \mathcal{N}_m$ are involved in $\mathcal{S}_h$; and since the convergence errors of $\mathcal{S}_h$ will propagate to $\mathcal{S}_a$ and $\mathcal{S}_b$, we choose to sacrifice the cost on some high performance sensors to provide better convergence properties for $\mathcal{S}_h$.

4.5.2 ISS of Subsystem $\mathcal{S}_a$

Consider a hybrid system with state vector $\xi = (\tilde{\xi}, k, \tau_e, \tau_S) \in \mathbb{X}$, where

$$\begin{aligned}
&\tilde{\xi} = [x^T, e^T, S^T]^T, \mathbb{X} = \Big\{(x, e, S, k, \tau_e, \tau_S) \in \mathbb{R}^{nn_x} \times \mathbb{R}^{nn_e} \times \mathbb{R}^{nn_s} \times \mathbb{N}^n \times \mathbb{R}^n_{\geq 0} \times \mathbb{R}^n_{\geq 0}\Big\}, \\
&x = [x_1^T, \cdots, x_n^T]^T,\ e = [e_1^T, \cdots, e_n^T]^T,\ S = [S_1^T, \cdots, S_n^T]^T, \\
&\tau_e = [\tau_{e_1}, \cdots, \tau_{e_n}]^T,\ \tau_s = [\tau_{s_1}, \cdots, \tau_{s_n}]^T, k = [k_1, \cdots, k_n]^T.
\end{aligned} \tag{4.39}$$

On the flow domain, the differential equation is given by

$$F(\xi, \varsigma) = (f(\tilde{\xi}, \varsigma), g_e(\tilde{\xi}, \varsigma), g_s(\tilde{\xi}, \varsigma), \mathbf{0}, \mathbf{1}),\ \xi \in C, \tag{4.40}$$

where $g_e(\tilde{\xi}, \varsigma) = (g_1^e(\tilde{\xi}, \varsigma), \cdots, g_n^e(\tilde{\xi}, \varsigma))$, $g_s(\tilde{\xi}, \varsigma) = (g_1^s(\tilde{\xi}, \varsigma), \cdots, g_n^s(\tilde{\xi}, \varsigma))$; $\varsigma \in \mathbb{R}^{n_\varsigma}$ represents the disturbances. The corresponding flow set C is given by $C = \cap_{i=1}^n C_i$, $C_i = \{\xi \in \mathbb{X} | (0 \leq \tau_{s_i} \leq \tau^i_{masp}) \vee (0 \leq \tau_{e_i} \leq \tau^i_{macp})\}$, where τ^i_{macp} and τ^i_{masp} represent the MACP for checking the ET condition and MASP for detection, respectively. On the jump domain, the set-valued mapping G satisfies

$$G(\xi) = G_s(\xi) \cup G_e(\xi),\ \xi \in D, \tag{4.41}$$

where G_s and D_s are in the same forms as (4.27); G_e and D_e are in the same forms as in (4.29), with $e_m = e_f = k_f = \tau_m = \tau_f = 0$, $e_u = e$, $\tau_u = \tau_e$, $\Gamma^u_i = \Gamma_i$, $\bar{\Lambda}^u_i = \bar{\Lambda}^e_i$; and $\bar{\Lambda}^e_i = \Lambda_i \otimes I_{n_e}$, $\Lambda_i \in \mathbb{R}^{n \times n}$ is a diagonal matrix with the i-th diagonal elements being 1 and others being 0 and $h_i(e_i, q_i, t)$ is the ET function to be specified later.

The following conditions are introduced to provide the ISS property for the hybrid system in (4.40)–(4.41).

Condition 5. ([82, 87]) Consider the hybrid system in (4.40)–(4.41). For each $i = 1, \cdots, n$, there exist a locally Lipschitz function $W^\pi_i : \mathbb{R}^{n_\pi} \times \mathbb{N} \to \mathbb{R}_{\geq 0}$, a continuous function $H^\pi_i : \mathbb{R}^{n_x} \times \mathbb{R}^{n_\pi} \to \mathbb{R}_{\geq 0}$ and $\underline{\alpha}^\pi_{W_i}$, $\bar{\alpha}^\pi_{W_i} \in \mathcal{K}_\infty$ such that the following hold:

- For any $\pi_i \in \mathbb{R}^{n_\pi}$ and $k_i \in \mathbb{N}$, $\underline{\alpha}^\pi_{W_i}(\|\pi_i\|) \leq W^\pi_i(\pi_i, k_i) \leq \bar{\alpha}_{W_i}(\|\pi_i\|)$.

- For almost all $\pi_i \in \mathbb{R}^{n_\pi}$, all $k_i \in \mathbb{N}$ and $(x, \varsigma) \in \mathbb{R}^{n_x} \times \mathbb{R}^{n_\varsigma}$, $\left\langle \frac{\partial W_i(\pi_i, k_i)}{\partial \pi_i}, g_i^\pi(\tilde{\xi}, \varsigma) \right\rangle \leq H_i^\pi(\tilde{\xi}, \varsigma)$.

Here π and π_i are replaced with e (e_i) and s (s_i) when the functions are related to e (e_i) and s (s_i), respectively.

Condition 6. ([82, 87]) There exist a locally Lipschitz function $V_x : \mathbb{R}^{n_x} \to \mathbb{R}_{\geq 0}$, $\underline{\alpha}_V$, $\bar{\alpha}_V$, α_V, α_W^π, $\sigma_{V_i} \in \mathcal{K}_\infty$, locally Lipschitz functions $\Psi_i : \mathbb{R}^{n_e} \to \mathbb{R}_{\geq 0}$ satisfying $\Psi_i(0) = 0$, continuous functions $J_i : \mathbb{R}^{n_x} \times \mathbb{R}^{n_e} \times \mathbb{R}^{n_\varsigma} \to \mathbb{R}_{\geq 0}$, $l_{\pi_i} > 0$, $i \in \mathcal{V}_f$, such that the following hold:

- For all $x \in \mathbb{R}^{nn_x}$, $\underline{\alpha}_V(\|x\|) \leq V_x \leq \bar{\alpha}_V(\|x\|)$.

- For almost all $x \in \mathbb{R}^{n_x}$ and all $(e, S, \varsigma) \in \mathbb{R}^{nn_e} \times \mathbb{R}^{nn_S} \times \mathbb{R}^{n_\varsigma}$,
$$\left\langle \nabla V_x(x), f(\tilde{\xi}, \varsigma) \right\rangle \leq -\alpha_V(\|x\|) - \alpha_W(\|[e^T, S^T]^T\|)$$
$$+ \sum_{i=1}^{n} \left((\sigma_{V_i}(\varsigma) + \sum_{\pi=e,\pi=S} \left({l_{\pi_i}}^2 W_i^{\pi 2}(\pi_i, k_i) - H_i^{\pi 2}(\tilde{\xi}, \varsigma) \right) - J_i(\tilde{\xi}, \varsigma) - \Psi_i(q_i(x)) \right),$$
where $q_i(x)$ is a locally Lipschitz function of x with $f_{q_i}(\tilde{\xi}, \varsigma) = \frac{\partial q_i(x)}{\partial x} f(\tilde{\xi}, \varsigma)$; W_i^π and H_i^π are the same as in Condition 5.

- For almost all $x \in \mathbb{R}^{n_x}$ and all $(e, S, \varsigma) \in \mathbb{R}^{nn_e} \times \mathbb{R}^{nn_S} \times \mathbb{R}^{n_\varsigma}$,
$$\left\langle \nabla \Psi_i(q_i), f_{q_i}(\tilde{\xi}, \varsigma) \right\rangle \leq L_i \Psi(q_i) + H_i^{e2}(\tilde{\xi}, \varsigma) + J_i(\tilde{\xi}, \varsigma).$$

According to Conditions 5 and 6, the ET function in (4.41) is designed as

$$h_i(e_i, q_i, t) = l_{e_i} W_i^{e2}(e_i, k_i) - \lambda_i \rho_i \Psi_i(q_i), \tag{4.42}$$

where $\rho_i = \frac{l_{e_i} \lambda_i}{1 - \lambda_i L_i}$, λ_i is introduced as a user-specified parameter to tune MACPs and event numbers and constrained by $\lambda_i \in [0, \lambda_i^*)$, with

$$\lambda_i^* = \begin{cases} 1, & L_i \leq -l_{e_i} \\ \min\{1, \frac{1}{L_i + l_{e_i}}\}, & L_i > -l_{e_i} \end{cases}.$$

Lemma 12. ([82, 87]) Consider the hybrid system in (4.40)-(4.41) with ET function given by (4.42). If (i) $\tau_{macp}^i = \frac{1}{l_{e_i}} \arctan \frac{1/\rho_i - \rho_i}{2}$, (ii) $\tau_{masp}^i = \frac{1}{l_{s_i}} \arctan \frac{\bar{\rho}_i - \underline{\rho}_i}{1 + \bar{\rho}_i \underline{\rho}_i}$, with $\bar{\rho}_i > \underline{\rho}_i > 0$, (iii) Conditions 5 and 6 hold; then the set $\Xi : \{\xi \in \mathbb{X} | \|\tilde{\xi}\| = 0\}$ is globally ISS w.r.t. ς.

Proof. Consider Lyapunov candidate

$$U(\xi) = V_x + \sum_{i\in\mathcal{N}_f}(l_{s_i}\phi_{s_i}W_i^{s2} + \max\{l_{e_i}\phi_{e_i}W_i^{e2}, \lambda_i\psi_i\}),$$

where ϕ_{e_i} and ϕ_{s_i} are auxiliary variables introduced, respectively, as

$$\begin{cases}\dot{\phi}_{e_i} = -l_{e_i}({\phi_{e_i}}^2+1)\\ \phi_{e_i}(0) = \bar{\rho}_i^e\\ \phi_{e_i}(\tau)\in[\underline{\rho}_i^e, \bar{\rho}_i^e]\end{cases} \quad\text{and}\quad \begin{cases}\dot{\phi}_{s_i} = -l_{s_i}({\phi_{s_i}}^2+1)\\ \phi_i^s(0) = \bar{\rho}_i\\ \phi_{s_i}(\tau)\in[\underline{\rho}_i, \bar{\rho}_i].\end{cases} \tag{4.43}$$

Here l_{e_i} and l_{s_i} are positive constants. The bound on ϕ_{e_i} satisfies $\underline{\rho}_i^e \geq \rho_i$ and $\bar{\rho}_i^e \leq \frac{1}{\rho_i}$. Let $V_{s_i} = l_{s_i}\phi_{s_i}W_i^{s2}$, we have

$$\langle\nabla V_{s_i}, F(\xi,\varsigma)\rangle \leq 2l_{s_i}\phi_{s_i}W_i^s(|H_i^s|) - (1+{\phi_{s_i}}^2)(l_{s_i}W_i^s)^2. \tag{4.44}$$

Let $V_{e_i} = \max\{l_{e_i}\phi_{e_i}W_i^{e2}, \lambda_i\psi_i\}$. Denote $\mathcal{V}_0(t,j)$ as the set includes the agents satisfying $l_{e_i}\phi_{e_i}W_i^{e2} \geq \lambda_i\Psi_i$, and $\mathcal{V}_1(t,j) = \mathcal{V}\backslash\mathcal{V}_0(t,j)$. On flow domain, for $i\in\mathcal{V}_0$,

$$\langle\nabla V_{e_i}, F(\xi,\varsigma)\rangle \leq 2l_{e_i}\phi_{e_i}W_i^e(|H_i^e|) - (1+{\phi_{e_i}}^2)(l_{e_i}W_i^e)^2;$$

and for $i\in\mathcal{V}_1$,

$$\langle\nabla V_{e_i}, F(\xi,\varsigma)\rangle \leq \lambda_i(L_i\Psi_i + J_i + H_i^{e2}).$$

Combining with Condition 6,

$$\begin{aligned}&\langle\nabla U(\xi), F(\xi,\varsigma)\rangle \leq\\ &-\alpha_V(\|x\|) - \alpha_W(\|[e^T, S^T]^T\|) + \sum_{i=1}^N\sigma_{V_i}(\|\varsigma\|) + \sum_{i\in\mathcal{V}_1}\big((l_{e_i}W_i^e)^2 - (1-\lambda_iL_i)\Psi_i\big).\end{aligned} \tag{4.45}$$

According to (4.42), we have

$$(l_{e_i}W_i^e)^2 - (1-\lambda_iL_i)\Psi_i < 0,$$

and

$$\langle\nabla U(\xi), F(\xi,\varsigma)\rangle \leq -\alpha_V(\|x\|) - \alpha_W(\|[e^T, S^T]^T\|) + \sum_{i=1}^N\sigma_{V_i}(\|\varsigma\|).$$

On jump domain, for $\xi \in G_i^e$, when there is no transmission, ${V_{e_i}}^+ = \max\{l_{e_i}\phi_{e_i}W_i^{e2}, \lambda_i\Psi_i\}$. According to (4.42), $l_{e_i}W_i^{e2} \leq \lambda_i\rho_i\Psi_i$, $l_{e_i}\frac{1}{\rho_i}W_i^{e2} \leq \lambda_i\Psi_i$. Since $\phi_{e_i} \leq \bar{\rho}_i^e \leq \rho_i$, we have $l_{e_i}\phi_{e_i}W_i^{e2} \leq \lambda_i\Psi_i$. Then,

$$ {V_{e_i}}^+ = \lambda_i\Psi_i = V_{e_i}. $$

When there is a transmission,

$$ W_i^{e+} = 0,\ {V_{e_i}}^+ = \lambda_i\Psi_i \leq \max\{l_{e_i}\phi_{e_i}W_i^{e2}, \lambda_i\Psi_i\} \leq V_{e_i}. $$

For $\xi \in G_i^s$, we have ${V_{s_i}}^+ = 0 \leq V_{s_i}$. Combining the above, when $\xi \in G$, $U^+ \leq U$. Using the standard Lyapunov arguments in [87], [78] and [82], the set Ξ is ISS w.r.t. ς. □

Remark 16. Conditions 5 and 6 are similar to Assumptions 1 and 2 in [82]. However, only PUSC was considered in the paper [82]; while, in order to include PULC, auxiliary variables τ_{s_i} and measurement error S are introduced in hybrid model (4.40)–(4.41). Subsequently, a different Lyapunov function candidate is proposed in the proof of Lemma 12 to provide the stability for the hybrid system under both PUSC and PULC.

According to (4.13), (4.15) and (4.18), the subsystems belong to $\mathcal{S}_a$ satisfying the dynamics in (4.40)–(4.41), which results in the following theorems to illustrate the ISS of $\mathcal{S}_a$.

Theorem 9. Consider the subsystem $\mathcal{S}_m$, if

(i) the initial state $\delta_i(0,0) \in \mathbb{X}_{i_1}$, where $\mathbb{X}_{i_1} = \{\xi_{m_i} | U(\xi_{m_i}) \leq \underline{\alpha}_u c_\delta^2\}$;

(ii) there exist positive constants ϵ_2, α_δ, α_e, l_u, ψ_u, $L_u > 0$, such that the following LMI is established

$$ \begin{bmatrix} -(2c(1-\psi_u)+(I-L_u)\psi_u+\epsilon_\Psi-\alpha_\delta)I+(1+\psi_u)\begin{bmatrix} 0 & 0 \\ 0 & \frac{1}{\epsilon_2^2} \end{bmatrix} & (1-\psi_u)I \\ (1-\psi_u)I & -(l_u^2-\alpha_e)I \end{bmatrix} = Q_m < 0; \tag{4.46} $$

(iii) the MACP is upper bounded by $\tau_{macp}^{u_i} < \frac{1}{l_u} \arctan \frac{\bar{\rho}_i^u - \underline{\rho}_i^u}{2}$, where $\bar{\rho}_i^u < \frac{1}{\rho_u}$, $\underline{\rho}_i^u > \rho_u$; ρ_u and λ_u are determined by (4.42), with $l_{e_i} = l_u$, $L_i = 0$; and the ET function is given by $h_{u_i}(e_{u_i}, \delta_i, t) = l_u e_{u_i}^2 - \lambda_u \rho_u \psi_u \delta_i^2$;

(iv) items (i)–(iii) in Theorem 8 are satisfied;

then, there exist sufficiently small $\epsilon_\eta > 0$ and $\epsilon_\chi > 0$ such that the steady state error of $\tilde{\xi}_{m_i}$ is given by $r_\delta = \sqrt{\frac{\bar{\alpha}_u}{\underline{\alpha}_u}} c_\delta$, where $\bar{\alpha}_u = \max\{\frac{1+\lambda_u\psi_u}{\alpha_\delta}, \frac{l_u \bar{\rho}_i^u}{\alpha_e}\}$ and $\underline{\alpha}_u = \min\{1 + \frac{\lambda_u \psi_u}{2}, \frac{l_u \underline{\rho}_i^u}{2}\}$.

Proof. Detailed proof is provided in Appendix A.2. □

Remark 17. The constant c_δ in (4.9) determines the convergence range of subsystem $\mathcal{S}_m$. According to (4.10), a lager c_δ results in a larger U_i, which further leads to a larger convergence error r_v. As a result, the trade-off between estimation performance and constraints on initial errors needs to be considered.

Theorem 10. For subsystem $\mathcal{S}_\pi$, where π is replaced by ω or v for the state $\tilde{\xi}_\omega$ or $\tilde{\xi}_v$, respectively, the set $\Xi_\pi = \{\xi \in \mathbb{X} | \|\tilde{\xi}_\pi^T\| = 0\}$ is globally ISS w.r.t. ς and ξ_h if

(i) Assumption 10 is satisfied;

(ii) there exist positive constants ϵ_π, ϵ_{π_j}, $j = 0, 1, 2$, L_{π_i}, l_{π_i}, ψ_{π_i}, α_{W_π}, α_{V_π}, ϵ_{π_e} and positive definite matrix P_π such that the following LMI can be established

$$\begin{aligned} &A_\pi - A_\pi^\psi - (I - L_\omega)\psi_\pi \begin{bmatrix} (L_{ff} - D_{fl})^T \\ -A_{ff}^T \end{bmatrix} [(L_{ff} - D_{fl}) \ -A_{ff}] \\ &- \begin{bmatrix} (\epsilon_{\pi_e} - \alpha_{V_\pi}) I & 0 \\ 0 & l_\pi^2 - \alpha_{W_\pi} I \end{bmatrix} = Q_\pi \leq 0; \end{aligned} \tag{4.47}$$

here, $L_\pi = \text{diag}(L_{\pi_{n_{m+1}}}, \cdots, L_{\pi_n})$, $l_\pi = \text{diag}(l_{\pi_{n_{m+1}}}, \cdots, l_{\pi_n})$, $\psi_\pi = \text{diag}(\psi_{\pi_{n_{m+1}}}, \cdots, \psi_{\pi_n})$,

$$\begin{aligned} A_\pi =& - \begin{bmatrix} P_\pi \\ \mathbf{0}_{(n_f, n_f)} \end{bmatrix} [c_\pi (L_{ff} - \frac{\epsilon_\pi^2}{2} I) - \frac{\epsilon_{\pi_0}^2}{2} I, \ L_{ff}] + [**]^T, \\ A_\pi^\psi =& \begin{bmatrix} (L_{ff} - D_{fl})^T \\ -A_{ff}^T \end{bmatrix} \psi_\pi \big(- c_\pi D_f [L_{ff} - \epsilon_{\pi_1}^2 (L_{ff} - D_{fl}), \ L_{ff} - \epsilon_{\pi_1}^2 A_{ff}] \\ &+ \epsilon_{\pi_2}^2 [(L_{ff} - D_{fl}), \ -A_{ff}] \big) + [**]^T, \end{aligned}$$

and $D_f, D_{fl} \in \mathbb{R}^{n_f \times n_f}$ are diagonal matrices with diagonal elements $[D_f]_{(i,i)} = \sum_{j \in \mathcal{N}_f} a_{ij}$ and $[D_{fl}]_{(i,i)} = \sum_{j \in \mathcal{N}_m} a_{ij}$, respectively;

(iii) the MACP for ET function h_{π_i} is upper bounded by $\tau^{\pi_i}_{macp} < \frac{1}{l_{\pi_i}} \arctan \frac{\bar{\rho}^{\pi}_i - \underline{\rho}^{\pi}_i}{2}$, where $\bar{\rho}^{\pi}_i < \frac{1}{\rho_{\pi_i}}$, $\underline{\rho}^{\pi}_i > \rho_{\pi_i}$ and ρ_{π_i} satisfies (4.42), with $l_{e_i} = l_{\pi_i}$, $L_i = L_{\pi_i}$; and the ET function is designed by $h_{\pi_i} = l_{\pi_i}\|e_{\pi_i}\|^2 - \lambda_{\pi_i}\rho_{\pi_i}\psi_{\pi_i}\|q_{\pi_i}\|^2$, where $q_{\pi_i} = \sum_{j \in \mathcal{N}_f} a_{ij}(\hat{\pi}_i(t) - \hat{\pi}_j(t^j_{k_j}))$.

Proof. Detailed proof is provided in Appendix A.3. □

The following matrices and parameters are defined to facilitate the analysis of subsystem $\mathcal{S}_\gamma$. Let

$$\begin{aligned} Q_{\gamma_f} = &- \Big(A_\gamma - A^{\psi}_\gamma - (1 - L_\gamma)\psi_\gamma \begin{bmatrix} (L_{ff} - D_{fl})^T \\ -A^T_{ff} \\ -I \end{bmatrix} [(L_{ff} - D_{fl}) \ - A_{ff} \ - I] \\ &- \begin{bmatrix} (\epsilon_{\gamma_e} - \alpha_{V_\gamma})I & 0 & 0 \\ 0 & {l_\gamma}^2 - \alpha_{W_\gamma} I & 0 \\ 0 & 0 & {l^s_\gamma}^2 - \alpha_{W_\gamma} I \end{bmatrix} \Big) \end{aligned} \tag{4.48}$$

where $L_\gamma = \text{diag}(L_{\gamma_{n_m+1}}, \cdots, L_{\gamma_n})$, $l_\gamma = \text{diag}(l_{\gamma_{n_m+1}}, \cdots, l_{\gamma_n})$ and $l^s_\gamma = \text{diag}(l^s_{\gamma_{n_m+1}}, \cdots, l^s_{\gamma_n})$;

$$\begin{aligned} A_\gamma &= c_\gamma \begin{bmatrix} P_\gamma \\ \mathbf{0}_{(n_f, n_f)} \\ \mathbf{0}_{(n_f, n_f)} \end{bmatrix} [-L_{ff} + (\epsilon^2_\gamma + \frac{\epsilon^2_\omega}{c_\gamma})I, -L_{ff}, I] + [**]^T, \\ Q_\gamma &= \begin{bmatrix} aQ_{\gamma_f} & 0 \\ 0 & bQ_\omega - a\beta^\omega_\gamma I \end{bmatrix}, \beta^\omega_\gamma = \frac{2}{\epsilon^2_\omega} + \frac{2}{\epsilon^2_{\gamma_2}}\bar{\lambda}(\psi_\gamma L_{ff}), \\ A^{\psi}_\gamma =& c_\gamma \begin{bmatrix} (L_{ff} - D_{fl})^T \\ -A^T_{ff} \\ -I \end{bmatrix} \psi_\gamma \big([L_{ff} + A_{ff}][-L_{ff} \ - L_{ff} \ I] \\ &+ \epsilon^2_{\gamma_2}[(L_{ff} - D_{fl}) \ - A_{ff} \ - I]\big) + [**]^T. \end{aligned}$$

Theorem 11. For subsystem $\mathcal{S}_\gamma$, the set $\Xi_\gamma = \{\xi \in \mathbb{X} | \|\tilde{\xi}^T_\gamma\| = 0\}$ is globally ISS w.r.t. ς and ξ_h if

(i) there exist positive constants ϵ_γ, ϵ_ω, ϵ_{γ_2}, ϵ_{γ_e}, l_{γ_i}, $l^s_{\gamma_i}$, L_{γ_i}, ψ_{γ_i}, α_{V_γ}, α_{W_γ} and positive definite matrix P_γ, such that $Q_{\gamma_f} \geq 0$, and positive constants a and b such that $Q_\gamma > 0$;

(ii) the MASP satisfies $\tau_{masp}^{\gamma_i} = \frac{1}{l_{\gamma_i}^s} \arctan \frac{\bar{\rho}_i - \underline{\rho}_i}{2}$ and the MACP satisfies $\tau_{macp}^{\gamma_i} = \frac{1}{l_{\gamma_i}} \arctan \frac{\bar{\rho}_i^{\gamma} - \underline{\rho}_i^{\gamma}}{2}$, with $\bar{\rho}_i^{\gamma} \leq \frac{1}{\rho_{\gamma_i}}$, $\underline{\rho}_{\gamma}^{i} \geq \rho_{\gamma_i}$ and ρ_{γ_i} satisfying (4.42); and ET condition is designed by $h_{\gamma_i}(e_{\gamma_i}, q_{\gamma_i}, t) = l_{\gamma_i} e_{\gamma_i}^2 - \lambda_{\gamma_i} \rho_{\gamma_i} \psi_{\gamma_i} q_{\gamma_i}^2$, where $e_{\gamma_i}(t) = \tilde{\gamma}_i - \hat{\gamma}_i$ and $q_{\gamma_i}(t) = \sum_{j \in \mathcal{N}_f} a_{ij}(\hat{\gamma}_i - \tilde{\gamma}_j - \bar{\gamma}_{ij})$.

(iii) items in Theorem 10 are satisfied.

Proof. Detailed proof is provided in Appendix A.4. □

Combining the results in Theorems 9–11, for subsystem $\mathcal{S}_a$, the set $\Xi_a = \{\xi \in \mathbb{X} \mid \|\tilde{\xi}_a^T\| = 0\}$ is ISS with respect to ς and ξ_h.

4.5.3 Strongly iISS of Subsystem $\mathcal{S}_b$

Consider the hybrid system with the state vector given by (4.39). The elements in ξ are participated into $\xi_a = (\tilde{\xi}_a, k, \tau_a, \tau_s)$ and $\xi_b = (\tilde{\xi}_b, k, \tau_b, \tau_s)$ according to a cascade structure, where $x_i = [x_{a_i}^T, x_{b_i}^T]^T$, $e_i = [e_{a_i}^T, e_{b_i}^T]^T$, $S_i = [S_{a_i}^T, S_{b_i}^T]^T$, $\tau_{e_i} = [\tau_{a_i}, \tau_{b_i}]$, with $x_\pi = [x_{\pi_1}^T, \cdots, x_{\pi_n}^T]^T$, $x_{\pi_i} \in \mathbb{R}^{n_{x_\pi}}$, $e_\pi = [e_{\pi_1}^T, \cdots, e_{\pi_n}^T]^T$, $e_{\pi_i} \in \mathbb{R}^{n_{e_\pi}}$, $S_\pi = [S_{\pi_1}^T, \cdots, S_{\pi_n}^T]^T$, $S_{\pi_i} \in \mathbb{R}^{n_{s_\pi}}$, $\tilde{\xi}_\pi = [x_\pi^T, e_\pi^T, S_\pi^T]^T$, $\tau_\pi = [\tau_{\pi_1}, \cdots, \tau_{\pi_n}]$, $\pi = \{a, b\}$. On the flow domain, the differential equation is given by

$$\begin{cases} \dot{\xi} = F(\xi, \varsigma) = (f(\tilde{\xi}, \varsigma), g_e(\tilde{\xi}, \varsigma), g_s(\tilde{\xi}, \varsigma), \mathbf{0}, \mathbf{1}), \\ \dot{\xi}_a = F_a(\xi_a, \varsigma) = (f_a(\tilde{\xi}_a, \varsigma), g_{e_a}(\tilde{\xi}_a, \varsigma), g_{s_a}(\tilde{\xi}_a, \varsigma), \mathbf{0}, \mathbf{1}), \\ \dot{\xi}_b = F_b(\xi, \varsigma) = (f_b(\tilde{\xi}, \varsigma), g_{e_b}(\tilde{\xi}, \varsigma), g_{s_b}(\tilde{\xi}, \varsigma), \mathbf{0}, \mathbf{1}), \end{cases} \tag{4.49}$$

with flow set C given by $C = \cap_{i=1}^n C_i$, $C_i = \{\xi \in \mathbb{X} | (0 \leq \tau_{s_i} \leq \tau_{masp}^i) \vee (0 \leq \tau_{e_{a_i}} \leq \tau_{macp}^{a_i}) \vee (0 \leq \tau_{e_{b_i}} \leq \tau_{macp}^{b_i})\}$. The set-valued mapping G and jump domain D are given by

$$G(\xi) = G_s(\xi) \cup G_e(\xi), \ \xi \in D, \tag{4.50}$$

where G_s and D_s have the same forms as in (4.27); G_e and D_e have the same forms as G_t and D_t in (4.28), with $e_u = k_u = \tau_u = 0$, $e_t = e$, $\tau_t = \tau_e$, $\Gamma_i^t = \Gamma_i$, $\Lambda_i^t = \Lambda_i$, $\bar{\Lambda}_i^t = \bar{\Lambda}_i^e$, $\bar{\Lambda}_\pi^t = \bar{\Lambda}_\pi$; and $\bar{\Lambda}_i^e = \Lambda_i \otimes I_{n_e}$, $\bar{\Lambda}_\pi = I_n \otimes \Lambda_j^\pi$, $\Lambda_i \in \mathbb{R}^{n \times n}$, $\Lambda_i^\pi \in \mathbb{R}^{2 \times 2}$ are diagonal matrices with the i-th diagonal elements being 1, and others being 0.

Condition 7. Consider the hybrid system in (4.49)–(4.50). If there exist positive definite matrices $P_a(\tau_a, \tau_s, k)$, $P_b(\tau_b, \tau_s, k)$ and positive constants $\bar{\alpha}_a \geq \underline{\alpha}_a > 0$, $\underline{\alpha}_b \geq \bar{\alpha}_b > 0$ such that

(i) $\underline{\alpha}_a I \leq P_a \leq \bar{\alpha}_a I$ and $\underline{\alpha}_b I \leq P_b \leq \bar{\alpha}_b I$ hold for all $\tau_{a_i} \in [0, \tau^{a_i}_{macp})$, $\tau_{b_i} \in [0, \tau^{b_i}_{macp})$, $\tau_{s_i} \in [0, \tau^{i}_{masp})$ and $k \in \mathbb{N}$;

(ii) there exists a positive definite matrix Q_b, such that storage function $U_b(\xi_b) = \tilde{\xi}_b^T P_b \tilde{\xi}_b$ satisfies

$$\begin{aligned} &\langle \nabla U_b(\xi_b), F_b(\xi, \varsigma) \rangle \leq \\ &- \tilde{\xi}_b^T Q_b \tilde{\xi}_b + \sum_{k_b=1}^{n_b} \|\tilde{\xi}_a\|^{2k_b} \tilde{\xi}_b^T Q_{k_b} \tilde{\xi}_b + \sum_{k_a=1}^{n_a} \alpha_{k_a} \|\tilde{\xi}_a\|^{2k_a} + \sigma_b(\|\varsigma\|), \xi \in C, \\ &U_b^+(\xi_b) - U_b(\xi_b) \leq 0, \ \xi \in D, \end{aligned} \tag{4.51}$$

where Q_{k_b} is either a positive definite matrix or a zero matrix, $\alpha_{k_a} \geq 0$ is a constant, and σ_b is a $\mathcal{K}_\infty$ function;

(iii) there exists a positive definite matrix Q_a and a $\mathcal{K}_\infty$ function σ_a such that storage function $U_a(\xi_a) = \tilde{\xi}_a^T P_a \tilde{\xi}_a$ satisfies

$$\begin{aligned} &\langle \nabla U_a(\xi_a), F_a(\xi_a, \varsigma) \rangle \leq -\tilde{\xi}_a^T Q_a \tilde{\xi}_a + \sigma_a(\|\varsigma\|), \ \xi \in C; \\ &U_a^+(\xi_a) - U_a(\xi_a) \leq 0, \ \xi \in D; \end{aligned} \tag{4.52}$$

(iv) there exist positive constants $\epsilon_{k1}, \ \epsilon_{k2}, \ \cdots, \ \epsilon_{k(j_k-1)}$, $\forall \ k \in \mathcal{O}$, where $\mathcal{O} = \cup_{i \in \mathbb{N}} \mathcal{O}_i$, $\mathcal{O}_0 = \{k| \ k \leq \max\{k_a, k_b\} \& (Q_k \neq 0 | \alpha_k \neq 0)\}$, $\mathcal{O}_i = \{k | k = 2k_0 - 2^{j_{k_0}}, k_0 \in \mathcal{O}_{i-1}\}$, such that $k\alpha_a - \epsilon_k - \beta_k - \sum\limits_{i \in \mathcal{S}_k} \varepsilon_i \geq 0$. Here j_k satisfies $2^{j_k - 1} < k \leq 2^{j_k}$, $\epsilon_k = (\frac{k}{2}\epsilon_{k1})^2 + \frac{\epsilon_{k2}^2}{2\epsilon_{k1}^2} + \cdots + \frac{\epsilon_{k(j_k-1)}^2}{2\epsilon_{k1}^2 \cdots \epsilon_{k(j_k-2)}^2}$, $\varepsilon_i = \frac{\epsilon_{ij_i}^2}{2\epsilon_{i1}^2 \cdots \epsilon_{i(j_i-1)}^2}$, and $i \in \mathcal{S}_k$ if $2i - 2^{j_i} = k$, $\alpha_a = \min\{\lambda \in \mathbb{R} : \det(Q_a - \lambda P_a) = 0, \ \forall \tau_{a_i} \in [0, \tau^{a_i}_{macp}), \tau^i_s \in [0, \tau^i_{masp}), i = 1, \cdots, n\}$, $\beta_k = \lambda_k + \alpha_k$, with $\lambda_k = \max\{\lambda \in \mathbb{R} : \det(Q_k - \lambda P_b) = 0, \ \forall \tau_{b_i} \in [0, \tau^{b_i}_{macp}), \tau_{s_i} \in [0, \tau^i_{masp}), i = 1, \cdots, n\}$.

Lemma 13. (Strongly iISS of cascade systems) Consider the hybrid system in (4.49)–(4.50). If Condition 7 is satisfied, then the set $\Xi : \{\xi \in \mathbb{X} | \ \|\tilde{\xi}\| = 0\}$ is globally strongly iISS w.r.t. ς.

Proof. Consider a Lyapunov candidate $U(\xi) = \ln(1 + U_b(\xi_b)) + \sum_{k=1}^{k_a} U_a^k(\xi_a)$. According to (4.51) and (4.52), when $\xi \in C$, we have

$$\langle \nabla U(\xi), F(\xi, \varsigma) \rangle = \frac{\langle \nabla U_b(\xi_b), F_b(\xi, \varsigma) \rangle}{1 + U_b(\xi_b)} + \sum_{k=1}^{k_a} \frac{\partial U_a^k(\xi_a)}{\partial U_a(\xi_a)} \langle \nabla U_a(\xi_a), F_a(\xi_a, \varsigma) \rangle . \tag{4.53}$$

For $U_a^k(\xi_a)$, we have

$$\begin{aligned} &\frac{\partial U_a^k(\xi_a)}{\partial U_a(\xi_a)} \langle \nabla U_a(\xi_a), F_a(\xi_a, \varsigma) \rangle \leq \\ &k\big((-\alpha_a + \epsilon_k)\|\tilde{\xi}_a\|^{2k} + \varepsilon_k \|\tilde{\xi}_a\|^{2(2k-2^{j_k})} + \varepsilon_{\sigma_k} \sigma_a^{2^{j_k}}(\|\varsigma\|)\big), \end{aligned} \tag{4.54}$$

where $\varepsilon_{\sigma_k} = \frac{1}{\epsilon_{k1}^2 \cdots \epsilon_{kj_k}^2}$. Then,

$$\begin{aligned} \langle \nabla U(\xi), F(\xi, \varsigma) \rangle \leq & - \frac{\tilde{\xi}_b^T Q_b \tilde{\xi}_b}{1 + \tilde{\xi}_b^T P_b \tilde{\xi}_b} + \sum_{k=1}^{k_a} \alpha_k \|\tilde{\xi}_a\|^{2k} + \sigma_b(\|\varsigma\|) \\ & + \sum_{k \in \mathcal{O}} k\big((-\alpha_a + \epsilon_k)\|\tilde{\xi}_a\|^{2k} + \varepsilon_k \|\tilde{\xi}_a\|^{2(2k-2^{j_k})} + \varepsilon_{\sigma_k} \sigma_a^{2^{j_k}}(\|\varsigma\|)\big) \\ \leq & - \frac{\tilde{\xi}_b^T Q_b \tilde{\xi}_b}{1 + \tilde{\xi}_b^T P_b \tilde{\xi}_b} + \sum_{k \in \mathcal{O}} \big(k(-\alpha_a + \epsilon_k) + (\alpha_k + \sum_{i \in \mathcal{S}_k} i\varepsilon_i)\big) \|\tilde{\xi}_a\|^{2k} \\ & + \sum_{k \in \mathcal{O}} k\varepsilon_{\sigma_k} \sigma_a^{2^{j_k}}(\|\varsigma\|) + \sigma_b(\|\varsigma\|) \\ \leq & - \lambda_F + \frac{\lambda_F}{1 + \tilde{\xi}_b^T P_b \tilde{\xi}_b} - \sum_{k \in \mathcal{O}} \lambda_{Lk} \|\tilde{\xi}_a\|^{2k} \\ & + \sum_{k \in \mathcal{O}} k\varepsilon_{\sigma_k} \sigma_a^{2^{j_k}}(\|\varsigma\|) + \sigma_b(\|\varsigma\|), \end{aligned} \tag{4.55}$$

where $\lambda_F = \min\{\lambda \in \mathbb{R} |\ \det(Q_b - \lambda P_b) = 0,\ \forall \tau_{b_i} \in [0, \tau_{macp}^{b_i}), \tau_{s_i} \in [0, \tau_{masp}^i), k \in \mathbb{N}, i = 1, \cdots, N\}$, $\lambda_{Lk} = k(-\alpha_a + \epsilon_k) + (\alpha_k + \sum_{i \in \mathcal{S}_k} i\varepsilon_i)$, $\sigma(\|\varsigma\|) = \sum_{k \in \mathcal{O}} k\varepsilon_{\sigma_k} \sigma_a^{2^{j_k}}(\|\varsigma\|) + \sigma_b(\|\varsigma\|)$. Since P_b and Q_b are positive definite, $\lambda_F > 0$; and according to the forth item in Condition 7, $\lambda_{Lk} > 0$. Therefore, there exist W, $W_b \in \mathcal{K}$, and σ, $W_a \in \mathcal{K}_\infty$ such that

$$\langle \nabla U(\xi), F(\xi, \varsigma) \rangle \leq -W_a(\|\tilde{\xi}_a\|) - W_b(\|\tilde{\xi}_b\|) + \sigma(\|\varsigma\|) \leq -W(\|\tilde{\xi}\|) + \sigma(\|\varsigma\|). \tag{4.56}$$

While on jump domain $\xi \in D$,

$$U^+(\xi) - U(\xi) \leq 0. \tag{4.57}$$

Case I. iISS:

By (4.56), there exists a positive definite function α_U such that

$$\langle \nabla U(\xi), F(\xi, \varsigma) \rangle \leq -\alpha_U(U(\xi)) + \sigma(\|\varsigma\|), \text{ and } U^+(\xi) \leq U(\xi).$$

Let $\underline{U}(t,j) = U(t,j) - \|V_t\|_\infty$, $t \in [t_j, t_{j+1}]$, where $V_t = \int_0^t \sigma(\|\varsigma\|)dt$. According to [88], we have

$$\dot{\underline{U}}(t,j) \leq -\alpha_U(\max\{\underline{U}(t,j) + V(t), 0\}).$$

Then, there exists $\beta \in \mathcal{KL}$ satisfies

$$\begin{aligned} &\beta(s,0) = s, \ \beta(\beta(s,t_1),t_2) = \beta(s,t_1+t_2), \\ &\underline{U}(t,j) \leq \max\{\beta(\underline{U}(t_j,j), t-t_j), \|V_t\|_\infty\}. \end{aligned} \tag{4.58}$$

In addition

$$\begin{aligned} \underline{U}(t_j, j-1) &= U(t_j, j-1) + \int_0^{t_j} \sigma(\|\varsigma(s)\|)ds \\ &\geq U(t_j, j) + \int_0^{t_j} \sigma(\|\varsigma(s)\|)ds = \underline{U}(t_j, j), \\ \underline{U}(t_j, j-1) &\leq \max\{\beta(\underline{U}(t_{j-1}, j-1), t_j - t_{j-1}), \|V_{t_j}\|_\infty\} \\ &\leq \max\{\beta(\underline{U}(t_{j-1}, j-1), t_j - t_{j-1}), \|V_t\|_\infty\}. \end{aligned} \tag{4.59}$$

Substitute (4.59) into (4.58),

$$\begin{aligned} \underline{U}(t,j) &\leq \max\{\beta(\max\{\beta(\underline{U}(t_{j-1}, j-1), t_j - t_{j-1}), \|V_t\|_\infty\}, t-t_j), \|V_t\|_\infty\} \\ &= \max\{\beta(\beta(\underline{U}(t_{j-1}, j-1), t_j - t_{j-1}), \beta(\|V_t\|_\infty, t_j - t_{j-1}), \|V_t\|_\infty\} \\ &\leq \max\{\beta(\underline{U}(t_{j-1}, j-1), t - t_{j-1}), \|V_t\|_\infty\}. \end{aligned} \tag{4.60}$$

Repeat (4.58)–(4.60) until $t_0 = 0$, $\underline{U}(t,j) \leq \max\{\beta(\underline{U}(0,0), t), \|V_t\|_\infty\}$. Since $U(t,j) = \underline{U}(t,j) + \|V_t\|_\infty$, we have $U(t,j) \leq \beta(U(0,0),t) + 2\int_0^t \sigma(\|\varsigma\|)ds$. Furthermore, since we have finite agents, and the sampling intervals for each

agent are lower bounded by $\tau_0 > 0$, there always exist finite ϵ_0 and ϵ_1 such that $\epsilon_0 j \leq t + \epsilon_1$, $t \in [t_j, t_{j+1}]$. Let

$$\bar{\beta}(s,t) = \begin{cases} e^{-t}\beta(s,0), \ t < 0 \\ \beta(s,t), \ t \geq 0. \end{cases} \tag{4.61}$$

Then, $\bar{\beta}(s,t)$ is decreasing and $U(t,j) \leq \bar{\beta}(U(0,0), 0.5t + 0.5\epsilon_0 j - 0.5\epsilon_1)$. Let $\hat{\beta}(s,t,j) = \bar{\beta}(s, 0.5t + 0.5\epsilon_0 j - 0.5\epsilon_1)$, we have $\hat{\beta}(s,t,j) \in \mathcal{KLL}$ and $U(t,j) \leq \hat{\beta}(U(0,0),t,j) + 2\int_0^t \sigma(\|\varsigma(s)\|)ds$. Then for all $(t,j) \in \text{dom } \xi$, there exists $\beta_\xi \in \mathcal{KLL}$ such that

$$\tilde{\xi}(t,j) \leq \beta_\xi(\tilde{\xi}(0,0),t,j) + \sigma_1 \sum_{i=0}^{i=I-1} \int_{t_i}^{t_{i+1}} \sigma_2(\|\varsigma(s,i)\|)ds + \sigma_1 \int_{t_I}^{t} \sigma_2(\|\varsigma(s,I)\|)ds. \tag{4.62}$$

Case II: ISS when $|\varsigma|_{(t,j)} < R$:

There exist $\underline{\alpha}$, $\bar{\alpha}$, $W \in \mathcal{K}$, such that $\underline{\alpha}(\|\tilde{\xi}\|) \leq U(\xi) \leq \bar{\alpha}(\|\tilde{\xi}\|)$. By (4.55), $W_b(\infty) = \lambda_F$. Let $R = \sigma^{-1}(\lambda_F)$ and $\epsilon(\|\varsigma\|) = \frac{1}{2}(1 - \frac{\sigma(\|\varsigma\|)}{\lambda_F})$. Then, when $|\varsigma|_{(t,j)} < R$, $\forall \|\tilde{\xi}\| \geq W^{-1}(\frac{\sigma(|\varsigma|_{(t,j)})}{1-\epsilon(|\varsigma|_{(t,j)})}) = r(|\varsigma|_{(t,j)})$ we have

$$\langle \nabla U(\xi), F(\xi,\varsigma) \rangle \leq -\epsilon(\|\varsigma\|) W_\xi(\|\tilde{\xi}\|) \leq -\epsilon(|\varsigma|_{(t,j)}) W_\xi(\|\tilde{\xi}\|), \tag{4.63}$$

and there exists a $\alpha_\xi \in \mathcal{K}$ such that, $\langle \nabla U(\xi), F(\xi,\varsigma) \rangle \leq -\alpha_\xi(\tilde{\xi})$. Then, for all $\xi \in \mathbb{X}$, $\mathbb{X}_r = \{\xi | \|\tilde{\xi}\| > r\}$,

$$\begin{aligned} U(\xi(t,j)) &\leq U(\xi(t_k,k)) - \alpha_\xi(r)(t - t_k), \ t \in [t_k, t_k + 1); \\ U(\xi(t,k+1)) &\leq U(\xi(t,k)), \ t = t_{k+1}. \end{aligned}$$

In addition, since the system is Zeno-free, for any $\xi(0,0) \in \mathbb{X}_r$, there exists a $T > 0$ such that

$$\begin{aligned} U(\xi(t,j)) &\leq U(\xi(0,0)) - \alpha_\xi(r)T \leq U(\underline{\alpha}(r)), \\ \|\tilde{\xi}(t,j)\| &\leq \underline{\alpha}^{-1} \circ (\bar{\alpha}(r)) = r_\xi, \end{aligned}$$

where $T = \frac{U(\xi(0,0)) - U(\underline{\alpha}(r))}{\alpha_\xi(r)}$. Denote the first time when ξ reach set $\mathbb{X}_\xi : \{\|\tilde{\xi}\| \leq r_\xi\}$ as T_r. Since $r_b \geq r$, $\langle \nabla U(\xi), F(\xi,\varsigma) \rangle < 0$ on the boundary of $\mathbb{X}_\xi$, $\mathbb{X}_\xi$ is an

invariant set. Combining the above facts with similar arguments in (4.61)–(4.62), there exists a class $\mathcal{KLL}$ function β such that

$$\|\tilde{\xi}(t,j)\| \leq \beta(\tilde{\xi}(0,0),t,j), \quad t \in [0,T_r),\ t_j \in [0,T_r),$$
$$\|\tilde{\xi}(t,j)\| \leq \underline{\alpha}^{-1} \circ \bar{\alpha}(|r(\varsigma)|_{(t,j)}), \quad t \in [T_r,\infty),\ t_{j+1} \in [T_r,\infty),$$

which leads to

$$\|\tilde{\xi}(t,j)\| \leq \beta(\tilde{\xi}(0,0),t,j) + \underline{\alpha}^{-1} \circ \bar{\alpha}(|r(\varsigma)|_{(t,j)}),\ \forall (t,j) \in \text{dom } \xi. \tag{4.64}$$

Combining (4.62) and (4.64), one comes to the conclusion that the set Ξ is strongly iISS in the sense of Definition 7. □

Remark 18. In Condition 7, the second item is used to reflect the cascade relationship between subsystems $\mathcal{S}_a$ and $\mathcal{S}_b$. By (4.51), higher order couplings exist, which introduce difficulties to provide the stability for the system. The third item is used to ensure the convergence of subsystem $\mathcal{S}_a$, and the forth item gives the constraints on the strengths of different order couplings. These constraints are determined by the inherent dynamics of subsystems $\mathcal{S}_a$ and $\mathcal{S}_b$. Notice that, strongly iISS is determined for the closed-loop system in Lemma 13. The higher order couplings between subsystems make it hard to find a Lyapunov candidate decaying with a $\mathcal{K}_\infty$ function of the states to provide ISS. As a result, a $\mathcal{K}$ function is used to provide strongly iISS.

Finally, we can provide the overall stability results for the system in (4.26)–(4.32) in the following theorem, where the expressions of some parameters and matrices are defined as follows.

Items in Theorem 12–(i)

$A_{\delta_0} =$

$$\begin{bmatrix} -c(I-\bar{\psi})-\frac{1}{2}\left((I-\bar{L}\bar{\psi})+\alpha_{V_\delta} I\right) & -cI+\bar{\psi}(c_\delta L_{ff}+c)+(I-\bar{L}\bar{\psi}) & c_\delta\bar{\psi}L_{ff} & -\bar{\psi} & -c_\delta\bar{\psi} \\ *^{\S\S} & -c_\delta(I-\bar{\psi})L_{ff}+c\bar{\psi}-\frac{1}{2}\left((I-\bar{L}\bar{\psi})+\alpha_{V_\Delta} I\right) & -c_\delta(I-\bar{\psi})L_{ff} & -\bar{\psi} & c_\delta(I-\bar{\psi}) \\ * & * & \frac{1}{2}(-l_\delta^2+\alpha_{W_e} I) & * & * \\ * & * & * & \frac{1}{2}(-l_u^2+\alpha_{W_u} I) & * \\ * & * & * & * & \frac{1}{2}(-l_\delta^{s\,2}+\alpha_{W_s} I) \end{bmatrix}$$
$$+ [* * \P\P]^T \tag{4.65}$$

$$A_{\sigma_1} = \begin{bmatrix} \frac{1}{\epsilon_7^2} & * & * \\ * & \frac{1}{\epsilon_2^2}+\frac{1}{\epsilon_4^2}+\frac{1}{\epsilon_5^2}+\frac{1}{\epsilon_6^2} & * \\ * & * & * \end{bmatrix} + [**]^T, A_{\sigma_2} = \frac{1}{2\epsilon_8^2}\Big(\begin{bmatrix} \begin{bmatrix} c_\delta \bar{\psi} L_{fl} \\ c_\delta(1-\bar{\psi})L_{fl} \end{bmatrix}^{[**]^T} & * \\ * & * \end{bmatrix} + [**]^T \Big),$$

$$A_{\sigma_3} = \frac{13}{2}\Big(\begin{bmatrix} * & \omega_0^2(1+\epsilon_3^2)[A_{nf}, A_{nf}, A_{nf}]^{[**]^T} & * & * \\ * & * & * & * \end{bmatrix} + [**]^T \Big),$$

$\bar{\psi} = \frac{\psi_\delta + \psi_u}{2}$, $\bar{L} = \frac{L_\delta + L_u}{2}$, $l_\pi = \text{diag}(l_{\pi_{n_m+1}}, \cdots, l_{\pi_n})$, $L_\pi = \text{diag}(L_{\pi_{n_m+1}}, \cdots, L_{\pi_n})$, $\psi_\pi = \text{diag}(\psi_{\pi_{n_m+1}}, \cdots, \psi_{\pi_n})$, $l_\delta^s = \text{diag}(l_{\delta_{n_m+1}}^s, \cdots, l_{\delta_n}^s)$.

Items in Theorem 12–(ii)

$\epsilon_{\pi_2} = \epsilon_{\pi_{21}}^2$, $\epsilon_{\pi_4} = 4\epsilon_{\pi_{41}}^2 + \frac{\epsilon_{\pi_{42}}^2}{2\epsilon_{\pi_{41}}^2}$;

for $\pi = \omega$, $\beta_{\omega_1} = \alpha_0^\omega + \alpha_1^\omega + \lambda_1^\omega$, $\beta_{\omega_2} = \alpha_2^\omega$;

for $\pi = v, m$, $\beta_{\pi_1} = \alpha_1^\pi$, $\beta_{\pi_2} = \alpha_2^\pi$;

for $\pi = \gamma$, $\beta_{\gamma_1} = \alpha_0^\gamma + \alpha_1^\gamma + \lambda_1^\gamma$, $\beta_{\gamma_2} = \alpha_2^\gamma + \lambda_2^\gamma$, $\beta_{\gamma_4} = \alpha_4^\gamma$.

$\lambda_k^\pi = \max\{\lambda \in \mathbb{R} : \det(Q_k^\pi - \lambda P_f) = 0,\ \forall \tau_{\delta_i} \in [0, \tau_{macp}^{\delta_i}), \tau_{s_i} \in [0, \tau_{masp}^i), i \in \mathcal{N}_f\}$, $k = 0, 1, 2$;

$\alpha_\pi = \min\{\lambda \in \mathbb{R} : \det(Q_\pi - \lambda P_\pi),\ \forall \tau_{\pi_i} \in [0, \tau_{macp}^{\pi_i}), \tau_{s_i} \in [0, \tau_{masp}^i), i \in \mathcal{N}\}$;

$\alpha_0^\omega = \frac{\lambda_0^{\omega\,2}}{2\epsilon_{\omega_0}^2}$, $\alpha_0^\gamma = \frac{\lambda_0^{\gamma\,2}}{2\epsilon_{\gamma_0}^2}$, $\alpha_1^\omega = 13\,(r_v^2\sigma^2(A_{nl}) + r_{\delta_m}\sigma^2(A_{nl}))$,

$\alpha_2^\omega = 13\,(\epsilon_\omega^2\sigma^4(A_{nl}) + \epsilon_9^2 r_{\delta_m}\sigma^4(A_{nl}))$, $\alpha_1^v = \epsilon_4^2$, $\alpha_2^v = \frac{\epsilon_2^2}{\epsilon_{10}^2} + 13\frac{1}{4\epsilon_f^2}\sigma^2(A_{ff})$,

$\alpha_1^\gamma = \epsilon_5^2 v_M^2 + 13(v_M + r_v)^2\sigma^2(L_{fl})$, $\alpha_2^\gamma = \epsilon_2^2\epsilon_{10}^2 + 13(\epsilon_\gamma^2 n_l^2 + v_M^2\sigma^2(A_{ff}))$,

$\alpha_4^\gamma = 13\epsilon_f^2\sigma^2(A_{ff})$, $\alpha_1^m = \epsilon_8^2 + 13\omega_M^2(1 + \frac{1}{4\epsilon_3^2})\sigma^2(A_{nl})$, $\alpha_2^m = 13\lambda^2(A_m)$;

$$Q_0^\omega = \begin{bmatrix} \epsilon_1^2 I & 0 & 0 \\ 0 & \frac{1}{\epsilon_1^2} I & 0 \\ 0 & 0 & 0 \end{bmatrix},\ Q_0^\gamma = \sigma(A_1) I,\ Q_1^\omega = (1 + \tfrac{1}{4\epsilon_9^2}) \begin{bmatrix} \begin{bmatrix} A_{nf}^T \\ A_{nf}^T \\ A_{nf}^T \end{bmatrix}^{[**]^T} & 0 \\ 0 & 0 \end{bmatrix},$$

$$Q_1^\gamma = 13 \begin{bmatrix} \omega_0^2[A_{nf}^T A_{nf}] & 0 & 0 \\ 0 & A_{ff}^T A_{ff} & 0 \\ 0 & 0 & 0 \end{bmatrix},\ Q_2^\gamma = 13 \begin{bmatrix} \begin{bmatrix} -cA_{ff}^T \\ -cA_{ff}^T \end{bmatrix}^{[**]^T} & 0 & \begin{bmatrix} -cA_{ff}^T \\ -cA_{ff}^T \end{bmatrix} A_{ff} & 0 \\ 0 & 0 & 0 & 0 \\ A_{ff}^T[-cA_{ff},\ -cA_{ff}] & 0 & A_{ff}^T A_{ff} & 0 \\ 0 & 0 & 0 & 0 \end{bmatrix},$$

$$P_f = \begin{bmatrix} I & 0 & 0 & 0 \\ 0 & l_\delta\phi_\delta & 0 & 0 \\ 0 & 0 & l_u\phi_u & 0 \\ 0 & 0 & 0 & l_\delta^s\phi_\delta^s \end{bmatrix},\ \phi_\delta = \text{diag}(\phi_{\delta_{n_m+1}}, \cdots, \phi_{\delta_n}),$$

$\phi_u = \text{diag}(\phi_{u_{n_m+1}}, \cdots, \phi_{u_n})$, $\phi_\delta^s = \text{diag}(\phi_{\delta_{n_m+1}}^s, \cdots, \phi_{\delta_n}^s)$,

Q_π and P_π are the same as the ones in Theorems 8–11.

§§ $*$ in a matrix represents zero matrix with compatible dimensions

¶¶ $**$ represents a copy of the matrix on its left side.

Theorem 12. Consider the hybrid system in (4.26)–(4.32), for sufficiently small ϵ_η and ϵ_χ, the set $\Xi_\delta = \{\xi \in \mathbb{X} | \|\tilde{\xi}^T\| = 0\}$ is locally strongly iISS w.r.t. ς if:

(i) for subsystem $\mathcal{S}_\delta$, there exist positive constants ϵ_k, $k = 2, \cdots, 8$, ψ_{π_i}, l_{π_i}, $l^s_{\delta_i}$, α_{V_δ}, α_{V_Δ}, α_{W_π}, α_{W_s}, $\pi = \delta, u$, such that the following LMI can be established: $A_\delta = A_{\delta_0} + A_{\sigma_1} + A_{\sigma_2} + A_{\sigma_3} \leq 0$;

(ii) there exist positive constants $\epsilon_{\pi_{pq}}$, $\pi = \gamma, \omega, v, m$, $p = 2, 4$, $q = 1, 2$, such that

$$\begin{aligned} &\alpha_\pi - \beta_{\pi_1} \geq 0,\ 2\alpha_\pi - \epsilon_{\pi_2} - \beta_{\pi_2} \geq 0, \pi = \omega, v, m; \\ &\alpha_\pi - \beta_{\pi_1} \geq 0,\ 2\alpha_\pi - \epsilon_{\pi_2} - \beta_{\pi_2} \geq 0,\ 4\alpha_\pi - \epsilon_{\pi_4} - \beta_{\pi_4} \geq 0,\ \pi = \gamma; \end{aligned} \tag{4.66}$$

(iii) the MASP satisfies $\tau^i_{masp} = \min\{\tau^{\pi_i}_{masp} |\ \pi = \delta, \gamma, v, \omega\}$, with $\tau^{\pi_i}_{masp} = \frac{1}{l^s_{\pi_i}} \arctan \frac{\bar{\rho}_i - \underline{\rho}_i}{2}$;

(iv) for $i \in \mathcal{N}_f$, the MACP satisfies $\tau^{\pi_i}_{macp} \leq \frac{1}{l_{\pi_i}} \arctan \frac{\bar{\rho}^\pi_i - \underline{\rho}^\pi_i}{2}$, with $\bar{\rho}^\pi_i \leq \frac{1}{\rho_{\pi_i}}$, $\underline{\rho}^i_\pi \geq \rho_{\pi_i}$ and ρ_{π_i} satisfying (4.42); and ET functions are designed by $h_{\pi_i}(e_{\pi_i}, q_{\pi_i}, t) = l_{\pi_i}\|e_{\pi_i}\|^2 - \lambda_{\pi_i}\rho_{\pi_i}\psi_{\pi_i}q^2_{\pi_i}$, where $q_{\pi_i} = \hat{\delta}_i$, $\pi = u, \delta$;

(v) for $i \in \mathcal{N}_m$, the MATP satisfies $\tau^i_{mati} \leq \frac{r_m}{\kappa_1},\ t \in [0, T_v)$; $\tau^i_{mati} \leq \frac{r_m}{\kappa_2},\ t \in [T_v, \infty)$. Here,
$\kappa_1 = \max\{l_{\eta_2}\omega_M,\ l_{\chi_2}v_M,\ (1 + \bar{d}_{i0})U_i + v_M + c_\delta\omega_M,\ \omega_M + U_i\}$,
$\kappa_2 = \max\{l_{\eta_2}r_\omega,\ l_{\chi_2}r_v,\ (1 + \bar{d}_{i0})U_i + v_M + c_\delta\omega_M,\ \omega_M + U_i\}$;

(vi) the items in Theorems 8–11 are established.

Proof. Detailed proof is given in Appendix A.5. □

Remark 19. The closed-loop MAS in (4.1) follows a cascade dynamics as described in Table. 4.3 and Figure 4.3 (b). Theorems 8–11 provide the finite time convergence of subsystem $\mathcal{S}_h$ and the ISS of subsystem $\mathcal{S}_a$. According to the cascade connection, when we analyse the dynamics of $\mathcal{S}_b$, the effects of $\mathcal{S}_h$ are considered as an L_∞ disturbances bounded by r_ω and r_v after short

convergence time T_ω and T_v; the influences of subsystem $\mathcal{S}_a$ are analyzed based on the novel Lyapunove function candidate proposed in Lemma 13; and the strongly iISS of the cascade system is provided. More specifically, the closed-loop system is proved to be ISS under a disturbance bounded by a computable threshold R, and is iISS otherwise. Since the amplitude of the disturbance is determined by the convergence error of $\mathcal{S}_h$, the inherent dynamics of $\mathcal{S}_a$ and $\mathcal{S}_b$, and the coupling strength between them, the threshold R can be served as a criterion when designing the event-triggered controller and the network infrastructure.

4.6 Simulations

In this section, we provide a numerical example to illustrate the effectiveness of the proposed method. Consider an MAS with one leader, six followers and a network as shown in Figure 4.1. The initial states and expected formation w.r.t. the leader are given by $d(0) = [1, 1, 4, 6, 6, 6]$, $\beta(0) = [\frac{\pi}{12}, -\frac{\pi}{12}, \frac{\pi}{12}, -\frac{\pi}{12}, 0]$, $\gamma(0) = [\frac{\pi}{12}, -\frac{\pi}{12}, \frac{\pi}{12}, -\frac{\pi}{12}, \frac{\pi}{12}, \frac{\pi}{12}]$ and $d_0 = [1.5, 1.5, 3, 3, 4, 4]$, $\beta_0 = [\frac{\pi}{6}, -\frac{\pi}{6}, -\frac{\pi}{5}, \frac{\pi}{5}, -\frac{\pi}{8}, \frac{\pi}{8}]$, respectively. The leader's velocities are given by $v_0(t) = 0.45 + 0.05\cos(t)$, $w_0(t) = 0.1\cos(t)$; the constant is chosen as $r_m = 0.05$, and the input saturation for $i \in \mathcal{N}_m$ is selected as $U_i = 2$.

First, we show the **finite time convergence of subsystem $\mathcal{S}_h$**. The constants in (4.6) and (4.8) are chosen as $\epsilon_\eta = 0.005$ and $\epsilon_\chi = 0.08$. The MASPs calculated by Lemma 10 and the MATPs before and after convergence are shown in Table 4.4. The simulation results are shown in Figure 4.4. Here, we divide each curve into two parts according to the time domain, where the left column illustrates the finite time convergence and the right column shows the convergence error. The values of convergence error and convergence time calculated by Theorem 8 and obtained by simulations are shown in Table 4.5.

For subsystems $\mathcal{S}_a$, $\mathcal{S}_b$, the corresponding MASPs calculated by Theorems 8 and 9 are summarized in Table 4.4, which shows that fast samplings are only

Table 4.4: MASPs of agents

Level	$i \in \mathcal{N}_m$		$i \in \mathcal{N}_f$			
Agent	1	2	3	4	5	6
MASP (10^{-2})	0.34×10^{-2}	0.34×10^{-2}	2.04	1.47	1.18	1.31
MATP(10^{-2}),$t \in (0, 1.2]$	0.125	0.125	-	-	-	-
MATP(10^{-2}),$t \in (1.2, \infty)$	1.1	1.1	-	-	-	-

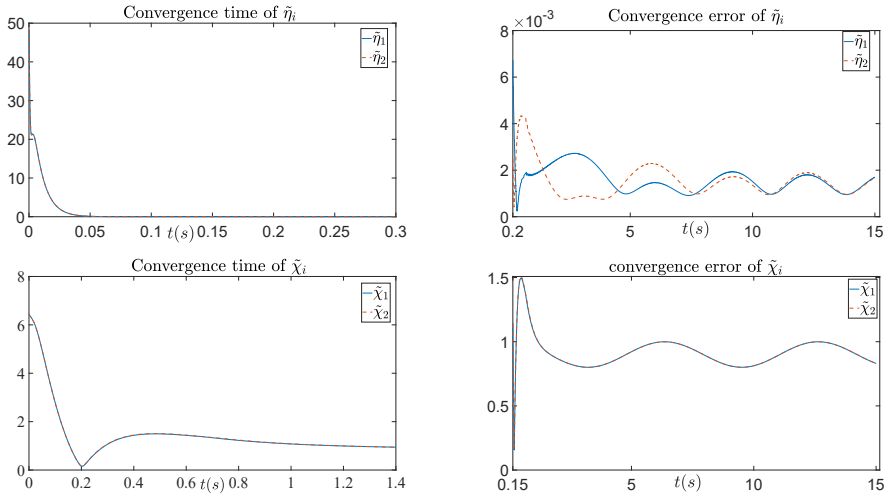

Figure 4.4: Finite-time convergence of subsystem $\mathcal{S}_h$

Table 4.5: Convergence errors and convergence times of $\mathcal{S}_h$

Subsystem	Agent	Computation		Simulation	
		Error	Time	Error	Time
$\mathcal{S}_\eta$	1	0.0059	0.4275	0.0016	0.2093
	2	0.0059	0.4188	0.0015	0.1484
$\mathcal{S}_\chi$	1	1.2590	1.1806	0.9183	0.1458
	2	1.2590	0.9759	0.9188	0.1456

Table 4.6: MACPs and average inter-event times of agents

Group	Subsystem	Level	State	MACP (10^{-2})				Inter-Event Time (10^{-2})				Distribution(%)			
			Agent	1(3)	2(4)	5	6	1(3)	2(4)	5	6	3	4	5	6
$\mathcal{S}_a$	$\mathcal{S}_m$	$i \in \mathcal{N}_m$	u_i	1.12	1.12	-	-	1.31	1.36	-	-	-	-	-	-
	$\mathcal{S}_\omega$	$i \in \mathcal{N}_f$	$\hat{\omega}_i$	1.62	0.97	0.78	3.5	0.41	0.36	0.35	0.40	19.0	26.1	24.5	0
	$\mathcal{S}_v$	*	$\hat{v}_i$	1.62	0.97	0.78	3.5	*	*	*	*	1.7	1.9	1.1	0
	$\mathcal{S}_\gamma$	*	$\hat{\gamma}_i$	1.86	0.55	0.42	0.44	*	*	*	*	6.4	38.4	50.2	5.7
$\mathcal{S}_b$	$\mathcal{S}_\delta$	*	$\hat{\delta}_i$	0.48	0.59	0.50	0.40	*	*	*	*	72.8	43.4	24.1	94.3
		*	u_i	2.4	1.80	1.09	2.09	4.92	3.57	2.22	4.09				

requested for agent $i \in \mathcal{N}_m$. Table 4.6 gives the MACPs for each state and the average inter-event times for each agent obtained by simulation. Since when an ET condition is satisfied, the agent transmits all the local information, the

Table 4.7: Steady-state error of $\mathcal{S}_a$ and $\mathcal{S}_b$

Group	State	Level	Steady-state error			
		Agent	1(3)	2(4)	5	6
$\mathcal{S}_a$	δ_i	$i \in \mathcal{N}_m$	0.0099	0.0097	-	-
	$\Delta\omega_i$	$i \in \mathcal{N}_f$	0.0892	0.0890	0.0885	0.0878
	Δv_i	*	0.0435	0.0434	0.0432	0.0428
	$\Delta\gamma_i$	*	0.0011	0.0013	0.0018	0.0026
$\mathcal{S}_b$	δ_i	*	0.2489	0.0594	0.2415	0.1105
	$\Delta\delta_i$	*	0.0935	0.1443	0.1200	0.1516

distributions of the source that generates a transmission are also summarized in Table 4.6. The control inputs are shown in Figure 4.5, which are only updated at each triggering instant. The trajectories of the states belongs to subsystem S_a and S_b are shown in Figure 4.6 and Figure 4.7, respectively, with the steady-state errors summarized in Table 4.7.

The steady-state errors of $\mathcal{S}_a$ and $\mathcal{S}_b$ are with different numerical magnitudes, which coincide with the cascade structure in a sense that the errors are accumulated in each level. The trajectories of all the agents in the MAS are shown in Figure 4.8, which shows that the formation in the leader's coordinate frame is realized.

The following example is used to discuss the conservativeness of the results. In this case, we increase amplitude of the external disturbances as $v_0(t) = 2 + 0.5\cos(t)$, $\omega_0(t) = 0.25 + 0.5\cos(1.5t)$. The simulation results are given in Figures 4.9–4.11. From Figures 4.9–4.10, we can tell that the finite time convergence for subsystem $\mathcal{S}_h$ and the ISS property of subsystem $\mathcal{S}_a$ are preserved. However, by Figure 4.11, subsystem $\mathcal{S}_b$ diverges because the external disturbances exceed the threshold to guarantee the ISS property, which means the strongly iISS might be the "best" stability result we can obtain for the closed-loop system.

4.7 Summary

A leader-follower formation tracking problem without velocity measurements has been solved in this chapter. PETMs were introduced for both

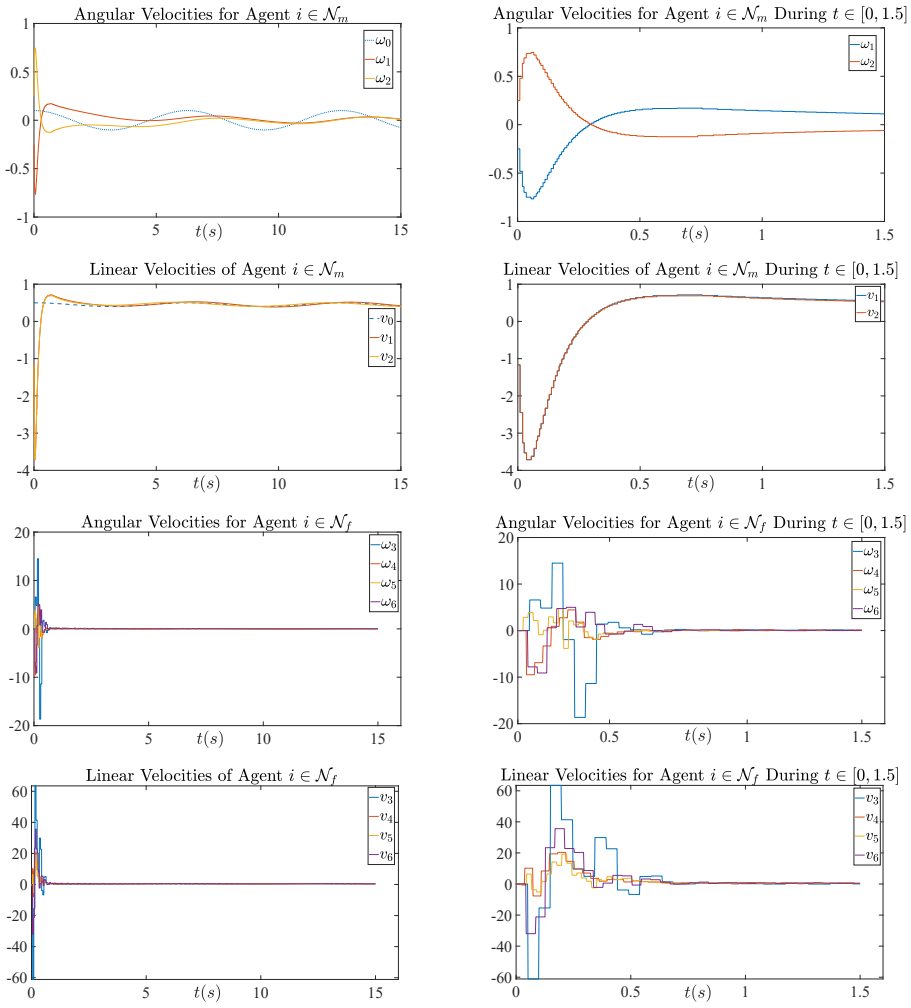

Figure 4.5: Control inputs to the agents

communication and controller updates, where continuous measurements were avoided. By reformulating the problem in a hybrid system framework, asynchronous samplings and checking instants among agents were analyzed without increasing the dimension of the system matrix. In addition, the underlying communication network was managed separately for PULC and PUSC, which took into account of their distinct features. The MAS was subject to a hierarchical structure, benefited from which, the acyclic assumption was removed. Novel Lyapunov function candidates were proposed to illustrate different stability properties of three subsystems, and by reconstructing the system into a cascade-connected structure, strongly iISS was provided for the overall sys-

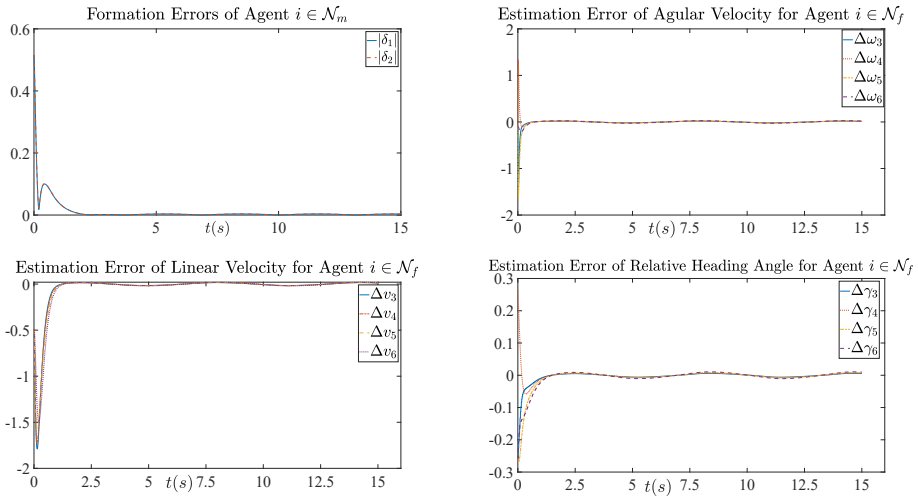

Figure 4.6: Trajectories of the states in subsystem $\mathcal{S}_a$

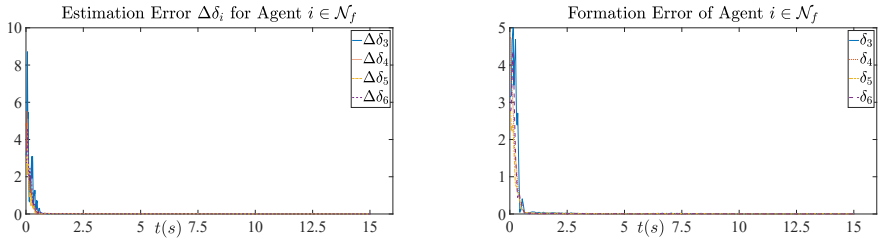

Figure 4.7: Trajectories of the states in subsystem $\mathcal{S}_b$

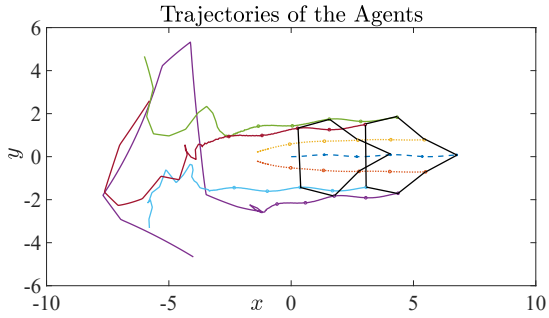

Figure 4.8: Trajectories of the agents. Here the solid lines represent the trajectories of agents in $\mathcal{N}_m$ and the dashed lines represent the trajectories of agents in $\mathcal{N}_f$.

tem. The effectiveness of the proposed methods were further illustrated by a numerical example.

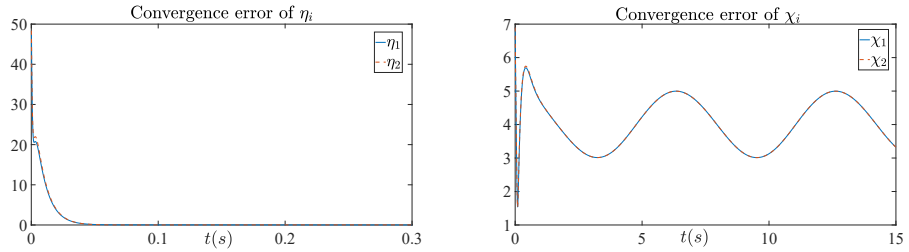

Figure 4.9: Finite-time convergence of subsystem $\mathcal{S}_h$ with larger disturbances

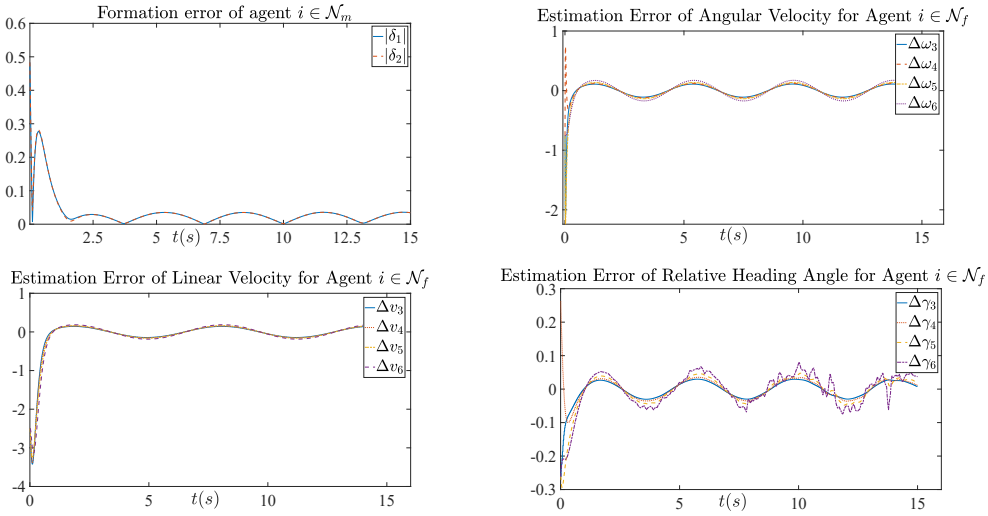

Figure 4.10: Trajectories of the states in subsystem $\mathcal{S}_a$ with larger disturbances

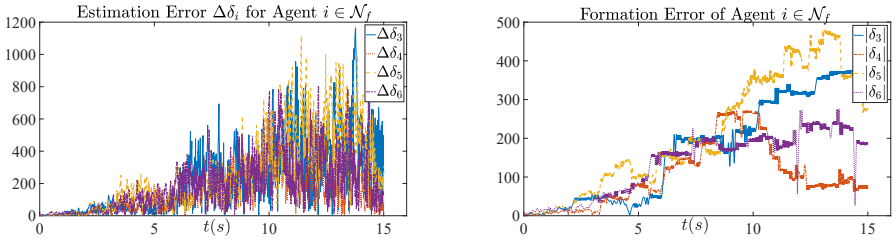

Figure 4.11: Trajectories of the states in subsystem $\mathcal{S}_b$ with larger disturbances

Chapter 5

Distributed Optimization-Based Formation Control under Event-Triggered Mechanism*

5.1 Overview

This chapter investigates an ETM for distributed optimization-based formation problems of MASs under directed graphs. In most of existing results [21, 22, 23], DOP was solved in a consensus sense, such that all agents in MASs shared an identical optimal solution. In order to cope with certain circumstances, like formation control of mobile robots [89], we consider the situation where the optimal points of agents form some specific configurations. The optimization-based formation problems were considered in [90] and [68] as well. However, in these results, the equality constraint introduced by formation configuration was treated as a penalty term in the global object function; therefore, the transformed DOP was only equivalent to the original one when the coefficient on the penalty term approached to infinity. In our work, the optimization-based formation problem is solved by the modified Lagrangian based (MLB) algorithm [22]. The formation errors are estimated by each agent locally, and a proportional-integral feedback structure is used to

*A version of this chapter has been submitted to *IEEE Transactions on Cybernetics* as: J. Yang, H. Yu, and T. Chen, Distributed optimization-based formation control: a dynamic event-triggered approach.

guarantee asymptotic stability of the closed-loop system.

In order to reduce network load, an ETM is proposed. Considering the situation where MASs are subject to unknown disturbances, an auxiliary variable was introduced to estimate the average influence of external disturbances in [65] and [23]. Single-loop systems were considered in [65] and MASs with connected underlying graphs were considered in [23]. However, their ETMs cannot be extended trivially to the case that the underlying graph is directed. Since the transmitted signals from neighbors are included explicitly in the controller, the auxiliary variable introduced in [65] and [23] might not be continuous between adjacent agent transmissions, which may lead to arbitrarily small inter-event times. Motivated by this, a novel dynamic ETM is implemented where a buffer variable is introduced to record the historical local information including the average values of measurement errors over one transmission interval. Subsequently, the transmission performance can be evaluated by a computable positive minimum inter-event time and the closed-loop MAS is proved to be ISES w.r.t. unknown disturbances.

Furthermore, two kinds of ET functions are investigated. By changing the input to the buffer variables, which leads to different requirements on integration capacity, we show the trade-off between network load and computation complexity. The effectiveness of the proposed method is verified by numerical examples.

5.2 Preliminaries and Problem Formulation

5.2.1 Preliminaries

Some preliminaries and notations on graph theory are the same as those in Section 2.2.1, and definition of $\mathcal{L}_\infty$ norm and properties of system stabilities are the same as those in Section 3.2.1. $\bar{\lambda}(\cdot)$ and $\underline{\lambda}(\cdot)$ represent the maximum and minimum eigenvalues of a symmetric matrix, respectively.

Definition 8. ([91]) A differentiable function $f : \mathbb{R}^n \to \mathbb{R}$ is ν-strongly convex

if for any $x, y \in \mathbb{R}^n$,

$$f(y) \geq f(x) + \nabla f(x)^T (y - x) + \frac{\nu}{2}\|x - y\|^2;$$

and it is μ-smooth if for any $x, y \in \mathbb{R}^n$,

$$\|\nabla f(x) - \nabla f(y)\| \leq \mu \|x - y\|,$$

where $\nabla f(x)$ stands for the gradient of f at point x.

A digraph $\mathcal{G}$ is strongly connected if for every pair of nodes there exists a directed path connecting them, and it is weight-balanced if $\sum_{j=1}^n a_{ij} = \sum_{k=1}^n a_{ki},\ i \in \mathcal{N}$ and $a_{ij} \geq 0,\ \forall i, j \in \mathcal{N}$. Let $d_i = \sum_{j=1}^n a_{ij}$ represent the out-degree of node i; and $L \in \mathbb{R}^{n\times n}$ be the Laplacian matrix of diagraph $\mathcal{G}$, where $[L]_{ij} = -a_{ij}$ if $i \neq j$, and $[L]_{ii} = \sum_{j\in\mathcal{N}_i} a_{ij}$

Lemma 14. ([57, 92]) For a strongly connected and weight-balanced digraph $\mathcal{G}$ with n nodes and Laplacian matrix L, one has

- $L + L^T \geq 0$ and 0 is a simple eigenvalue;
- $Lx = 0$ iff $x \in \mathbb{R}^n$ and all the elements in x are the same;
- there exists a nonnegative constant ϵ_L satisfying

$$\frac{1}{2}\epsilon_L(L + L^T) \geq \frac{1}{4}(L^T - L)(L - L^T);$$

- there exists a matrix $\Gamma > 0$ such that $\frac{L+L^T}{2}\Gamma = \Gamma\frac{L+L^T}{2} = \Pi$ with $\Pi = I_n - \frac{1}{n}\mathbf{1}_n\mathbf{1}_n^T$.

Lemma 15. ([23]) Consider the function $m(t) = \text{ave}_{[t_0,t]}(|s|), t > t_0$, with a given initial instant t_0, a nonnegative signal $s : \mathbb{R} \to \mathbb{R}_{\geq 0}$ and $\text{ave}_{[t_0,t]}(s) = \int_{t_0}^t \frac{1}{t-t_0}s(\tau)d\tau$, then the following two equations hold: $\lim_{t\to t_0^+} m(t) = s(t_0)$; and $\dot{m}(t) = -\frac{1}{t-t_0}m(t) + \frac{1}{t-t_0}s(t),\ t > t_0$.

5.2.2 Event-Triggered Optimization-Based Formation Control

Consider a MAS with n agents modeled by single integrators subject to unknown disturbances

$$\dot{x}_i = u_i + \omega_i, \quad i = 1, \cdots, n, \tag{5.1}$$

where $x_i \in \mathbb{R}$ is the state, $\omega_i \in \mathbb{R}$ is the unknown disturbance, and $u_i \in \mathbb{R}$ is the control input to be designed. Each agent i is only aware of its local object function $f_i(x_i) : \mathbb{R} \to \mathbb{R}$, which is not shared with others, and can communicate with each other via the interaction network described by $\mathcal{G}$. The goal of the MAS is to minimize a global object function

$$f(x) = \sum_{i \in \mathcal{N}} f_i(x_i), \ x = [x_1, \cdots, x_n]^T, \tag{5.2}$$

and, at the same time, converge to the formation given by

$$L(x - h) = 0, \tag{5.3}$$

where L is the Laplacian matrix associated with $\mathcal{G}$ and $h = [h_1, \cdots, h_n]^T \in \mathbb{R}^n$ is the desirable configuration known to all agents.

Assumption 11. The local objective function $f_i(x)$ is μ_i-smooth and ν_i-strongly convex.

Assumption 12. The underlying digraph $\mathcal{G}$ is strongly connected and weight-balanced.

Under Assumption 11, the optimization problem in (5.2) and (5.3) has an unique optimal solution. The corresponding Lagrange function is given by $L(x, \lambda) = \sum_{i \in \mathcal{N}} f_i(x_i) + \lambda^T L(x - h)$ with a Lagrange multiplier $\lambda \in \mathbb{R}^n$; and the constrained optimization problem is solved iff the Karush–Kuhn–Tucker condition

$$L_{x^*} = \begin{bmatrix} \nabla f_1(x_1^*) \\ \vdots \\ \nabla f_n(x_n^*) \end{bmatrix} + L^T \lambda = 0 \tag{5.4}$$

is satisfied, where $x^* = [x_1^*, \cdots, x_n^*]^T \in \mathbb{R}^n$ is the optimal solution.

Assuming agents can transmit local information continuously, controller u_i is designed according to the MLB algorithm as

$$\begin{cases} u_i = -\alpha \nabla f_i(x_i) - \beta \sum_{j \in \mathcal{N}_i} a_{ij}(x_i - x_j - h_i + h_j) - v_i, \\ \dot{v}_i = \gamma \sum_{j \in \mathcal{N}_i} a_{ij}(x_i - x_j - h_i + h_j). \end{cases} \tag{5.5}$$

When $\omega_i = 0$, the equilibrium point in (5.1) and (5.5) satisfies

$$\begin{cases} \sum_{j \in \mathcal{N}_i} a_{ij}(x_i - x_j - h_i + h_j) = 0 \\ -\alpha \nabla f_i(x_i) - v_i = 0. \end{cases} \tag{5.6}$$

Under Assumption 12, $\sum_{i \in \mathcal{N}} \dot{v}_i = 0$. If $\sum_{i \in \mathcal{N}} v_i(0) = 0$, we have $\sum_{i \in \mathcal{N}} v_i(t) = 0$. Since $\text{span}\{L^T\} \perp \mathbf{1}_n$, there always exists a λ satisfying $v = L^T \lambda$ and (5.4), where $v = [v_1, \ldots, v_n]^T$ is decided from (5.6). Therefore, the goal in (5.2) and (5.3) is achieved if the state x can converge to the equilibrium decided by (5.6).

Remark 20. It should be noted that using the Kronecker product on Laplacian matrix L, the MAS in (5.1) can be generalized to the case where $x_i, u_i, \omega_i \in \mathbb{R}^m$. For notational simplicity, we only consider the scalar case in this work.

Since the communication among MASs is inherently discrete in digital channels, in this paper, we focus on designing an ETM for system (5.1) and (5.5) such that agents only transmit local information when some predetermined ET conditions are violated. Let $\hat{x}_i$ represent the value of x_i at its latest transmission instants; then the dynamics of the event-triggered system can be represented as

$$\begin{cases} \dot{x}_i = u_i + \omega_i \\ u_i = -\alpha \nabla f_i(x_i) - \beta \sum_{j \in \mathcal{N}_i} a_{ij}(\hat{x}_i - \hat{x}_j - h_i + h_j) - v_i \\ \dot{v}_i = \gamma \sum_{j \in \mathcal{N}_i} a_{ij}(\hat{x}_i - \hat{x}_j - h_i + h_j), \end{cases} \tag{5.7}$$

under the initial condition constraint $\sum_{i \in \mathcal{N}} v_i(0) = 0$, where

$$\begin{cases} \hat{x}_i(t) = x_i(t), & t = t_{k_i}^i \\ \hat{x}_i(t) = x_i(t_{k_i}^i), & t \in [t_{k_i}^i, t_{k_i+1}^i), \end{cases}$$

and $t^i_{k_i}$ represents the transmission instant of agent i generated by the following dynamic ETM:

$$t^i_{k_i+1} = \inf\{t > t^i_{k_i} | g_i(t) < 0\}. \tag{5.8}$$

Here, $g_i : \mathbb{R}_{\geq 0} \to \mathbb{R}$ is an auxiliary (buffer) variable to be specified later.

In the subsequent section, we will provide a detailed design for the ETM in (5.8) such that the closed-loop system in (5.7) is ISES w.r.t. disturbances. Furthermore, Zeno-freeness is ensured by a computable positive minimum inter-event time.

5.3 Event-Triggered Optimization Algorithm

Inspired by [65] and [23], we introduce an auxiliary average variable η_i to estimate the effects of unknown disturbances

$$\begin{aligned} \eta_i =& \frac{1}{t - t^i_{k_i}} \max\Big\{ \|\hat{x}_i - x_i\| - \int_{t^i_{k_i}}^{t} \|\alpha \nabla f_i \\ &+ \beta \sum_{j \in \mathcal{N}_i} a_{ij}(\hat{x}_i - \hat{x}_j - h_i + h_j) + v_i \| d\tau, 0 \Big\},\ i \in \mathcal{N}. \end{aligned} \tag{5.9}$$

Then, a novel dynamic ETM is proposed based on the following buffer variable:

$$\begin{aligned} \dot{g}_i =& - p_i g_i - a_i \|\hat{x}_i - x_i\|^2 + m_i(\alpha \nabla f_i + v_i)^2 \\ &+ l_i \big(\beta \sum_{j \in \mathcal{N}_i} a_{ij}(\hat{x}_i - \hat{x}_j - h_i + h_j)\big)^2 + c_i \eta_i^2, \end{aligned} \tag{5.10}$$

with $g_i(0) = 0$, where a_i, p_i, m_i, $c_i > 0$ are parameters to be determined later.

The following lemma discusses Zeno-freeness of the closed-loop system with the ETM described in (5.8)–(5.10).

Lemma 16. For each agent i, the ETM given in (5.8)–(5.10) admits a positive minimum inter-event time ΔT_i satisfying

$$\Delta T_i^2 e^{p_i \Delta T_i} = \frac{\min\{l_i, m_i, c_i\}}{2a_i}.$$

Proof. Let $e_{t_i} = \hat{x}_i - x_i$ represent the measurement error of agent i with the augmented vector $e_t = [e_{t_1}, \cdots, e_{t_n}]^T$. By (5.7), e_{t_i} is differentiable and bounded for $t \in (t^i_{k_i}, t^i_{k_i+1})$. According to L'Hospital's rule, we have

$$\lim_{t\to(t^i_{k_i})^+} \frac{\|e_{t_i}(t)\|}{t - t^i_{k_i}}$$

is well defined and finite. Similar arguments are applied to

$$\lim_{t\to(t^i_{k_i})^+} \frac{\int_{t^i_{k_i}}^t \|\beta \sum_{j\in\mathcal{N}_i} a_{ij}(\hat{x}_i - \hat{x}_j - h_i + h_j) + \alpha\nabla f_i + v_i\| d\tau}{t - t^i_{k_i}}.$$

As a result, according to (5.9), for $t \in [t^i_{k_i}, t^i_{k_i+1})$, we have

$$\|e_{t_i}\| \leq \int_{t^i_{k_i}}^t \|\beta \sum_{j\in\mathcal{N}_i} a_{ij}(\hat{x}_i - \hat{x}_j - h_i + h_j) + \alpha\nabla f_i + v_i\| d\tau + (t - t^i_{k_i})\eta_i.$$

Use Cauchy-Schwartz inequality

$$\|e_{t_i}\|^2 \leq 2(t - t^i_{k_i})^2\eta_i^2 + 2(t - t^i_{k_i})\xi_i(t).$$

where

$$\xi_i(t) = \int_{t^i_{k_i}}^t \big(\beta \sum_{j\in\mathcal{N}_i} a_{ij}(\hat{x}_i - \hat{x}_j - h_i + h_j) + \alpha\nabla f_i + v_i\big)^2 d\tau.$$

Integrate on both sides,

$$\begin{aligned}
\int_{t^i_{k_i}}^t \|e_{t_i}\|^2 d\tau \leq& \int_{t^i_{k_i}}^t \big(2(\tau - t^i_{k_i})^2\eta_i^2 + 2(\tau - t^i_{k_i})\xi_i(\tau)\big) d\tau \\
\leq& 2(t - t^i_{k_i})^2 \int_{t^i_{k_i}}^t \eta_i^2 d\tau + (t - t^i_{k_i})^2\xi_i(t) \\
\leq& 2(t - t^i_{k_i})^2 \int_{t^i_{k_i}}^t \eta_i^2 d\tau + 2(t - t^i_{k_i})^2 \\
&\times \int_{t^i_{k_i}}^t (\beta \sum_{j\in\mathcal{N}_i} a_{ij}(\hat{x}_i - \hat{x}_j - h_i + h_j))^2 + (\alpha\nabla f_i + v_i)^2 d\tau,
\end{aligned} \tag{5.11}$$

By (5.10), we have

$$\begin{aligned}
&\int_{t^i_{k_i}}^{t^i_{k_i+1}} e^{p_i(\tau - t^i_{k_i})} a_i \|e_{t_i}(\tau)\|^2 d\tau \\
=& \int_{t^i_{k_i}}^{t^i_{k_i+1}} e^{p_i(\tau - t^i_{k_i})} \big(l_i(\beta \sum_{j\in\mathcal{N}_i} a_{ij}(\hat{x}_i - \hat{x}_j - h_i + h_j))^2 + m_i(\alpha\nabla f_i + v_i)^2 + c_i\eta_i^2\big) d\tau.
\end{aligned}$$

Then,

$$\int_{t^i_{k_i}}^{t^i_{k_i+1}} a_i \|e_{t_i}(\tau)\|^2 d\tau \geq$$
$$e^{-p_i \Delta T^i_{k_i}} \int_{t_{k_i}}^{t_{k_i+1}} \big(l_i(\beta \sum_{j\in\mathcal{N}_i} a_{ij}(\hat{x}_i - \hat{x}_j - h_i + h_j))^2 + m_i(\alpha \nabla f_i + v_i)^2 + c_i \eta_i^2\big) d\tau, \tag{5.12}$$

where $\Delta T^i_{k_i} = t^i_{k_i+1} - t^i_{k_i}$. Combining (5.11) and (5.12), the minimum inter-event time can be calculated from

$$\Delta T_i^2 e^{p_i \Delta T_i} = \frac{\min\{l_i, m_i, c_i\}}{2a_i}. \tag{5.13}$$

□

The stability of the system is shown in Theorem 13. In order to guarantee ISES w.r.t. unknown disturbances, a Lyapunov method is used to facilitate the selection of parameters in auxiliary variable (5.10) and the feedback gains in (5.7).

Theorem 13. Consider the sampled-data system in (5.7) under ETM in (5.8–5.10); for any given $p_i > 0$, there always exist small enough l_i, m_i, $c_i > 0$, large enough α, β, a_i, $i \in \mathcal{N}$, and well designed $\gamma > 0$, such that the closed-loop system is ISES w.r.t. unknown disturbance $\omega = [\omega_1, \cdots, \omega_n]^T$.

Proof. By (5.7), we have

$$\|\dot{e}_{t_i}\| \leq \|\alpha \nabla f_i(x_i) + \beta \sum_{j\in\mathcal{N}_i} a_{ij}(\hat{x}_i - \hat{x}_j - h_i + h_j) + v_i\| + \|\omega_i\|. \tag{5.14}$$

Integrate on both sides,

$$\|e_{t_i}(t)\| \leq \int_{t^i_{k_i}}^{t} \|\alpha \nabla f_i(x_i) + \beta \sum_{j\in\mathcal{N}_i} a_{ij}(\hat{x}_i - \hat{x}_j - h_i + h_j) + v_i\| d\tau + \int_{t^i_{k_i}}^{t} \|\omega_i\| d\tau.$$

Combining with (5.8) and (5.9), we have

$$\|\eta_i\| \leq \|\omega_i\|_\infty. \tag{5.15}$$

Let $e_{x_i} = x_i - x_i^*$, $e_{v_i} = v_i - v_i^*$, $i \in \mathcal{N}$, with the corresponding augmented vector $e_x = [e_{x_1}, \cdots, e_{x_n}]^T$, $e_v = [e_{v_1}, \cdots, e_{v_n}]^T$, and $g = \sum_{i=1}^n g_i$. Consider a Lyapunov function

$$V = \frac{1}{2}\big(a e_x^T e_x + (be_x + e_v)^T \Gamma (be_x + e_v)\big) + g, \tag{5.16}$$

where a, b are positive constants to be specified later. When there is no event, the derivative of (5.16) can be represented as

$$\begin{aligned}
\dot{V} =& \frac{1}{2} a\big(e_x^T(-\alpha q - \beta L(e_t + e_x) - e_v + \omega) + (-\alpha q - \beta L(e_t + e_x) - e_v + \omega)^T e_x\big) \\
&+ \frac{1}{2}(be_x + e_v)^T \Gamma (b(-\alpha q - \beta L(e_t + e_x) - e_v + \omega) + \gamma L(e_t + e_x)) + \dot{g} \\
&+ \frac{1}{2}(b(-\alpha q - \beta L(e_t + e_x) - e_v + \omega) + \gamma L(e_t + e_x))^T \Gamma (be_x + e_v)\big) \\
=& \frac{1}{2} e_x^T\big(- a\beta(L + L^T) + b(\gamma - b\beta)(\Gamma L + L^T \Gamma)\big) e_x + e_v^T(-\Gamma) e_v \\
&+ e_x^T\big(- a - b^2 \Gamma + (\gamma - b\beta) L^T \Gamma\big) e_v \\
&+ e_x^T\big(- a\beta L + b(\gamma - b\beta)\Gamma L\big) e_t + e_v^T(\gamma - b\beta)\Gamma L e_t \\
&+ e_x^T(a + b^2\Gamma)(-\alpha q + \omega) + e_v^T b\Gamma(-\alpha q + w) + \dot{g}
\end{aligned}$$

where $\omega = [\omega_1, \cdots, \omega_n]^T$. Under Assumption 12, according to Lemma 14, we have

$$\begin{aligned}
e_v^T \Gamma L e_x =& e_v^T \Gamma (\frac{L + L^T}{2}) e_x + e_v^T \Gamma (\frac{L - L^T}{2}) e_x \\
=& e_v^T (I - \frac{1}{N} \mathbf{1}_N \mathbf{1}_N^T) e_x + e_v^T \Gamma (\frac{L - L^T}{2}) e_x \\
=& e_v^T e_x + e_v^T \Gamma (\frac{L - L^T}{2}) e_x \\
\leq& e_v^T e_x + e_v^T \Gamma \sqrt{\epsilon_L (\frac{L + L^T}{2})} e_x.
\end{aligned}$$

Under Assumption 11, let $a = \gamma - b\beta$. Then, by introducing some free parameters δ_{k_1}, $k_1 \in \{1, 2, 3, 4, 5, 6\}$, $\delta_\omega^{k_2}$, $k_2 \in \{x, v\}$, based on the Young's inequality,

we have

$$
\begin{aligned}
&\dot{V} \leq \\
&\big(- a\alpha\nu + \frac{\delta_\omega^x}{2}(a + b^2\lambda(\Gamma)) + \frac{\delta_3}{2}b^2\bar{\lambda}(\Gamma) + \frac{\delta_4}{2}a\beta\bar{\lambda}(L) + a(\frac{\delta_2}{2} + b + \frac{\delta_5}{2}b)\lambda_M\big)e_x^T e_x \\
&+ \big(- \underline{\lambda}(\Gamma) + b\bar{\lambda}(\Gamma)\frac{\delta_\omega^v}{2} + (\frac{2}{\delta_3}b^2 + \alpha b\mu)\bar{\lambda}(\Gamma) + (\frac{2}{\delta_2} + \frac{\delta_6}{2})a\lambda_M + \frac{1}{2\delta_1}\bar{\lambda}(\Gamma)^2\big)e_v^T e_v \\
&+ \big(a\beta\bar{\lambda}(L)\frac{2}{\delta_4} + (\frac{2}{\delta_5}b + \frac{2}{\delta_6}a)\lambda_M\big)e_t^T e_t + (\frac{2}{\delta_\omega^v}b\bar{\lambda}(\Gamma) + \frac{2}{\delta_\omega^x}(a + b^2\bar{\lambda}(\Gamma)))\omega^T\omega \\
&+ e_x^T\big(- a\beta + \frac{\delta_1}{2}\epsilon_L a\big)(\frac{L^T + L}{2})e_x + \dot{g}.
\end{aligned}
$$

Here $\lambda_M = \bar{\lambda}(\Gamma)\bar{\lambda}(L)$, ν and μ represent the minimum and maximum of ν_i and μ_i for all $i \in \mathcal{N}$, respectively. Therefore, for any given a, δ_3, $\delta_5 > 0$, there always exist large enough α, β, δ_1, $\delta_2 > 0$ and small enough b, δ_ω^x, δ_ω^v, δ_4, $\delta_6 > 0$ such that

$$
\begin{cases}
-a\alpha\nu + \frac{\delta_\omega^x}{2}(a + b^2\bar{\lambda}(\Gamma)) + \frac{\delta_4}{2}a\beta\bar{\lambda}(L) + a(\frac{\delta_2}{2} + b + \frac{\delta_5}{2}b)\lambda_M + \frac{\delta_3}{2}b^2\bar{\lambda}(\Gamma) = -\epsilon_x' \\
< 0 \\
-\underline{\lambda}(\Gamma) + b\bar{\lambda}(\Gamma)\frac{\delta_\omega^v}{2} + (\frac{2}{\delta_3}b^2 + \alpha b\mu)\bar{\lambda}(\Gamma) + (\frac{2}{\delta_2} + \frac{\delta_6}{2})a\lambda_M + \frac{1}{2\delta_1}\bar{\lambda}(\Gamma)^2 = -\epsilon_v' < 0 \\
-a\beta + \frac{\delta_1}{2}\epsilon_L a < 0.
\end{cases}
$$

Then, we have $\gamma = a + b\beta$, and

$$
\dot{V} \leq -\epsilon_x' e_x^T e_x - \epsilon_v' e_v^T e_v + \epsilon_t' e_t^T e_t + \epsilon_\omega' \|\omega\|_\infty^2 + \dot{g}, \tag{5.17}
$$

where

$$
\begin{aligned}
\epsilon_t' &= a\beta\bar{\lambda}(L)\frac{2}{\delta_4} + (\frac{2}{\delta_5}b + \frac{2}{\delta_6}a)\lambda_M \\
\epsilon_\omega' &= \frac{2}{\delta_\omega^v}b\bar{\lambda}(\Gamma) + \frac{2}{\delta_\omega^x}(a + b^2\bar{\lambda}(\Gamma)).
\end{aligned}
$$

According to (5.10) and (5.15), we have

$$
\begin{aligned}
\dot{V} \leq & - \epsilon_x'\|e_x\|^2 - \epsilon_v'\|e_v\|^2 + \epsilon_t'\|e_t\|^2 + \epsilon_\omega'\|\omega\|_\infty^2 + \sum_{i\in\mathcal{N}}\big(- p_i g_i - a_i\|e_{t_i}\|^2 \\
& + m_i(\alpha q_i + e_{v_i})^2 + c_i\eta_i^2 + l_i\big(\beta\sum_{j\in\mathcal{N}_i}a_{ij}(\hat{x}_i - \hat{x}_j - h_i + h_j)\big)^2\big) \\
\leq & (-\epsilon_x' + 8\bar{l}\beta^2\bar{d}^2 + 2\alpha^2\max_{i\in\mathcal{N}}\{m_i\mu_i^2\})\|e_x\|^2 + (-\epsilon_v' + 2\bar{m})\|e_v\|^2 \\
& + (-\underline{a} + \epsilon_t' + 8\bar{l}\beta^2\bar{d}^2)\|e_t\|^2 - \underline{p}g + (\bar{c} + \epsilon_\omega')\|\omega\|_\infty^2,
\end{aligned} \tag{5.18}
$$

where $\bar{l}$, $\bar{d}$ and $\bar{m}$ represent the maximum of l_i, d_i and m_i for all $i \in \mathcal{N}$, respectively; and $\underline{c}$, $\underline{p}$ and $\underline{a}$ represent the minimum of c_i, p_i and a_i for all $i \in \mathcal{N}$, respectively. By (5.18), the parameters in (5.10) can be designed based on the following condition

$$\begin{aligned} -\epsilon_x' + 8\bar{l}\beta^2\bar{d}^2 + 2\alpha^2 \max_{i\in\mathcal{N}}\{m_i\mu_i^2\} &= -\epsilon_x < 0 \\ -\epsilon_v' + 2\bar{m} &= -\epsilon_v < 0 \\ -\underline{a} + \epsilon_t' + 8\bar{l}\beta^2\bar{d}^2 &= -\epsilon_t < 0. \end{aligned}$$

According to (5.16), we have

$$\begin{aligned} V &\le \frac{1}{2}\big(a + b^2\bar{\lambda}(\Gamma) + b\bar{\lambda}(\Gamma)\big)\|e_x\|^2 + \frac{1}{2}\big(1 + b\bar{\lambda}(\Gamma)\big)\|e_v\|^2 + g \\ V &\ge \frac{1}{2}(a + \underline{\lambda}(\Gamma)(1 - \frac{1}{\delta_v})b^2)\|e_x\|^2 + \frac{1}{2}\underline{\lambda}(\Gamma)(1-\delta_v)\|e_v\|^2 + g, \end{aligned} \tag{5.19}$$

where $0 < \delta_v < 1$ and satisfies $a + \underline{\lambda}(\Gamma)(1 - \frac{1}{\delta_v})b^2 > 0$. Then,

$$\dot{V} \le -\epsilon V + \epsilon_\omega \|\omega\|_\infty^2, \tag{5.20}$$

where $\epsilon = \min\{\frac{2\epsilon_x}{a+b^2\bar{\lambda}(\Gamma)+b\bar{\lambda}(\Gamma)}, \frac{2\epsilon_v}{1+b\bar{\lambda}(\Gamma)}, \underline{p}\}$ and $\epsilon_\omega = \bar{c} + \epsilon_\omega'$. When agent i transmits its local information at $t_{k_i}^i$, we have $V(t_{k_i}^{i+}) = V(t_{k_i}^i)$. Therefore, the closed-loop system is proved to be ISES w.r.t. w from (5.20). □

Remark 21. Event-triggered DOP was considered in [23] under connected graphs. Since the underlying graph was undirected, the feedback gain β in (5.7) could be set as zero, which means that agents would not be directly affected by neighbors' transmitted information. As a result, the ETM proposed in [23] was in the following static form independent of any buffer variables:

$$t_{k_i+1}^i = \inf\left\{t > t_{k_i}^i |\ \|\hat{x}_i - x_i\| > \max\{b_i\|\bar{\mu}_i\|, c_i\|\bar{\eta}_i\|\}\right\}, \tag{5.21}$$

where b_i, $c_i > 0$ were constants, $\bar{\mu}_i$ was a vector related to its own state x_i, and $\bar{\eta}_i$ was the auxiliary variable introduced following a similar motivation as η_i in (5.9):

$$\bar{\eta}_i = \frac{\max\{\|\hat{x}_i - x_i\| - a_i(t - t_{k_i}^i)\max\{\|\bar{\mu}_i(t)\|, \|\hat{x}_i - x_i\|\}, 0\}}{m_i(t - t_{k_i}^i)}, \tag{5.22}$$

with a_i, $m_i > 0$ to be designed. Since (5.21) and (5.22) only depended on agent's own state, $\bar{\eta}_i$ is always continuous before the next transmission instant $t^i_{k_i+1}$. However, the underlying graph considered in this work is directed. In order to ensure stability, β must be positive resulting in explicit dependence of u_i on neighbors' broadcast information. Since the transmissions among MASs are asynchronous and independent, we use an integral term in (5.9) and a buffer state g_i in (5.10) to record the transmitted information from agent's neighbors before the next transmission instant $t^i_{k_i+1}$.

Remark 22. The ETM proposed in this work is applied to the distributed formation problem with time-varying desirable configuration h considered in [68]. In that case, the dynamics of h is estimated by auxiliary variable η_i, and the closed-loop system is ISES w.r.t. disturbances and $\dot{h}$.

5.4 ETM with Less Computation Complexity

The auxiliary variable in (5.9) includes integration of a piece-wise constant term $\sum_{j\in\mathcal{N}_i} a_{ij}(\hat{x}_i - \hat{x}_j)$ and continuous terms $\alpha\nabla f_i$ and v_i. Clearly, the computation complexity for the first one is much less than the second. In order to reduce the load on microprocessors, we consider another design of the auxiliary average variable η_i as

$$\eta_i = \frac{1}{t - t^i_k}\max\{\|\hat{x}_i - x_i\| - \int_{t^i_{k_i}}^{t} \|\beta \sum_{j\in\mathcal{N}_i} a_{ij}(\hat{x}_i - \hat{x}_j - h_i + h_j)\| d\tau, 0\}. \quad (5.23)$$

Correspondingly, the ETM is given by

$$\begin{aligned} t^i_{k_i+1} &= \min\{t^i_{k_i} + T, \tilde{t}^i_{k_i+1}\}, \\ \tilde{t}^i_{k_i+1} &= \inf\{t > \tilde{t}^i_{k_i} : g_i(t) < 0\}. \end{aligned} \quad (5.24)$$

Here, $T > 0$ is a user-specified upper bound of inter-event times, and the buffer signal is given as

$$\dot{g}_i = -p_i g_i - a_i\|\hat{x}_i - x_i\|^2 + l_i\big(\beta \sum_{j\in\mathcal{N}_i} a_{ij}(\hat{x}_i - \hat{x}_j - h_i + h_j)\big)^2 + c_i\eta_i^2, \quad (5.25)$$

with $g_i(0) = 0$, where p_i, l_i, a_i, $c_i > 0$ are positive constants to be specified later. Consequently, the analytical solutions of η_i and g_i can be obtained in a piece-wise form.

Theorem 14. Consider the sampled-data system in (5.7) under ETM in (5.23)–(5.25). For any given $p_i > 0$, there always exist small enough c_i, $l_i > 0$, large enough α, β, a_i, $i \in \mathcal{N}$, and well designed $\gamma > 0$, such that the closed-loop system is ISES w.r.t. unknown disturbance $\omega = [\omega_1, \cdots, \omega_n]^T$. Furthermore, Zeno-freeness is guaranteed by a computable minimum inter-event time satisfying $\inf\{t_{k+1}^i - t_k^i\} \geq \min\{T, \Delta T_i\}$, with ΔT_i being the unique positive solution of

$$\Delta T_i^2 e^{p_i \Delta T_i} = \frac{\min\{l_i, c_i\}}{2a_i}.$$

Proof. The Zeno-free behavior can be proved following a similar line in Lemma 16. By (5.7), (5.8) and (5.23) we have

$$\|\eta_i\| \leq \text{ave}_{[t_k^i, t]} \|\alpha q_i\| + \text{ave}_{[t_k^i, t]} \|e_{v_i}\| + \|\omega_i\|_\infty. \tag{5.26}$$

For notational convenience, in the following, we drop the subscript $[t_{k_i}^i, t]$ in $\text{ave}(\cdot)_{[t_{k_i}^i, t]}$ if there is no ambiguity. Considering a storage function as in (5.16), when there is no event, the derivative of (5.16) can be represented as

$$\begin{aligned}
\dot{V} \leq & -\epsilon_x' \|e_x\|^2 - \epsilon_v' \|e_v\|^2 + \epsilon_t' \|e_t\|^2 + \epsilon_\omega' \|\omega\|_\infty^2 + \sum_{i \in \mathcal{N}} \big(- p_i g_i + c_i \eta_i^2 \\
& - a_i \|e_{t_i}\|^2 + l_i \big(\beta \sum_{j \in \mathcal{N}_i} a_{ij} (\hat{x}_i - \hat{x}_j - h_i + h_j) \big)^2 \big) \\
\leq & (-\epsilon_x' + 8\bar{l}\beta^2 \bar{d}^2) \|e_x\|^2 - \epsilon_v' \|e_v\|^2 + (-\underline{a} + \epsilon_t' + 8\bar{l}\beta^2 \bar{d}^2) \|e_t\|^2 \\
& - \underline{p} g + \epsilon_\omega' \|\omega\|_\infty^2 + \sum_{i \in \mathcal{N}} c_i \big((1 + \delta_{\omega x} + \delta_{xv}) \text{ave} \|e_{x_i}\|^2 \\
& + (1 + \frac{1}{\delta_{\omega v}} + \frac{1}{\delta_{xv}}) \text{ave} \|e_{v_i}\|^2 + (1 + \frac{1}{\delta_{\omega x}} + \delta_{\omega v}) \text{ave} \|\omega_i\|^2 \big) \\
\leq & - \epsilon_x e_x^T e_x - \epsilon_v e_v^T e_v - \epsilon_t e_t^T e_t - \underline{p} g + \epsilon_\omega \|\omega\|_\infty^2 \\
& + \sum_{i \in \mathcal{N}} c_i \big((1 + \delta_x) \alpha^2 \mu_i^2 \text{ave} \|e_{x_i}\|^2 + (1 + \delta_v) \text{ave} \|e_{v_i}\|^2 \big),
\end{aligned}$$

where ϵ_x', ϵ_v', ϵ_t' and ϵ_ω' have the same expressions as in (5.17) and $\delta_x = \delta_{\omega x} + \delta_{xv}$, $\delta_v = \frac{1}{\delta_{\omega v}} + \frac{1}{\delta_{xv}}$, $\epsilon_x = \epsilon_x' - 8\bar{l}\beta^2\bar{d}^2$, $\epsilon_v = \epsilon_v'$, $\epsilon_t = \underline{a} - \epsilon_t' - 8\bar{l}\beta^2\bar{d}^2$

and $\epsilon_\omega = 1 + \epsilon'_\omega + \frac{1}{\delta_{\omega x}} + \delta_{\omega v}$. According to (5.19), we have

$$\dot{V} = -\epsilon V + \epsilon_\omega \|\omega\|_\infty^2 + \sum_{i\in\mathcal{N}} c_i\big((1+\delta_x)\alpha^2\mu_i^2 \text{ave}\|e_{x_i}\|^2 + (1+\delta_v)\text{ave}\|e_{v_i}\|^2\big),$$

where ϵ has the same expression as in (5.20). According to (5.19), when

$$V \geq \max_{i\in\mathcal{N}} \left\{ \frac{1}{2}(a + \bar{\lambda}(\Gamma)(1-\frac{1}{\delta_v})b^2)\text{ave}\|e_{x_i}\|^2, \frac{1}{2}\bar{\lambda}(\Gamma)(1-\delta_v)\text{ave}\|e_{v_i}\|^2 \right\},$$

the derivative of V satisfies

$$\begin{aligned} \dot{V} \leq & -\epsilon V + \epsilon_\omega \|\omega\|_\infty^2 + \big(\bar{c}\sum_{i\in\mathcal{N}}(1+\delta_x)\alpha^2\mu_i^2 \frac{2V}{a + \bar{\lambda}(\Gamma)(1-1/\delta_v)b^2}\big) \\ & + \bar{c}n(1+\delta_v)\frac{2V}{\bar{\lambda}(\Gamma)(1-\delta_v)}. \end{aligned} \tag{5.27}$$

As a result, when

$$\frac{\epsilon}{2\bar{c}} \geq \sum_{i\in\mathcal{N}}(1+\delta_x)\alpha^2\mu_i^2 + \bar{c}n(1+\delta_v), \tag{5.28}$$

we have

$$\dot{V} \leq -\frac{\epsilon}{2}V + \epsilon_\omega\|\omega\|_\infty^2, \tag{5.29}$$

and there always exist small enough c_i, $i \in \mathcal{N}$, such that the condition in (5.28) can be established.

Consider a Lyapunov function as

$$O(t) = \max_{i\in\mathcal{N}} \left\{ V,\ \frac{1}{4}(a + \bar{\lambda}(\Gamma)(1-\frac{1}{\delta_v})b^2)\text{ave}\|e_{x_i}\|^2, \frac{1}{4}\bar{\lambda}(\Gamma)(1-\delta_v)\text{ave}\|e_{v_i}\|^2 \right\}.$$

Case I: $O(t) = V(t)$. When there is no jump, we have (5.29).

Case II: $O(t) = \frac{1}{4}(a + \bar{\lambda}(\Gamma)(1-\frac{1}{\delta_v})b^2)\text{ave}\|e_{x_i}\|^2$ and

$$\text{ave}\|e_{x_i}\|^2 \geq \frac{4V(t)}{a + \bar{\lambda}(\Gamma)(1-1/\delta_v)b^2} \geq 2e_x^T e_x \geq 2e_{x_i}^T e_{x_i}.$$

Then, it follows from the user-specified upper bound T of inter-event times that

$$\dot{O}(t) \leq -\frac{1}{t - t_{k_i}^i}(O(t) - \frac{O(t)}{2}) \leq -\frac{1}{2T}O(t).$$

Case III: $O(t) = \frac{1}{4}\bar{\lambda}(\Gamma)(1-\delta_v)\text{ave}\|e_{v_i}\|^2$. This is similar to Case II.

When agent i transmits its local information at $t^i_{k_i}$, we have $V(t^{i+}_{k_i}) = V(t_{k_i})$. When $O(t^i_{k_i}) = \frac{1}{4}(a+\bar{\lambda}(\Gamma)(1-\frac{1}{\delta_v})b^2)\text{ave}\|e_{x_i}\|^2$, according to Lemma 15, we have

$$\lim_{t\to t^{i+}_{k_i}} O(t) = \frac{1}{4}(a+\bar{\lambda}(\Gamma)(1-\frac{1}{\delta_v})b^2)\|e_{x_i}(t^i_{k_i})\|^2 \leq \frac{1}{2}V(t^i_{k_i}).$$

Similar conclusions can be applied when $O(t) = \frac{1}{4}\bar{\lambda}(\Gamma)(1-\delta_v)\text{ave}\|e_{v_i}\|^2$. As a result $O(t^{i+}_{k_i}) = O(t^i_{k_i})$. Combining the cases above with

$$\dot{O}(t) \leq -\min\left\{\frac{\epsilon}{2}, \frac{1}{2T}\right\} O(t) + \epsilon_\omega\|\omega\|^2_\infty,$$

one can prove ISES of the closed-loop system w.r.t. w. □

Remark 23. Comparing equations (5.8)–(5.10) and (5.23)–(5.25), the inter-event time in the second method is upper bounded by a user-specified constant T. In addition, besides ω_i, the upper bounds on η_i in (5.23) is related to $\text{ave}(e_{v_i})$ and $\text{ave}(e_{x_i})$. As a result, the ETM in (5.24) would be more conservative than the one in (5.8). This reveals the trade-off between computation complexity and network load.

5.5 Simulations

Numerical examples are used to illustrate the effectiveness of the proposed methods in this section. Consider a MAS with four agents. The underlying graph is described by the Laplacian matrix

$$L = \begin{bmatrix} 0.5 & 0 & 0 & -0.5 \\ -0.5 & 0.5 & 0 & 0 \\ 0 & -0.5 & 0.5 & 0 \\ 0 & 0 & -0.5 & 0.5 \end{bmatrix}.$$

The desirable formation is give as $h = [-1, -0.5, 0, 0.5]^T$, and the local object functions are $f_1 = x^2 + \ln(x^2+1)$, $f_2 = x^2 - 2x$, $f_3 = (x-4)^2$ and $f_4 = 1.25x^2$. The optimal values are $x^* = [0.316, 0.816, 1.314, 1.814]^T$. The gains in controller (5.7) are chosen as $\alpha = 5$, $\beta = 8$, $\gamma = 0.48$, and the parameters of auxiliary variables η_i and g_i in (5.9) and (5.10) are chosen as $p_i = 1$, $a_i = 50$,

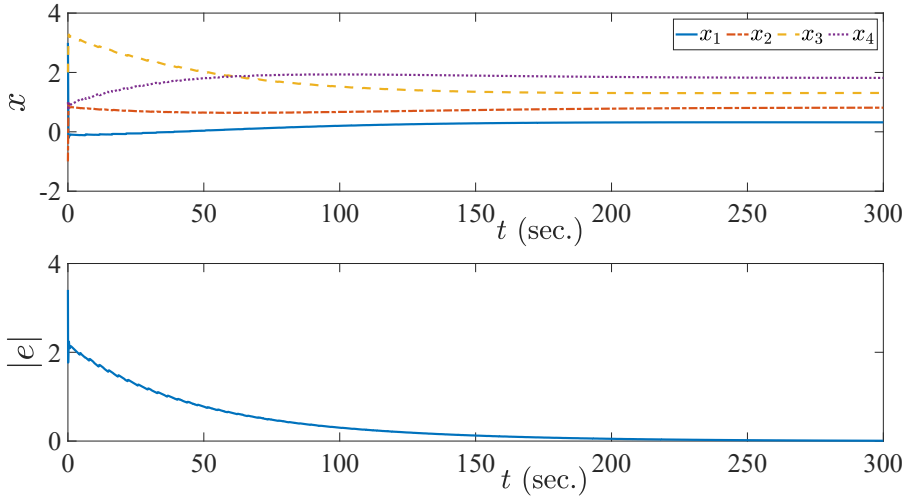

Figure 5.1: Trajectories under the ET function in (5.9) and (5.10) without disturbances

$l_i = 0.016$, $m_i = 0.005$ and $c_i = 1$.

Figure 5.1 shows the simulation result without disturbances and Figure 5.3 shows the corresponding inter-event times with the minimum, average and theoretical inter-event times listed in Table 5.1. Figure 5.2 shows the simulation result subject to disturbances $\omega_i(t) = 0.1\cos(0.5t)$, and the steady-state error is $\|e_x\| = 0.1183$. Figure 5.4 shows the corresponding inter-event times with the minimum and average inter-event times listed in Table 5.1, which illustrates that (i) Zeno behavior can be excluded in the absence and presence of disturbances, (ii) the existence of disturbances generates more transmissions, and (iii) our proposed ETM can adaptively allocate communication resources based on the on-line demands.

Table 5.1: Statistic properties of inter-event times under the ET function in (5.9) and (5.10)

	Agents	1	2	3	4
No Disturbances	Minimum	0.0151	0.0085	0.0085	0.0117
	Average	4.0988	2.5388	2.8033	3.5590
With Disturbances	Minimum	0.0043	0.0077	0.0065	0.0114
	Average	0.8422	0.6721	0.4701	0.8980
Theoretical	Minimum	0.0040			

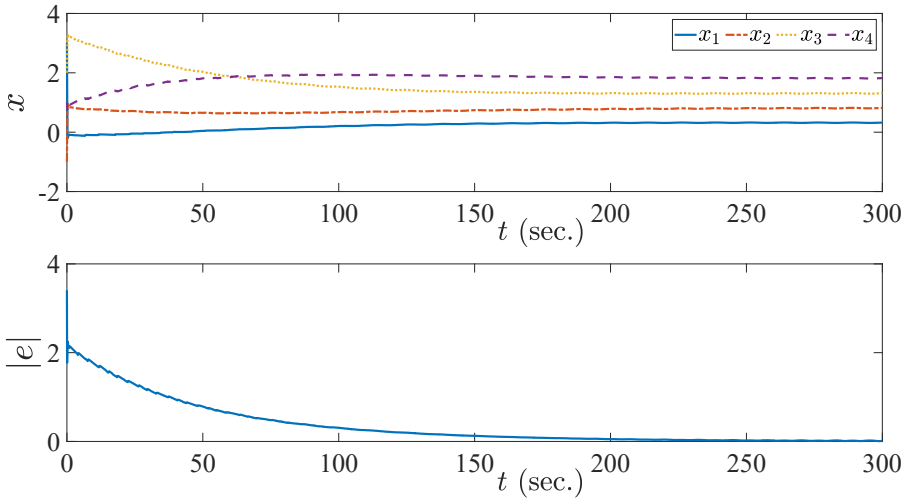

Figure 5.2: Trajectories under the ET function in (5.9) and (5.10) with disturbances

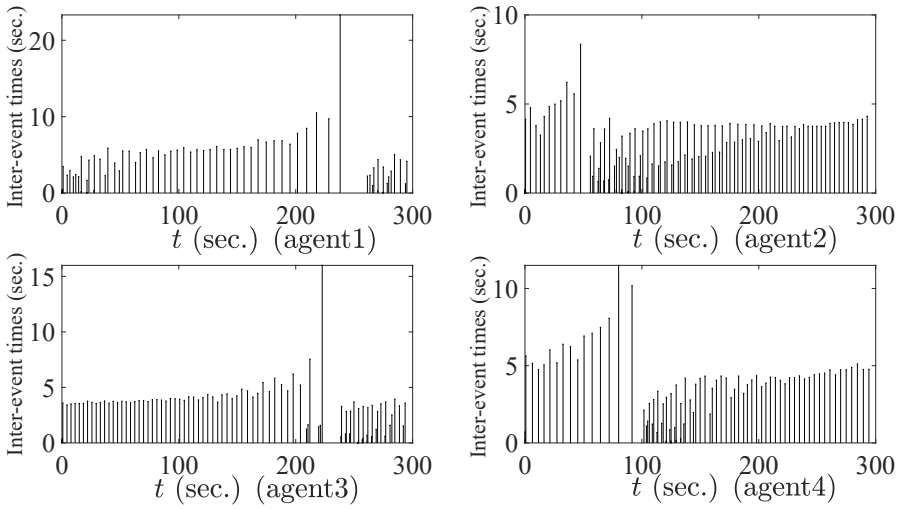

Figure 5.3: Inter-event times under the ET function in (5.9) and (5.10) without disturbances

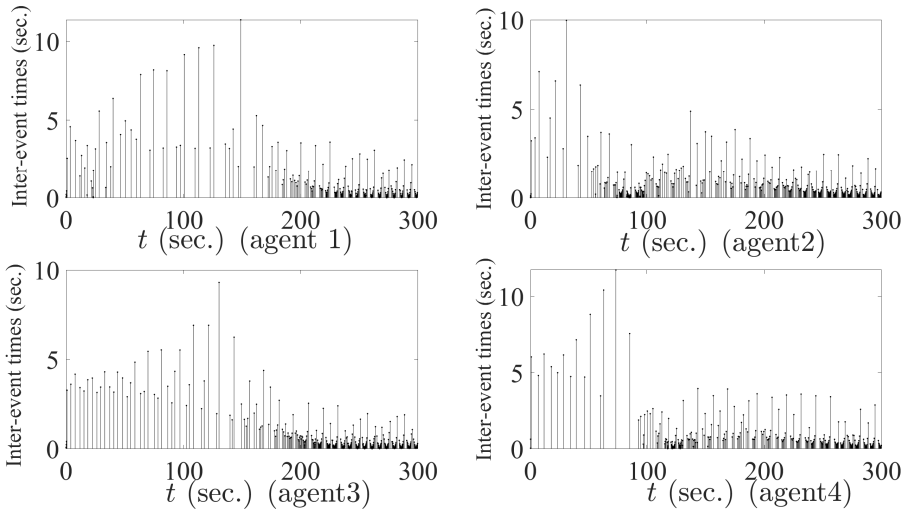

Figure 5.4: Inter-event times under the ET function in (5.9) and (5.10) with disturbances

The parameters of auxiliary variables η_i and g_i in (5.23) and (5.25) are chosen as $a_i = 50$, $l_i = 0.016$, $c_i = 0.0001$ and $T = 20$. Figures 5.5 and 5.6 show the simulation results without disturbances and with disturbances $\omega_i(t) = 0.1\cos(0.5t)$, respectively. The steady-state error for the disturbed case is $\|e_x\| = 0.1190$. Some statistic properties of inter-event times are summarized in Table 5.2. Comparing the results given in Tables 5.1 and 5.2, the

Table 5.2: Statistic properties of inter-event times under the ET function in (5.23) and (5.25)

	Agents	1	2	3	4
No	Minimum	0.0031	0.0022	0.0057	0.0058
Disturbances	Average	1.4304	1.1802	1.3764	1.8707
With	Minimum	0.0022	0.0022	0.0022	0.0022
Disturbances	Average	0.0907	0.2392	0.0600	0.3469
Theoretical	Minimum	0.0010			

inter-event times of the first method in Section 5.3 are larger than the ones of the second method in Section 5.4. This supports the discussions in Remark 23.

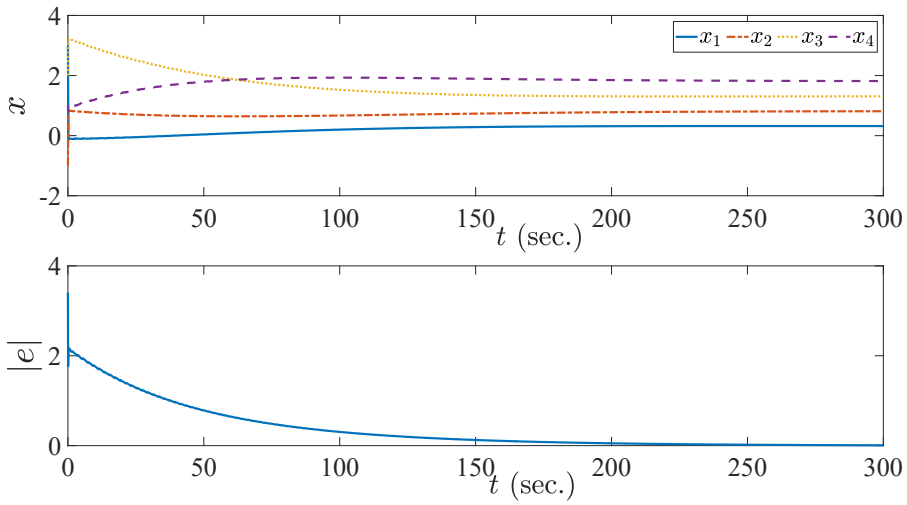

Figure 5.5: Trajectories under the ET function in (5.23) and (5.25) without disturbances

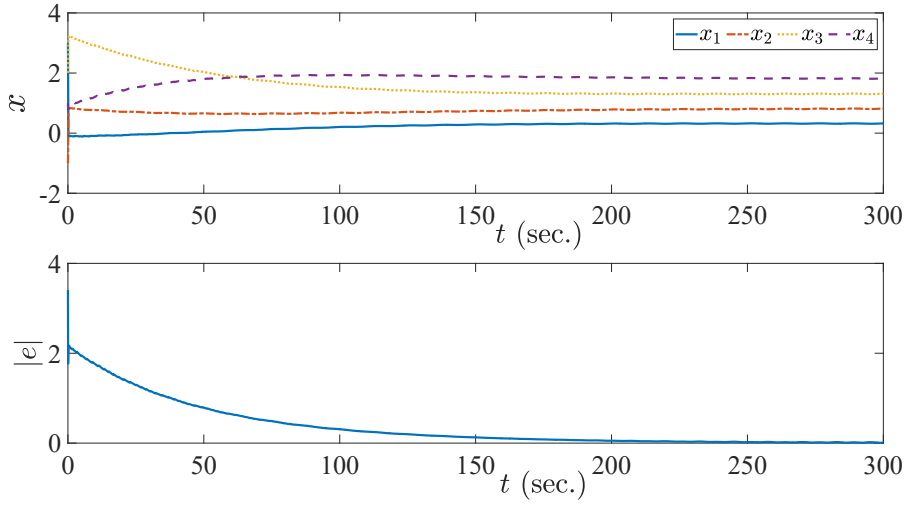

Figure 5.6: Trajectories under the ET function in (5.23) and (5.25) with disturbances

5.6 Summary

In this chapter, we proposed an ETM to solve a distributed optimization-based formation problem under strongly connected and weight-balanced digraph. Under the proposed method, MASs could minimize a global object function and converge to a desirable configuration simultaneously. An auxiliary average variable was introduced to estimate the influence of unknown disturbances between adjacent transmissions, and a novel dynamic ETM was used to deal with asynchronous transmissions among agents. Benefited from the novel ETM, the closed-loop system is ISES w.r.t. unknown disturbances, and Zeno-freeness is guaranteed for each agent by a computable positive minimum inter-event time. Furthermore, the trade-off between network load and computation complexity was discussed by constructing different ETMs that used different signals in the auxiliary variables. The effectiveness of the methods was verified by numerical examples.

Chapter 6

Conclusions and Future Work

In this chapter, remarks are provided to conclude this thesis, and then some potential research directions are pointed out for future work.

6.1 Conclusions

This thesis studies a variety of cooperative control problems for MASs. To reduce network load and energy consumption, ETMs are proposed to generate data transmissions and/or controller updates for the considered problems. The outcomes of the work in this thesis are summarized as follows:

1. An affine formation of general nonholonomic systems on the SE(3) is studied. A distributed control protocol is proposed, under which, MASs can converge to the desirable configuration. The control protocol only relies on relative information detected by agents' onboard sensors, and the configuration of MASs can be manipulated by only a few agents in the system. In addition, a distributed algorithm is proposed to reconstruct a k-rooted graph when some edges are lost. Taking the advantage of that, the proposed control protocol can be implemented under switching graphs. Furthermore, an ETM is proposed, such that the controller updates and data transmissions occur only when it is necessary to maintain system stability. To guarantee Zeno-freeness, an absolute term is introduced to the ET function with some sacrifice of system performance.

2. A COR problem is studied in a hybrid system framework. Considering inevitable network-induced imperfections, robustness against asynchronous transmissions and time-varying delays are analyzed in terms of MATIs and MADs, respectively. A novel Lyapunov candidate is proposed to facilitate stability analysis, by which, a more intuitive trade-off relationship between MATIs and MADs is given.

3. A formation tracking of nonholonomic systems without velocity measurements is studied. The information flow through detection networks and communication networks are considered separately. The first kind is defined as PULC, and we assume that the detected information is used directly; while the second kind is defined as PUSC, and PETMs are proposed to generate transmission events. Furthermore, a hierarchical structure is proposed to remove the acyclic assumption. Based on this structure, estimation and control strategies are proposed to the agents in different levels. The closed-loop MAS follows a cascade structure, and novel Lyapunov candidates are proposed to facilitate stability analysis, where finite time convergence, ISS and strongly iISS are provided for the corresponding subsystems.

4. A distributed optimization-based formation problem is studied, where each agent is only aware of its local object function and can communicate with its neighbors. A distributed control protocol is proposed based on MLB algorithms, such that the MAS can agree on the global optimal solution and converge to the desirable formation. An ETM is proposed to generate transmission events. To guarantee Zeno-freeness under disturbed cases, an auxiliary variable is introduced to estimate the average effect of disturbances to the MAS. Furthermore, the closed-loop system is proved to be ISES w.r.t the disturbances.

The effectiveness and applicability of the proposed methods are validated by case studies using numerical examples.

6.2 Future Work

This thesis studied several cooperative control problems of MASs, including affine formation control, COR, foramtion tracking and distributed optimization-based formation. Considering inevitable network-induced imperfections, the robustness against asynchronous samplings and time-varying delays was investigated. To reduce network load and energy consumption, ETMs were proposed, such that the controller updates and/or data transmissions only occurred when some predetermined thresholds were violated. However, the robust analysis and ETM designs were proposed for the MASs with specific dynamics. A method that is available to general MASs is still required. In addition, as one of the most critical problem in ETMs, Zeno-behavior has not been solved systematically. To meet the demands in some general and systematic methods to analyze the influence of network-induced imperfections and facilitate Zeno-free ETM designs, the following promising directions deserve efforts for future work.

Robustness Against Network-Induced Imperfections for MASs with General Dynamics

Cooperative control of MASs relies on the information flow among agents. However, the introduction of communication networks comes with network-induced imperfections inevitably, such as asynchronous samplings, time-varying delays, quantization errors, communication constraints and data dropouts. There are plenty of literature focusing on investigating the influence of these imperfections on NCSs, and most of them formulated and solved the problem in a hybrid system framework. But the Lyaounov function used in the existing results on NCSs ignored some distinct features of sampled-data MASs, which would led to some inconsistency and unintuitive analysis. In Chapter 3, we studied the robustness against network-induced imperfections for a COR problem under a hybrid system framework. The tolerance of asynchronous transmissions and time-varying delays were given in terms of MATIs

and MADs. A novel Lyapunov function candidate was proposed to facilitate the analysis of system stability, which led to a more intuitive trade-off design of MATIs and MASs. In practice, several types of communication imperfections always come simultaneously and the system dynamics are more complex. Therefore, a method which can cope with different types of communication imperfections and be applied to general system dynamics is required.

Zeno-Free Event-Triggered Mechanism for MASs

In order to reduce network load and energy consumption, ETMs are proposed as an improvement over the classical time-triggered mechanisms. Consequently, the exclusion of Zeno-behavoir needs to be taken into consideration. In Chapter 2, an absolute term was used to guarantee Zeno-freeness in the price of sacrificing asymptotic convergence. In Chapter 3, PETCs were applied, the continuous measurements and Zeno-behavior were excluded simultaneously. However, the system might degrade to classical periodic sampling when there exist disturbances. In Chapter 4, a dynamic ETM was proposed and an auxiliary variable was introduced to estimate the influence of disturbances. The closed-loop system was Zeno-free and ISES w.r.t. disturbances. But the robustness against network-induced imperfections was not provided, and continuous monitoring of system states was required. Based on the above analysis, it is worthy to investigate a systemic method that can provide ISS property against external disturbances with guaranteed Zeno-freeness, and at the same time, be free of continuous monitoring and robust to network-induced imperfections.

Bibliography

[1] R. Olfati-Saber and R. M. Murray, "Consensus problems in networks of agents with switching topology and time-delays," *IEEE Transactions on Automatic Control*, vol. 49, no. 9, pp. 1520–1533, 2004.

[2] J. A. Fax and R. M. Murray, "Information flow and cooperative control of vehicle formations," *IEEE Transactions on Automatic Control*, vol. 49, no. 9, pp. 1465–1476, 2004.

[3] K.-K. Oh, M.-C. Park, and H.-S. Ahn, "A survey of multi-agent formation control," *Automatica*, vol. 53, pp. 424–440, 2015.

[4] L. Krick, M. E. Broucke, and B. A. Francis, "Stabilisation of infinitesimally rigid formations of multi-robot networks," *International Journal of control*, vol. 82, no. 3, pp. 423–439, 2009.

[5] Z. Sun, S. Mou, B. D. Anderson, and M. Cao, "Exponential stability for formation control systems with generalized controllers: A unified approach," *Systems & Control Letters*, vol. 93, pp. 50–57, 2016.

[6] Q. Yang, M. Cao, H. G. de Marina, H. Fang, and J. Chen, "Distributed formation tracking using local coordinate systems," *Systems & Control Letters*, vol. 111, pp. 70–78, 2018.

[7] H. G. De Marina, B. Jayawardhana, and M. Cao, "Taming mismatches in inter-agent distances for the formation-motion control of second-order agents," *IEEE Transactions on Automatic Control*, vol. 63, no. 2, pp. 449–462, 2017.

[8] M. H. Trinh, S. Zhao, Z. Sun, D. Zelazo, B. D. O. Anderson, and H.-S. Ahn, "Bearing-based formation control of a group of agents with leader-first follower structure," *IEEE Transactions on Automatic Control*, vol. 64, no. 2, pp. 598–613, 2018.

[9] S. Zhao and D. Zelazo, "Translational and scaling formation maneuver control via a bearing-based approach," *IEEE Transactions on Control of Network Systems*, vol. 4, no. 3, pp. 429–438, 2015.

[10] W. Wang, J. Huang, C. Wen, and H. Fan, "Distributed adaptive control for consensus tracking with application to formation control of nonholonomic mobile robots," *Automatica*, vol. 50, no. 4, pp. 1254–1263, 2014.

[11] X. Yu and L. Liu, "Distributed formation control of nonholonomic vehicles subject to velocity constraints," *IEEE Transactions on Industrial Electronics*, vol. 63, no. 2, pp. 1289–1298, 2015.

[12] S. Zhao, "Affine formation maneuver control of multiagent systems," *IEEE Transactions on Automatic Control*, vol. 63, no. 12, pp. 4140–4155, 2018.

[13] Z. Lin, L. Wang, Z. Chen, M. Fu, and Z. Han, "Necessary and sufficient graphical conditions for affine formation control," *IEEE Transactions on Automatic Control*, vol. 61, no. 10, pp. 2877–2891, 2015.

[14] Y. Su and J. Huang, "Cooperative output regulation of linear multi-agent systems," *IEEE Transactions on Automatic Control*, vol. 57, no. 4, pp. 1062–1066, 2012.

[15] M. Lu and L. Liu, "Distributed feedforward approach to cooperative output regulation subject to communication delays and switching networks," *IEEE Transactions on Automatic Control*, vol. 62, no. 4, pp. 1999–2005, 2016.

[16] R. Olfati-Saber, "Flocking for multi-agent dynamic systems: Algorithms and theory," *IEEE Transactions on Automatic Control*, vol. 51, no. 3, pp. 401–420, 2006.

[17] J. Tsitsiklis, D. Bertsekas, and M. Athans, "Distributed asynchronous deterministic and stochastic gradient optimization algorithms," *IEEE Transactions on Automatic Control*, vol. 31, no. 9, pp. 803–812, 1986.

[18] A. Nedic and A. Ozdaglar, "Distributed subgradient methods for multi-agent optimization," *IEEE Transactions on Automatic Control*, vol. 54, no. 1, pp. 48–61, 2009.

[19] W. Shi, Q. Ling, G. Wu, and W. Yin, "Extra: An exact first-order algorithm for decentralized consensus optimization," *SIAM Journal on Optimization*, vol. 25, no. 2, pp. 944–966, 2015.

[20] J. Lu and C. Y. Tang, "Zero-gradient-sum algorithms for distributed convex optimization: The continuous-time case," *IEEE Transactions on Automatic Control*, vol. 57, no. 9, pp. 2348–2354, 2012.

[21] B. Gharesifard and J. Cortes, "Distributed continuous-time convex optimization on weight-balanced digraphs," *IEEE Transactions on Automatic Control*, vol. 59, no. 3, pp. 781–786, 2013.

[22] S. S. Kia, J. Cortes, and S. Martinez, "Distributed convex optimization via continuous-time coordination algorithms with discrete-time communication," *Automatica*, vol. 55, pp. 254–264, 2015.

[23] H. Yu and T. Chen, "A new Zeno-free event-triggered scheme for robust distributed optimal coordination," *Automatica*, vol. 129, p. Artical 109639, 2021.

[24] W. Heemels, A. R. Teel, N. Van de Wouw, and D. Nesic, "Networked control systems with communication constraints: Tradeoffs between trans-

mission intervals, delays and performance," *IEEE Transactions on Automatic Control*, vol. 55, no. 8, pp. 1781–1796, 2010.

[25] K. Liu, A. Selivanov, and E. Fridman, "Survey on time-delay approach to networked control," *Annual Reviews in Control*, vol. 48, pp. 57–79, 2019.

[26] M. Lemmon, "Event-triggered feedback in control, estimation, and optimization," in *Networked Control Systems*. Springer, 2010, pp. 293–358.

[27] L. Ding, Q.-L. Han, X. Ge, and X.-M. Zhang, "An overview of recent advances in event-triggered consensus of multiagent systems," *IEEE Transactions on Cybernetics*, vol. 48, no. 4, pp. 1110–1123, 2017.

[28] X.-M. Zhang, Q.-L. Han, and B.-L. Zhang, "An overview and deep investigation on sampled-data-based event-triggered control and filtering for networked systems," *IEEE Transactions on Industrial Informatics*, vol. 13, no. 1, pp. 4–16, 2016.

[29] D. P. Borgers and W. Heemels, "Event-separation properties of event-triggered control systems," *IEEE Transactions on Automatic Control*, vol. 59, no. 10, pp. 2644–2656, 2014.

[30] X.-M. Zhang, Q.-L. Han, and X. Yu, "Survey on recent advances in networked control systems," *IEEE Transactions on Industrial Informatics*, vol. 12, no. 5, pp. 1740–1752, 2015.

[31] M. Donkers, W. Heemels, N. Van de Wouw, and L. Hetel, "Stability analysis of networked control systems using a switched linear systems approach," *IEEE Transactions on Automatic Control*, vol. 56, no. 9, pp. 2101–2115, 2011.

[32] V. Dolk, D. P. Borgers, and W. Heemels, "Output-based and decentralized dynamic event-triggered control with guaranteed $\mathcal{L}_p$-gain performance and Zeno-freeness," *IEEE Transactions on Automatic Control*, vol. 62, no. 1, pp. 34–49, 2016.

[33] E. Garcia and P. J. Antsaklis, "Model-based event-triggered control for systems with quantization and time-varying network delays," *IEEE Transactions on Automatic Control*, vol. 58, no. 2, pp. 422–434, 2012.

[34] D. Nesic and A. R. Teel, "Input-output stability properties of networked control systems," *IEEE Transactions on Automatic Control*, vol. 49, no. 10, pp. 1650–1667, 2004.

[35] L. Zou, Z. Wang, Q.-L. Han, and D. Zhou, "Ultimate boundedness control for networked systems with try-once-discard protocol and uniform quantization effects," *IEEE Transactions on Automatic Control*, vol. 62, no. 12, pp. 6582–6588, 2017.

[36] W. Wang, D. Nesic, and R. Postoyan, "Observer design for networked control systems with FlexRay," *Automatica*, vol. 82, pp. 42–48, 2017.

[37] X.-M. Zhang, Q.-L. Han, X. Ge, D. Ding, L. Ding, D. Yue, and C. Peng, "Networked control systems: A survey of trends and techniques," *IEEE/CAA Journal of Automatica Sinica*, vol. 7, no. 1, pp. 1–17, 2019.

[38] M. Shen, S. K. Nguang, C. K. Ahn, and Q.-G. Wang, "Robust H_2 control of linear systems with mismatched quantization," *IEEE Transactions on Automatic Control*, vol. 64, no. 4, pp. 1702–1709, 2018.

[39] Z.-G. Wu, Y. Xu, Y.-J. Pan, H. Su, and Y. Tang, "Event-triggered control for consensus problem in multi-agent systems with quantized relative state measurements and external disturbance," *IEEE Transactions on Circuits and Systems I: Regular Papers*, vol. 65, no. 7, pp. 2232–2242, 2018.

[40] S. Xiong, Q. Wu, and Y. Wang, "Distributed coordination of heterogeneous multi-agent systems with dynamic quantization and L_2-L_∞ control," *International Journal of Control, Automation and Systems*, vol. 18, no. 10, pp. 2468–2481, 2020.

[41] Y.-J. Pan, H. Werner, Z. Huang, and M. Bartels, "Distributed cooperative control of leader–follower multi-agent systems under packet dropouts for quadcopters," *Systems & Control Letters*, vol. 106, pp. 47–57, 2017.

[42] Z. Liu, W. Yan, H. Li, and M. Small, "Cooperative output regulation problem of multi-agent systems with stochastic packet dropout and time-varying communication delay," *Journal of the Franklin Institute*, vol. 355, no. 17, pp. 8664–8682, 2018.

[43] H. Yang, S. Ju, Y. Xia, and J. Zhang, "Predictive cloud control for networked multiagent systems with quantized signals under dos attacks," *IEEE Transactions on Systems, Man, and Cybernetics: Systems*, vol. 51, no. 2, pp. 1345–1353, 2019.

[44] G. C. Walsh, O. Beldiman, and L. G. Bushnell, "Asymptotic behavior of nonlinear networked control systems," *IEEE Transactions on Automatic Control*, vol. 46, no. 7, pp. 1093–1097, 2001.

[45] D. Nesic, A. R. Teel, and D. Carnevale, "Explicit computation of the sampling period in emulation of controllers for nonlinear sampled-data systems," *IEEE Tansactions on Automatic Control*, vol. 54, no. 3, pp. 619–624, 2009.

[46] J. Berneburg and C. Nowzari, "Distributed dynamic event-triggered coordination with a designable minimum inter-event time," in *IEEE American Control Conference*, 2019, pp. 1424–1429.

[47] G. Zhao, C.-C. Hua, and X. Guan, "A hybrid event-triggered approach to consensus of multi-agent systems with disturbances," *IEEE Transactions on Control of Network Systems*, vol. 7, no. 3, pp. 1259–1271, 2020.

[48] F. Xiao and L. Wang, "Consensus protocols for discrete-time multi-agent systems with time-varying delays," *Automatica*, vol. 44, no. 10, pp. 2577–2582, 2008.

[49] Y. Gao, J. Yu, J. Shao, and M. Yu, "Group consensus for second-order discrete-time multi-agent systems with time-varying delays under switching topologies," *Neurocomputing*, vol. 207, pp. 805–812, 2016.

[50] V. Dolk, M. Abdelrahim, and W. Heemels, "Event-triggered consensus seeking under non-uniform time-varying delays," *IFAC-PapersOnLine*, vol. 50, no. 1, pp. 10 096–10 101, 2017.

[51] F. Xiao and T. Chen, "Sampled-data consensus in multi-agent systems with asynchronous hybrid event-time driven interactions," *Systems & Control Letters*, vol. 89, pp. 24–34, 2016.

[52] F. Xiao, Y. Shi, and W. Ren, "Robustness analysis of asynchronous sampled-data multiagent networks with time-varying delays," *IEEE Transactions on Automatic Control*, vol. 63, no. 7, pp. 2145–2152, 2017.

[53] M. Mazo and P. Tabuada, "Decentralized event-triggered control over wireless sensor/actuator networks," *IEEE Transactions on Automatic Control*, vol. 56, no. 10, pp. 2456–2461, 2011.

[54] X. Wang and M. Lemmon, "Event-triggering in distributed networked control systems," *IEEE Transactions on Automatic Control*, vol. 56, no. 3, pp. 586–601, 2010.

[55] D. Yang, W. Ren, X. Liu, and W. Chen, "Decentralized event-triggered consensus for linear multi-agent systems under general directed graphs," *Automatica*, vol. 69, pp. 242–249, 2016.

[56] G. S. Seyboth, D. V. Dimarogonas, and K. H. Johansson, "Event-based broadcasting for multi-agent average consensus," *Automatica*, vol. 49, no. 1, pp. 245–252, 2013.

[57] Z. Li, Z. Wu, Z. Li, and Z. Ding, "Distributed optimal coordination for heterogeneous linear multiagent systems with event-triggered mech-

anisms," *IEEE Transactions on Automatic Control*, vol. 65, no. 4, pp. 1763–1770, 2019.

[58] J. Yang, F. Xiao, and J. Ma, "Model-based edge-event-triggered containment control under directed topologies," *IEEE Transactions on Cybernetics*, vol. 49, no. 7, pp. 2556–2567, 2018.

[59] F. Xiao, T. Chen, and H. Gao, "Synchronous hybrid event-and time-driven consensus in multiagent networks with time delays," *IEEE Transactions on Cybernetics*, vol. 46, no. 5, pp. 1165–1174, 2015.

[60] ——, "Consensus in time-delayed multi-agent systems with quantized dwell times," *Systems & Control Letters*, vol. 104, pp. 59–65, 2017.

[61] M. Abdelrahim, R. Postoyan, J. Daafouz, and D. Nesic, "Stabilization of nonlinear systems using event-triggered output feedback controllers," *IEEE Transactions on Automatic Control*, vol. 61, no. 9, pp. 2682–2687, 2015.

[62] V. Dolk, D. P. Borgers, and W. Heemels, "Dynamic event-triggered control: Tradeoffs between transmission intervals and performance," in *53rd Conference on Decision and Control*, 2014, pp. 2764–2769.

[63] D. P. Borgers, V. Dolk, and W. Heemels, "Riccati-based design of event-triggered controllers for linear systems with delays," *IEEE Transactions on Automatic Control*, vol. 63, no. 1, pp. 174–188, 2017.

[64] H. Yu and F. Hao, "Input-to-state stability of integral-based event-triggered control for linear plants," *Automatica*, vol. 85, pp. 248–255, 2017.

[65] T. Liu, P. Zhang, and Z.-P. Jiang, "Event-triggered input-to-state stabilization of nonlinear systems subject to disturbances and dynamic uncertainties," *Automatica*, vol. 108, p. Artical 108488, 2019.

[66] J. Yang, F. Xiao, and T. Chen, "Event-triggered formation tracking control of nonholonomic mobile robots without velocity measurements," *Automatica*, vol. 112, p. Artical 108671, 2020.

[67] X. Yu, L. Liu, and G. Feng, "Distributed circular formation control of nonholonomic vehicles without direct distance measurements," *IEEE Transactions on Automatic Control*, vol. 63, no. 8, pp. 2730–2737, 2018.

[68] C. Sun, Z. Feng, and G. Hu, "Time-varying optimization-based approach for distributed formation of uncertain Euler-Lagrange systems," *IEEE Transactions on Cybernetics*, 2021, doi=10.1109/TCYB.2021.3055206.

[69] T. Lee, M. Leok, and N. H. McClamroch, "Geometric tracking control of a quadrotor UAV on SE (3)," in *49th IEEE Conference on Decision and Control*, 2010, pp. 5420–5425.

[70] H. A. Hashim, L. J. Brown, and K. McIsaac, "Nonlinear stochastic position and attitude filter on the special Euclidean group SE(3)," *Journal of the Franklin Institute*, vol. 356, no. 7, pp. 4144–4173, 2019.

[71] A. Khosravian, J. Trumpf, R. Mahony, and T. Hamel, "State estimation for invariant systems on Lie groups with delayed output measurements," *Automatica*, vol. 68, pp. 254–265, 2016.

[72] Z. Lin, L. Wang, Z. Han, and M. Fu, "Distributed formation control of multi-agent systems using complex Laplacian," *IEEE Transactions on Automatic Control*, vol. 59, no. 7, pp. 1765–1777, 2014.

[73] R. Connelly, "Generic global rigidity," *Discrete & Computational Geometry*, vol. 33, no. 4, pp. 549–563, 2005.

[74] N. J. Higham and F. Tisseur, "Bounds for eigenvalues of matrix polynomials," *Linear Algebra and its applications*, vol. 358, no. 1-3, pp. 5–22, 2003.

[75] Y. Xu, S. Zhao, D. Luo, and Y. You, "Affine formation maneuver control of multi-agent systems with directed interaction graphs," in *37th Chinese Control Conference*, 2018, pp. 4563–4568.

[76] L. Chen, J. Mei, C. Li, and G. Ma, "Distributed leader–follower affine formation maneuver control for high-order multiagent systems," *IEEE Transactions on Automatic Control*, vol. 65, no. 11, pp. 4941–4948, 2020.

[77] Y. Xu, S. Zhao, D. Luo, and Y. You, "Affine formation maneuver control of high-order multi-agent systems over directed networks," *Automatica*, vol. 118, p. Artical 109004, 2020.

[78] S. R. G. Goebel, Rafal and A. R. Teel, "Hybrid dynamical systems," *IEEE Control Systems Magazine*, vol. 29, no. 2, pp. 28–93, 2009.

[79] D. Liuzza, D. V. Dimarogonas, M. Di Bernardo, and K. H. Johansson, "Distributed model based event-triggered control for synchronization of multi-agent systems," *Automatica*, vol. 73, pp. 1–7, 2016.

[80] I. Sarras, J. Marzat, S. Bertrand, and H. Piet-Lahanier, "Collaborative multiple micro air vehicles localization and target tracking in GPS-denied environment from range–velocity measurements," *International Journal of Micro Air Vehicles*, vol. 10, no. 2, pp. 225–239, 2018.

[81] Z. Han, K. Guo, L. Xie, and Z. Lin, "Integrated relative localization and leader–follower formation control," *IEEE Transactions on Automatic Control*, vol. 64, no. 1, pp. 20–34, 2018.

[82] W. Wang, R. Postoyan, D. Nesic, and W. Heemels, "Periodic event-triggered control for nonlinear networked control systems," *IEEE Transactions on Automatic Control*, vol. 65, no. 2, pp. 620–635, 2019.

[83] A. Chaillet, D. Angeli, and H. Ito, "Combining iISS and ISS with respect to small inputs: the strong iISS property," *IEEE Transactions on Automatic Control*, vol. 59, no. 9, pp. 2518–2524, 2014.

[84] C. Cai and A. R. Teel, "Characterizations of input-to-state stability for hybrid systems," *Systems & Control Letters*, vol. 58, no. 1, pp. 47–53, 2009.

[85] L. A. Montestruque and P. J. Antsaklis, "On the model-based control of networked systems," *Automatica*, vol. 39, no. 10, pp. 1837–1843, 2003.

[86] J. Huang, C. Wen, W. Wang, and Z.-P. Jiang, "Adaptive output feedback tracking control of a nonholonomic mobile robot," *Automatica*, vol. 50, no. 3, pp. 821–831, 2014.

[87] D. Carnevale, A. R. Teel, and D. Nesic, "A Lyapunov proof of an improved maximum allowable transfer interval for networked control systems," *IEEE Transactions on Automatic Control*, vol. 52, no. 5, pp. 892–897, 2007.

[88] D. Angeli, E. D. Sontag, and Y. Wang, "A characterization of integral input-to-state stability," *IEEE Transactions on Automatic Control*, vol. 45, no. 6, pp. 1082–1097, 2000.

[89] J. P. Desai, J. P. Ostrowski, and V. Kumar, "Modeling and control of formations of nonholonomic mobile robots," *IEEE Transactions on Robotics and Automation*, vol. 17, no. 6, pp. 905–908, 2001.

[90] J. Alonso-Mora, E. Montijano, M. Schwager, and D. Rus, "Distributed multi-robot formation control among obstacles: A geometric and optimization approach with consensus," in *IEEE International Conference on Robotics and Automation*, 2016, pp. 5356–5363.

[91] G. Qu and N. Li, "Harnessing smoothness to accelerate distributed optimization," *IEEE Transactions on Control of Network Systems*, vol. 5, no. 3, pp. 1245–1260, 2017.

[92] W. Chen and W. Ren, "Event-triggered zero-gradient-sum distributed

consensus optimization over directed networks," *Automatica*, vol. 65, pp. 90–97, 2016.

Appendix A

Proofs of Theorems

A.1 Proof of Theorem 8

Step 1: Convergence of subsystem $\mathcal{S}_\eta$.

According to (4.6), the hybrid system model of $\mathcal{S}_\eta$ can be represented as in (4.33)–(4.34) with state vector ξ_η, disturbances $\varsigma_1 = \varsigma_\eta = [0, \dot{\omega}_0]^T$, $\varsigma_2 = \varsigma_s = 0$. Introduce auxiliary variable ϕ_η as in (4.35). Since A_η is Hurwitz, the positive definite matrices P_η, Q_η satisfying (4.38) always exist for a small enough ϵ_η. Then, the MASP can be calculated by Lemma 10. Consider Lyapunov candidate $U_\eta(\xi_{\eta_i}) = \eta_i^T P_\eta \eta_i + l_\eta \phi_\eta S_{\eta_i}^2$, on flow domain, we have

$$\langle \nabla U_\eta(\xi_{\eta_i}) \rangle \leq \frac{1}{\epsilon_\eta} \tilde{\xi}_{\eta_i}^T \begin{bmatrix} -Q_\eta + \left[\begin{smallmatrix} 0 & 0 \\ 0 & \epsilon_\eta \end{smallmatrix}\right] & P_\eta B_\eta \\ * & -l_\eta^2 \alpha_\eta^s \end{bmatrix} \tilde{\xi}_{\eta_i} + 2\eta_i^T P_\eta \left[\begin{smallmatrix} c0 \\ \dot{\omega}_0 \end{smallmatrix}\right]. \tag{A.1}$$

By the LMI in (4.38), we have $\langle \nabla U_\eta(\xi_{\eta_i}), F(\xi_{\eta_i}, \varsigma_\eta) \rangle \leq -\frac{\alpha_\eta}{\epsilon_\eta} \|\tilde{\xi}_{\eta_i}\|^2 + 2\bar{\alpha}_\eta \|\dot{\omega}_0\| \|\eta_i\|$. On jump domain, $U_\eta(\xi_{\eta_i})^+ \leq U_\eta(\xi_{\eta_i})$. Then, Condition 4 is satisfied with

- $\underline{\alpha}_\eta \|\tilde{\xi}_{\eta_i}\|^2 \leq U_\eta(\xi_{\eta_i}) \leq \bar{\alpha}_\eta \|\tilde{\xi}_{\eta_i}\|^2$
- $\langle \nabla U_\eta(\xi_{\eta_i}), F(\xi_{\eta_i}, \varsigma_\eta) \rangle \leq -\frac{1}{\epsilon_\eta} \frac{\alpha_\eta \underline{\alpha}_\eta}{\bar{\alpha}_\eta} U_\eta + 2\bar{a}_\omega \frac{\bar{\alpha}_\eta}{\sqrt{\underline{\alpha}_\eta}} \sqrt{U_\eta}, \quad \xi_{\eta_i} \in C$
- $U_\eta(\xi_{\eta_i})^+ \leq U_\eta(\xi_{\eta_i}), \quad \xi_{\eta_i} \in D$

By Lemma 11, the convergence error and convergence time can be calculated as $r_\omega = \frac{4\epsilon_\eta \bar{\alpha}_\eta^2}{\alpha_\eta^s \underline{\alpha}_\eta^{1.5}} a_\omega$ and $T_\omega = \frac{2\epsilon_\eta}{\alpha_\eta} \ln \frac{U_\eta(\xi_\eta(0,0))}{r_\omega^2}$, respectively.

Step 2: Convergence of subsystem $\mathcal{S}_\chi$.

According to (4.8), the hybrid system model of subsystem $\mathcal{S}_\chi$ can be represented as in (4.33)–(4.34) with state vector ξ_χ and disturbances $\varsigma_1 = \varsigma^i_{\chi 1}$, $\varsigma_2 = \varsigma^i_{\chi 2}$, $\varsigma_s = \varsigma^i_s$. Introduce auxiliary variable ϕ_χ as in (4.35). Since A_χ is Hurwitz, the positive definite matrices P_χ and Q_χ satisfying (4.38) always exist for a small enough ϵ_χ and the MASP can be calculated by (4.36). Consider a Lyapunov candidate $U_\chi(\xi_{\chi i}) = {\chi_i}^T P_\chi \chi_i + l_\chi \phi_\chi S^2_{\chi_i}$, on flow domain, we have

$$\begin{aligned}\langle \nabla U(\xi_{\chi_i}), F(\xi_{\chi_i}, \varsigma_{\chi_i})\rangle \leq & \frac{1}{\epsilon_\chi}\tilde{\xi}^T_{\chi i}\begin{bmatrix} -Q_\chi + \left[\begin{smallmatrix} 0 & 0 \\ 0 & \epsilon_\chi \end{smallmatrix}\right] & P_\chi B_\chi \\ * & -l^2_\chi \alpha^s_\chi I \end{bmatrix}\tilde{\xi}_{\chi i} \\ & + 2\frac{\chi_i^T P_\chi}{\epsilon_\chi}\varsigma^i_{\chi 2} + 2\chi_i^T P_\chi \varsigma^i_{\chi 1} + 2 l_\chi \phi_\chi S_\chi \varsigma^i_s.\end{aligned} \tag{A.2}$$

Referring to (4.8), the disturbances $\varsigma^i_{\chi 2}$ and ς^i_s involve the convergence error $\Delta\omega_i$, formation error δ_i, sampling error S_{η_i} and control input u_i. Since the control input is saturated by (4.11) and $\mathbb{V}_i$ is an open set, if $\delta_i(0) \in \mathbb{V}_i$, there exists a $(T_c, j_c) \neq (0,0)$ such that for all $(t,j) \in \mathbb{T}_m = \{(t,j) | t \in [t_j, t_{j+1}), j = 0, \cdots, j_c - 1\}$, $\xi_{m_i}(t,j) \in \mathbb{X}_i$, where $\mathbb{X}_i = \{\xi_{m_i} | \delta_i \in \mathbb{V}_i\}$. By the convergence property in Step 1, for a small enough ϵ_η, we have $T_\omega < T_c$. Then for $(t,j) \in \mathbb{T}_m \cap \mathbb{T}_\omega$, where $\mathbb{T}_\omega = \{(t,j) | t \in [t_k, t_{k+1}), t_k \geq T_\omega\}$, we have

$$\|\varsigma^i_{\chi 2}\| \leq r_\eta (c + \frac{U_i}{\sqrt{1 + \bar{d}^2_{i0}}} \max(1, \bar{d}_{i0})) = c^i_{\chi 2}$$

and

$$\|\varsigma^i_s\| \leq \frac{U_i}{\sqrt{1 + \bar{d}^2_{i0}}} \max(1, \bar{d}_{i0}) + c r_\eta = c^i_S.$$

Combining with the LMI in (4.38), we have

$$\left\langle \nabla U(\xi_{\chi_i}), F(\tilde{\xi}_{\chi_i}, \varsigma_{\chi_i}) \right\rangle \leq -\frac{\alpha_\chi}{\epsilon_\chi}\|\chi_i^T, S^T_{\chi_i}\|^2 + 2\bar{\alpha}_\chi (\frac{1}{\epsilon_\chi} c^i_{\chi 2} + c^i_{\chi 1})\|\chi_i\| + 2\bar{\alpha}_\chi c^i_S \|S_{\chi_i}\|.$$

On jump domain, $U_\chi(\xi_{\chi_i})^+ \leq U_\chi(\xi_{\chi_i})$. Then, Condition 4 is satisfied with

- $\underline{\alpha}_\chi \|\tilde{\xi}_{\chi_i}\|^2 \leq U(\xi_{\chi_i}) \leq \bar{\alpha}_\chi \|\tilde{\xi}_{\chi_i}\|^2$
- $\langle \nabla U_\eta(\xi_{\chi_i}), F(\xi_{\chi_i}, \varsigma_\chi)\rangle \leq -\frac{1}{\epsilon_\chi}\frac{\alpha_\chi \underline{\alpha}_\chi}{\bar{\alpha}_\chi} U_\chi + 2\frac{\bar{\alpha}_\chi}{\sqrt{\underline{\alpha}_\chi}}(\max\{c^i_{\chi 1}, c^i_S\} + \frac{1}{\epsilon_\chi} c^i_{\chi 2})\sqrt{U_\chi}$, $\xi_{\chi_i} \in C$
- $U^+_\chi(\xi_{\chi_i}) \leq U_\chi(\xi_{\chi_i}), \quad \xi_{\chi_i} \in D$

According to Lemma 11, the convergence error and convergence time can be calculated by $r_v = \frac{4\epsilon_\chi \bar{\alpha}_\chi^2}{\alpha_\chi \underline{\alpha}_\chi^2}(\max\{c_{\chi 1}^i, c_S^i\} + \frac{c_{\chi 2}^i}{\epsilon_\chi})$ and $T_v = \frac{2\epsilon_\chi}{\alpha_\chi} \ln \frac{U_\chi(\xi_\chi(0,0))}{r_v^2}$. By a small enough ϵ_χ, we have $T_v < T_c$. Furthermore, since at each detection instant, the agent collects all the relative information from its neighbors, the MASP of agent i is given as $\tau_{masp}^i = \min\{\tau_{masp}^{\eta_i}, \tau_{masp}^{\chi_i}\}$.

A.2 Proof of Theorem 9

According to (4.13), the hybrid model of subsystem $\mathcal{S}_m$ can be represented in the form of (4.40)–(4.41) with state vector ξ_m. Let $W_i^e = \|e_{u_i}\|$, $V_x = V_{\delta_i} = \delta_i^T \delta_i$, $\Psi_i = \Psi_{u_i}$ with $\Psi_{u_i} = \psi_u \delta_i^T \delta_i$. By (4.13), there always exists an $H_i^e(\tilde{\xi}_{m_i}, \tilde{\xi}_h, \varsigma)$ such that $\dot{W}_i^e \leq H_i^e(\tilde{\xi}_{m_i}, \tilde{\xi}_h, \varsigma)$. Let

$$J_i(\tilde{\xi}_{m_i}, \tilde{\xi}_h, \varsigma) = \dot{\Psi}_{u_i} - L_u \Psi_{u_i} - H_i^e + \epsilon_\Psi \delta_i^2.$$

According to Theorem 8, for $(t,j) \in \mathbb{T}_m$, $\xi_{m_i}(t,j) \in \mathbb{X}_i$; for $(t,j) \in \mathbb{T}_1 = \mathbb{T}_m \cap \mathbb{T}_\omega \cap \mathbb{T}_v$, $\|\tilde{\xi}_{\eta_i}\| \leq r_\omega$ and $\|\tilde{\xi}_{\chi_i}\| \leq r_v$. Assume Δ_u in (4.11) satisfies $\Delta_u \geq \sqrt{2(d_{i0}^2+1)} r_v$, and there is no input saturation during $\mathbb{T}_1$. Then, combining with (4.46), the following inequalities can be established with $\sigma_v(\xi_h) = (1+\psi_u)\epsilon_2^2 \|\Delta v_i\|^2$:

$$\begin{aligned}
\dot{V}_{\delta_i} \leq & -a_\delta \|\delta_i\|^2 - a_e \|e_i\|^2 + \sigma_v(\xi_h, \varsigma) + l_u \|e_{u_i}\|^2 - H_i^e(\tilde{\xi}_{m_i}, \xi_h, \varsigma) \\
& - J_i(\tilde{\xi}_{m_i}, \xi_h, \varsigma) - \Psi_{u_i}(\delta_i), \qquad \text{(A.3)} \\
\dot{\Psi}_{u_i} \leq & L_u \Psi_{u_i}(\delta_i) + H_i^e(\tilde{\xi}_{m_i}, \xi_h, \varsigma) + J_i(\tilde{\xi}_{m_i}, \xi_h, \varsigma).
\end{aligned}$$

Then, Conditions 5 and 6 are satisfied during $(t,j) \in \mathbb{T}_1$. Consider Lyapunov candidate

$$U(\xi_{m_i}) = \delta_i^T \delta_i + \max\{l_u \phi_u e_{u_i}^2, \lambda_u \psi_u \delta_i^2\},$$

if $\tau_{macp}^i < \frac{1}{l_u} \arctan \frac{\bar{\rho}_i^u - \underline{\rho}_i^u}{2}$, on flow domain,

$$\left\langle \nabla U(\xi_{m_i}), F(\tilde{\xi}_{m_i}, \xi_h, \varsigma) \right\rangle \leq -\alpha_\delta \|\delta_i\|^2 - \alpha_e \|e_i\|^2 + (1+\psi_u)\epsilon_2^2 r_v^2, \qquad \text{(A.4)}$$

during $(t,j) \in \mathbb{T}_1$. Let $c_{\delta_1} = \sqrt{(1+\psi_u)}\epsilon_2 r_v$, and $c_{\delta_1} < \min\{\sqrt{\alpha_\delta}, \sqrt{\alpha_e}\} \sqrt{\frac{\underline{\alpha}_u}{\bar{\alpha}_u}} c_\delta$, which can always be satisfied with a small enough ϵ_χ. In addition, let $\mathbb{X}_{i_1} =$

$\{\xi_{m_i}|U(\xi_{m_i}) \leq \underline{\alpha}_u c_\delta^2\}$, and $\mathbb{X}_{i_2} = \{\xi_{m_i}|\xi_{m_i} \in \mathbb{X}_i, \xi_{m_i} \notin \mathbb{X}_{i_1}\}$. Then, $\mathbb{X}_i = \mathbb{X}_{i_1} \cup \mathbb{X}_{i_2}$ and $\mathbb{X}_{i_1} \cap \mathbb{X}_{i_2} = \emptyset$. When $\xi_{m_i} \in \mathbb{X}_{i_1}$, according to (A.4), $U(\xi_{m_i})$ might increase. Since the control input is bounded, ξ_{m_i} will enter $\mathbb{X}_{i_2}$ before it exceeds $\mathbb{X}_i$. When $\xi_{m_i} \in \mathbb{X}_{i_2}$, $U(\xi_{m_i})$ decrease, ξ_{m_i} never exceeds $\mathbb{X}_{i_1}$ for all $(t, j) \in$dom ξ_{m_i}. On jump domain, $U^+(\xi_{m_i}) \leq U(\xi_{m_i})$. As a result, $\mathbb{X}_{i_1}$ is an invariant set. Furthermore, $U(\xi_{m_i})$ decreases when ξ_{m_i} reaches the boundary of $\mathbb{X}_{i_1}$. Therefore, the steady state error of $\|\tilde{\xi}_{m_i}\|$ can be calculated by $r_\delta = \sqrt{\frac{\bar{\alpha}_u}{\underline{\alpha}_u}} c_\delta$.

A.3 Proof of Theorem 10

According to (4.15), the dynamics of subsystem $\mathcal{S}_\pi$ can be written in the form of (4.40)–(4.41) with $\xi = \xi_\pi$. By (iii) in Theorem 10, the MACP for h_{π_i} is upper bounded by $\tau_{macp}^{\pi_i} < \frac{1}{l_{\pi_i}} \arctan \frac{\bar{\rho}_i^\pi - \underline{\rho}_i^\pi}{2}$. Let $\Psi_{\pi_i} = \psi_{\pi_i} q_{\pi_i}^2$, $W_{\pi_i}^e = \|e_{\pi_i}\|$, and $V_\pi = \Delta\pi_f^T P_\pi \Delta\pi_f$ be the storage function. By (4.15), on flow domain, we have

$$\begin{aligned}
\dot{V}_\pi =& - c_\omega \Big(\Delta\pi_f^T (P_\pi L_{ff} + L_{ff}^T P_\pi) \Delta\pi_f + 2\Delta\pi_f^T P_\pi (L_{ff} e_{\pi_f} + L_{fl} e_{\pi_m} + L_{fl} \Delta\pi_m) \Big) \\
& - 2\Delta\pi_f^T P_\pi \mathbf{1}_n \dot{\pi}_0 \\
\leq & [\Delta\pi_f^T, e_{\pi_f}^T] A_\pi \begin{bmatrix} \Delta\pi_f \\ e_{\pi_f} \end{bmatrix} + \frac{c_\pi}{\epsilon_\pi^2} \sigma_M^2(L_{fl}) (\|e_{\pi_m}\| + \|\Delta\pi_m\|)^2 + \frac{1}{\epsilon_{\pi_0}^2} n_f^2 \|a_\pi\|^2.
\end{aligned}$$

In addition, let $\Psi_\pi = \sum_{i \in \mathcal{N}_f} \Psi_{\pi_i}$, we have

$$\begin{aligned}
\dot{\Psi}_\pi \leq & [\Delta\pi_f^T \ e_{\pi_f}^T] A_\pi^\psi \begin{bmatrix} \Delta\pi_f \\ e_{\pi_f} \end{bmatrix} + \frac{2c_\pi}{\epsilon_{\pi_1}^2} (\sigma_M(\psi_\pi D_f L_{fl})^2 (\|e_{\pi_m}\| + \|\Delta\pi_m\|)^2 \\
& + \frac{2}{\epsilon_{\pi_2}^2} (\sigma_M(\psi_\pi (L_{ff} - D_{fl})) n_f a_\pi)^2.
\end{aligned} \tag{A.5}$$

By (4.15), there always exists an H_{π_i} such that $\dot{W}_{\pi_i}^e < H_{\pi_i}$. Let $J_i = \dot{\Psi}_{\pi_i} - L_{\pi_i} \Psi_{\pi_i} - H_{\pi_i}^2 + \epsilon_{\pi_e} \Delta\pi_i^2$. Combining with the LMI in (4.47), Conditions 5 and 6 are satisfied with $\alpha_W = \alpha_{W_\pi}$, $\alpha_V = \alpha_{V_\pi}$, which lead to the conclusion that the set $\Xi_\pi := \{\xi \in \mathbb{X} | \|\tilde{\xi}_\pi\| = 0\}$ is ISS w.r.t. ς and ξ_h.

A.4 Proof of Theorem 11

According to (4.18), subsystem $\mathcal{S}_\gamma$ can be represented in the form of (4.40)–(4.41). Introduce auxiliary variables ϕ_{γ_i} and $\phi^s_{\gamma_i}$ as in (4.43), then, the MACP and MASP can be calculated by $\tau^{\gamma_i}_{macp} \leq \frac{1}{l_{\gamma_i}} \arctan \frac{\bar{\rho}^\gamma_i - \underline{\rho}^\gamma_i}{2}$, $\tau^{\gamma_i}_{masp} \leq \frac{1}{l^s_{\gamma_i}} \arctan \frac{\bar{\rho}_i - \underline{\rho}_i}{1+\bar{\rho}_i \underline{\rho}_i}$. In addition, let $W^e_i = a\|e_{\gamma_i}\| + b\|e_{\omega_i}\|$, $\Psi_i = \Psi_{\gamma_i} = \psi_{\gamma_i} q^2_{\gamma_i}$, $W^s_i = \|S_{\gamma_i}\|$ and $V_x = aV_\gamma + bV_\omega, V_\gamma = \Delta\gamma_f{}^T P_\gamma \Delta\gamma_f$. By (4.18), there always exists $H^e_{\gamma_i}$, such that $W^e_i \leq H^e_{\gamma_i}$. Let

$$J_i = J_{\gamma_i} := \dot{\Psi}_{\gamma_i} - L_{\gamma_i}\Psi_{\gamma_i} - H^{e\,2}_{\gamma_i} + \epsilon_{\gamma_2}\Delta\gamma^2_i.$$

Combining with the LMI in (4.48), Conditions 5 and 6 can be checked with
$\sigma_\gamma(\varsigma, \xi_h) = b(\sigma_v + \sigma_{v_0}) + a\beta^m_\gamma e^2_{\gamma_m}$, $\beta^m_\gamma = 2\frac{c_\gamma}{\epsilon^2_\gamma}\sigma^2_M(L_{fl})$,
$\sigma_v = \left(\frac{c_\pi}{\epsilon^2_\pi}\sigma^2_M(L_{fl}) + \frac{2c_\pi}{\epsilon^2_{\pi_1}}\sigma^2_M(\psi_\pi D_f L_{fl})\right)(\|e_{v_m}\| + \|\Delta v_m\|)^2$,
$\sigma_{v_0} = \left(\frac{1}{\epsilon^2_{\pi_0}} + \frac{2}{\epsilon^2_{\pi_2}}\sigma^2_M(\psi_\pi(L_{ff} - D_{fl}))\right) n^2_f \|a_v\|^2$.

A.5 Proof of Theorem 12

Due to the dependency of the conditions in Theorems 8 and 9, the stability in this theorem can be only ensured in a local sense.

Step 1: The set $\Xi_b = \{\xi \in \mathbb{X} | \|\tilde{\xi}^T_b\| = 0\}$ is ISS w.r.t. $\tilde{\xi}_a$ and ς

According to (4.23) and (4.24), the hybrid system model of subsystem $\mathcal{S}_b$ can be written in the form of (4.49)–(4.50) with state vector ξ_δ shown in Table 4.7. Introduce auxiliary variables ϕ_{π_i} and $\phi^s_{\delta_i}$ satisfying (4.43), then, the MACP and MASP can be calculated by $\tau^{\pi_i}_{macp} \leq \frac{1}{l_{\pi_i}} \arctan \frac{\bar{\rho}^\pi_i - \underline{\rho}^\pi_i}{2}$, $\tau^{\delta_i}_{masp} \leq \frac{1}{l^s_{\delta_i}} \arctan \frac{\bar{\rho}_i - \underline{\rho}_i}{1+\bar{\rho}_i \underline{\rho}_i}$. Let $W^e_{\pi_i} = \|e_{\pi_i}\|$, $W^s_{\delta_i} = \|S_{\delta_i}\|$, $\Psi_{\pi_i} = \psi_{\pi_i} q^2_{\pi_i}$, $V_{\delta_f} = \delta^T_f \delta_f + \Delta\delta^T_f \Delta\delta_f$ and consider Lyapunov candidate

$$U_{\delta_f} = V_{\delta_f} + \sum_{i \in \mathcal{N}_f} \left(l^s_{\delta_i} \phi^s_{\delta_i} W^{s\,2}_{\delta_i} + \max\left\{ l_{\delta_i} \phi_{\delta_i} W^{e\,2}_{\delta_i} \right\} + \max\left\{ l_{u_i} \phi_{u_i} W^{e\,2}_{u_i} \right\} \right).$$

Then, we have $U_{\delta_f} = \tilde{\xi}^T_{\delta_f} P_f \tilde{\xi}_{\delta_f}$. In addition, by (4.23) and (4.24), there always exists an $H^e_{\pi_i}$ such that $\dot{W}^e_{\pi_i} \leq H^e_{\pi_i}$. Let $J_{\pi_i} = \dot{\Psi}_{\pi_i} - L_\pi \Psi_{\pi_i} - H^{e\,2}_{\pi_i} + \epsilon_{\pi_e} \pi^2_i$. Since $\mathcal{S}_h$ converges to r_v and r_ω in a finite time, combining item (i) with the

matrix in (4.65), Conditions 5 and Condition 6 are satisfied with $\sigma_\delta = \beta_V(\delta_f, \Delta\delta_f, e_{\delta_f}, e_{u_f}, S_{\delta_f})\sigma_{V_\delta} + \sigma_{V_0} + \sigma_{V_f}$, where

$$\begin{aligned}
\beta_V\sigma_{V_\delta} \leq & \tilde{\xi}_{\delta_f}^T \left(\|\tilde{\xi}_\omega\| Q_0^\omega + \|\tilde{\xi}_\omega\|^2 Q_1^\omega + \|\tilde{\xi}_\gamma\| Q_0^\gamma + \|\tilde{\xi}_\gamma\|^2 Q_1^\gamma + \|\tilde{\xi}_\gamma\|^4 Q_2^\gamma \right) \tilde{\xi}_{\delta_f}, \\
\sigma_{V_0} \leq & \alpha_1^\omega \|\tilde{\xi}_\omega\|^2 + \alpha_2^\omega \|\tilde{\xi}_\omega\|^4 + \alpha_1^v \|\tilde{\xi}_v\|^2 + \alpha_2^v \|\tilde{\xi}_v\|^4 + \alpha_1^\gamma \|\tilde{\xi}_\gamma\|^2 + \alpha_2^\gamma \|\tilde{\xi}_\gamma\|^4 \\
& + \alpha_4^\gamma \|\tilde{\xi}_\gamma\|^8 + \alpha_1^m \|\tilde{\xi}_{\delta_m}\|^2 + \alpha_2^m \|\tilde{\xi}_{\delta_m}\|^4, \\
\sigma_{V_f} \leq & \, r_v^2 c_\delta^2 \sigma^2(L_{fl})(\epsilon_6^2(1+\psi_M^2) + \epsilon_7^2\psi_M^2) + 13\left(\epsilon_m^2 {r_m}^2 + \omega_M^2 \sigma^2(A_{nl}) r_v^2\right),
\end{aligned} \tag{A.6}$$

and ψ_M represents the maximum value of matrix $\bar{\psi}$. Then, when $\xi \in C$, $\left\langle \nabla U_{\delta_f}, F(\xi_{\delta_f}, \tilde{\xi}_a, \tilde{\xi}_h, \varsigma) \right\rangle \leq -\tilde{\xi}_{\delta_f}^T A_\delta \tilde{\xi}_{\delta_f} + \sigma_\delta$; and when $\xi \in D$, $U_{\delta_f}^+ - U_{\delta_f} \leq 0$. By using the standard Lyapunov arguments, the set Ξ_b is ISS w.r.t. $\tilde{\xi}_a$ and ς.

Step 2: The set $\Xi = \{\xi \in \mathbb{X} | \|\tilde{\xi}^T\| = 0\}$ is strongly iISS w.r.t. ς

Let

$$U_m = V_m + \sum_{i \in \mathcal{N}_m} \max\{l_{u_i} \phi_{u_i} {W_{u_i}^e}^2, \lambda_{u_i} \psi_{u_i}\},$$

$$U_\pi = V_\pi + \sum_{i \in \mathcal{N}_f} \max\{l_{\pi_i} \phi_{\pi_i} {W_{\pi_i}^e}^2, \lambda_{\pi_i} \psi_{\pi_i}\}, \ \pi = v, \omega,$$

and

$$U_\gamma = V_\gamma + \sum_{i \in \mathcal{N}_f} (l_{\gamma_i}^s \phi_{\gamma_i}^s {W_s^{\gamma_i}}^2 + \max\{l_{\gamma_i} \phi_{\gamma_i} {W_{\gamma_i}^e}^2, \lambda_{\gamma_i} \psi_{\gamma_i}\}).$$

According to Theorems 9–11, the first item in Condition 7 is satisfied. By step 1, the second term is satisfied and the third term can be established by

$$\begin{cases}
\left\langle \nabla U_\gamma(\xi_\gamma), F_{\gamma_f}(\tilde{\xi}_{\gamma_f}, \tilde{\xi}_h, \varsigma), F_\omega(\tilde{\xi}_\omega, \tilde{\xi}_h, \varsigma) \right\rangle \leq -\tilde{\xi}_\gamma^T Q_\gamma \tilde{\xi}_\gamma + \sigma_\gamma(\varsigma_\gamma); \ \xi_\gamma \in \ C_\gamma; \\
U_\gamma(\tilde{\xi}_\gamma)^+ \leq U_\gamma(\tilde{\xi}_\gamma), \ \xi_\gamma \in D_\gamma, \\
\left\langle \nabla U_m(\xi_m), F_m(\tilde{\xi}_m, \tilde{\xi}_h, \varsigma) \right\rangle \leq -\tilde{\xi}_{\delta_m}^T Q_m \tilde{\xi}_{\delta_m} + \sigma_m(\varsigma_{\delta_m}), \ \xi_m \in \cap_{i \in \mathcal{N}_m} C_{u_i}; \\
U_m^+(\xi_{\delta_m}) \leq U_{\delta_m}, \ \xi_m \in \cup_{i \in \mathcal{N}_m} D_{u_i}, \\
\left\langle \nabla U_\omega(\xi_\omega), F_\omega(\tilde{\xi}_\omega, \tilde{\xi}_h, \varsigma) \right\rangle \leq -\tilde{\xi}_\omega^T Q_\omega \tilde{\xi}_\omega + \sigma_\omega(\varsigma_\omega), \ \xi_\omega \in C_\omega; \\
U_\omega^+(\xi_\omega) \leq U_\omega, \ \xi_\omega \in D_\omega, \\
\left\langle \nabla U_v(\xi_v), F_v(\tilde{\xi}_v, \tilde{\xi}_h, \varsigma) \right\rangle \leq -\tilde{\xi}_v^T Q_v \tilde{\xi}_v + \sigma_v(\varsigma_v), \ \xi_v \in C_v; \\
U_v^+(\xi_v) \leq U_v, \ \xi_v \in D_v,
\end{cases} \tag{A.7}$$

where $\sigma_M = (1+\psi_u)\epsilon_2^2 r_v^2$, $\sigma_V = \left(\frac{c_\pi}{\epsilon_\pi^2}\sigma_M^2(L_{fl}) + \frac{2c_\pi}{\epsilon_{\pi_1}^2}\sigma_M^2(\psi_\pi D_f L_{fl})\right)(r_m + r_v)^2 + \sigma_{v_0}$, $\sigma_\Omega = \left(\frac{c_\omega}{\epsilon_\omega^2}\sigma_M^2(L_{fl}) + \frac{2c_\omega}{\epsilon_{\omega_1}^2}\sigma_M^2(\psi_\omega D_f L_{fl})\right)(r_m + r_\omega)^2 + \sigma_{\omega_0}$, $\sigma_\Gamma = b(\sigma_V + \sigma_{v_0}) + a\beta_\gamma^m r_m^2$. Furthermore, the last item can be checked by the inequalities in (4.66). Then, strongly iISS of set $\Xi_\delta = \{\xi \in \mathbb{X} | \|[\tilde{\xi}_a^T, \tilde{\xi}_b^T]^T\| = 0\}$ w.r.t. ς, $\tilde{\xi}_h$ can be proved. Finally, by Theorem 8, since $\tilde{\xi}_h$ converges to a small ball with a radius related to ς in a finite time, we have that $\Xi = \{\xi \in \mathbb{X} | \|\tilde{\xi}^T\| = 0\}$ is locally strongly iISS w.r.t. ς.

Step 3: Determine the threshold R of disturbances.

Consider Lyapunov candidate

$$U(\xi_a, \xi_b) = \ln U(\xi_b) + \sum_{\pi=\omega,v,m} \Big(\sum_{k_\pi=1,2} U^{k_\pi}(\xi_\pi) \Big) + \sum_{k_\gamma=1,2,4} U^{k_\gamma}(\xi_\gamma).$$

According to step 1, $\lambda_F = \min\{\lambda \in \mathbb{R} | \det(A_\delta - \lambda \bar{P}_f) = 0\}$ and

$$\bar{P}_f = \begin{bmatrix} I & 0 & 0 & 0 \\ 0 & l_e\bar{\rho}_e & 0 & 0 \\ 0 & 0 & l_u\bar{\rho}_u & 0 \\ 0 & 0 & 0 & l_\delta^s\bar{\rho}_s \end{bmatrix},$$

where $\bar{\rho}_\pi$ represents the diagonal matrix with the i-th element being $\bar{\rho}_i^\pi$ for $\pi = e, u$, and $\bar{\rho}_i$ for $\pi = s$. The disturbances in the closed-loop system are introduced by the dynamics of the leader and the constant r_m related to the MATPs. On flow domain, the disturbances have an influence on the differential equation $\langle \nabla U(\xi_a, \xi_b) \rangle$ by σ_f, where

$$\sigma_f = \sigma_{V_f} + \sum_{(\Pi,\pi)=(\Omega,\omega),(V,v),(M,m),(\Gamma,\gamma)} (\sigma_\Pi + \frac{1}{\epsilon_{\pi_{21}}^2}\sigma_\Pi) + \frac{1}{\epsilon_{\gamma_{41}}^2\epsilon_{\gamma_{42}}^2}\sigma_\Gamma.$$

By similar arguments to the proof of Lemma 13, the system is ISS when $\sigma_f \leq \lambda_F$. As a result, the threshold $R = \lambda_F$.